Functional analysis of purinergic signaling in the control of adult neurogenesis in mice: the hippocampal and hypothalamic neurogenic niche

Dissertation
zur Erlangung des Doktorgrades
der Naturwissenschaften

vorgelegt beim Fachbereich Biowissenschaften
der Goethe - Universität
in Frankfurt am Main

von
Jennifer Stefani
aus Göppingen

Frankfurt 2016
(D 30)

Vom Fachbereich Biowissenschaften der Goethe – Universität Frankfurt als Dissertation angenommen.

Dekanin:	Prof. Dr. M. Piepenbring
Gutachter :	Prof. Dr. A. Acker-Palmer
	Prof. Dr. H. Zimmermann

Datum der Disputation: 21.03.2017

Für meine Eltern

Helga und Johann Stefani

Summary

In the adult mammalian brain stem cells within defined neurogenic niches retain the capacity for lifelong de novo generation of neurons. The subventricular zone (SVZ) of the lateral ventricles and the subgranular layer (SGL) of the hippocampal dentate gyrus (DG) have been identified as the two major sites of adult neurogenesis. Moreover, the third ventricle in the hypothalamus is emerging as a new neurogenic niche in the adult brain. Extracellular purine and pyrimidine nucleotides are involved in the control of both embryonic and adult neurogenesis. These nucleotides act via ionotropic P2X or metabotropic P2Y receptors and studies of the adult SVZ and the DG provide strong evidence that ATP promotes progenitor cell proliferation in this stem cell rich regions. Previous studies have shown that the extracellular nucleotide-hydrolyzing enzyme NTPDase2 is highly expressed by adult neural stem and progenitor cells of the SVZ and the rostral migratory stream (RMS), the hippocampal SGL, and the third ventricle. NTPDase2 preferentially hydrolyzes extracellular nucleoside triphosphates (NTPs) and, to a lower extent, diphosphates, thus modulating their effect on nearby nucleotide receptors. Deletion of the enzyme increases extracellular NTP concentrations, and might indicate roles of purinergic signaling in adult neurogenesis. As shown by enzyme histochemistry, genetic deletion of NTPDase2 essentially eliminates ATPase activity in neurogenic niches but does not affect protein expression levels and activity of other ectonucleotidases. Lack of NTPDase2 leads to expansion of the hippocampal stem cell pool as well as of the intermediate progenitor type-2 cells. Cell expansion is lost at around type-3 stage, paralleled by increased labeling for caspase-3, indicating increased apoptosis, and decreased levels in CREB phosphorylation in doublecortin-expressing cells, diminishing survival in this cell population. In line with increased cell death, $P2Y_{12}$ receptor-expressing microglia is enriched at the hilus orientated side of the granule cell layer. These data strongly suggest that NTPDase2 functions as central homeostatic regulator of nucleotide-mediated neural progenitor cell proliferation and expansion in the adult brain by balancing extracellular nucleotide concentrations and activation of purinergic receptors.

In order to further characterize the role of purinergic signaling in adult neurogenesis, the ADP-sensitive $P2Y_{13}$ receptor was identified as a potential candidate whose activation might inhibit neurogenesis in the hippocampal dentate gyrus and the newly identified neurogenic niche at the third ventricle. Deletion of *P2ry13* increased progenitor cell proliferation and long-term progenitor survival as well as new neuron formation in the hippocampal neurogenic

niche. This was further paralleled by increased thickening of the granule cell layer, CREB phosphorylation, and expression of the neuronal activity marker c-Fos. Increased progenitor cell proliferation and progenitor survival persist in aged *P2ry13* knockout animals. However, in the ventral dentate gyrus proliferation and expansion levels of progenitor cells did not differ significantly from the wild type. This study strongly supports the notion that extracellular nucleotides significantly contribute to the control of adult neurogenesis in the dentate gyrus in situ. Data in this work suggest that activation of the $P2Y_{13}$ receptor dampens progenitor cell proliferation, new neuron formation, and neuronal activity. In contrast to several in vitro studies and studies in the SVZ in situ, a contribution of the ATP/ADP-sensitive $P2Y_1$ receptor could not be confirmed in the dentate gyrus in vivo.

To unravel implications of purinergic signaling and $P2Y_{13}$ receptor action in the control of adult hypothalamic neurogenesis a pilot study was performed. Mice null for *P2ry13* revealed increased progenitor cell proliferation at the third ventricle as well as long-term progeny survival and new neuron formation in the hypothalamus. In contrast to results obtained in the dentate gyrus expression of the neuronal activity marker c-Fos was significantly decreased in hypothalamic nuclei, indicating increased inhibition of appetite-regulating neuronal circuits by surplus neurons in knockout animals. These data provide first evidence that extracellular nucleotide signaling contributes to the control of adult hypothalamic neurogenesis in situ. Activation of the $P2Y_{13}$ receptor inhibits progenitor cell proliferation, long-term survival and neuron formation and therefore controls inhibition of appetite-regulating circuits in the adult rodent hypothalamus.

Zusammenfassung

Lange Zeit galt das von Ramon y Cajal postulierte, unangefochtene Dogma, dass das erwachsene Säugerhirn nach der Embryonalentwicklung in ein weitgehend postmitotisches Stadium übergehe und nicht mehr zur Proliferation von Vorläuferzellen sowie zur Neubildung von Nervenzellen fähig sei. Obwohl es bereits zuvor Hinweise auf sich teilende Zellen im erwachsenen Rattenhirn gab, wurde dieses Dogma erst mit der Wiederentdeckung des Konzepts der adulten Neurogenese im Gehirn von Singvögeln, Mitte der 80er Jahre des letzten Jahrhunderts in Frage gestellt. Heute gilt es als gesichert, dass auch im erwachsenen Säugerhirn, in mindestens zwei sogenannten neurogenen Nischen, Zellen die Fähigkeit beibehalten, sich zu teilen und reife Nervenzellen oder Gliazellen hervorzubringen. Diese neurogenen Nischen sind die subventrikuläre Zone am Seitenventrikel, sowie die subgranuläre Zone im Gyrus dentatus des Hippokampus. In den letzten Jahren häuften sich zudem die Hinweise auf die Existenz weiterer neurogener Nischen im erwachsenen Säugerhirn. Eine davon befindet sich am dritten Ventrikel im Hypothalamus. Das Konzept der adulten Neurogenese ist in allen Nischen vergleichbar, unterscheidet sich jedoch in einigen wichtigen Punkten. Im Allgemeinen beherbergen alle neurogenen Nischen ruhende Stammzellen die, nach ihrer Aktivierung durch interne und/oder externe Faktoren, beginnen, sich langsam zu teilen. Die Population der ruhenden Stammzellen scheint jedoch nicht homogen zu sein. Studien deuten vermehrt auf eine Heterogenität innerhalb der Stammzellpopulation hin. Dies könnte darauf hinweisen, dass unterschiedliche Stammzelltypen auf unterschiedliche Signalfaktoren reagieren, um so eine bestmögliche Anpassung an sich verändernde Umweltbedingungen zu garantieren. Im Hippokampus reifen langsam proliferierende Stammzellen, sogenannte Typ-1 Zellen, zu sich schnell teilenden Typ-2 Zellen heran. Aus Typ-2 Zellen gehen Typ-3 Zellen, auch Neuroblasten genannt, hervor, die aus der subgranulären Zone tiefer in die Körnerzellschicht einwandern, wo sie schließlich zu reifen Körnerzellen differenzieren und sich synaptisch in das hippokampale, neuronale Netzwerk integrieren. Am dritten Ventrikel gelten spezielle Ependymzellen, die Tanyzyten, als die eigentliche Stammzellpopulation. Generell ist bisher wenig über die dynamischen Prozesse der Proliferation und Differenzierung von Stammzellen zu reifen Neuronen im Hypothalamus bekannt. Subtypen von Tanyzyten, die die Ventrikelwand auskleiden, scheinen durch periphere Signale aktiviert zu werden, die sie über die Cerebrospinalflüssigkeit oder fenestrierte Blutgefäße der Blut-Hirn-Schranke in der Eminentia mediana erreichen. Sie beginnen zu proliferieren und bringen reife Neuronen hervor, die ins Parenchym auswandern, um dort verschiedene hypothalamische Nuklei zu bevölkern und sich

in Appetit-regulierende Netzwerke des Hypothalamus zu integrieren. Generell stellt der Prozess der adulten Neurogenese eine Abfolge von Ereignissen dar, die in Proliferation, Determinierung des Zellschicksals, Überleben, sowie Differenzierung und Integration der jungen Nervenzellen unterteilt werden kann. Es bedarf einer Reihe von Faktoren die diese Ereignisse auf der Einzelzellebene streng regulieren. Die in dieser Arbeit untersuchten purinergen Signalmechanismen, die ihre Wirkung über extrazelluläre Nukleotide vermitteln, stellen dabei potentielle Kandidaten dar.

Extrazelluläre Nukleotide können im zentralen Nervensystem von Säugern von einer Vielzahl von Zellen freigesetzt werden. Freisetzungsmechanismen beinhalten aktive Freisetzung von Vesikeln über Exozytose, Freisetzung über spannungsgesteuerte Ionenkanäle oder Kanalproteine, Transporter, Hemikanäle oder Konnexone sowie unkontrollierte Diffusion aus beschädigten oder toten Zellen. Nach ihrer Freisetzung fungieren extrazelluläre Nukleotide als Signalmoleküle, die in einer Reihe physiologischer und pathologischer Ereignisse eine Rolle spielen und ihre auto- oder parakrine Signalwirkung über ionotrope P2X-Rezeptoren oder metabotrope P2Y- oder P1-Rezeptoren vermitteln. Purinerge Rezeptoren unterscheiden sich in ihrer Ligandenspezifität und membranständige Enzyme, sogenannte Ektonukleotidasen, hydrolysieren extrazelluläre Nukleotide, verändern damit deren Verfügbarkeit und terminieren oder modifizieren auf diese Weise Signalwege, die durch die Bindung der Liganden an den jeweiligen Rezeptor intrazellulär ausgelöst werden. In der Literatur finden sich vermehrt Hinweise, dass purinerge Signalwege maßgeblich an der Kontrolle embryonaler und adulter Neurogenese beteiligt sind. So wurde auf kultivierten neuralen Stammzellen, die aus der subventrikulären Zone isoliert wurden, die Expression funktioneller purinerger Rezeptoren nachgewiesen. Die ATP-vermittelte Aktivierung des $P2Y_1$-Rezeptors veranlasst etwa das Freisetzen von Ca^{2+} aus intrazellulären Kalziumspeichern des endoplasmatischen Retikulums, was zur Freisetzung von Neurotransmittern, Wachstumsfaktoren sowie ATP führt und sowohl die Proliferation als auch Migration der Vorläuferzellen fördert. Erste klare Hinweise auf eine Beteiligung purinerger Signalwege bei der Kontrolle der adulten Neurogenese, lieferten Erkenntnisse aus unserer Arbeitsgruppe, die zeigen konnten, dass die Ektonukleotidase NTPDase2 auf primären Stammzellen der beiden klassischen neurogenen Nischen, der subventrikulären Zone und der subgranulären Zone, exprimiert wird. In reifen Neuronen oder Astrozyten konnte hingegen keine Expression des Enzyms nachgewiesen werden. Ein Großteil der Daten, die eine Beteiligung purinerger Signalwege an der adulten Neurogenese demonstrieren, stammt aus in vitro Kultursystemen. Neuere in vivo Studien, die ebenfalls auf

eine zentrale Rolle extrazellulärer Nukleotide bei der Kontrolle der adulten Neurogenese hinweisen, konzentrieren sich auf die Untersuchung der subventrikulären Zone. Eine kürzlich veröffentlichte Studie unsere Arbeitsgruppe zeigt, dass die Deletion der NTPDase2 in situ zu einer deutlich erhöhten Proliferation von Vorläuferzellen in den beiden klassischen neurogenen Nischen führt, wohingegen das Langzeit-Überleben sowie die Bildung reifer Nervenzellen unverändert bleiben.

Ziel dieser Arbeit war es daher, anhand verschiedener Knockout-Mausmodelle die Rolle purinerger Signalwege bei der Kontrolle der adulten Neurogenese, vor allem im Gyrus dentatus des Hippokampus in situ zu charakterisieren. Darüber hinaus wurde in einer Pilotstudie eine mögliche funktionelle Rolle purinerger Signalmechanismen in der neuentdeckten neurogenen Nische am dritten Ventrikel im Hypothalamus untersucht.

Die ATP-hydrolysierende Ekto-Nukleotidase NTPDase2 wird von primären Stammzellen in den beiden neurogenen Hauptnischen exprimiert. Die Deletion des Enzyms führt zu einer erhöhten Proliferation von Vorläuferzellen in neurogenen Nischen, ohne das Langzeit-Überleben oder die Bildung von Nervenzellen zu verändern. Die Akkumulation extrazellulären ATPs in den neurogenen Nischen dürfte in Folge der Deletion der NTPDase2 erhöht sein. Um die Morphologie der primären Stammzellen genauer betrachten zu können, wurde eine NTPDase2-/- Mauslinie generiert, die das grün-fluoreszierende Protein EGFP unter der Kontrolle des Nestinpromotors exprimiert. In Gefrierschnitten von Wildtyp- und Knockout-Mäusen konnten keine Unterschiede in der allgemeinen Hirnmorphologie oder in der Verteilung oder Morphologie der Nestin-exprimierenden Stammzellen gefunden werden. Mittels enzymhistochemischer Detektion von ATPase-Aktivität wurde die NTPDase2 als Hauptenzym für die Hydrolyse extrazellulärer Nukleotide in den neurogenen Nischen identifiziert. In NTPDase2+/+ Mäusen, ist die durch Hydrolyse von ATP vermittelte Färbung stark auf primären Stammzellen beider neurogenen Nischen lokalisiert, wohingegen in NTPDase2-/- Tieren keinerlei Markierung detektiert werden konnte. Semiquantitative Western-Blot-Analysen in Membranfraktionen von Wildtyp- und Knockout-Mäusen unterstützen die Beobachtung, dass die Deletion der NTPDase2 keine kompensatorische Überexpression anderer nukleotidhydrolysierender Enzyme zur Folge hat. Mittels eines immunhistochemischen Ansatzes wurde die stadiumsspezifische Proliferationsrate von Vorläuferzellen entlang der Differenzierungskaskade im Gyrus dentatus analysiert. Hoch signifikant erhöhte Proliferationsraten konnten in NTPDase2-/- Mäusen im Typ-1 und Typ-2

Zellstadium nachgewiesen werden, wohingegen die Zahl der Typ-3 Zellen zwischen Wildtyp- und Knockout-Mäusen unverändert war. Dies deutet auf eine erhöhte Expansion früher Vorläuferzellen hin, wohingegen interne regulatorische Mechanismen ein Überleben der Zellen verhindern. Gestützt wurde diese Hypothese durch Hinweise auf eine symmetrische Teilung der langsam proliferierenden Typ-1 Zellen, was die Ausdehnung des Typ-1 Zellpools erklären könnte, sowie durch den Nachweis einer erhöhten Apoptoserate im Gyrus dentatus von NTPDase2-/- Mäusen. Darüber hinaus konnte nachgewiesen werden, dass das Ausmaß der Phosphorylierung von CREB (cAMP response-element binding protein) in Typ-3 Zellen von Knockout-Mäusen deutlich erniedrigt ist. Die Phosphorylierung von CREB wurde in früheren Studien als essentiell für das Überleben dieses Zelltyps beschrieben. Der Verlust von Überlebensfaktoren stellt daher eine mögliche Erklärung für das Absterben der zuvor im Überschuss gebildeten Vorläuferzellen dar. Die Ergebnisse dieser Studie legen nahe, dass die NTPDase2 als homöostatischer Regulator der Nukleotid-vermittelten Proliferation und Ausdehnung von Vorläuferzellen im Gyrus dentatus des Hippokampus fungiert und damit eine entscheidende Rolle bei der Kontrolle der adulten Neurogenese übernimmt. Die NTPDase2 dürfte dabei die Aktivierung pro-mitotisch und anti-mitotisch wirkender Signalwege über die Kontrolle extrazellulärer ATP- und ADP- Konzentrationen und entsprechender purinerger Rezeptoraktivierung kontrollieren. Das warf die Frage auf, welche purinergen Rezeptoren diese Effekte vermitteln.

Vorausgegangene in vitro und in vivo Analysen hatten den beiden metabotropen ATP-sensitiven Rezeptoren $P2Y_1$ und $P2Y_2$ eine pro-mitotische Rolle bei der Neurogenese zugewiesen. Ausgehend von in situ-Hybridisierungsdaten die im Allen Brain Atlas publiziert wurden, wurde der ADP-sensitive $P2Y_{13}$-Rezeptor als potentieller Kandidat ausgemacht, der anti-mitotische Signalwege vermitteln könnte. Inkorporationsanalysen des chemischen Thymidinanalogons BrdU (Bromodesoxyuridin) zeigten eine deutlich erhöhte Anzahl BrdU-markierter Zellen in der subgranulären Zone des Gyrus dentatus von *P2ry13* Knockout-Mäusen. Darüber hinaus war das Überleben dieser Zellen 28 Tage nach der BrdU-Injektion signifikant erhöht und es konnte eine Verdopplung der Anzahl neugebildeter Neuronen nachgewiesen werden. Die neurogene Kapazität, also der Anteil initial gebildeter Vorläuferzellen, die sich zu Neuronen differenzieren, blieb jedoch unverändert zwischen Wildtyp- und Knockout-Tieren. Dies spricht gegen eine vermehrte Bildung von Astroglia zu Lasten von Neuronen in Knockout-Mäusen. Begleitet wurden die proliferativen Effekte in der $P2Y_{13}$-Rezeptor-KO-Maus von einer Verdickung der Körnerzellschicht, sowie einer signifikant er-

höhten Phosphorylierungsrate von CREB in Doublecortin-exprimierenden Neuroblasten. Immunhistochemische Analysen der Expression von c-Fos, einem häufig genutzten Marker für neuronale Aktivität in situ, deuten zudem auf eine erhöhte neuronale Aktivität im Gyrus dentatus von Knockout-Mäusen hin. Diese Beobachtung könnte durch die erhöhte Anzahl reifer Neuronen erklärt werden oder aber durch potentielle Veränderungen in der Freisetzung von Neurotransmittern nach Deletion des $P2Y_{13}$-Rezeptors. Interessanterweise wurden die proliferativen Effekte in Knockout-Tieren nicht gleichmäßig entlang der dorsoventralen Achse des Hippokampus beobachtet. Im ventralen Gyrus dentatus wurde keine Erhöhung der Proliferation oder des Überlebens von Vorläuferzellen detektiert, was auf eine regionenspezifische Expression des $P2Y_{13}$-Rezeptors hindeuten könnte und einmal mehr auf potentielle Unterschiede in der Regulierung und Funktion der adulten Neurogenese entlang der dorsoventralen Achse des Hippokampus hinweist.

Die Neurogeneserate in Säugern ist abhängig vom Alter des Individuums und in gealterten Tieren wurde eine deutliche Abnahme der adulten Neurogenese nachgewiesen. Trotz des altersabhängigen Rückgangs der Neurogenese konnte auch in 6 Monate alten $P2Y_{13}$-Rezeptor-KO-Mäusen eine erhöhte Proliferation und ein erhöhtes Überleben von Vorläuferzellen nachgewiesen werden.

Zusammengefasst implizieren die Daten dieser Studie eine maßgebliche Beteiligung purinerger Signalwege an der Kontrolle adulter Neurogenese im Hippokampus. Darüber hinaus wurde in dieser Arbeit zum ersten Mal der Nachweis erbracht, dass die Aktivierung des $P2Y_{13}$-Rezeptors die Proliferation von Vorläuferzellen, die Neubildung von Neuronen sowie die neuronale Aktivität abschwächt. Diese Erkenntnis stützt die These, dass die kontrollierte Aktivierung von pro-mitotisch und anti-mitotisch wirkenden purinergen Rezeptoren, vermutlich vermittelt durch die katalytische Aktivität der Ekto-Nukleotidase NTPDase2, eine funktionelle Rolle bei der adulten hippokampalen Neurogenese spielt.

Der Hypothalamus fungiert als zentrale regulatorische Schaltstelle im Säugerhirn und kontrolliert lebenserhaltende Funktionen wie Wachstum und Entwicklung, Fortpflanzung, Schlaf und Wachheit, Blutdruck aber auch Nahrungsaufnahme und Energiemetabolismus. Der dritte Ventrikel im Hypothalamus wurde als neurogene Nische identifiziert und adulte Neurogenese in dieser Region steht in engem Zusammenhang mit der Kontrolle von Nahrungsaufnahme sowie der Regulation von Hunger und Sattheit. Eine zentrale Rolle in diesem Kontext nehmen

Tanyzyten ein. Sie kleiden die Ventrikelwand aus und fungieren als chemosensorische Pförtner, die peripher freigesetzte Signalmoleküle wie etwa Glukose wahrnehmen und diese metabolischen Informationen an sensitive Neuronen weiterleiten. Tanyzyten, oder Subpopulationen dieses Zelltyps, repräsentieren die primäre hypothalamische Stammzellpopulation. Die Tatsache, dass Tanyzyten die Ekto-Nukleotidase NTPDase2 exprimieren, lieferte erste Hinweise auf eine funktionelle Beteiligung purinerger Signalmechanismen in der adulten hypothalamischen Neurogenese. Darüber hinaus wurde gezeigt, dass das Erfassen von Glukosekonzentrationen im Blut durch Tanyzyten von einem $P2Y_1$-Rezeptor-abhängigen, durch ATP-Freisetzung vermittelten, Signalweg reguliert wird. Zudem konnte die Expression funktioneller purinerger Rezeptoren auf Neuronen in hypothalamischen Nuklei nachgewiesen werden.

In dieser Arbeit wurde zum ersten Mal gezeigt, dass die Deletion des $P2Y_{13}$-Rezeptors die Proliferation und Neurogenese am dritten Ventrikel signifikant erhöht. Dieser Effekt war besonders deutlich in der Eminentia mediana, wo in $P2Y_{13}$-Rezeptor-Knockout-Mäusen 85% mehr BrdU-positive Zellen detektiert wurden. Die Analyse der BrdU-markierten Zellen nach vier Wochen zeigte, dass der Großteil der initial markierten Vorläuferzellen ins Parenchym eingewandert war, wo sie in hypothalamische Nuklei integriert wurden und neuronale Marker wie HuC/D oder NeuN exprimierten. Im dorsomedialen Nukleus sowie im Nucleus arcuatus war die Zahl neugebildeter Neuronen in Knockout-Mäusen beinahe verdoppelt. Im ventromedialen Nukleus konnte lediglich ein Trend ($p=0,15$) für eine Erhöhung nachgewiesen werden, der ebenfalls auf eine erhöhte Neubildung von Neuronen hindeutet. Mittels immunhistochemischer Analyse der Expression von c-Fos, wurde der neuronale Aktivitätszustand im Hypothalamus von Knockout- und Wildytyp-Mäusen untersucht. In allen drei hypothalamischen Nuklei (dorsomedialer Nukleus, ventromedialer Nukleus und Nucleus arcuatus) war das Aktivitätsniveau in $P2Y_{13}$–Rezeptor-Knockout-Mäusen deutlich erniedrigt. Diese Beobachtung deutet auf eine verstärkte inhibierende Wirkung von neugebildeten Neuronen auf Appetit-regulierende neuronale Netzwerke im Hypothalamus hin. Zusammengefasst legen diese Daten eine Beteiligung purinerger Signalmechanismen, insbesondere des $P2Y_{13}$-Rezeptors, an der adulten hypothalamischen Neurogenese und an der Kontrolle des Energiestoffwechsels nahe. Unter physiologischen Bedingungen übt die Aktivierung des $P2Y_{13}$-Rezeptors vermutlich einen negativen Effekt auf Zellproliferation, Zellüberleben und die Bildung von Nervenzellen aus, was eine mutmaßlich verringerte inhibitorische Wirkung auf Appetit-regulierende Netzwerke im adulten murinen Hypothalamus zur Folge hat. Die Befun-

de unterstützen damit auch die Hinweise zweier Studien die nachweisen konnten, dass die Aktivierung des $P2Y_1$-Rezeptors im Hypothalamus die Nahrungsaufnahme von Ratten erhöht und dass die Beschränkung der Nahrungsaufnahme die Expression des $P2Y_1$-Rezeptors negativ beeinflusst.

Wie bereits eingangs erwähnt, legen die Befunde dieser Arbeit die Vermutung nahe, dass die NTPDase2 die Aktivierung entgegengesetzter, pro- und anti-mitotisch wirkender purinerger Rezeptoren kontrolliert. Der ADP-sensitive $P2Y_{13}$-Rezeptor wurde in dieser Arbeit als anti-mitotisch wirkender, purinerger Rezeptor der adulten hippokampalen und hypothalamischen neurogenen Nische identifiziert. Vorausgegangene in vitro und in vivo Analysen lassen die Vermutung zu, dass der ATP/ADP-sensitive $P2Y_1$-Rezeptor als potentieller Gegenspieler des $P2Y_{13}$-Rezeptors im Hippokampus und Hypothalamus fungiert. Die Anzahl c-Fos-positiver Zellen war im Gyrus dentatus des Hippokampus von $P2Y_1$-/- Tieren deutlich verringert, was eine erniedrigte neuronale Aktivität nahelegt. Es bedarf weiterführender Studien, um eindeutig zu klären, ob es sich hierbei tatsächlich um einen Neurogenese-abhängigen Effekt oder aber um eine veränderte Freisetzung von Neurotransmittern infolge der Deletion des Rezeptors handelt. Ein durch den $P2Y_1$-Rezeptor vermittelter proliferativer Effekt ließ sich allerdings im vorliegenden in vivo-Modelsystem nicht nachweisen. Sowohl im Hippokampus als auch im Hypothalamus blieb die Anzahl BrdU-markierter Zellen in $P2Y_1$-/- und $P2Y_1$+/+ Tieren zwei Stunden nach der Injektion von BrdU unverändert. Es ist nicht auszuschließen, dass kompensatorische Mechanismen, entweder durch Überexpression struktur- und funktionsverwandter Proteine oder durch regulatorische Netzwerkanpassungen zu diesen Abweichungen führten. Es ist denkbar, dass die Deletion des ATP/ADP-sensitiven $P2Y_1$-Rezeptors etwa durch verstärkte Aktivierung des ATP/UTP-sensitiven $P2Y_2$-Rezeptors kompensiert werden könnte. Die Aktivierung des $P2Y_2$-Rezeptors erhöht nachweislich die Proliferation von Vorläuferzellen in vitro. Auch eine verstärkte Aktivierung von ATP-sensitiven P2X-Rezeptoren oder Adenosin-sensitiven P1-Rezeptoren erscheint nicht unwahrscheinlich. Umfangreiche semi-quantitative Western-Blot-Analysen oder real-time PCR Analysen könnten aufklären, ob die Deletion des $P2Y_1$-Rezeptors die Expression anderer purinerger Rezeptoren beeinflusst. Eine weitere Möglichkeit, kompensatorische Mechanismen aufzuspüren, stellt der zellspezifische Knockout des $P2Y_1$-Rezeptors in der GLAST-exprimierenden Stammzellpopulation dar. Hierzu könnten neuerlich generierte (GLAST-$CreER^{T2}$)_$P2Y_1^{flox/flox}$ Mäuse zum Einsatz kommen. Damit würde die Deletion auf die Stammzellpopulation beschränkt und potentielle kompensatorische Mechanismen würden eingeschränkt.

Die Daten veranschaulichen einmal mehr, dass zwischen in vitro- und in vivo-Modellsystemen deutlichen Unterschiede bestehen können. Sie legen zudem nahe, dass die adulte Neurogenese in der subventrikulären Zone der Seitenventrikel, der subgranulären Zone des Gyrus dentatus sowie am dritten Ventrikel einer stark nischenabhängigen Regulation unterliegt. Daher müssen nischenspezifische Effekte stets gesondert betrachtet werden und können nicht zwingend vereinheitlicht werden.

Table of contents

1 Introduction

1.1 Adult neurogenesis in the mammalian brain

It was the prominent histologist Ramon y Cajal establishing the neuronal doctrine in the late 19th century postulating that: "once the development was ended, the founts of growth and regeneration of the axons and dendrites dried up irrevocably. In the adult centers, the nerve paths are something fixed, ended, and immutable. Everything may die, nothing may be regenerated. It is for the science of the future to change, if possible, this harsh decree." Over 100 years later the pioneering work of Altman and Das (1965), providing anatomical evidence for the presence of dividing cells in the postnatal rat hippocampus, was challenging this long-held dogma for the first time. Met with criticism, it took more than two more decades for general acceptance, that new neurons are continuously generated from precursor cells throughout the life of mammals in discrete regions of the brain. Rediscovery of the concept of adult neurogenesis started with work in songbirds from Paton and Nottebohm (1984) demonstrating that new neurons are functionally integrated into neural circuits in the adult central nervous system (CNS). After the first isolation of multipotent neural stem cells (NSCs) derived from the adult mammalian brain (Reynolds and Weiss, 1992; Richards et al., 1992) the acceptance of the concept of adult neurogenesis started to grow. The neurosphere assay represents one widely used tool to identify stem cells and to study neural stem and progenitor cell properties (van Doze and Perez, 2012). The sphere-formation assay is making use of the self-renewal and pluripotent capacity of stem cells (Reynolds and Weiss, 1992). Under non-adherent conditions cultured stem cells form free-floating cell aggregates or spheres that can be differentiated into neurons or glia cells in vitro (Reynolds and Rietze, 2005). More and more studies were published indicating that cells capable of long-term expansion and differentiation into neurons and glia reside in the adult rodent (Palmer et al., 1997; Doetsch et al., 1999; Palmer et al., 1999) and human brain (Eriksson et al., 1998; Kukekov et al., 1999; Roy et al., 2000). Today it is widely accepted that in the adult mammalian brain, new neurons are continuously generated from neural stem and progenitor cells in two main neurogenic regions: the subventricular zone (SVZ) of the lateral ventricles and the subgranular layer (SGL) of the hippocampal dentate gyrus (DG) (Urban and Guillemot, 2014) (Figure 1). Precursor cells in the SGL generate new neurons for the granule cell layer of the dentate gyrus whereas neural stem cells of the SVZ generate neurons for the olfactory bulb (OB) (Zhao et al., 2008). Several studies report adult neurogenesis at new sites besides the classic neurogenic regions, including

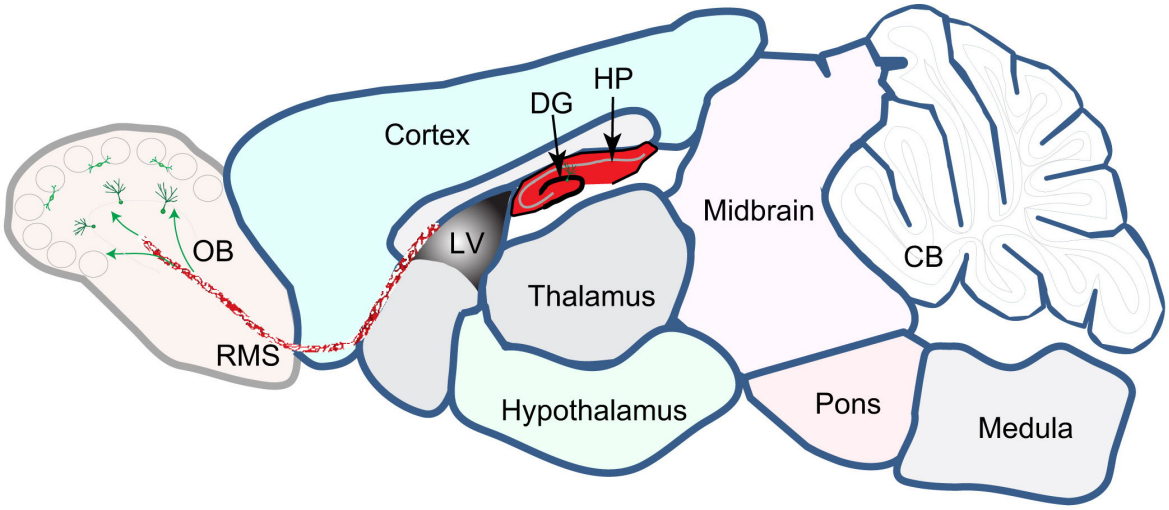

Figure 1: Sites of adult neurogenesis in the rodent brain. Sagittal view of an adult rodent brain depicting in red and dark grey shades the two main sites of adult neurogenesis: the dentate gyrus (DG) in the hippocampus and the lateral ventricle (LV), where newly generated neurons migrate along the rostral migratory stream (RMS) to the olfactory bulb (OB). CB, cerebellum; DG, dentate gyrus; HP, hippocampal formation; OB, olfactory bulb; RMS, rostral migratory stream. From Ming and Song (2011)

the neocortex (Gould et al., 1999), substantia nigra (Zhao et al., 2003), striatum (Dayer et al., 2005), the piriform cortex (Shapiro et al., 2007) or the hypothalamus (Kokoeva et al., 2005). However, at least some of them remain controversial (Bonfanti and Peretto, 2011).

1.1.1 Neural stem and progenitor cells and the development and maturation of adult-born neurons in the hippocampal dentate gyrus

The term stem cell refers to a cell fulfilling the features of self-renewal, proliferation and multipotency (the ability of a cell to differentiate into more than one cell type) (Braun and Jessberger, 2014). The existence or persistence of a neurogenic cell type with this hallmark stem cell properties in the adult DG is still the basis for controversial discussion (Bonaguidi et al., 2011; Encinas et al., 2011). Moreover, the debate about the cell type within the SGL representing the "real" stem cell is still ongoing (Bonaguidi et al., 2012). Another yet partially unresolved question addresses the ontogenetic origin of adult neural stem cells. In the classic model, glial fibrillary acidic protein (GFAP)-expressing cells originate from the dentate neuroepithilium, a part of the embryonic ventricular zone of the telencephalon, that migrate along with neuronal precursor cells to the newly formed SGL, where they give rise to granule neurons through the lifespan of mammals. However, this model is defied by studies on the

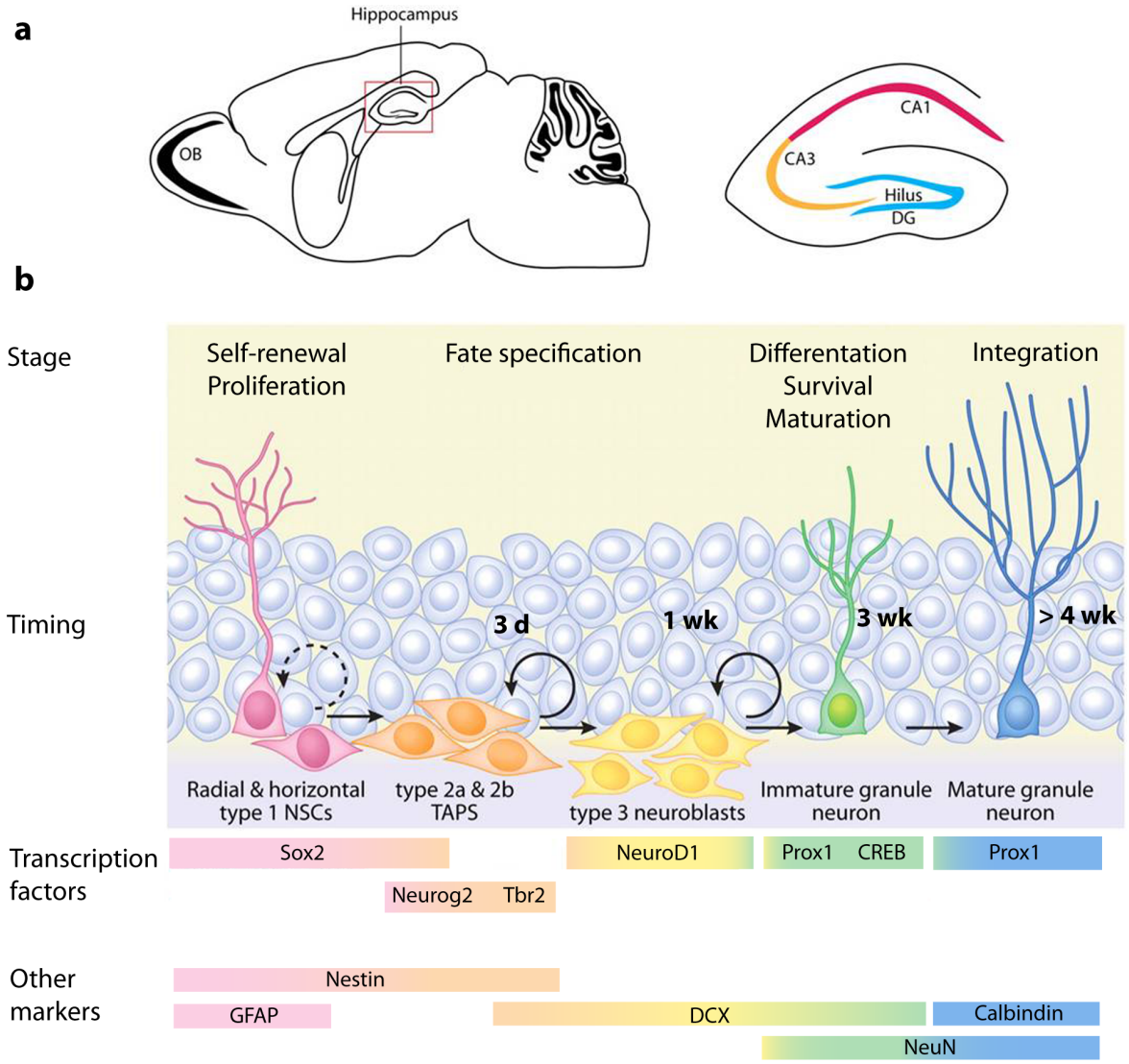

Figure 2: Adult neurogenesis in the SGL of the hippocampal dentate gyrus. a: Sagittal view of the mouse brain depicting the localization of the hippocampal formation. The scheme on the right side in **a** represents a close-up of the boxed region in the left sagittal overview roughly outlining the structure of the hippocampal formation including the cornu ammonis 1 and 3 (CA1 and CA3), dentate gyrus (DG) and hilus. **b:** Type-1 NSCs (pink) give rise to highly proliferating TAPs, subdivided into type-2a and type-2b cells (orange) that mature into type-3 neuroblasts (yellow) and finally into immature granule neurons (green) and mature granule neurons (blue) over the time course of several weeks (indicated in the middle). The differentiation and maturation of a type-1 cell to a mature granule neuron is a multistep process that can be subdivided in different stages (labeled on top). The progression is controlled by the expression of various transcription factors. Some examples mentioned in the text are depicted in the bottom colored panels. Cell type-specific marker combinations allow for a solid discrimination of individual cell types along the differentiation cascade (lower colored panels). CA, cornu ammonis; CREB, cAMP response element-binding protein; DCX, doublecortin; DG, dentate gyrus; GFAP, glial fibrillary acidic protein; NeuN, neuronal nuclei; NeuroD1, neurogenic differentiation 1; Neurog2, neurogenin 2; NSC, neural stem cell; Prox1, prospero homeobox 1; Sox2, sex determining region Y-box 2; TAP, transit amplifying progenitor; Tbr2, t-box brain protein 2. Modified from Hsieh (2012).

secretion of sonic hedgehog (Shh) from the amygdala at perinatal stages in a restricted region close to the lateral ventricle at the ventral-most side of the hippocampus, inducing NSCs which thereupon migrate, to populate all regions of the DG (reviewed by Urban and Guillemot, 2014). It is undisputed, that the whole process of adult neurogenesis is the sum of distinct steps along a differentiation cascade over the time course of several weeks including cell proliferation, cell migration, neuronal differentiation, cell survival and functional integration of the newborn neuron, each of them being strictly controlled by either niche-derived or intrinsic factors, that ensure the appropriate levels of neurogenesis suiting the tissue's demand (Kempermann et al., 2004) (Figure 2). The largely quiescent NSCs, also referred to as type-1 cells or radial-glia like cells, reside in the SGL, located at the border between the hilus and the granule cell layer (GCL) (Kempermann et al., 2004; Steiner et al., 2006; Zhao et al., 2008). Type-1 cells extend a single radial process spanning the entire granule cell layer, reaching the molecular layer, and forming bushy ramifications there (Steiner et al., 2006). Type-1 cells directly contact blood vessels and express the intermediate filament nestin, GFAP, the ectonucleotidase NTPDase2 and the transcription factor sex determining region Y-box 2 (Sox2) (Braun et al., 2003; Kempermann et al., 2004; Shukla et al., 2005; Hsieh, 2012). Recent studies suggest the existence of a second class of type-1 cells, having a short, horizontal process that is highly branching into the border of the outer granule cell layer and the inner molecular layer that appears not to proliferate (Lugert et al., 2010; Gebara et al., 2016). Moreover, studies in inducible reporter mouse lines such as GLAST-CreER^{T2} and Nestin-CreER^{T2}, suggest the co-existence of distinct populations of antigenically heterogeneous NSCs that contribute differently to long-term neurogenesis (Decarolis et al., 2013). The morphological characteristics of type-1 cells along with their distinct marker expression profile suggests, that they display astrocytic features (Seri et al., 2001; Bracko et al., 2012). Upon activation by intrinsic and/or extrinsic factors, slowly proliferating type-1 cells give rise to type-2 cells through asymmetric division. As mentioned earlier, it is still under debate whether, under certain circumstances, type-1 cells, or at least a subpopulation of them, can replicate through symmetric division (Bonaguidi et al., 2011). Type-2 cells, or transit-amplifying progenitors (TAPs) represent a highly proliferative cell type, enlarging the neurogenic cell pool, that can terminally differentiate into neurons or astrocytes (Kronenberg et al., 2003; Kempermann et al., 2004; Lugert et al., 2010). However, it is still controversial when exactly and at what levels astrocytes are formed (Bonaguidi et al., 2011; Encinas et al., 2011). Type-2 cells have only a short process and express nestin (Kempermann et al., 2004). They can further be subdivided in type-2a cells and type-2b cells by means of their cell type

specific marker expression profile (Kronenberg et al., 2003; Suh et al., 2007). While type-2a cells still express the transcription factor Sox2, type-2b cells were found to be Sox2-negative. Moreover, type-2b cells start to express the microtubule-associated protein doublecortin (DCX) (Kempermann et al., 2004). Fate specification in TAPs, defined as the transition from

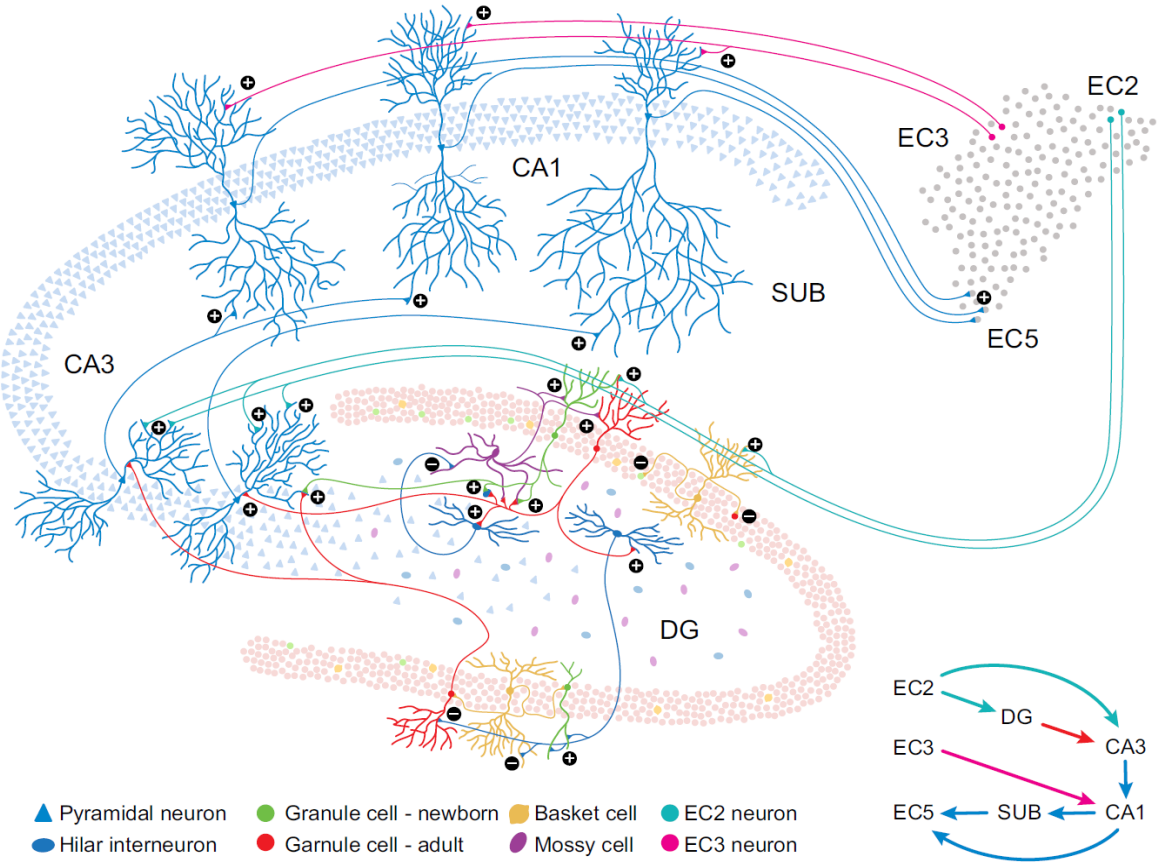

Figure 3: Hippocampal circuit anatomy. Neurogenesis is localized to the dentate gyrus (DG, highlighted in rose) and gives rise to excitatory granule cells throughout the lifespan of mammals. The hippocampus receives major input from the entorhinal cortex (EC) via axons of the perforant path. Axons arising from neurons in layer II of the EC (EC2 neurons, turquoise) form connections with dentate granule neurons (red and green) and interneurons (basket cells, yellow) as well as CA3 pyramidal neurons (blue, indicated with a triangular shape), while axons arising from layer III neurons (EC3 neurons, pink) project to pyramidal cells of the CA1 (blue, indicated with a triangular shape) and the subiculum (SUB). The complex local circuitry of the DG is composed of inhibitory interneurons (hilar interneurons, blue, indicated with a round shape) and excitatory feedback neurons (mossy cells, lilac) participating in the network's behavior. Granule cells in the DG project to the CA3 pyramidal neurons, which then project to the pyramidal neurons in the CA1 region via the Schaffer collateral pathway (indicated with a blue arrow in the lower right cartoon), as well as to CA1 cells in the contralateral hippocampus via the associational commissural pathway (not shown). The CA1 pyramidal cells then project back to the entorhinal cortex (EC) particularly to neurons in layer V (EC5) and subiculum (SUB), closing the "hippocampal loop". Plus and minus in the cartoon indicate excitatory or inhibitory action. From Aimone et al. (2014)

a multipotent cell type to a neuronal lineage-committed progenitor cell type, is marked by the upregulation of the transcription factors Neurog2 and Tbr2 (Hodge et al., 2008; Hsieh, 2012).

TAPs exhibit limited rounds of proliferation and mature into nestin- but DCX+ type-3 cells or neuroblasts (Kempermann et al., 2004; Steiner et al., 2006; Dhaliwal and Lagace, 2011; Berg et al., 2015). Neuroblasts migrate tangentially along blood vessels in the SGL and develop into immature neurons that radially migrate deeper up in the granule cell layer (Sun et al., 2015), slowly becoming post-mitotic, beginning to extend processes, and to express neuronal markers such as NeuN or Calbindin (Kempermann et al., 2004). Moreover, they start to express transcription factors such as pCREB, NeuroD1 and Prox1, that have been suggested to be important for the survival of this cell type (Gao et al., 2009; Lavado et al., 2010; Karalay et al., 2011; Merz et al., 2011; Jagasia et al., 2009). Over a time course of three weeks, neuroblasts mature into glutamatergic excitatory granule neurons extending dendrites into the molecular layer and establishing functional synapses with hilar interneurons, mossy cells and CA3 pyramidal cells in the hippocampus (Ming and Song, 2011; Zhao et al., 2006; Toni et al., 2008; van Praag et al., 2002). Only a small subset of the initially generated neurons (around 20-40%) manages to survive and to integrate into pre-existing circuits within the hippocampus (Figure 3). The majority of cells is undergoing programed cell death by apoptosis (Ming and Song, 2011; Kuipers et al., 2015). Therefore, similar to embryonic development, a surplus of progenitor cells is generated in the adult brain and neuronal survival is regulated via a selection process that exhibits two critical periods, one at the transition from the TAP to the neuroblast cell stage (Sierra et al., 2010), and another at 3-4 weeks of age of a newborn neuron, that requires N-Methyl-D-aspartate (NMDA) receptor expression and glutamate synaptic activation of newborn neurons (Tashiro et al., 2006).

1.1.2 The neurogenic niche in the adult hippocampus

The term niche, refers to a complex cellular microenvironment that surrounds stem cells and controls their development on a functional level (Ming and Song, 2011; Urban and Guillemot, 2014). The niche is build up by various cell types and structures that, on the one hand, permit and support differentiation and integration of new neurons, and on the other hand, create an appropriate environment that keeps the majority of stem cells quiescent and undifferentiated to maintain tissue homeostasis (Morrison and Spradling, 2008). The special architecture of the hippocampal neurogenic niche, where quiescent stem cells reside in direct vicinity to determined amplifying progenitors and immature neurons, is highly demanding for a strict control on a single-cell level (Braun and Jessberger, 2014). Neurogenesis in the DG is

promoted by signals from non-cellular components including secreted molecules and extracellular matrix molecules, such as the Reelin signaling pathway (Teixeira et al., 2012) or integrins (Porcheri et al., 2014). Moreover, direct cell to cell contact also modulates adult neurogenesis (Aimone et al., 2014). Neural stem and progenitor cells in the SGL are situated in close contact to the dense granule cell layer of the DG, build up by mature and immature neurons (Figure 4a). Immature neurons respond to the neurotransmitters glutamate and GABA, and neuronal activity is one main regulator in progenitor cell differentiation (Deisseroth et al., 2004; Tozuka et al., 2005; Song et al., 2012). Astrocytes were shown to represent one of the major contributors to the neurogenic niche. Co-culturing of neural precursor cells with astrocytes isolated from the adult hippocampus promoted neuronal differentiation (Song et al., 2002). Astrocytes are a source of a variety of paracrine niche factors such as ephrins, particularly ephrin-B2 (Ashton et al., 2012), cytokines like IL-6 (Oh et al., 2010), Wnt or Wnt inhibitors (Lie et al., 2005; Jang et al., 2013), Sonic hedgehog (Shh) (Ahn and Joyner, 2005) bone morphogenetic proteins (BMPs) (Mira et al., 2010) or Notch (Ables et al., 2010; Kawaguchi et al., 2013; Breunig et al., 2007; Seib et al., 2013). Furthermore astrocytes were shown to release adenosine 5'-triphosphate (ATP), promoting hippocampal progenitor cell proliferation in vitro (Cao et al., 2013). Resting microglia reside in the hilus and along the border of the granule cell layer in the hippocampal neurogenic niche (Wirenfeldt et al., 2003). They selectively shape neurogenesis via phagocytosis (Sierra et al., 2010; Sierra et al., 2014) while activation of microglia upon inflammation impairs neurogenesis (Ekdahl et al., 2003). Neural stem and precursor cells lie in close proximity to blood vessels (Figure 4a and b). Palmer et al. (2000) provided first evidence for the existence of a vascular niche, consisting of neural progenitors, newly generated neurons and mitotically active or quiescent endothelial cells that might control neurogenesis via direct cell-cell-contact or blood-circulating factors. Indeed, vascular endothelial growth factor (VEGF) (Jin et al., 2002; Fabel et al., 2003; Cao et al., 2013; Cao et al., 2004; Schanzer et al., 2004) or insulin-like growth factor (IGF) (Trejo et al., 2001; Carro et al., 2000) were shown to modulate neurogenesis. Moreover, circulating blood-derived factors have been directly linked to the impairment of neurogenesis in aged mice (Villeda et al., 2011; Smith et al., 2015). Notably, also NSCs themselves might influence each other via autocrine or paracrine mechanisms. Gap junction coupling and connexin expression of neural stem cells but not precursor cells is required for intact neurogenesis in the adult dentate gyrus (Kunze et al., 2009). In addition, expression of both, the VEGF

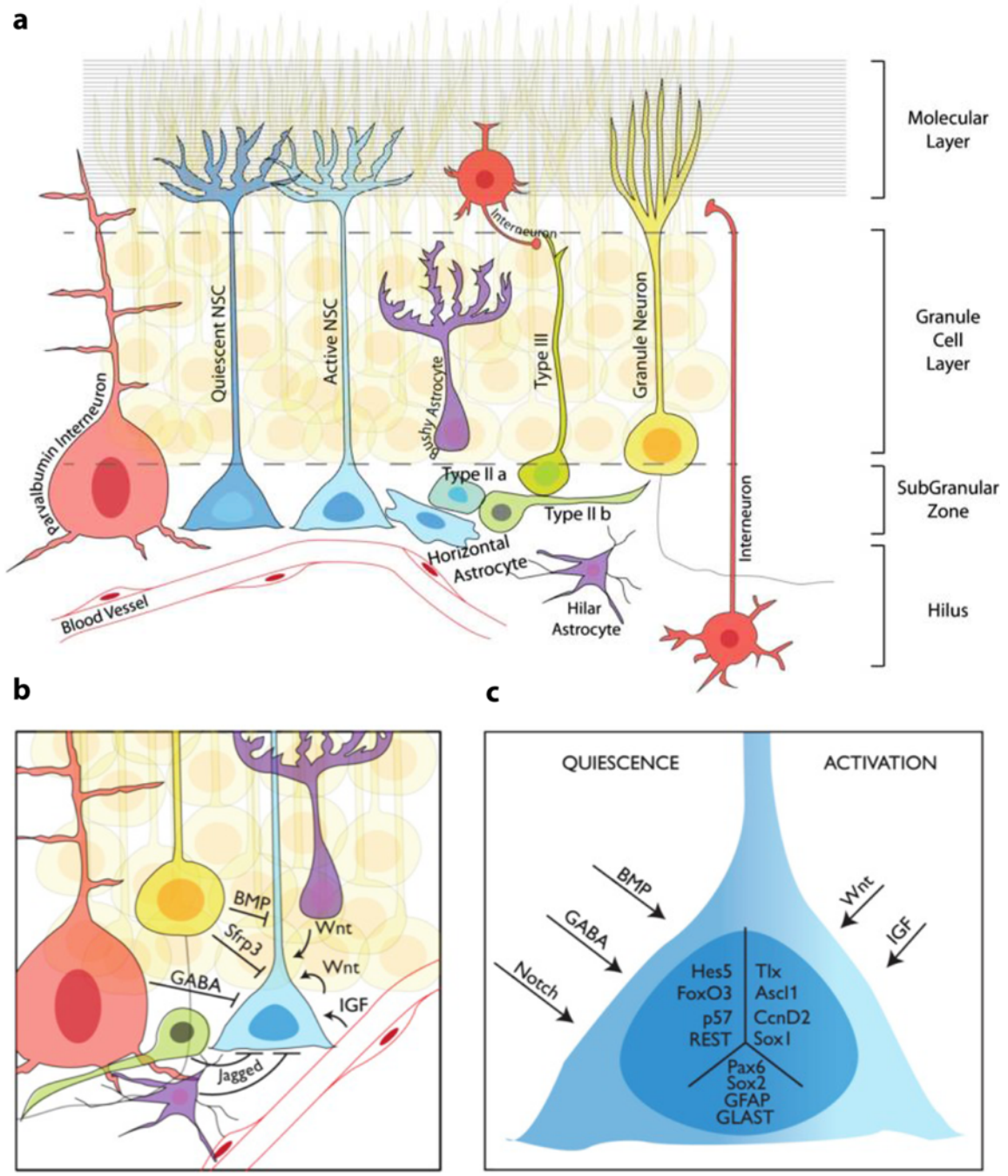

Figure 4: The hippocampal neurogenic niche. a: Graphic representation of the hippocampal neurogenic nice. Different cell types residing in the niche are highlighted in different colors. The niche is made up of quiescent and active neural stem cells (NSCs, light and dark blue), intermediate precursor cells (IPCs, typeIIa (turquoise), typeIIb (light green)), neuroblasts (typeIII, green), and granule neurons (light and bright yellow). Moreover, astrocytes (lilac), various types of interneurons (red), blood vessels, microglia (not shown) and axonal projections in the molecular layer (horizontal lines) contribute to the niche. **b:** Illustration of exemplary interactions within the SGL providing quiescence cues (BMP, GABA, Jagged or Sfrp3) or activation cues (Wnt, IGF). **c:** Examples of proteins, secreted molecules or transcription factors that have been linked to quiescence or activation of NSCs in the adult DG. Factors in the central part of the schematized cell (Sox2, Pax6, GFAP and GLAST) have been shown to be essential in NSCs, though no clear mechanism in the control of quiescence or activation has been reported yet (Hsieh, 2012). Modified from Urban and Guillemot (2014)

receptor 3 and its ligand VEGF-C by NSCs mediates intracellular activation of AKT and ERK pathways and controls activation and proliferation of quiescent radial-glia like stem cells (Han et al., 2015).

1.1.3 Functional significance of adult hippocampal neurogenesis

Thousands of new neurons are generated every day in the adult mammalian brain and adult neurogenesis is emerging as an important player in brain homeostasis and disease (Deng et al., 2010; Braun and Jessberger, 2014). Adult hippocampal neurogenesis does not only serve simple cell-replacement functions, but rather balances stability and plasticity of the hippocampal neuronal circuit to guarantee its proper function (Ming and Song, 2011; Christian et al., 2014; Abraham and Robins, 2005; Lledo et al., 2006). Hippocampus-dependent learning is the major physiological function adult hippocampal neurogenesis has been related to. Improved performance in hippocampus-dependent learning and memory tasks is directly correlated to increased levels of neurogenesis (Kempermann et al., 1997; van Praag et al., 1999) whereas reduction of hippocampal neurogenesis impairs hippocampus-dependent learning (Shors et al., 2001). Particularly long-term spatial memory and pattern separation have been reported to be modulated by adult neurogenesis (Deng et al., 2010; Sahay et al., 2011). Pattern separation describes a process, where highly similar representations or experiences or close located spatial positions are transformed into distinct, non-overlapping neural representations (Braun and Jessberger, 2014). It is one of the key functions of the dentate gyrus (Aimone et al., 2014; Leutgeb et al., 2007). Classical tasks related to pattern separation such as the radial arm maze (Saxe et al., 2007; Clelland et al., 2009), fear contextual discrimination (Sahay et al., 2011; Nakashiba et al., 2012) or two-choice discrimination (Clelland et al., 2009; McTighe et al., 2009; Creer et al., 2010) ruled out functional implications of adult neurogenesis in this context. Besides its function in memory formation, a role for adult neurogenesis in memory consolidation (Kitamura et al., 2009) and forgetting (Frankland et al., 2013; Akers et al., 2014) emerges. Immature adult born dentate granule cells are hyper-excitable and exhibit a lower threshold for the induction of long-term potentiation (LTP), with an increased potentiation amplitude as compared to mature neurons (Ge et al., 2007; Ge et al., 2008; Esposito et al., 2005; Schmidt-Hieber et al., 2004). This distinct period of elevated plasticity seems to be essential for the differential contribution to information coding of adult-born immature neurons compared to adult-born mature neurons or developmentally born neurons (Marin-Burgin et al., 2012). Immature neurons are preferentially recruited into circuits that support

spatial memory (Kee et al., 2007) and they display a significantly higher contribution to the formation of robust long-term spatial memory than mature dentate granule cells do (Deng et al., 2009). Not only in the healthy, but also in the diseased brain a functional relevance of adult neurogenesis has been described. Disruptions in adult hippocampal neurogenesis are directly linked to several neurological or neuropsychiatric disorders such as depression and epilepsy (Zhao et al., 2008; Sahay and Hen, 2007; Parent and Murphy, 2008; Snyder et al., 2011). All these implications in physiological and pathological situations attribute a significant role to adult neurogenesis in the rapid adaption to environmental or internal changes and challenges.

1.2 The third ventricle in the hypothalamus – a novel neurogenic niche

The concept of adult neurogenesis in classical neurogenic niches is nowadays widely accepted (Zhao et al., 2008; Ming and Song, 2011; Urban and Guillemot, 2014). Moreover, acceptance is growing that active neurogenesis may be more widespread in the adult brain (Gould, 2007). One potential novel neurogenic region that attracted more and more attention during the last decade is the hypothalamus (Migaud et al., 2010; Cheng, 2013). In 2001, Pencea et al. demonstrated that intraventricular administration of neurotrophic factors together with the cell proliferation marker bromodeoxyuridine (BrdU) into the lateral ventricle does not only stimulate the proliferation and differentiation of cells in the SVZ, lining the lateral ventricle. Numerous BrdU-positive cells were found in addition in the parenchyma of other brain regions lining the lateral and third ventricles in the adult forebrain, including the hypothalamus. Evans et al. (2002) were the first to isolate and culture mitotically active neural precursors from the adult rat hypothalamus. These cultured cells can form neurospheres and express distinct markers that are typically expressed by neural stem and progenitor cells such as Sox2 or nestin (Li et al., 2012). They also generate several subtypes of neuropeptide-expressing neurons, including those found in the neuroendocrine system (Markakis et al., 2004). These in vitro studies marked the starting-point for the awareness of the existence of a local neural stem and progenitor cell niche within the adult mammalian hypothalamus. Only three years after the first discovery of neurogenic action in the adult hypothalamus, the ependymal layer of the third ventricle in the hypothalamus was described as a neurogenic niche harboring BrdU-incorporating nestin- and GFAP-positive neural progenitor cells, that migrate to the hypothalamic parenchyma and functionally integrate into neuronal networks (Xu et al., 2005). Several in vivo studies demonstrated that cell proliferation and neurogenesis in periventricular and parenchymal areas of the adult hypothalamus can directly be stimulated

by the infusion of neurotrophic factors or growth factors into the third ventricle (Kokoeva et al., 2005; Xu et al., 2005; Perez-Martin et al., 2010). Taking advantage of more sophisticated labeling techniques, lentiviral YFP-tracking of Sox2-positive cells lining the third ventricle wall, revealed neuronal differentiation of these progenitors in normal brain physiology (Li et al., 2012). In line with another study published in the same year by Lee et al., these Sox2-positive progenitors were found to co-localize with nestin in tanycytes, a subpopulation of specialized ependymal cells, at the third ventricle wall and in the median eminence. Genetic fate mapping of tanycytes and their progeny suggested that at least a subpopulation of these cells directly gives rise to functionally active neurons in vivo (Lee et al., 2012). Compared to the two major neurogenic niches, neuronal differentiation of adult hypothalamic neural stem and progenitor cells (hNSPCs) is rather slow (Li et al., 2012). Nevertheless, a substantial post-natal turnover of neurons in the hypothalamic arcuate nucleus was reported. Within 4 to 12 weeks, hNSPCs replace around half of the neurons residing in this region (McNay et al., 2012).

1.2.1 The hypothalamus – a central homeostatic regulator in the mammalian brain

In mammals, the hypothalamus functions as a critical regulator in the vital control of body homeostasis including feeding behavior and energy expenditure, growth, reproduction and stress (Morton et al., 2006; Rizzoti and Lovell-Badge, 2016). Defects of hypothalamic maturation or lesions in specific areas of the hypothalamus result in obesity or weight loss (Maggi et al., 2014; Olney, 1969; Brobeck et al., 1943; Anand and Brobeck, 1951). Already in the early 20th century Anton Julius Carlson came up with the idea, that hunger and satiety might be triggered by plasma glucose concentrations (Carlson, 1919). A direct link of plasma glucose concentrations and food intake was suggested by Mayer (1953), who proposed that hypothalamic neurons might be responsible for sensing of alterations in blood glucose concentrations after a meal, leading to appetite regulation and meal termination. Indeed, the control of feeding behavior and glucose homeostasis strongly depends on the integration of energy-related hormonal signals, reflecting nutritional and energetic states such as leptin, insulin, ghrelin and glucose that are released by secretory cells in the periphery and circulate through the blood-stream (Frayling et al., 2011; Elizondo-Vega et al., 2015; Holmes et al., 2016). Responsive groups of neurons reside within anatomically distinct nuclei in the hypothalamic parenchyma, surrounding the third ventricle (3V) and regulating different

physiological functions (Rizzoti and Lovell-Badge, 2016; Haan et al., 2013). Nuclei that are involved in the control of feeding behavior include the arcuate nucleus (ARC), the paraventricular nucleus (PVN), the lateral hypothalamic area (LHA), the ventromedial nucleus (VMN), and the dorsomedial nucleus (DMN) (Figure 5). The median eminence (ME) is situated in the mediobasal hypothalamus (MBH) at the ventral-most side of the third ventricle. It represents a privileged region of the blood-brain-barrier, composed of fenestrated capillaries that allow the passage of circulating hormones and nutrients (Yu and Kim, 2012). This feature defines the median eminence as a circumventricular organ (Miyata, 2015), that promotes bi-directional exchange of molecules from the hypophyseal portal system to the hypothalamus

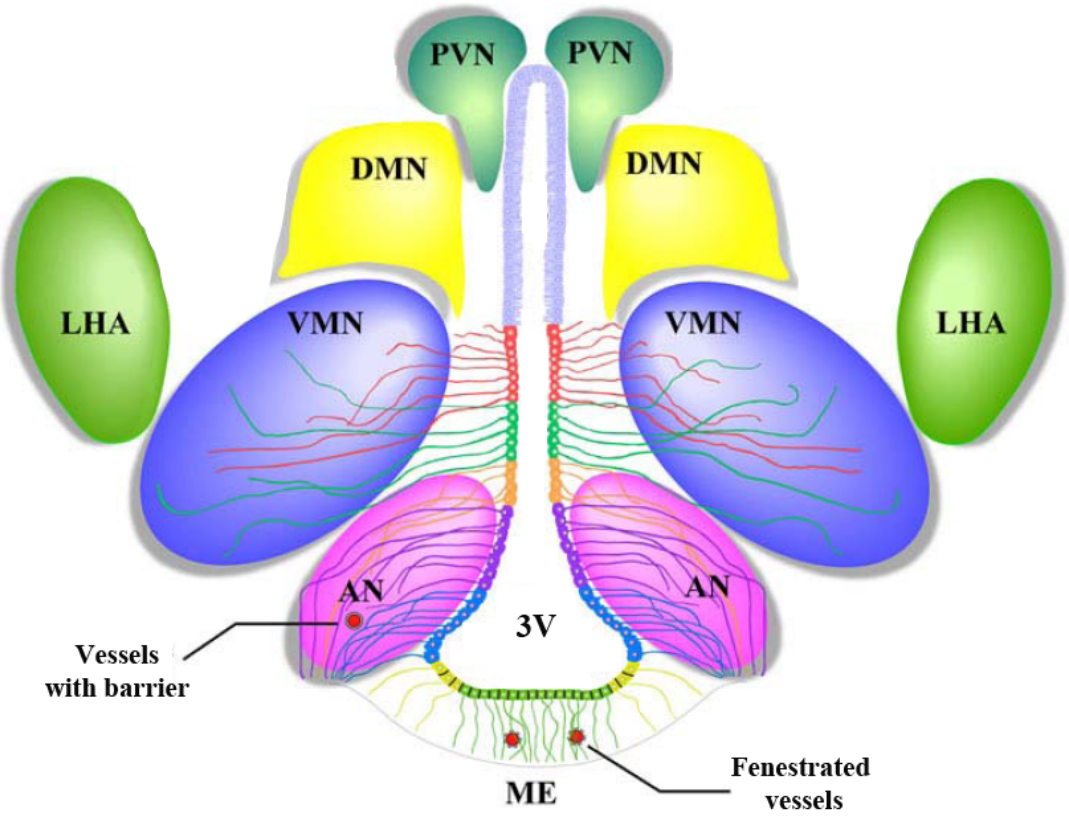

Figure 5: The cytoarchitecture of hypothalamic nuclei involved in the regulation of food intake. Schematic representation of hypothalamic nuclei and hypothalamic areas that are involved in the control of hunger and satiety. The distribution of tanycytes lining the third ventricle wall is depicted in different colors depending on their distinct location at the ventricle. AN, arcuate nucleus; DMN, dorsomedial nucleus; LHA, lateral hypothalamic area; PVN, paraventricular nucleus; VMN, ventromedial nucleus. Modified from Elizondo-Vega et al. (2015)

and vice versa (Figure 6). Hypothalamic nuclei are interconnected and build a neuronal network that integrates peripheral nutritional signals to maintain energy homeostasis (Blouet and Schwartz, 2010; Schwartz et al., 2000; Yu and Kim, 2012). The arcuate nucleus lies adjacent to the median eminence at the ventral side of the third ventricle (Figure 5). Thus, circulating

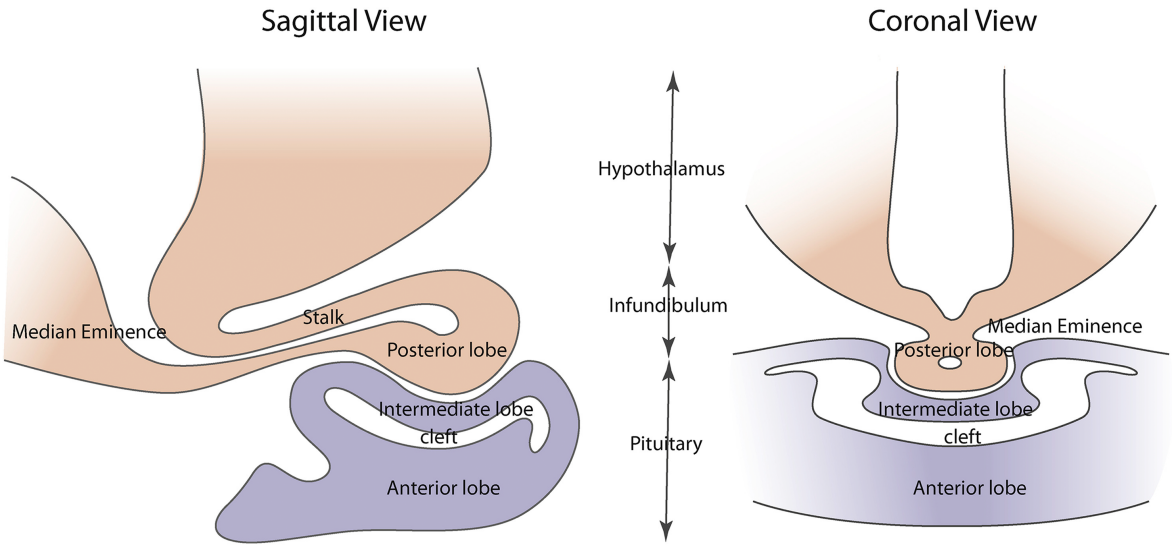

Figure 6: Anatomy of the hypothalamo-hypophyseal tract. Graphic representation of the link between the hypothalamus and the pituitary. The infundibulum is the direct connection between the hypothalamus and the pituitary and extends from the median eminence at the base of the third ventricle (sagittal view, left); with the pituitary stalk representing the direct physical link between the median eminence and the pituitary. The pituitary is divided in three sections: the anterior, the intermediate and the posterior lobe that have different homeostatic functions. From Rizzoti and Lovell-Badge (2016)

hormones and nutrients can directly access the arcuate nucleus through the median eminence and the cerebrospinal fluid (CSF) (Sousa-Ferreira et al., 2014). Due to this privileged anatomical position, the arcuate nucleus is widely considered as the main hypothalamic area responsible for sensing and internalizing peripheral metabolic signals (Yu and Kim, 2012). The arcuate nucleus harbors two populations of neurons: anorexigenic proopiomelanocortin (POMC)-expressing neurons and orexigenic neuropeptide Y (NPY)/agouti related protein (AgRP)-expressing neurons responsive for peripheral metabolic signals that include leptin, insulin, ghrelin, and nutrients. Axonal projections of POMC neurons innervate target neurons in the paraventricular nucleus, the ventromedial nucleus, and the lateral hypothalamic area. POMC neurons release α-melanocyte-stimulating hormone (α-MSH) that binds to melanocortin-3 and -4 receptors (MC3R, MC4R), expressed on neurons in the target regions to activate anabolic or catabolic actions (Huszar et al., 1997). These neurons then secrete neuropeptides such as the corticotrophin-releasing hormone, thyrotropin-releasing hormone, somatostatin, vasopressin, and oxytocin (Yu and Kim, 2012). The effect of α-MSH is antagonized by release of AgRP from NPY/AgRP-expressing neurons (Ollmann et al., 1997). Axonal projections from the arcuate nucleus also innervate neurons in the ventromedial nucleus, that have been shown to be involved in glucose sensing, therefore playing a pivotal role in maintaining glucose homeostasis (Gonzalez et al., 2009). VMN neurons innervate

target neurons in the arcuate nucleus, the dorsomedial nucleus, the lateral hypothalamic area, and in brainstem regions (Yu and Kim, 2012). Innervations by NPY and α-MSH terminals originating from the arcuate nucleus are also present in the dorsomedial nucleus (Yu and Kim, 2012). The lateral hypothalamic area represents another region being innervated by ARC neuronal terminals expressing NPY/AgRP and α-MSH. Orexin-expressing neurons in the lateral hypothalamic area undertake important regulatory functions in glucose sensing but also in the control of sleep and wakefulness (Ono et al., 2014).

1.2.2 Tanycytes and the hypothalamic neurogenic niche

Little is known about the identity and biology of adult hypothalamic neural stem and precursor cells (hNSPCs) and the dynamics of the neurogenic process (Haan et al., 2013). To date, the identity of stem cells is still not completely clear. Several studies suggest that tanycytes, or subpopulations of these cells, represent hNSPCs (Lee et al., 2012; Robins et al., 2013; Haan et al., 2013). Tanycytes are specialized types of ependymal cells that are non-ciliated (Altman and Bayer, 1978) but possess a long basal process that penetrates into the hypothalamic parenchyma (Rodriguez et al., 2005). They line the ventricular wall of the third ventricle. Based on their location (Akmayev and Popov, 1977) and marker expression profile (Cortes-Campos et al., 2011; Robins et al., 2013) they are subdivided into distinct subpopulations (Figure 7). The α1-tanycytes and α2-tanycytes are found at the level of the ventromedial nucleus and arcuate nucleus, respectively. α1-tanycytes project to the ventromedial nucleus whereas α2-tanycytes project mainly towards the arcuate nucleus. β1-tanycytes project to the median eminence and to the arcuate nucleus. β2-tanycytes reside on the floor of the third ventricle projecting to the median eminence, where they have direct access to fenestrated capillaries of the hypophyseal portal system (Ciofi et al., 2009; Langlet, 2014). Tight junctions between β2-tanycytes form a barrier between the median eminence and the ventricular cerebrospinal fluid (Peruzzo et al., 2000; Mullier et al., 2010) whereas tight junctions of β1-tanycytes form a barrier to limit the diffusion of blood-derived molecules to the arcuate nucleus (Rodriguez et al., 2005). However, barrier permeability can be modulated in response to changes in physiological situations such as fasting (Langlet et al., 2013). During development, tanycytes arise in the infundibulum (Sousa-Ferreira et al., 2014; Rizzoti and Lovell-Badge, 2016). They are generated from E18.5 onward by differentiation of early sonic hedgehog-expressing progenitors (Alvarez-Bolado et al., 2012; Rodriguez et al., 2005) in a process that highly

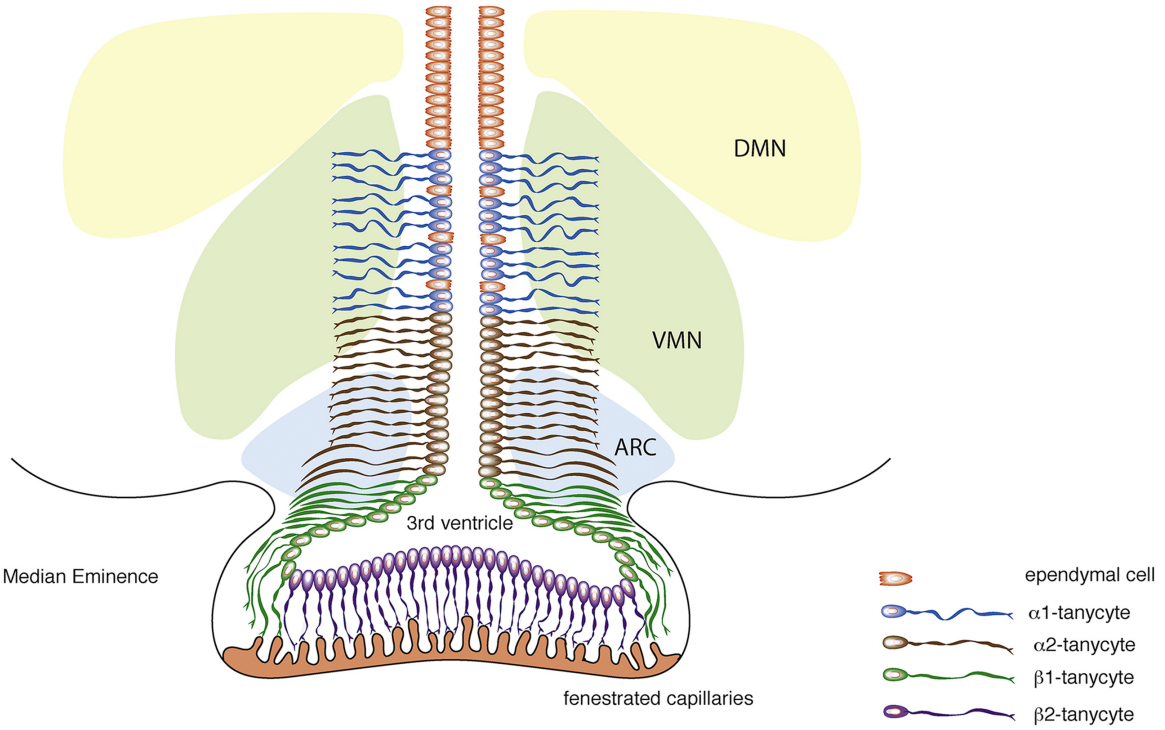

Figure 7: Tanycytes lining the third ventricle in the adult hypothalamus. The cartoon depicts the dorso-ventral organization of tanycytes and ependymal cells along the third ventricle wall. Ependymal cells are located at the dorsal part of the third ventricle. α1-tanycytes (blue) and α2-tanycytes (brown) reside in the medial part projecting to target neurons in the VMN and ARC. β1-tanycytes (green) project to the median eminence and the ARC and β2-tanycytes (lilac) reside on the base of the third ventricle, projecting to the median eminence. They are in direct contact to the portal system, composed of fenestrated capillaries. ARC, arcuate nucleus; DMN, dorsomedial nucleus; VMN, ventromedial nucleus. From Rizzoti and Lovell-Badge (2016)

depends on the expression of the transcription factors LHX2 and RAX and Wnt signaling (Rizzoti and Lovell-Badge, 2016). Several lines of evidence suggest that tanycytes represent hNSPCs. Radial glia cells release ATP acting on $P2Y_1$ receptors, to propagate calcium waves that control proliferation of these cells (Weissman et al., 2004; Pearson et al., 2005; Dale, 2008). Moreover, expression of the ectonucleotidase NTPDase2 is associated with distinct stem cell populations (Braun et al., 2003; Shukla et al., 2005). Indeed, tanycytes arise from radial glia cells (Sousa-Ferreira et al., 2014), they release ATP and signal via waves of intracellular Ca^{2+} (Frayling et al., 2011). They express functional $P2Y_1$ receptors (Bjelobaba et al., 2015) and NTPDase2 (Braun et al., 2003). Moreover, tanycytes express several markers associated with stem cell populations in other neurogenic niches including nestin, vimentin, GFAP and Sox2 (Robins et al., 2013). As described earlier, the two main characteristics of neural stem cells are their capacity to self-renew and to differentiate into other cell types, probably through asymmetric cell division (Gage, 2000; Suh et al., 2007). α- and β-tanycytes proliferate under basal and stimulated conditions (Lee et al., 2012; Robins et al., 2013; Haan et al., 2013). β2-tanycytes proliferate and generate neurons that migrate to several hypothalamic nuclei in

young adult mice, however their rate of proliferation dramatically decreases during adulthood (Lee et al., 2012; Haan et al., 2013). Only α-tanycytes were shown to form neurospheres in vitro and only α2-tanycytes showed the ability to unlimitedly self-renew (Robins et al., 2013). Whether β2-tanycytes might represent transient hypothalamic hNSPCs that are later replaced by α2-tanycytes is still a matter of debate (Maggi et al., 2014). α -tanycytes were shown to give rise to cells, that migrate ventrally towards the foot of the third ventricle and become β-tanycytes (Robins et al., 2013; Rizzoti and Lovell-Badge, 2016). This suggests that these cells might represent stem cells and committed progenitors rather than distinct subpopulations of progenitors. Different populations of hNSPCs possibly undertake distinct functions. This is further supported by the notion, that different growth factors modulate stem and progenitor cell proliferation in different hypothalamic areas. Whereas BDNF increases levels of cell proliferation in the paraventricular nucleus (Pencea et al., 2001), IGF-I stimulates neurogenesis in periventricular and parenchymal zones of the whole hypothalamus (Perez-Martin et al., 2010). FGF-2 and CNTF promote neurogenesis in the arcuate nucleus (Pierce and Xu, 2010). Apart from tanycytes, proliferative subependymal astrocytes and other types of proliferating cells within the hypothalamic parenchyma were identified (Kokoeva et al., 2007; Perez-Martin et al., 2010) (Figure 8). All these findings are indicative of a region- or subtype specific activation of progenitors that might be important to implement different metabolic cues according to the organisms need.

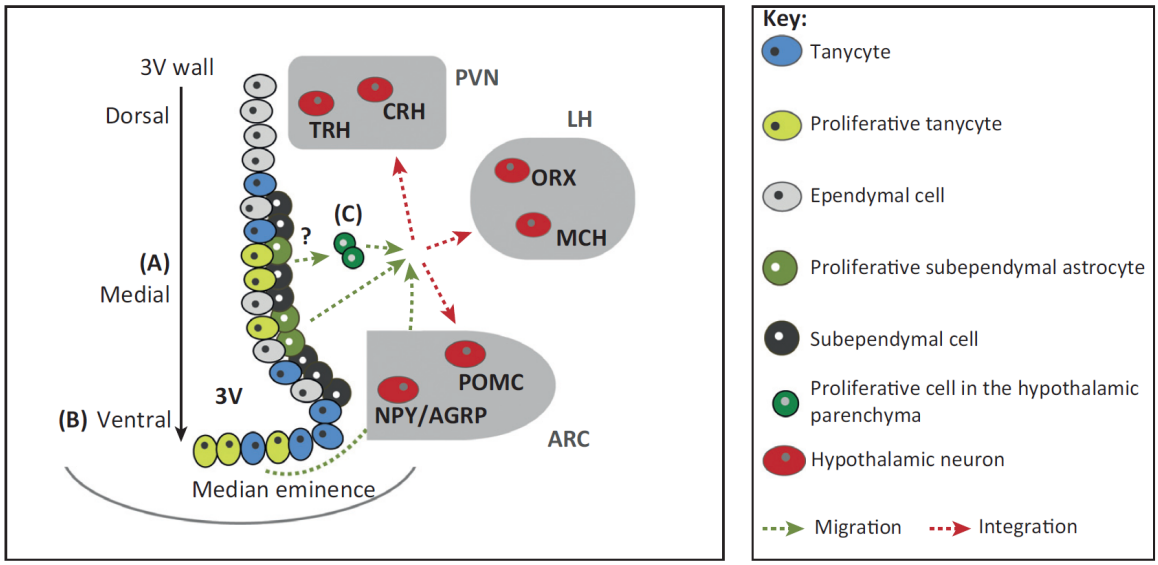

Figure 8: The hypothalamic neurogenic niche in the adult rodent brain. Graphic representation of cell types and hypothalamic areas involved in adult hypothalamic neurogenesis. Ependymal cells (grey), tanycytes (blue) and subependymal cells (dark brown) line the third ventricular wall. Different proliferative zones have been described in the medial (A) and ventral (B) part of the 3V as well as in the parenchyma (C). Proliferative tanycytes (light green) and proliferative subependymal astrocytes (dark green) reside in the medial part (A), whereas the ventral part (B) contains only proliferative

tanycytes (light green). Proliferative cells in the parenchyma might arise from proliferative progenitors at the 3V wall as indicated (green arrows). Green arrows depict the migration of distinct populations of hNSPCs to their target regions in hypothalamic nuclei where they mature to distinct sub-populations of hypothalamic neurons (red) and integrate into the hypothalamic neural network. 3V, third ventricle; AgRP, agouti-related protein; ARC, arcuate nucleus; CRH, corticotropin-releasing hormone, LH, lateral hypothalamus; MCH, melanin concentrating hormone; NPY, neuropeptide Y; ORX, orexin; POMC, proopiomelanocortin; PVN, paraventricular nucleus; TRH, thyrotropin-releasing hormone. From Sousa-Ferreira et al. (2014)

1.2.3 Functional implications of adult hypothalamic neurogenesis in the control of energy balance

Due to the central regulatory function of the hypothalamus in the control of food intake and energy balance (Morton et al., 2006), a contribution of adult hypothalamic neurogenesis to the plasticity of hypothalamic networks involved in energy metabolism was hypothesized (Bolborea and Dale, 2013). Recent studies show, that adult hypothalamic neurogenesis persist in the aging brain of mice and retains the capacity to generate neurons for hypothalamic nuclei throughout the lifespan of the animal (Chaker et al., 2016). The majority of hypothalamic progenitor cells terminally differentiates into NPY/AgRP- and POMC-expressing neurons and integrates into hypothalamic areas that are mainly involved in the regulation of hunger and satiety including the arcuate nucleus, the ventromedial nucleus and the dorsomedial nucleus (Kokoeva et al., 2005; Pierce and Xu, 2010). Neural growth factors play a major role in the control of adult hypothalamic neurogenesis. Ciliary neurotrophic factor (CNTF) promotes neurogenesis in the arcuate nucleus and the ventromedial nucleus and this is directly associated with weight loss in obese mice (Kokoeva et al., 2005, 2007). Chronic high-fat diet is accompanied with increased levels of apoptosis in several hypothalamic nuclei including the arcuate nucleus and the lateral hypothalamic area (Moraes et al., 2009). In line with these findings, Li et al. (2012) reported that high-fat diet induced inflammation and upregulation of IKKbeta/NF-kappaB, and inhibits proliferation of α- and β1-tanycytes and proliferative cells in the hypothalamic parenchyma, which finally leads to obesity in mice. In contrast, short-term feeding of a high-fat diet stimulated β2-tanycyte proliferation and neuronal differentiation in the median eminence, specifically in female mice (Lee et al., 2012; Lee et al., 2014). Moreover, reduced proliferation and neurogenesis in the median eminence correlates with caloric restriction (Lee et al., 2014). Adult hypothalamic neurogenesis is the driving force in the constant neuronal turnover of NPY/AgRP- and POMC-expressing neurons in feeding circuits

and it was shown to be impaired in obese mice (McNay et al., 2012; Li et al., 2012). A direct correlation of seasonal changes in food intake and body weight with changes in tanycyte function and neurogenesis in syrian hamsters has been reported (Ebling, 2015; Samms et al., 2015). Tanycytes are considered to represent hNSPCs (Sousa-Ferreira et al., 2014). Their distinct location in direct proximity to fenestrated capillaries in the median eminence provides unrestricted access to blood-borne signals and to the ventricular CSF. This feature places them in a privileged position to sense and implement nutritional cues from the periphery such as glucose, hormones and neurotrophic factors and to transfer this metabolic information to responsive neurons residing in the regulatory feeding-centers in hypothalamic nuclei (Rodriguez et al., 2005; Lee et al., 2012; Langlet et al., 2013; Balland et al., 2014; Frayling et al., 2011; Rizzoti and Lovell-Badge, 2016). Although concrete studies unraveling the molecular mechanisms underlying hNSPC proliferation and differentiation are still missing, it is nowadays widely accepted that adult hypothalamic neurogenesis is one key component in the central regulation of energy metabolism and feeding control, providing neuronal circuits with the structural plasticity to adapt to changes in diet or energy expenditure.

1.3 Purinergic signaling mechanisms – Focus on the central nervous system

Intercellular communication is maintained through molecules released from one cell into the extracellular space and diffusion to another cell or through coupling of cells via channels such as gap junctions (Verkhratsky and Burnstock, 2014). Extracellular nucleotides like ATP, ADP, UTP, UDP and UDP glucose can trigger this messenger release (Zimmermann, 2016) and function as regulatory molecules in a variety of physiological and pathological events through autocrine or paracrine mechanisms (Glaser et al., 2012). Mechanisms, using purines and pyrimidines as signaling molecules, are evolutionary very old, possibly due to the fact that nucleotides such as ATP represent the underlying components for the genetic code and serve as major molecules involved in energy storage and supply (Verkhratsky and Burnstock, 2014). Ligand-gated ion-channels sensitive for ATP, so called P2X purinoreceptors are already present in rather primitive organisms such as protozoa and algae (Burnstock and Verkhratsky, 2009). Due to its involvement in vital cellular functions, cells contain millimolar concentrations of intracellular ATP. The nucleotide can be actively released from virtually every cell type of an organism into the extracellular space by various mechanisms such as vesicular exocytosis, voltage-gated ion channels or channel proteins, transporters or hemichannels but also

by uncontrolled leakage from damaged or lysed cells (Abbracchio et al., 2009; Lohman et al., 2012; Zimmermann, 2016). Multiple cells express different subtypes of purinergic receptors that exhibit different ligand specificity and/or affinity, activating different intracellular signaling cascades (Cavaliere et al., 2015; Zimmermann, 2016). The nomenclature of purinergic receptors was changed several times throughout the years. In this work, a consequent nomenclature will be provided. Protein symbols will be indicated in capital letters, followed by the subtype that is subscripted (e.g. $P2Y_{13}$). Gene symbols for purinergic receptors are italicized, with only the first letter in upper-case (e.g. *P2ry13*). Extracellular nucleotides can bind different cell surface-located receptors whose catalytic site faces the cell exterior (Neary and Zimmermann, 2009). As indicated earlier, these purinergic receptors represent evolutionary very old receptors that are already found in single-cell organisms (Burnstock and Verkhratsky, 2009). Purinergic receptors can be subdivided in groups of ionotropic ATP-sensitive P2X receptors, of which seven subtypes have been described ($P2X_{1\text{-}7}$), metabotropic G protein-coupled P2Y receptors ($P2Y_1$, $P2Y_2$, $P2Y_4$, $P2Y_6$, $P2Y_{11}$, $P2Y_{12}$, $P2Y_{13}$, and $P2Y_{14}$), and P1 receptors (A_1, A_{2A}, A_{2B}, and A_3) (Burnstock, 2007) (Figure 9). Whereas P1 receptors are activated by adenosine, P2Y receptors – depending on subtype - are sensitive for ATP, ADP, UTP, UDP or UDP-sugar with differing affinity (Ralevic and Burnstock, 1998) (Figure 9). A recently discovered fourth class of purinergic receptors, termed P0 receptors or AdeR, has been shown to be activated by the nucleobase adenine (Thimm et al., 2013). Receptors of the P2Y and P1 type display the classical membrane topology of G protein-coupled receptors (GPCRs) with seven hydrophobic transmembrane regions connected by three extracellular loops and three intracellular loops with the N-terminus located extracellularly and a cytoplasmic C-terminus that couples to the respective G protein (von Kügelgen and Hoffmann, 2016). Crystal structures recently published for the $P2Y_1$ and $P2Y_{12}$ receptor provide evidence that parts of the predicted transmembrane regions 3, 6 and 7 form the ligand binding pocket (von Kügelgen and Harden, 2011). Like other GPCRs, P2Y receptors can form homo- and heterodimers which, in some cases, leads to changes in their pharmacological properties (von Kügelgen and Hoffmann, 2016). Receptor action of P2Y receptors is mediated through the coupled G-proteins and intracellular secondary messenger molecules, such as cyclic AMP (cAMP), phospholipase C (PLC), inositol 1,4,5-trisphosphate (IP3), diacylglycerol (DAG) as well as Ca^{2+} (Burnstock, 2007). P2Y receptors are subdivided into two classes based on their pharmacology, signal transduction and structural similarity (Abbracchio et al., 2006; von Kügelgen, 2006; von Kügelgen and Harden, 2011). $P2Y_1$, $P2Y_2$, $P2Y_4$, $P2Y_6$ and $P2Y_{11}$ receptors form the first subclass. They couple via G_q-proteins and stimulate phospholipase C

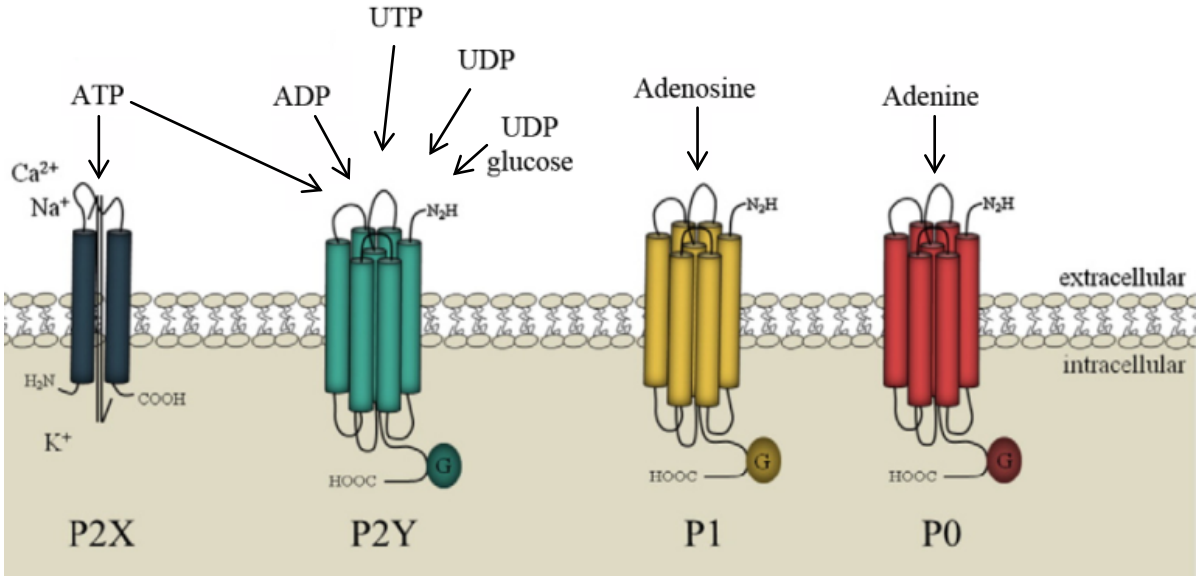

P2Y receptor subtype	$P2Y_1$	$P2Y_2$	$P2Y_4$	$P2Y_6$	$P2Y_{11}$	$P2Y_{12}$	$P2Y_{13}$	$P2Y_{14}$
Native agonist	ADP ATP (in rodents)	UTP ATP	UTP	UDP	ATP	ADP	ADP	UDP UDP glucose
EC_{50} (µM)	8.1	0.085 0.06	0.09	0.53	17.3	0.06	0.011	0.16 0.4
Subclass and G protein	Class I G_q	Class I G_q	Class I G_q	Class I G_q	Class I G_q, G_s	Class II G_i	Class II G_i	Class II G_i

Figure 9: Purinergic receptor families and native P2Y receptor agonists. Purinergic receptors are divided into subtypes of receptors including P2 receptors, P1 receptors and the recently identified P0 receptors. P2 receptors can be further subdivided into ionotropic P2X receptors activated by ATP and metabotropic G-protein-coupled P2Y receptors sensitive for ATP, ADP, UTP, UDP or UDP-sugar. Subclasses of P2Y receptors couple to different G-proteins. Metabotropic P1 receptors are preferentially activated by adenosine whereas P0 receptors were shown to be adenine sensitive. Modified from Kaebisch et al. (2015) and Zimmermann (2016)

followed by increases in inositol phosphates and Ca^{2+} mobilization from intracellular stores (von Kügelgen and Hoffmann, 2016). The second subclass consists of $P2Y_{12}$, $P2Y_{13}$, and $P2Y_{14}$ receptors that couple to G_i proteins, therefore inhibiting adenylate cyclase activity which in turn leads to reduced formation of intracellular cyclic AMP (Abbracchio et al., 2006).

A substantial role for ATP in the central nervous system has been reported in the context of regulation of neurogenesis, growth and differentiation of neural cells and mediation of neuron-glia communication (del Puerto et al., 2013). In neurons, ATP can be released from secretory vesicles by the presynaptic terminal, either alone or as co-transmitter, and from the postsynaptic membrane (del Puerto et al., 2013) (Figure 10). Upon release, ATP can activate

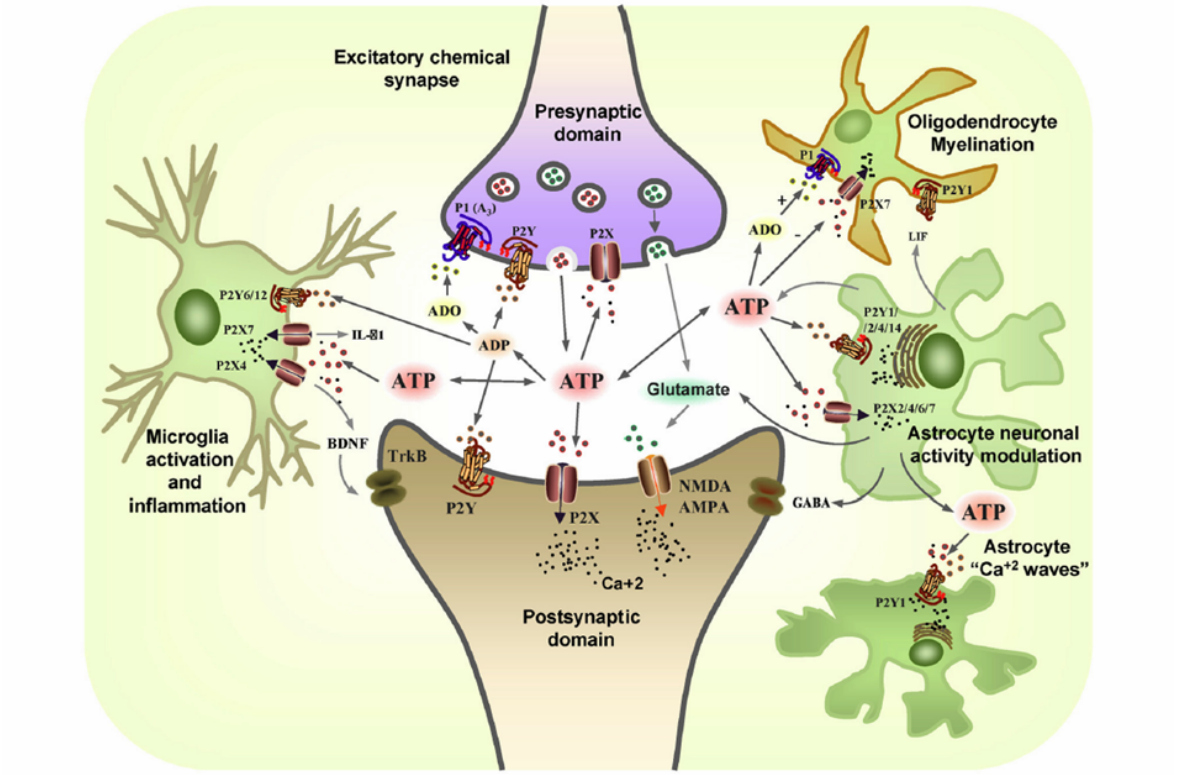

Figure 10: Coordinated action of nucleotide signaling in the central nervous system. ATP is released from presynaptic terminals via exocytosis either alone or as co-transmitter (here shown together with glutamate). Cell-surface located enzymes hydrolyze extracellular ATP to ADP and AMP and finally to adenosine (ADO). ATP and ADP activate P2X and P2Y receptors at the postsynaptic domain. Additionally glutamate acts on α-amino-3-hydroxy-5-methyl-4-isoxazole propionic acid (AMPA) receptors receptors and/or *N*-methyl-d-aspartate (NMDA) receptors. Activation of P2X, P2Y, and P1 (A_3 subtype) receptors, respectively at the presynaptic domain by ATP, ADP and ADO modulates neurotransmitter release. Resting microglia express $P2X_4$ and $P2X_7$ receptors that are involved in neuropathic pain. Upon ATP-binding IL-1β or brain-derived neurotrophic factor (BDNF) are released. BDNF then acts on TrkB receptors on neurons. Migration of resting microglia is mediated by $P2X_7$ and $P2Y_1$ receptor activation. Activation of $P2Y_6$ on activated microglia mediates phagocytosis. Astrocytic ATP release modulates neuronal activity (when co-released with GABA and glutamate) and promotes propagation of astrocytic Ca^{2+} waves through activation of $P2Y_1$ receptors and subsequent release of Ca^{2+} from internal stores. ATP binding to astrocytic purinergic receptors promotes release of leukemia inhibiting factor (LIF) that in turn promotes myelination by oligodendrocytes. Oligodendrocytes express $P2X_7$ receptors that mediate apoptosis. Activation of P1 receptors through ADO exerts opposing effects. From del Puerto et al. (2013)

P2X receptors and P2Y receptors at the postsynaptic terminal, triggering intracellular signaling cascades. Moreover, ATP might act at the presynaptic terminal via P2X or P2Y receptors enhancing the release probability of distinct neurotransmitters by increasing sodium, potassium and calcium permeability which promotes rapid changes in membrane potential (del Puerto et al., 2013; Zimmermann, 2016). ATP is released from astrocytes by connexin 43 and 30 hemichannels, pannexin 1 hemichannels, $P2X_7$ receptors or regulated lysosomal exocytosis (Zimmermann, 2016). Binding of ATP to purinergic receptors expressed on astrocytes induces release of glutamate and GABA which modulates neuronal activity (del Puerto et al.,

2013). Moreover, ATP mediates its own release and propagates astrocytic Ca^{2+} waves through activation of $P2Y_1$ receptors and Ca^{2+} release from internal stores (Zimmermann, 2016). Apart from astrocytes other glial cell types in the central nervous system such as oligodendrocytes and microglia express functional purinergic receptors (Abbracchio et al., 2009) involving purinergic signaling mechanisms in several other physiological and pathological processes such as myelination, mediation of phagocytosis and apoptosis, neuroinflammation and neuropathic pain (Burnstock, 2008). The complexity of purinergic signaling is further increased by the expression of various cell-surface located nucleotide-hydrolyzing enzymes that break down nucleoside triphosphates, diphosphates and monophosphates to the respective nucleoside (Zimmermann et al., 2012; Abbracchio et al., 2009). Eliminating ligands for one receptor subtype and, at the same time, generating ligands for another receptor, finally terminates or modulates nucleotide signaling.

1.3.1 Purinergic receptors – Focus on the $P2Y_{13}$ receptor

The $P2Y_{13}$ receptor is one of the most recently identified P2Y receptors (Zhang et al., 2002). It is mainly activated by ADP (Communi et al., 2001; von Kügelgen and Harden, 2011), with ATP and 2-methylthio-ATP acting only as a weak partial agonist (Marteau et al., 2003). As described before, the $P2Y_{13}$ receptor belongs to the second subclass of P2Y receptors, coupling to G_i proteins and inhibiting adenylyl cyclase and cyclic AMP formation (von Kügelgen and Hoffmann, 2016). Receptor antagonists have been described for the human $P2Y_{13}$ receptor, including suramin, reactive blue- 2, PPADS, MRS2211 and cangrelor (Marteau et al., 2003). Effective blocking of receptor activity with cangrelor was also reported for the rat $P2Y_{13}$ receptor (Fumagalli et al., 2004). Apart from its expression in spleen, bone marrow, peripheral leukocytes, liver, pancreas, and heart, high expression levels of the $P2Y_{13}$ receptor have been allocated to the brain (Communi et al., 2001). In the brain $P2Y_{13}$ is expressed by neurons and astroglial cell populations including microglia (von Kügelgen, 2006). Of note in situ hybridization (ISH) data from Allen Brain Atlas allocates high expression levels of *P2ry13* mRNA to regions involved in adult neurogenesis. The $P2Y_{13}$ receptor has been functionally implicated in allergic conditions as it mediates ADP-dependent degranulation in rat mast cells (Gao et al., 2010). The terminal differentiation of bone marrow progenitors and bone mass is balanced by mechanisms involving $P2Y_{13}$ receptor activation (Blom et al., 2010; Orriss et al., 2011; Biver et al., 2013; Wang et al., 2014a). Inhibition of insulin-release in pancreatic beta cells was attributed to ADP acting via $P2Y_{13}$ receptors (Amisten et al., 2010). Moreover,

hepatic lipoprotein and reverse cholesterol transport are altered in *P2ry13* knockout mice (Blom et al., 2010; Fabre et al., 2010; Lichtenstein et al., 2015). Loss of *P2ry13* prevents myenteric neurons from apoptosis induced by high-fat-diet (Voss et al., 2014) and protects pancreatic beta cells from glucolipotoxicity (Tan et al., 2013). In contrast, in the central nervous system protective effects in astrocytes and neurons have been reported upon $P2Y_{13}$ receptor activation (Espada et al., 2010; Ortega et al., 2011; Morente et al., 2014; Perez-Sen et al., 2015). In vitro studies implicate that the $P2Y_{13}$ receptor suppresses neuronal differentiation and axon outgrowth (Yano et al., 2012; del Puerto et al., 2012). Moreover, direct involvement of the ADP-sensitive $P2Y_{13}$ receptor in the control of neuropathic pain has been reported (Tatsumi et al., 2015; Malin and Molliver, 2010).

1.3.2 Extracellular nucleotide hydrolysis – The family of ecto-nucleoside triphosphate diphosphohydrolases (E-NTPDases)

Extracellular nucleotides act as key molecules of cellular communication. Among these nucleotides ATP, ADP, UTP, UDP, UDP-glucose and other nucleotide sugars, and dinucleoside polyphosphates bind to different types of purinergic receptors that differ in terms of signal specificity and affinity (Burnstock, 2007). ATP is released from various cell types in the central nervous system via different mechanisms (Abbracchio et al., 2009). However, extracellular action of purinergic signaling molecules such as ADP or adenosine requires hydrolysis of ATP. The hydrolysis of extracellular nucleotides is performed by various cell surface-located enzymes, called ectonucleotidases (Zimmermann, 2006). Four major groups of ectonucleotidases have been described: the ecto-nucleoside triphosphate diphosphohydrolases (E-NTPDases), ecto-5'-nucleotidase (eN), ecto-nucleotide pyrophosphatase/phosphodiesterases (E-NPPs), and alkaline phosphatases (APs) (Zimmermann et al., 2012). Another ecto-enzyme, adenosine deaminase, deaminates extracellular adenosine to inosine and the interconversion or transphosphorylation of extracellular nucleotides is catalyzed by the ecto-enzymes ecto-nucleoside diphosphate kinase and ecto-adenylate kinase (Zimmermann et al., 2012). E-NPPs directly hydrolyze ATP to AMP that can further be degraded to adenosine by the ecto-5'-nucleotidase (Figure 11). Alkaline phosphatases hydrolyze nucleoside tri-, di-, and monophosphates about equally well, however the tissue non-specific alkaline phosphatase (TNAP) represents the only isoform that is expressed in the

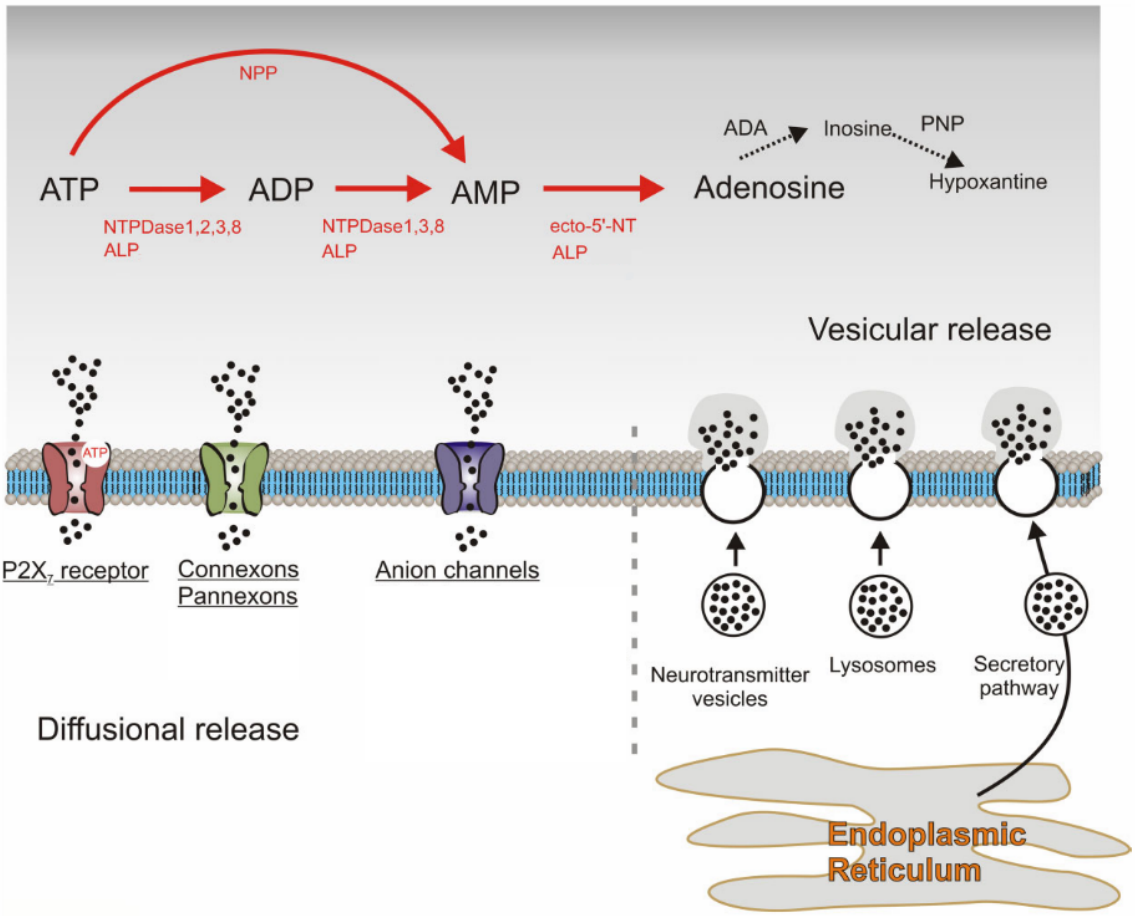

Figure 11: Release and hydrolysis of extracellular nucleotides. ATP is released from cells via diffusion or vesicular exocytosis. Upon release ATP can be degraded by several classes of cell surface-located nucleotide hydrolyzing enzymes, so called ecto-nucleotidases. Nucleoside triphosphate diphosphohydrolases (NTPDases) represent the major class of ecto-nucleotidases, and they hydrolyze ATP to ADP and AMP. Nucleotide pyrophosphatase/phosphodiesterases (NPPs) directly hydrolyze ATP to AMP. AMP is further degraded to adenosine by ecto-5'-nucleotidase (ecto-5'-NT) or alkaline phosphatases (ALP). Moreover, ALP hydrolyzes ATP, ADP and AMP about equally well. The conversion from adenosine to inosine is performed by adenosine deaminase (ADA) whereas purine nucleoside phosphorylase coverts inosine to hypoxantine. Modified from Verkhratsky and Burnstock (2014)

mammalian brain (Abbracchio et al., 2009). The group of ecto-nucleoside triphosphate diphosphohydrolases (E-NTPDases) hydrolyzes nucleoside triphosphates and diphosphates to nucleoside monophosphates and represents the major class of nucleotide-hydrolyzing enzymes involved in purinergic signaling (Zimmermann et al., 2012). The family of E-NTPDases consist of eight members (NTPDase1-8) of which four members, namely the NTPDase1, NTPDase2, NTPDase3 and NTPDase8, are located at the cell surface whereas the NTPDases4-7 are located intracellularly (Robson et al., 2006). E-NTPDases have their highest activity in the presence of millimolar concentrations of Ca^{2+} or Mg^{2+}at physiological extracellular pH of 7 to 8 (Zimmermann et al., 2012). In general, ATP is more rapidly hydrolyzed by extracellular E-NTPDases than ADP, but NTPDase2 shows a significantly higher

preference for ATP over ADP (Heine et al., 1999; Robson et al., 2006). NTPDase1 hydrolyzes ATP directly to AMP without releasing ADP from the catalytic active site (Heine et al., 1999; Kukulski et al., 2005). In contrast, hydrolysis of ATP by NTPDase2 produces accumulating amounts of ADP as an intermediate hydrolyzation product (Zimmermann, 2006). Whereas the NTPDase8 is expressed in the liver, kidney, and intestine, expression of the other extracellular E-NTPDases1-3 has also been allocated to the rodent brain (Kukulski et al., 2011). NTPDase 3 is expressed by subsets of neurons and NTPDase 1 was found to be predominantly expressed by microglia and vascular endothelial cells (Robson et al., 2006; Langer et al., 2008; Braun et al., 2000). In the rodent brain NTPDase2 is highly expressed by adult neural stem cells in neurogenic niches (Braun et al., 2003; Shukla et al., 2005), where it represents the major nucleotide hydrolyzing enzyme (Gampe et al., 2015).

1.3.3 Extracellular nucleotides modulate adult neurogenesis

Accumulating evidence suggest a major contribution of purinergic signaling mechanisms in the control of adult neurogenesis. Cultured neural stem cells derived from the subventricular zone (SVZ) express a variety of functional purinergic receptors, including $P2X_4$ and $P2X_7$ receptors, all P2Y receptor subtypes except $P2Y_4$ and $P2Y_{11}$ as well as all adenosine P1 receptors, apart from the subtype A_3 (Stafford et al., 2007; Grimm et al., 2009; Messemer et al., 2013; Migita et al., 2008; Lin et al., 2007). It is well established that purinergic signaling mechanisms, particularly ATP-signaling through the $P2Y_1$ receptor, take over major regulatory functions in the control of embryonic neurogenesis (Zimmermann, 2006). ATP-dependent activation of $P2Y_1$ receptors evokes Ca^{2+} release from internal stores that promotes rapid release of neurotransmitters, growth factors and ATP which in turn acts on $P2Y_1$ receptors in neighboring cells, promoting proliferation and migration of neural progenitors in cortical development (Scemes et al., 2003; Weissman et al., 2004; Liu et al., 2010; Striedinger et al., 2007). Moreover, survival and neuronal differentiation of mouse embryonic stem cells involve $P2X_7$ receptor signaling (Thompson et al., 2012; Tsao et al., 2013).

In 2003, Braun et al. had demonstrated that the ecto-nucleotidase NTPDase2 is highly expressed on stem and progenitor cells in the SVZ and the rostral migratory stream (RMS) in situ whereas it is absent from mature cell types along the transition cascade. These findings provided the first line of evidence for the contribution of purinergic signaling mechanisms not only during CNS development, but also in the maintenance of neurogenesis in the adult

rodent brain. NTPDase2 was further revealed to be expressed in progenitors in the adult hippocampal neurogenic niche (Shukla et al., 2005). In vitro studies showed that neurospheres derived from the adult SVZ express functional P2Y receptors, that, upon activation, produce transient increases in intracellular Ca^{2+}, and increase cell proliferation and migration (Mishra et al., 2006; Grimm et al., 2010). Moreover, both purinergic receptor activation and growth factor receptor activation led to the phosphorylation of the MAP kinase ERK1/2 and the transcription factor CREB, indicating coordinate action of purinergic and growth factor signaling in neurogenesis at least in vitro (Grimm et al., 2009). Notably, higher concentrations of growth factors seem to revert pro-mitotic functions of the $P2Y_1$ receptor (Stafford et al., 2007).

It has to be said that when this work was started hardly anything was known regarding the contribution of individual nucleotide receptors to adult neurogenesis. ATP was recently found to be released from B1 cells in acute brain slices (Lacar et al., 2012) and from hippocampal astrocytes in vivo (Cao et al., 2013). Studies on organotypic slice cultures of the SVZ revealed, that the expression of connexin45 hemichannels and ATP-signaling via P2X channels are required for precursor cell proliferation (Khodosevich et al., 2012). Functional $P2X_7$ receptors are located in cultured adult nestin-EGFP-expressing stem and progenitor cell populations of the mouse SVZ (Messemer et al., 2013). High levels of extracellular ATP and prolonged $P2X_7$ receptor activation lead to precursor cell death in vitro (Delarasse et al., 2009). In line with these findings, a slight increase in BrdU incorporation in the hippocampal granule cell layer was observed upon deletion of $P2X_7$ (Csölle et al., 2013). In vivo studies on the adult SVZ provide evidence, that ATP-mediated activation of $P2Y_1$ promotes proliferation of progenitors that could be reversed by application of the selective antagonist MRS2179 (Suyama et al., 2012). Application of the stable $P2Y_1$ receptor agonist ADPβS promotes proliferation and differentiation of SVZ progenitor cells in the subventricular zone. Moreover, administration of ADPβS into the lateral ventricle provokes reactive gliosis and subsequently increases stem cell proliferation and expansion of transit amplifying progenitors and neuroblasts (Boccazzi et al., 2014). In the adult dentate gyrus ATP is released from hippo-campal astrocytes and ATP was shown to promote progenitor cell proliferation at least in vitro (Cao et al., 2013). More recently the NTPDase2 was shown to be the major ecto-nucleotidase within neurogenic niches of the adult mouse brain. Deletion of the enzyme strongly increased progenitor cell proliferation in situ, however, long-term progenitor cell survival or neuron formation were unaffected (Gampe et al., 2015). Cultured neural stem and progenitor cells are capable of self-

renewal and have pluripotent capacity (Reynolds and Weiss, 1992). Non-adherent conditions allow to culture neural stem and progenitor cells as free-floating, self-renewing cell aggregates or spheres that can be differentiated into neurons, astrocytes and oligodendrocytes (Reynolds and Rietze, 2005). Thanks to the advantage that cultured neural stem and progenitor cells can be easily accessed and/or pharmacologically manipulated, the sphere-formation assay has been used in a variety of studies investigating adult neurogenesis. Likewise most of the work mentioned above, investigating the role of purinergic mechanisms in the control of neurogenesis referes to data obtained from in vitro cultured progenitor cells. In vitro systems resemble to some extent in situ conditions and can provide important indications on the functional role of purinergic signaling in adult neuro-genesis. However unconfined transferability of in vitro data is restricted. Limitations of the neurosphere culture system, concerning changes in gene expression profile of progenitor cells and sensitivity to methodological variations have been reviewed in detail (Reynolds and Rietze, 2005; Jensen and Parmar, 2006; Pastrana et al., 2011). This is pointing at the importance to assess in vitro data also in vivo.

1.3.4 Aims of this study

As mentioned above, in vivo analyses are essential for the reliable assessment of purinergic mechanisms in the control of adult neurogenesis. To date the in vivo analysis of purinergic signaling in adult neurogenesis mainly focused on the subventricular niche (Suyama et al., 2012; Boccazzi et al., 2014). The ectonucleotidase NTPDase2 is highly expressed on neural stem and progenitor cells within the neurogenic niches (Braun et al., 2003; Shukla et al., 2005). We recently showed in an *Entpd2* null mouse model (Vandenbeuch et al., 2013) that nucleotide-mediated progenitor cell proliferation was increased in the subventricular niche and in the hippocampal neurogenic niche. Yet in either niche progenitor cell survival and neuron formation were unaffected (Gampe et al., 2015). In order to exclude compensatory mechanisms of other ectonucleotidases expressed in the adult mouse brain, levels of protein expression and functionality of these enzymes between NTPDase2 wild type and knockout animals were compared in the first part of this thesis. The question, at what stages of the transition cascade progenitor cells specifically in the hippocampal neurogenic niche die off, was addressed making use of an immunohistochemical staging approach. Moreover, unraveling the potential mechanisms underlying increased progenitor cell death in knockout animals was pursued.

Astrocytes in the adult hippocampal neurogenic niche release ATP (Cao et al., 2013). NTPDase2 hydrolyzes nucleoside triphosphates to nucleoside diphosphates and, to a lower extent, to nucleoside monophosphates, thus modulating ligand availability at purinergic receptors. Loss of *Entpd2* should increase extracellular ATP concentrations in neurogenic niches while, at the same time, extracellular ADP concentrations are decreased. According to the Allen Brain Atlas high levels of mRNA of the ADP-sensitive $P2Y_{13}$ receptor can be allocated to regions involved in adult neurogenesis, particularly to the hippocampal neurogenic niche. If progenitor cell proliferation in the adult hippocampal dentate gyrus is controlled by balancing the activation of pro-mitotic and anti-mitotic purinergic receptors, loss of function of these proteins should affect the activity of neural stem and progenitor cells in vivo. Thus, in the second part of the thesis a *P2ry13* null mouse model (Fabre et al., 2010) was used to gain in situ information on the functional role of this receptor subtype on progenitor cell proliferation, neuron formation and neuronal activity in the adult hippocampus under basal conditions.

The third part of this thesis aims at evaluating the contribution of purinergic signaling to hypothalamic neurogenesis. The third ventricle in the hypothalamus was recently discovered as a novel neurogenic niche and adult hypothalamic neurogenesis has been implicated in the control of energy metabolism (Sousa-Ferreira et al., 2014). Functional nucleotide receptors are expressed in food intake regulating nuclei of the adult hypothalamus (Bjelobaba et al., 2015). Moreover, purinergic signaling mechanisms have been shown to be implicated in sensing metabolic cues from the periphery as well as in the control of food intake (Bolborea and Dale, 2013; Kittner et al., 2006). A pilot study in *P2ry13* null mice persecuted the objective to unravel the impact of the $P2Y_{13}$ receptor on adult hypothalamic neurogenesis. It has previously been reported that $P2Y_1$ and $P2Y_{13}$ receptors act in an antagonistic manner in several cellular contexts including axonal outgrowth, insulin-release and neuropathic pain (del Puerto et al., 2012; Amisten et al., 2010; Malin and Molliver, 2010). Both receptor subtypes are expressed by NSCs cultured from the subventricular zone (Grimm et al., 2009). Part of this work therefore aimed at providing insight into the potential antagonistic action of $P2Y_1$ and $P2Y_{13}$ nucleotide receptors in the control of adult neurogenesis.

2 Results

2.1 Analysis of purinergic signaling in adult hippocampal neurogenesis

In the adult rodent brain nerve cells are continuously generated from stem/progenitor cells in the subventricular zone (SVZ) lining the lateral ventricles and the hippocampal dentate gyrus (reviewed by Gage, 2000). However, the underlying cellular and molecular mechanisms are still poorly understood. A multitude of factors like hormones (Gould et al., 1992; Chow et al., 2013) neurotrophic factors (Shimazu et al., 2006; Bath et al., 2008), growth factors (Craig et al., 1996; Zhao et al., 2007), or transcription factors (Ferri et al., 2004; Mu et al., 2012) are implicated in the control of adult neurogenesis. Increasing evidence suggests that extracellular purine and pyrimidine nucleotides are involved in the control of embryonic (Weissman et al., 2004; Scemes et al., 2003; Thompson et al., 2012) and adult neurogenesis (Neary and Zimmermann, 2009). Several studies revealed that functional purinergic receptors are expressed on cultured neural stem cells (Stafford et al., 2007; Grimm et al., 2009; Messemer et al., 2013; Lin et al., 2007). Moreover, release of ATP was reported from cultured SVZ-derived neural progenitors (Stafford et al., 2007; Striedinger et al., 2007; Lin et al., 2007), from B1 cells in acute brain slices (Lacar et al., 2012) and from hippocampal astrocytes (Cao et al., 2013). Extracellular nucleotides were shown to stimulate proliferation and/or migration of neural progenitor cells in vitro (Scemes et al., 2003; Mishra et al., 2006; Striedinger et al., 2007; Grimm et al., 2010; Cao et al., 2013; Lin et al., 2007) and in vivo (Suyama et al., 2012; Boccazzi et al., 2014).

2.1.1 The functional role of NTPDase2 in adult hippocampal neurogenesis

Previous reports have shown that the ectonucleotidase NTPDase2 is highly expressed by adult neural progenitor cells of the SVZ/RMS and SGL (Braun et al., 2003; Shukla et al., 2005; Langer et al., 2008). Furthermore, deletion of the enzyme increased progenitor cell proliferation without affecting long-term progeny survival or neuron formation (Gampe et al., 2015). NTPDase2 catalyzes the dephosphorylation of nucleoside triphosphates and, to a lower extent, diphosphates (Zimmermann et al., 2012). Deletion of this enzyme presumably

increases local extracellular nucleoside triphosphates concentrations and might indicate roles of purinergic signaling in adult neurogenesis.

2.1.1.1 The ectonucleotidase NTPDase2 is expressed in neurogenic niches of the adult mouse brain

Heterozygous *Entpd2*+/- mice were inbred to generate wild type and knockout animals in a litter. Genotyping PCR allowed for solid discrimination of wild type from knockout alleles (Figure 12). In the upper panel, amplified fragments could be detected at 309 bp and 263 bp with lysates from animal #1699, indicating that this mouse represents an *Entpd2*+/- mouse. For animal #1701 a product could be detected at 309 bp, whereas no product could be detected at 263 bp. In consequence this mouse corresponds to an *Entpd2*-/- mouse. In contrast, no product could be detected at 309 bp for animal #1704, whereas an amplified fragment was detectable at 263 bp. Hence, this animal carried the wild type allele homozygously. Furthermore, PCR allowed to detect animals carrying EGFP under control of the nestin promoter (Mignone et al., 2004). As depicted in the lower panel of Figure 12, amplified fragments could be detected at 510 bp, with lysates from both animals #1701 and #1704, showing that both animals correspond to nestin-EGFP expressing mice.

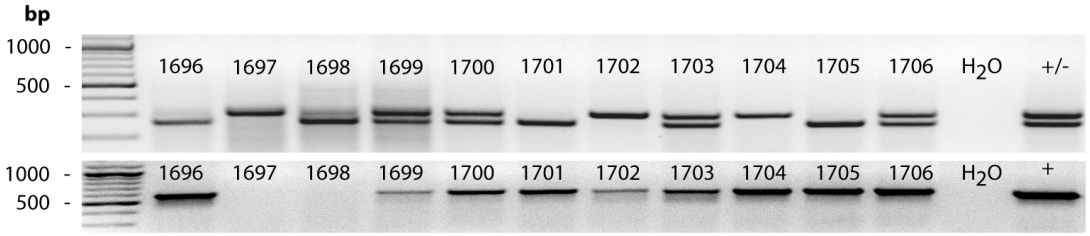

Figure 12: Identification of NTPDase KO mice. *Entpd2*+/- mice were inbred and offspring was genotyped via PCR. Primer pairs amplifying fragments of the mutated allele (263 bp) and the wild type allele (309 bp) allowed discrimination of WT and KO mice (upper panel). In the lower panel amplified fragments could be detected at 510 bp, representing nestin-EGFP+ animals.

In a first series of experiments, expression of NTPDase2 was analyzed in sagittal cryosections from adult 8-12 week old NTPDase2 wild type and knockout mice expressing nestin-EGFP (Figure 13). Nestin is transiently expressed in primary stem cells as well as early progenitor cells (Mignone et al., 2004). Immunohistochemical staining for NTPDase2 in WT animals colocalizes with the signal for nestin-EGFP in regions involved in adult neurogenesis, namely

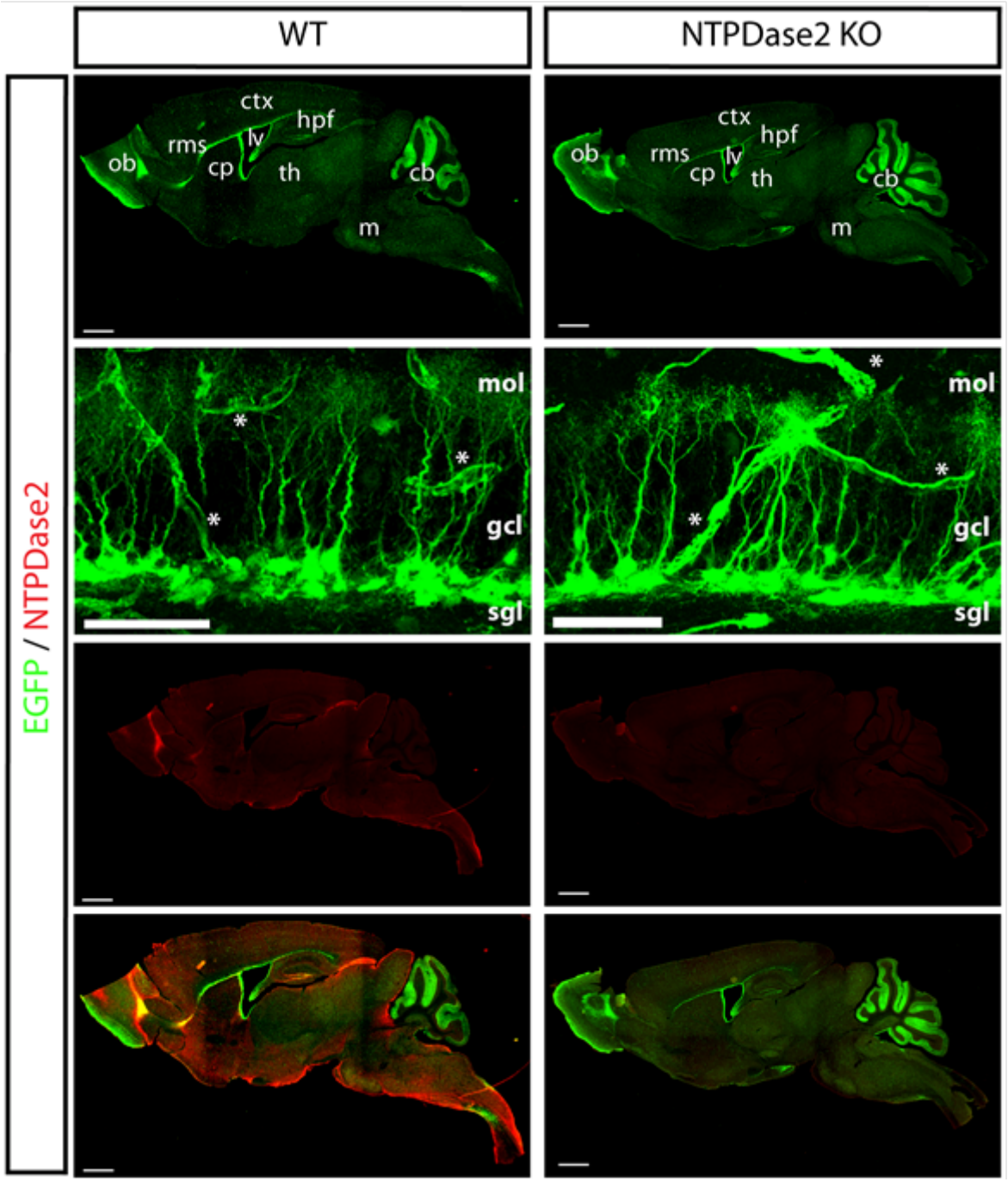

Figure 13: Expression of the ectonucleotidase NTPDase2 in neurogenic niches of the adult mouse brain. Sagittal sections of wild type and knockout mice expressing nestin-EGFP (green). Sections were immunohistochemically stained for NTPDase2 (red). Immunosignal for NTPDase2 colocalizes with fluorescence for EGFP in neurogenic niches (lower panel). Deletion of *Entpd2* leads to complete loss of staining for NTPDase2 (middle panel, right image). No obvious changes in overall brain structure (upper panel) or in the structure and distribution of nestin-EGFP positive cells in the hippocampal neurogenic niche (close-up) were detected in *Entpd2*-/- mice. Asterisks in close-up images indicate nestin-expressing ependymal cells. cb, cerebellum; cp, caudoputamen; ctx, cerebral cortex; gcl; granule cell layer; hpf, hippocampal formation; lv, lateral ventricle; m, medulla oblongata; mol, molecular layer; ob, olfactory bulb; rms, rostral migratory stream; sgl, subgranular layer; th, thalamus. Fluorescence images were taken with a Keyence BZ-9000 II microscope. Close-up images were taken with a Leica TCS SP5 II confocal laser scanning microscope. (Scale bars, 500 µm, overview; 50 µm, close-up)

in the subventricular zone (SVZ) lining the lateral ventricles, along the rostral migratory stream, in the olfactory bulb as well as in the hippocampal dentate gyrus (Figure 13, left). Deletion of *Entpd2* leads to complete loss of staining for NTPDase2 (Figure 13, right). However, no apparent changes in overall brain structure could be observed between WT and KO (Figure 13). Moreover, no gross changes were observed in the structure and distribution of nestin-EGFP positive cells in the hippocampal neurognic niche (Figure 13, close-up) indicating that deletion of *Entpd2* has no general effect on brain or stem cell morphology.

2.1.1.2 Loss of NTPDase2 is not compensated by other extracellular nucleotide hydrolyzing enzymes in the adult mouse brain

NTPDase2 is strongly expressed in regions involved in neurogenesis (Figure 13). Previous reports have shown that NTPDase2 is expressed by the neural progenitor cells of the hippocampus (Shukla et al., 2005) and the SVZ (Braun et al., 2003). NTPDase2 has a high preference for the hydrolysis of ATP over ADP and it does not hydrolyze AMP (Zimmermann et al., 2012). Enzyme histochemistry visualizes reaction products of ecto-nucleotidase and alkaline phosphatase activity in sections of mouse brain (Figure 14a). Genetic deletion of *Entpd2* results in a strong overall reduction of ecto-ATPase catalytic activity (Figure 14a, upper panel) with significant reaction product remaining in the caudoputamen and the substantia nigra. Enzyme histochemical staining with ATP as the substrate further depicts catalytic ecto-ATPase activity on the cell population with the characteristic morphology of primary neural stem and progenitor cells in the hippocamus and the SVZ (Figure 14a, insert). This is completely lost in the KO in both neurogenic niches with strong biochemical ectonucleotidase activity remaining in the blood vessels. These findings suggest that NTPDase2 is a major enzyme involved in the hydrolysis of extracellular ATP in the mouse brain, particularly in neurogenic niches. Catalytic ADPase activity shows only weak enzyme staining in the WT and no further substantial reduction in KO animals (Figure 14a). Residual enzyme staining on blood vessels can be attributed to the expression of NTPDase1 that hydrolyzes ATP and ADP about equally well (Braun et al., 2000). Ecto-5'-nucleotidase hydrolyzes AMP and is highly expressed in the caudoputamen (Langer et al., 2008). Catalytic AMPase activity denotes this distribution and staining remains unaltered in brain sections from *Entpd2* knockout mice (Figure 14a). Alkaline phosphatase (AP) activity is detected throughout the brain (Figure 14a), and can be attributed to expression of tissue nonspecific alkaline phosphatase (TNAP), the isoform of alkaline phosphatases found in mouse brain,

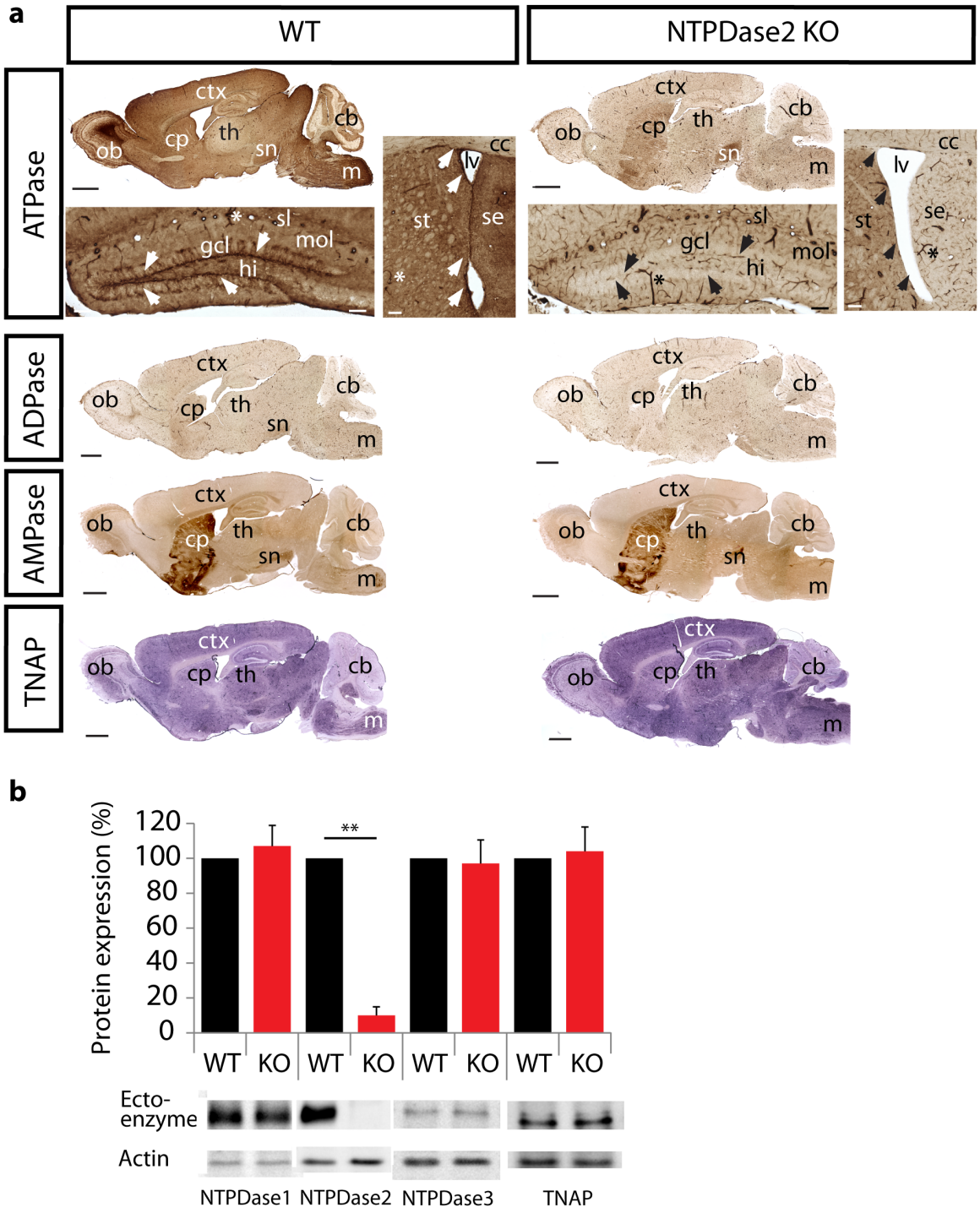

Figure 14: Distribution of ectonucleotidase/alkaline phosphatase activity in WT and KO mice. **a:** Enzyme histochemical reaction product in sagittal sections using ATP, ADP and AMP as a substrate for visualizing ectonucleotidase activity and NBT/BCIP as a substrate for alkaline phosphatase (TNAP) activity. Arrows in close-up of dentate gyrus (top left) depict position of type-1 cells with their typical ramifications being intensely stained for ATPase activity in WT sections of the dentate gyrus. This staining was not detectable in KO sections. Arrows in close-up of the lateral ventricle (top right) depict enhanced ATPase activity in the SVZ and its dorsal extension that was completely lost in KO mice. Asterisks indicate NTPDase1-expressing blood vessels. **b:** Immunoblotting revealed lack of up-regulation of other ectonucleotidases in *Entpd2* KO mice. Bar graph (means ± SEM) represents quantitative analysis of immunoblots for NTPDase1, NTPDase2, NTPDase3 and TNAP in WT and KO mice. Actin served as a loading control. Molecular masses correspond to 72 kDa for NTPDase1,

70 kDa for NTPDase2, 75 kDa for NTPDase3, and 75 kDa for TNAP. n=10 mice for each condition. **p<0.01, significant relative to control. cb, cerebellum; cc, corpus callosum; cp, caudoputamen; ctx, cerebral cortex; gcl, granule cell layer; hi, hilus; m, medulla oblongata; lv, lateral ventricle; mol, molecular layer; ob, olfactory bulb; sl, stratum lacunosum; sn substantia nigra; st, striatum, se, septum, th, thalamus. Bright field images were taken with a Keyence BZ-9000 II microscope. (Scale bars, 500 µm, overview; 100 µm, close-up)

hydrolyzing ATP to adenosine (Brun-Heath et al., 2011). However, deletion of NTPDase2 does not result in altered staining intensity for alkaline phosphatase activity. To further exclude compensatory upregulation of other ectonucleotidases or alkaline phosphatases upon deletion of *Entpd2*, quantitative Western Blots of membrane fractions derived from total mouse brain were performed (Figure 14b). Whereas the immunosignals for NTPDase1, NTPDase3 and TNAP are unchanged in mutant mice, the immunosignal for NTPDase2 is abolished. In summary these data demonstrate that deletion of NTPDase2 does not affect levels of activity and protein of other extracellular nucleotide hydrolyzing enzymes in the adult mouse brain.

2.1.1.3 Precursor cells are expanded in the subgranular zone of NTPDase2 KO mice

Deletion of *Entpd2* in adult mice is perturbing purinergic signaling, boosting progenitor cell proliferation without affecting long-term cell survival and neuron formation in both the SVZ and the dentate gyrus (Gampe et al., 2015). In order to analyze at which stage of stem cell development progenitor cells are eliminated, the abundance of individual progenitor cell types was compared between wild type and knockout mice. To ease identification of type-1 cells *Entpd2* WT and KO mice expressing nestin-EGFP were used. Mice were perfused and sagittal cryosections were immunohistochemically stained (Figure 15). The number of nestin-EGFP-positive cells with a radial process traversing the entire granule cell layer and representing adult neural stem cells was counted (Figure 15a). Cell numbers were increased in *Entpd2* KO mice by 29.3% compared to the WT (Figure 15c). To further verify the expansion of the progenitor cell pool, numbers of additional individual cell types along the transition cascade to mature neurons were counted in the same sections (Figure 15a, b). According to the nomenclature and protein expression profile of individual transition stages proclaimed by Kempermann et al. (2004) and Steiner et al. (2006) and along with morphological characteristics, individual cell types were assigned to four different stages. Type-1 cells represent the slowly proliferating primary neural stem cells and expressed nestin-EGFP, GFAP and the transcription factor Sox2 and displayed at least a short process (Figure 15a, white arrowheads). Type-2a cells

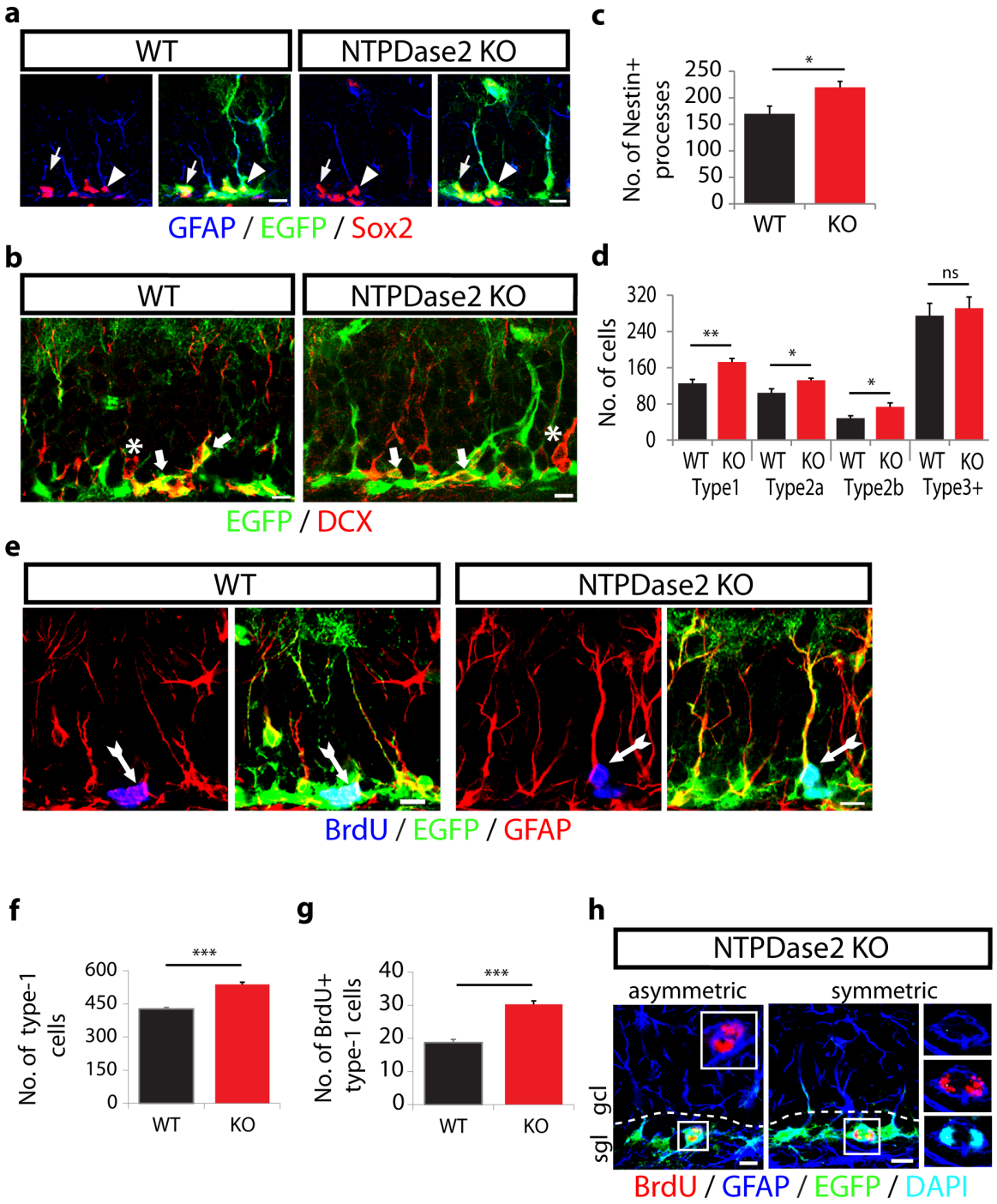

Figure 15: Expansion of precursor cells in the subgranular layer of WT and NTPDase2 KO mice. a, b: Analysis of fluorescence for nestin-EGFP (green), GFAP (blue) and Sox2 (red) (**a**), or nestin-EGFP (green) and DCX (red) (**b**) in precursor cells in the SGL. Cell types were differentiated as follows: type-1 (positive for nestin-EGFP, GFAP and Sox2 and showing at least a short process facing the granule cell layer; arrow heads in **a**), type-2a (positive for nestin-EGFP and Sox2; arrows in **a**), type-2b (positive for nestin-EGFP and DCX; thick arrows in **b**), type-3+ (immunopositive for DCX only; asterisks in **b**). **c:** Total number of nestin-positive processes (four sections per animal) in WT and KO animals (n=9). **d:** Corresponding abundance of individual cell types (total number of cells, four sections per animal) in WT and KO animals (n=9). **e:** 2 h after the final BrdU injection (3 pulses at 2 h interval) animals were perfused and proliferating type-1 cells (arrows) were identified by labeling for BrdU (blue), EGFP (green) and GFAP (red). Left images: double labeling for BrdU and GFAP; right images: triple labeling for BrdU, EGFP and GFAP. **f:** Total number of type-1 cells (10 sections per animal) in WT and KO mice (n=7). **g:** A disproportionally higher increase in the total number of

BrdU-labeled type-1 cells (10 sections per animal) in KO animals compared to WT control (n=7) was detected. **h:** Examples of asymmetric (left) and symmetric (right) division of BrdU-labelled (red) type-1 cells in the SGL of KO mice. Type-1 cells were identified by double labeling for GFAP (blue) and EGFP (green). The boxed regions are enlarged and include labeling for DAPI to better visualize the cleavage plane of the cell. Bar graphs represent means ± SEM. *p<0.05, **p<0.01; ***p<0.001, significant relative to control, ns, difference not significant. gcl, granule cell layer; sgl, subgranular layer. Confocal images were taken with a Leica TCS SP5 II microscope. (Scale bars, 10 μm)

expressed nestin-EGFP and Sox2 but no longer GFAP (Figure 15a, arrows). Type-2b cells expressed nestin-EGFP and the microtubule-associated protein DCX (Figure 15b, arrows) and type-3+ cells (represent neuroblasts and immature young neurons) were only immunopositive for DCX (Figure 15b, asterisks). Quantification of cell numbers revealed an increase in 33% in the number of type-1 cells in knockout mice compared to the wild type control (Figure 15d). Moreover, the number of type-2a and type-2b cells was also increased in knockout animals by 23% and 29%, respectively. In contrast, the number of type-3+ cells remained unchanged between WT and KO. To exclude, that findings in the slow-proliferating type-1 cell stage result from changes during embryonic or early postnatal development, levels of cell proliferation in EGFP/GFAP-positive cells (type-1 cells) in *Entpd2* KO mice were analyzed (Figure 15e). Mice received three consecutive intraperitoneal BrdU injections at 2 h interval. Two hours after the final pulse BrdU incorporation into type-1 cells was quantified (Figure 15g). In line with previous quantifications the total number of type-1 cells was increased in KO animals by 26% (Figure 15f). Noteworthy, the number of type-1 cells that had incorporated BrdU was disproportionally increased by 62% in knockout mice (Figure 15g). In WT animals 4.4% of all type-1 cells were found to be BrdU-positive, whereas in the KO 5.6% of all type-1 cells had incorporated BrdU. This corresponds to an increase of 27% in overall BrdU labeling of type-1 cells in knockout mice compared to the wild type control. This suggests that increased levels in the number of type-1 cells result from increased proliferation rates in this cell type in the KO rather than from changes during development. During development neurons of the CNS are generated by neural stem and progenitor cells by asymmetric and symmetric division (Götz and Huttner, 2005). In the conventional model of adult neurogenesis neuronal cells derive from polarized progenitor cells that undergo an asymmetric division (Encinas et al., 2011). However, expansion of the stem cell pool through symmetric self-renewal has recently been reported under certain conditions (Bonaguidi et al., 2011). This prompted the question whether expansion of the type-1 cell pool in NTPDase2 knockout animals might result from expansion through symmetric divisions. The type of division is closely linked to the orientation of the cleavage-plane (Götz and Huttner, 2005). Cleavage planes typical for symmetric (horizontal) or asymmetric (vertical) division modes

were detected in dividing type-1 cells in knockout animals (Figure 15h), indicating potential symmetric self-renewal and expansion of stem cells in *Entpd2* KO mice. In summary this data suggests, that NTPDase2 controls the expansion of the hippocampal stem and progenitor cell pool in the adult dentate gyrus. As deletion of NTPDase2 results in an increase of the progenitor cell pool, NTPDase2 activity would contribute to attenuating progenitor cell formation.

2.1.1.4 Apoptosis is increased in *Entpd2* KO mice

The hippocampal pool of progenitor cells is initially increased in the KO mice. However, cell expansion is lost at the level of maturing young neurons. Therefore increased levels of

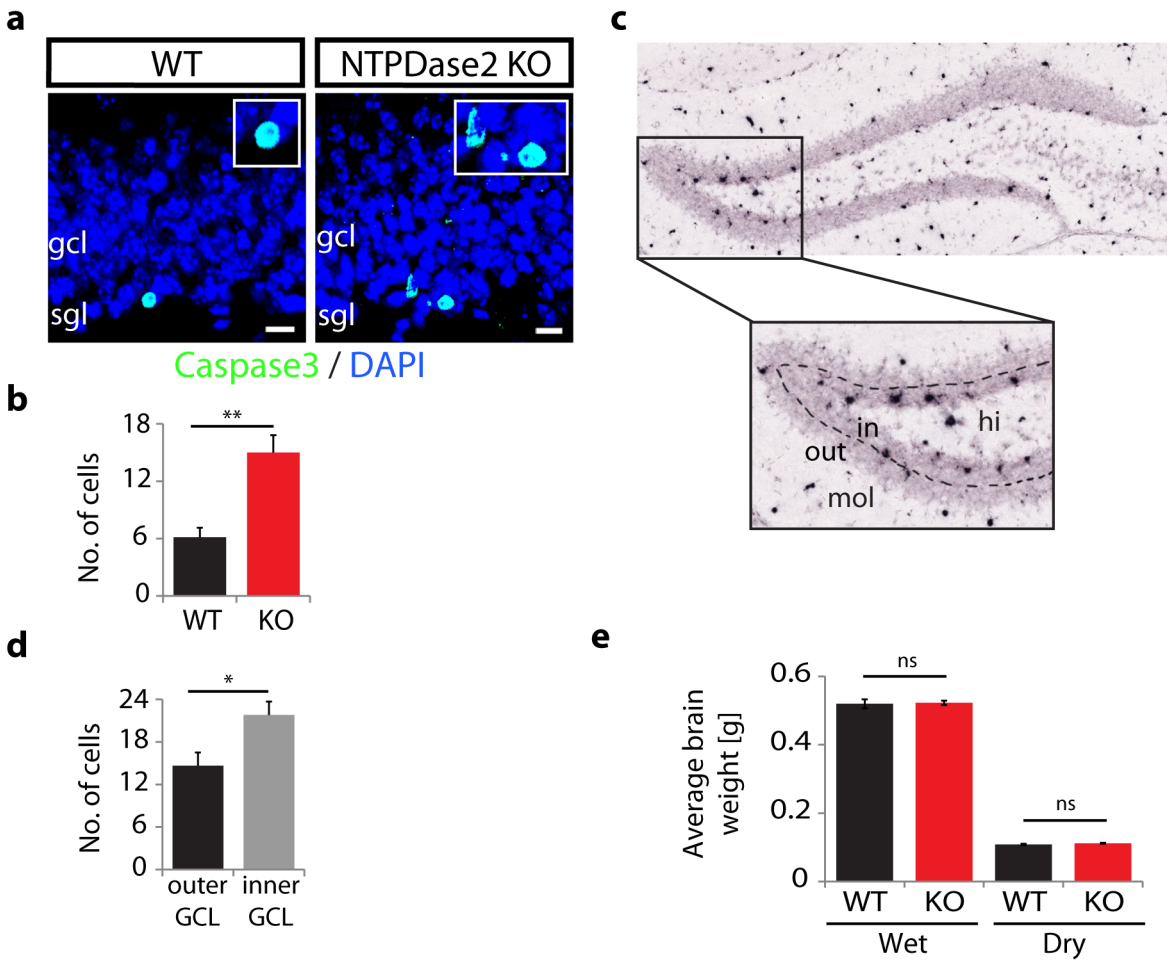

Figure 16: Increased levels of apoptosis in *Entpd2* knockout mice. a: Immunofluorescence for activated caspase-3 (green) and DAPI (blue). Boxed inserts in **a** represent enlarged images of caspase-3-positive cells. **b:** Corresponding quantification of caspase-3-positive cells (total number of cells, six sections per animal) in the SGL of WT (n=7) and KO (n=6) mice. **c:** Analysis of $P2Y_{12}$ receptor-expressing cells in adult WT animals (ISH, from Allen Brain Atlas). Boxed insert in **c** represents an

enlarged image of $P2Y_{12}$ receptor-expressing cells in the adult granule cell layer. The granule cell layer was manually divided in two identical parts, an inner part facing the hilar side of the GCL and an outer part, facing the molecular layer. **d:** Corresponding quantification of *P2ry12* expressing cells (total number of cells, six sections per animal) revealed an enrichment of microglia at the hilar side of the hippocampal granule cell layer. **e:** Analysis of wet brain weight or dry brain weight after 4 days of drying at 60 °C in WT and KO mice (n=7-10). Bar graphs represent means ± SEM. *$p<0.05$, **$p<0.01$, significant relative to control, ns, difference not significant. gcl, granule cell layer; hi, hilus; mol, molecular layer; sgl, subgranular layer. Confocal images were taken with a Leica TCS SP5 II microscope. (Scale bars, 10 μm)

apoptosis in the mutant mice were expected. Immunohistochemical staining for cleaved caspase-3 revealed indeed a 2.5-fold increase in the number of positive cells in KO mice (Figure 16b), however the absolute number of cells identified was rather low. Apoptotic cells were observed exclusively in the subgranular layer (Figure 16a). Microglial cells rapidly remove apoptotic cells in the adult hippocampal dentate gyrus (Sierra et al., 2010). Expression of the $P2Y_{12}$ nucleotide receptor can be used as a marker for resting microglia (Burnstock and Knight, 2004). To scrutinize the effect of apoptotic cell removal in the subgranular zone by microglia, chromogenic labeled cells for *P2ry12* mRNA were analyzed. In situ hybridization (ISH) data was obtained from Allen Brain Atlas and the number of labeled cells was counted in the inner half and outer half of the granule cell layer (Figure 16c). Expression of *P2ry12* mRNA was enriched at the hilar side of the granule cell layer, supporting a role of microglia in the removal of apoptotic progenitor cells (Figure 16d). In line with the lack of overall structural changes in brain morphology (comp. Fig. 13) average brain weight was unchanged between wild type and knockout animals (Figure 16e).

2.1.1.5 DCX-positive cells show decreased levels of CREB phosphorylation in NTPDase2 KO mice

Previous reports by Merz et al. (2011) have shown that the transcription factor pCREB is transiently expressed in DCX-expressing cells in the adult dentate gyrus and loss of CREB phosphorylation compromises the survival of newborn neurons (Jagasia et al., 2009). Therefore the extent of CREB-phosphorylation in DCX-expressing cells was compared between NTPDase2 wild type and knockout animals (Figure 17a). In line with previous findings the total number of DCX-immunopositive cells was unchanged between WT and KO mice (Figure 17b, left bars). However, the number of DCX-positive cells expressing pCREB was decreased by 30% in knockout animals (Figure 17b, right bars).

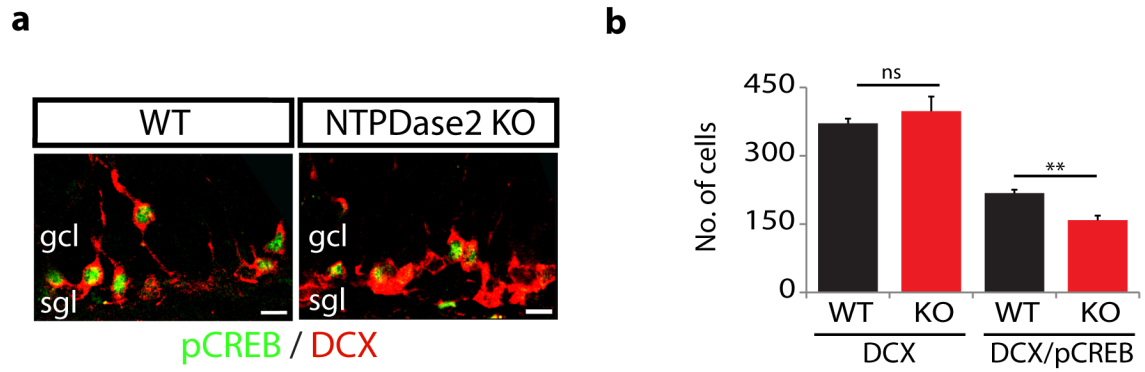

Figure 17: Decrease of immunofluorescence for pCREB in NTPDase2 KO animals. a: Immunofluorescence for pCREB (green) and DCX (red) in the SGL. b: Corresponding quantification of DCX-positive cells (left bars) and pCREB-labeled DCX-positive cells (right bars) in WT (n=7) and KO (n=5) animals (total number of cells, four sections per animal). Bar graphs represent means ± SEM. **p<0.01, significant relative to control, ns, difference not significant. gcl, granule cell layer, sgl, subgranular layer. Confocal images were taken with a Leica TCS SP5 II microscope. (Scale bars, 10 µm)

Taken together these data indicate that expansion of the stem cell pool as well as of the intermediate progenitor type-2 cells is increased in *Entpd2* KO mice. Cell expansion is subsequently lost at around type-3 stage and the progenitor cell pool is reduced to WT control levels by increased apoptosis. This is paralleled by loss of support by survival factors as indicated by decreases in CREB phosphorylation in the DCX-expressing progenitor cell population.

2.1.2 Functional characterization of $P2Y_{13}$ receptor knockout mice in adult neurogenesis

The data obtained with mice KO for the ATP/ADP-hydrolyzing NTPDase2 suggested that nucleotide receptors are involved in the control of adult neurogenesis. This raises the question which receptors could be involved and which could be the nucleotide agonists responsible. One of the most recently identified P2Y receptors is the $G_{i/o}$-coupled $P2Y_{13}$ receptor (Zhang et al., 2002). Expression in the brain was allocated to neuronal and astroglial cell populations. The $P2Y_{13}$ receptor is preferentially activated by ADP (Burnstock, 2007; von Kügelgen and Harden, 2011). Extracellular action of ADP requires extracellular hydrolysis of ATP, carried out by ectonucleotidases. NTPDase2 might function as a homeostatic regulator of neurogenesis by providing ligands for ATP-sensitive and ADP-sensitive P2 receptors, exhibiting opposing functions. In situ hybridization data from Allen Brain Atlas allocate high expression levels of *P2ry13* mRNA to regions involved in neurogenesis (Figure 18). This is particularly obvious in the enlarged view of the hippocampal dentate gyrus where a strong signal can be

detected in the subgranular layer (Figure 18, close-up). The $P2Y_{13}$ receptor would thus be a candidate nucleotide receptor relevant for the control of adult neurogenesis. In order to verify the hypothesis of a contribution of the $P2Y_{13}$ receptor and extracellular nucleotides to the control of adult hippocampal neurogenesis, mice null for *P2ry13* were analyzed.

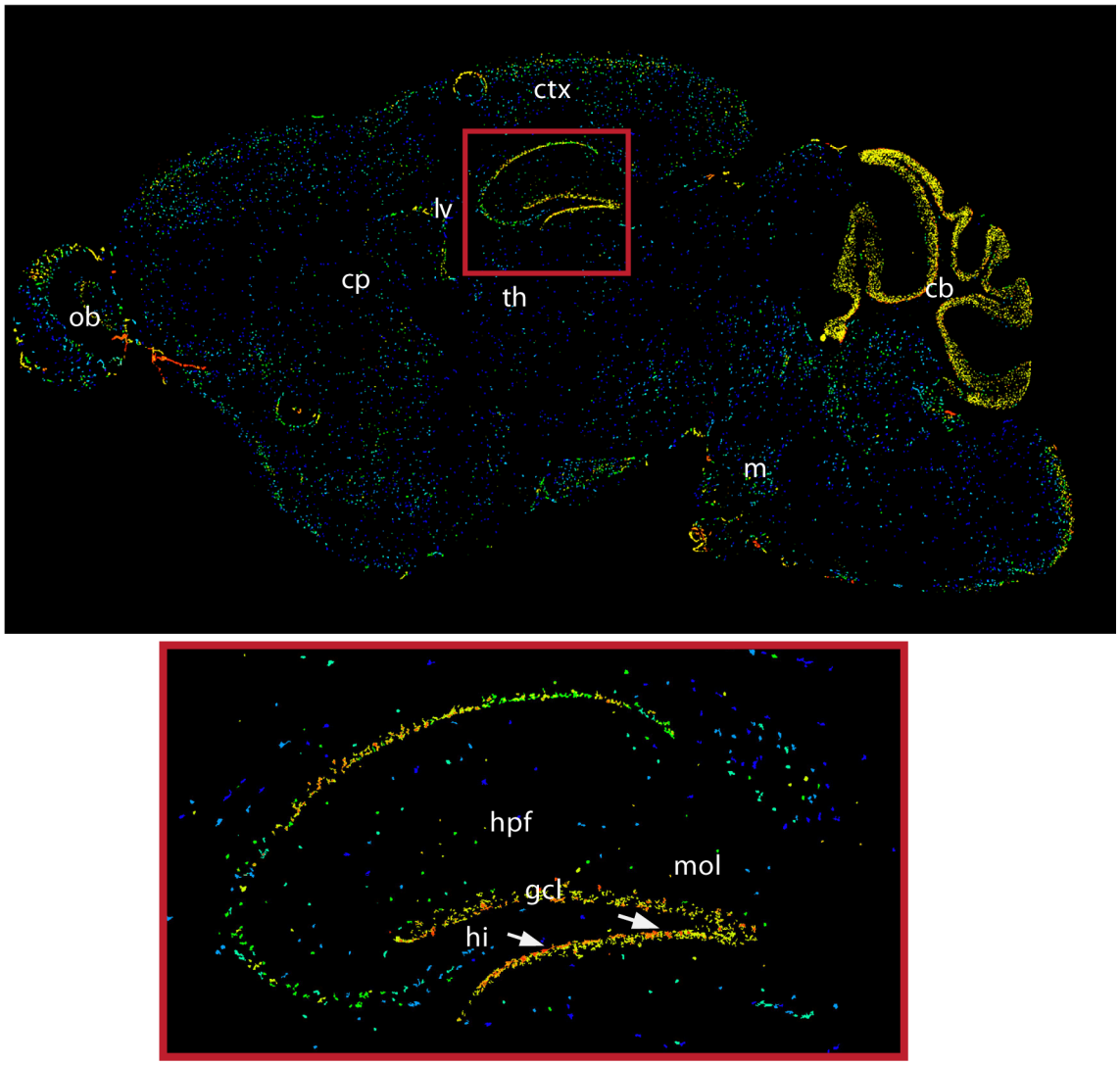

Figure 18: Expression of *P2ry13* mRNA in the hippocampal dentate gyrus. ISH data for *P2ry13* mRNA in adult WT animals (from Allen Brain Atlas). Boxed insert represents an enlarged image of the adult DG. High expression levels of *P2ry13* were allocated to the highly proliferative SGL (arrows). cb, cerebellum; cp, caudoputamen; ctx, cerebral cortex; gcl, granule cell layer; hi, hilus; hpf, hippocampal formation; m, medulla oblongata; lv, lateral ventricle; mol, molecular layer; ob, olfactory bulb; th, thalamus.

2.1.2.1 The granule cell layer is thicker in *P2ry13*-/- mice

To scrutinize potential effects of *P2ry13* deletion on general dentate gyrus morphology, the granule cell layer of wild type and *P2ry13* knockout mice was selected based on immunostaining for the neuronal marker NeuN (Figure 19a) and the area of the GCL was analyzed semiautomatically using the Contour Surface Tool in Bitplane Imaris (Figure 19b). Increased thickening of the average area of the GCL by 10% could be detected in *P2ry13* KO animals compared to WT controls (Figure 19c).

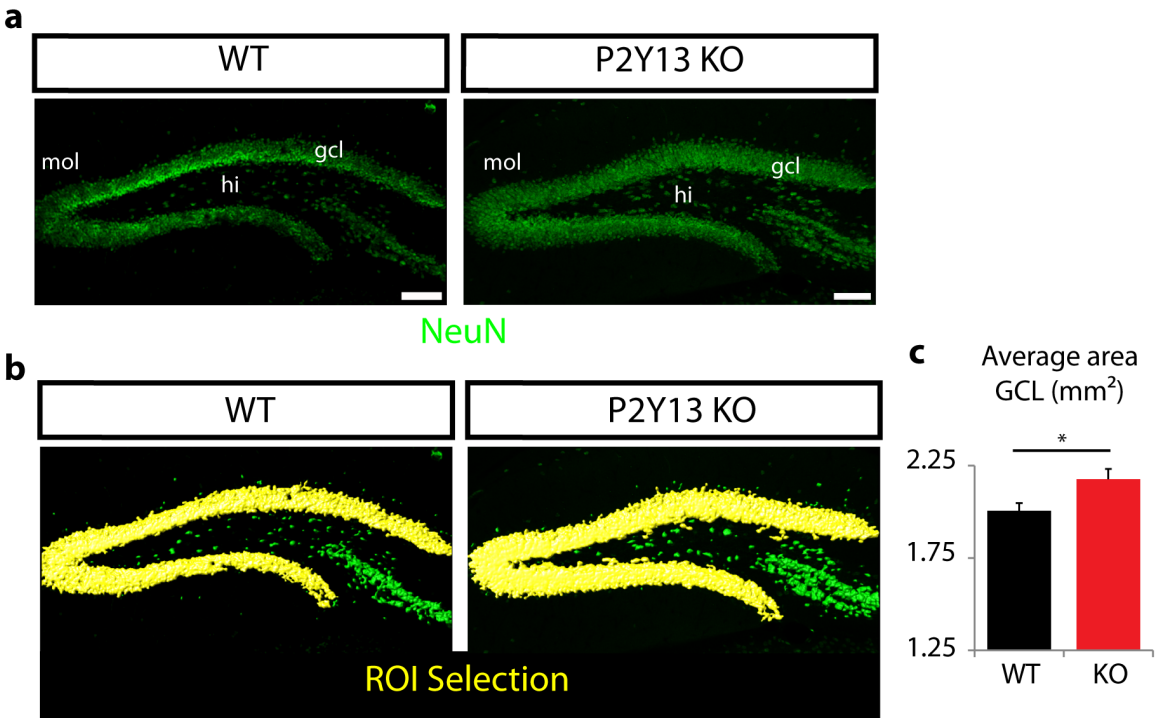

Figure 19: Increased thickening of the granule cell layer in *P2ry13* -/- mice. a: Immunofluorescence for NeuN (green) in the GCL of WT and KO mice. **b:** Semiautomatic selection of the region of interest (ROI) (yellow) with the Contour Surface Tool in Bitplane Imaris. **c:** Corresponding quantification of the average area of the GCL in WT (n=7) and KO (n=6) animals (average area in mm^2, six corresponding sections per animal) revealed an increased average area in KO animals. Bar graphs represent means ± SEM. *$p<0.05$, significant relative to control. gcl, granule cell layer; hi, hilus; mol, molecular layer. Confocal images were taken with a Leica TCS SP5 II microscope. (Scale bars, 100 µm)

2.1.2.2 Deletion of *P2ry13* increases proliferation and long-term survival of precursor cells

The granule cell layer was thickened in $P2Y_{13}$ receptor knockout animals. This was indicative of a constant increased supply of granule neurons to the GCL. To prove this hypothesis, the

effect of $P2Y_{13}$ purinergic receptor deletion on progenitor cell proliferation and long-term cell survival in the dentate gyrus was analyzed (Figure 20). WT and $P2Y_{13}$ receptor KO mice received either one single intraperitoneal BrdU injection and were perfused 2 h after the BrdU pulse or 3 injections at 2 h interval and were perfused 3 d or 28 d later, respectively (Figure 20a). Immunohistochemistry depicts the proliferative pool of progenitor cells in the granule cell layer that incorporated BrdU during the S-Phase of the cell cycle (Figure 20b). Quantitative evaluation of BrdU-positive cells 2 h after the final BrdU pulse revealed an increase in the knockout animals of 40% (Figure 20c). This suggests that activation of the $P2Y_{13}$ receptor dampens nucleotide-mediated cell proliferation in the hippocampal dentate gyrus. BrdU-positive cells were almost exclusively observed in the subgranular layer of the dentate gyrus. A few scattered cells were observed in the hilar region (Figure 20b, upper panel). However, quantification of these cells did not reveal significant differences between WT and KO animals (Figure 20h). Fast-proliferating progenitor cells migrate into their target region, the granule cell layer of the dentate gyrus, and either undergo death by apoptosis or differentiate into interneurons (Zhao et al., 2008). Two critical periods of survival have been reported during this neurogenic cascade, one main period during the first four days in the life of a transit amplifying progenitor cell at the transition to the neuroblast state (Sierra et al., 2010) and a second selection process 1-3 weeks after birth of a young immature neuron, dependent upon NMDA receptor ex-pression and glutamate synaptic input (Tashiro et al., 2006). Therefore, BrdU-labeling was quantified at two additional time points after BrdU injection. Quantification in mice perfused 3 d after the final BrdU pulse (Figure 20b, middle panel) revealed an increase of 30% in the number of BrdU-positive cells in KO animals (Figure 20d). The number of BrdU-labeled cells in the hilar region of WT and KO animals was unchanged at this time point (Figure 20h). 28 days after BrdU-labeling the initially labeled cells had migrated deeper into the granule cell layer (Figure 20b, lower panel), became postmitotic and had encountered a critical selection process denoted either by integration of the newborn neuron into the hippocampal circuitry or by apoptosis (Encinas and Sierra, 2012). At this stage a duplication of BrdU-positive cells in knockout animals as compared to wild type controls was observed (Figure 20e). This indicates that upon deletion of *P2ry13* more progenitor cells pass the critical selection process. Quantification of the BrdU-positive cells in the hilus did not reveal changes in cell number in KO animals (Figure 20h). Ongoing neurogenesis occurs throughout the length of the dentate gyrus and across the transverse axis (suprapyramidal and infrapyramidal blade) though heterogeneity across both blades has been reported concerning

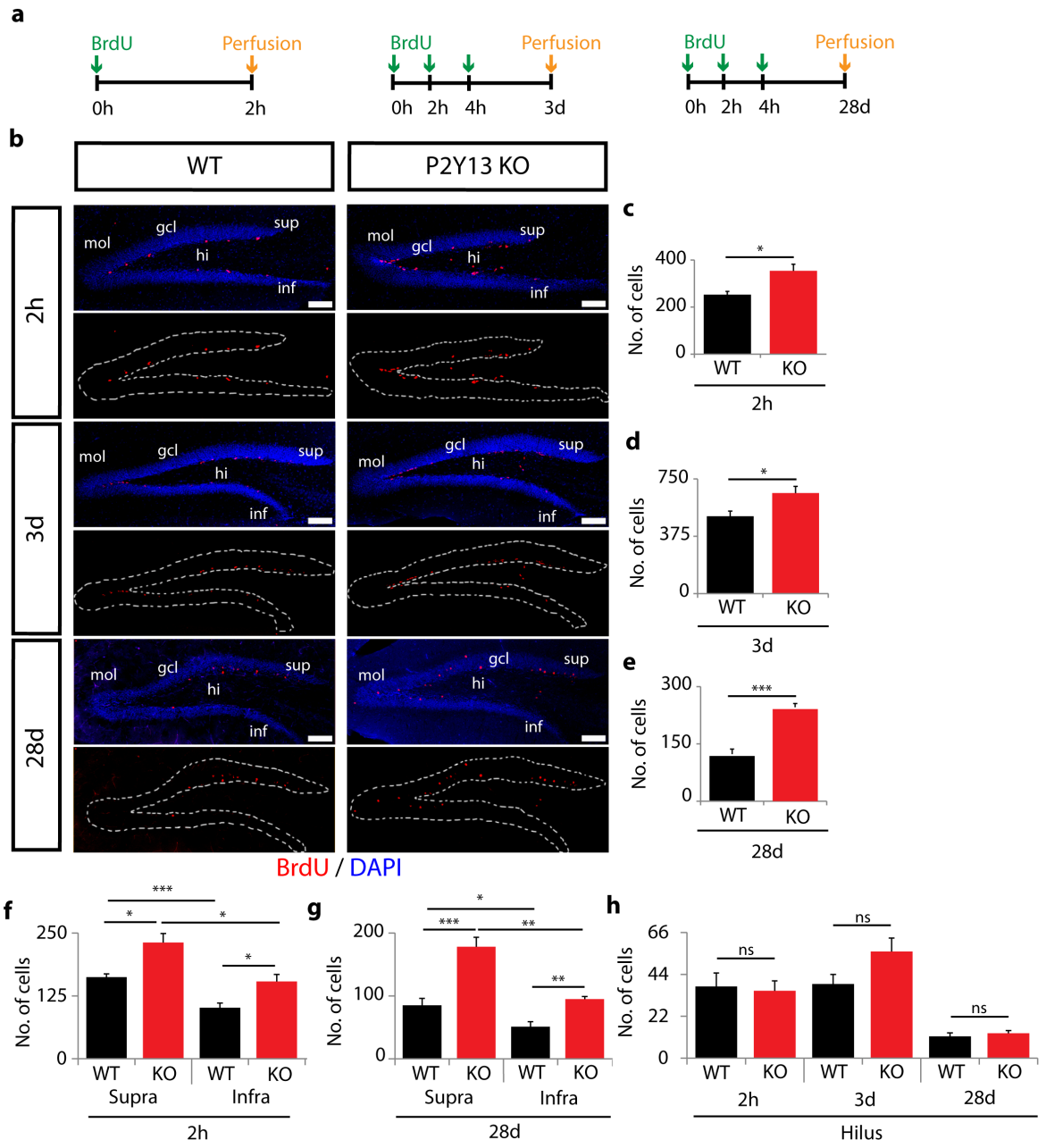

Figure 20: Increased levels of precursor cell proliferation and long-term survival in KO mice. a: Schematic overview of the different BrdU injection protocols. **b:** Analysis of immunofluorescence for BrdU (red) and DAPI (blue) in the GCL of adult WT and KO mice 2 h, 3 d or 28 d after BrdU injection. **c:** Corresponding quantification of BrdU+ cells 2 h after BrdU injection in WT and KO mice (total number of cells, 14 sections per animal, n=7). **d:** Quantitative evaluation of BrdU-labeled cells 3 d after BrdU injection (total number of cells, 14 sections per animal, n=7 per genotype) corresponding to **b** (middle panel). **e:** Quantification of cell numbers 28 d after BrdU injection(total number of cells, 14 sections per animal, n=7 per genotype) corresponding to **b** (lower panel), revealed increased survival of progenitor cells in KO mice. **f**: Individual quantification of BrdU+ cells in the suprapyramidal vs. infrapyramidal layer of the GCL in KO animals compared to WT control (total number of cells, 14 sections per animal, n=7) corresponding to **b** (upper panel).**g:** Individual quantification of BrdU+ cells in the suprapyramidal vs. infrapyramidal layer of the GCL in KO animals compared to WT control (total number of cells, 14 sections per animal, n=7 per genotype) corresponding to **b** (lower panel). **h:** No changes in the number of BrdU+ cells in the hilar region of WT and KO mice were detected (total number of cells, 14 sections per animal, n=7)**.** Bar graphs represent means ± SEM. *p<0.05, **p<0.01, ***p<0.001, significant relative to control, ns, difference not

significant. gcl, granule cell layer, hi, hilus; inf, infrapyramidal blade; mol, molecular layer; sup, suprapyramidal blade. Confocal images were taken with a Leica TCS SP5 II microscope. (Scale bars, 100 μm)

size of the dendritic tree of granule neurons, the ratio of inhibitory interneurons, connectivity and experience-induced activation (Snyder et al., 2012). Neurogenesis was reported to be initially higher in the infrapyramidal than suprapyramidal blade, however survival was diminished in the infrapyramidal blade, resulting in similar densities of neurons in the two blades by four weeks (Snyder et al., 2012). Individual quantification of dentate gyrus blades was performed in $P2Y_{13}$ WT and KO mice. 2 h after BrdU injection higher numbers of BrdU+ cells were found in the suprapyramidal compared to the infrapyramidal blade in both genotypes (Figure 20f). 60% more cells were found in the suprapyramidal blade of WT animals compared to the infrapyramidal blade. In KO animals an increase of around 50% in the number of BrdU-positive cells in the suprapyramidal blade was observed. Moreover, the number of BrdU+ cells was significantly increased in both blades in the KO compared to the WT control by 42% in the suprapyramidal blade, and 51% in the infrapyramidal blade, respectively. In order to determine the number of surviving cells, cell numbers were quantified 28 d after BrdU injection. In line with findings in the proliferating cell population, more cells were detected in the suprapyramidal blade in both genotypes (Figure 20g). Again, the number of BrdU+ cells was significantly higher in KO animals compared to WT mice. 109% and 85% more cells were found in the suprapyramidal blade and in the infrapyramidal blade, respectively. Taken together this suggests that under basal conditions activation of the ADP-sensitive $P2Y_{13}$ receptor inhibits proliferation and survival of progenitor cells, therefore acting as a brake on adult hippocampal neurogenesis. Of note, this effect could not be observed in the olfactory bulb, the target regions of new neurons generated in the SVZ. In wild type mice 4812.83 ± 446.92 BrdU-labeled cells were counted in the olfactory bulb as compared to 5793.67 ± 521.85 cells in the knockout. This increase was not significant ($p=0.22$, four sections per animal, mean ± S.E.M., $n=6$).

2.1.2.3 DCX-positive cells but not type-1 cells are expanded in the subgranular layer of *P2ry13*-/- mice

As shown above, type-1 cells in *Entpd2* KO mice revealed enhanced levels of proliferation (comp. Figure 15). Yet, mature progenitor cell types (type-3+ cells) lost responsiveness to survival factors and underwent increased apoptosis. In contrast, in *P2ry13* knockout mice, increased numbers of BrdU-labeled cells were still detectable four weeks after BrdU injections.

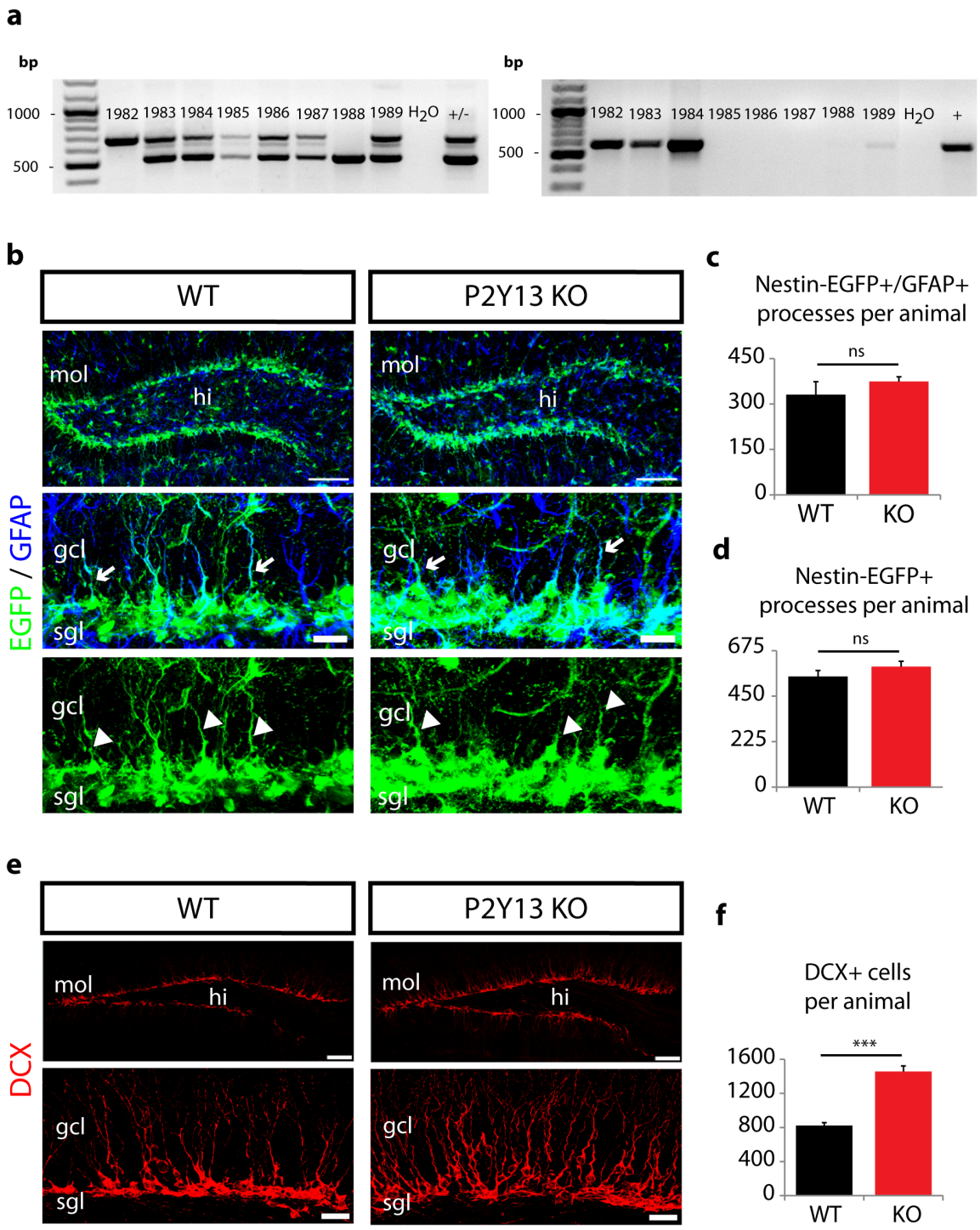

Figure 21: Expansion of DCX+ cells but not type-1 cells in the SGL of KO mice. a: Identification of *P2ry13* KO mice. *P2ry13*+/-, nestin-EGFP+ mice were inbred and offspring was genotyped via PCR. Primer pairs amplifying fragments of the wild type allele (500 bp) and mutated allele (700 bp) allowed solid discrimination of WT and KO mice (left panel). Amplified fragments detected at 510 bp (right panel), correspond to nestin-EGFP+ animals. **b:** Immunofluorescence for nestin-EGFP (green) and GFAP (blue) in precursor cells in the SGL. Middle and lower panel are close-up images of the upper panel. Processes facing the granule cell layer positive for nestin-EGFP and GFAP (arrows in middle panel) or nestin-EGFP (arrowheads in lower panel) were analyzed in WT and KO mice. **c:** Quantification of nestin-EGFP/GFAP double+ processes (total number of processes, four sections per animal, n=3-6) corresponding to **b** (middle panel). **d:** Quantitative evaluation of labeled processes positive for nestin-EGFP only (total number of processes, four sections per animal, n=3-6) corre-

sponding to **b** (lower panel). **e:** Immunolabeling of DCX (red) in WT and KO mice. Lower panels represent enlarged images of the upper panel. **f:** Corresponding quantification revealed a strong increase in the number of DCX+ cells in KO animals (total number of cells, six sections per animal, n=7 for both genotypes). Bar graphs represent means ± SEM. ***p<0.001, significant relative to control, ns, difference not significant. gcl, granule cell layer; hi hilus; mol, molecular layer; sgl, subgranular layer. Confocal images were taken with a Leica TCS SP5 II microscope. (Scale bars, 100 μm, b, e (upper panel); 20 μm, b (middle panel); 25 μm, e (lower panel))

This argues against increased levels of cell death in the neuroblast stage of *P2ry13* knockout mice and should result in differences in total cell numbers in the dentate gyrus between wild type and knockout mice. Numbers of individual cell types were therefore quantified in wild type and knockout animals. To ease the identification of type-1 cells, *P2ry13*-/- mice were bread to nestin-EGFP expressing mice. Identification of nestin-EGFP+ WT and KO mice was based on genotyping PCR (Figure 21a). Amplified fragments were detected at 500 bp and 700 bp with PCR products detected at 500 bp corresponding to the wild type allele and PCR products detected at 700 bp corresponding to the mutated allele (Figure 21a, left). At the same time, the PCR reaction allowed for a clear discrimination of EGFP+ mice, with amplified fragments detectable at 510 bp, and EGFP- mice, with no fragment amplified (Figure 21a, right). Type-1 cells were quantified based on the identification of distinct marker profiles together with morphological criteria as described before. Cells positive for nestin-EGFP and GFAP, having at least a short process reaching into the granule cell layer, were considered to represent type-1 cells (Figure 21b, upper and middle panel, white arrows). In analogy to previous experiments, the number of nestin-EGFP-positive processes was analyzed (Figure 21b, lower panel, white arrowheads). In contrast to previous findings in *Entpd2* knockout mice (comp. Figure 15c), no alterations in the number of nestin-EGFP+ processes (Figure 21d) or in the number of nestin-EGFP+/GFAP+ processes (Figure 21c) was detected. The total number of DCX+ cells was, however, strongly increased by 77% in *P2ry13* null mice (Figure 21f). Notably, this could already be detected by eye (Figure 21e, enlarged images). The data suggest that in *P2ry13* null mice the number of DCX+ cells is constitutively increased.

2.1.2.4 *P2ry13* deletion leads to increased CREB phosphorylation and apoptosis in the hippocampal dentate gyrus

Loss of CREB phosphorylation in DCX+ cells compromises the survival of young, immature neurons (Jagasia et al., 2009). To address the question whether increased survival of progenitor cells in *P2ry13*-deleted animals results in increased levels of CREB phosphorylation in DCX+ cells, immunostaining for DCX and pCREB was performed (Figure 22a). The extent

of CREB phosphorylation in the DCX-expressing cell population was analyzed. In WT mice 55% of all DCX+ cells were found to be immunopositive for pCREB whereas in KO mice around 64% of the DCX-expressing cell population was found to co-express pCREB (Figure 22b), demonstrating that DCX+ neuroblasts exhibit higher levels of CREB phosphorylation upon deletion of *P2ry13*. As progenitor cell proliferation was strongly increased in KO mice (comp. Figure 20) and neuroblasts displayed higher levels of CREB phosphorylation, possibly promoting survival of these cells, one would assume decreased rates of apoptosis in mutant mice. In the DG of WT and KO mice Caspase-3 positive cells were exclusively observed in the SGL (Figure 22c). Quantification of cleaved caspase-3-labeled cells rather revealed a strong increase of 140% in the number of apoptotic cells in the GCL of KO mice (Figure 22d).

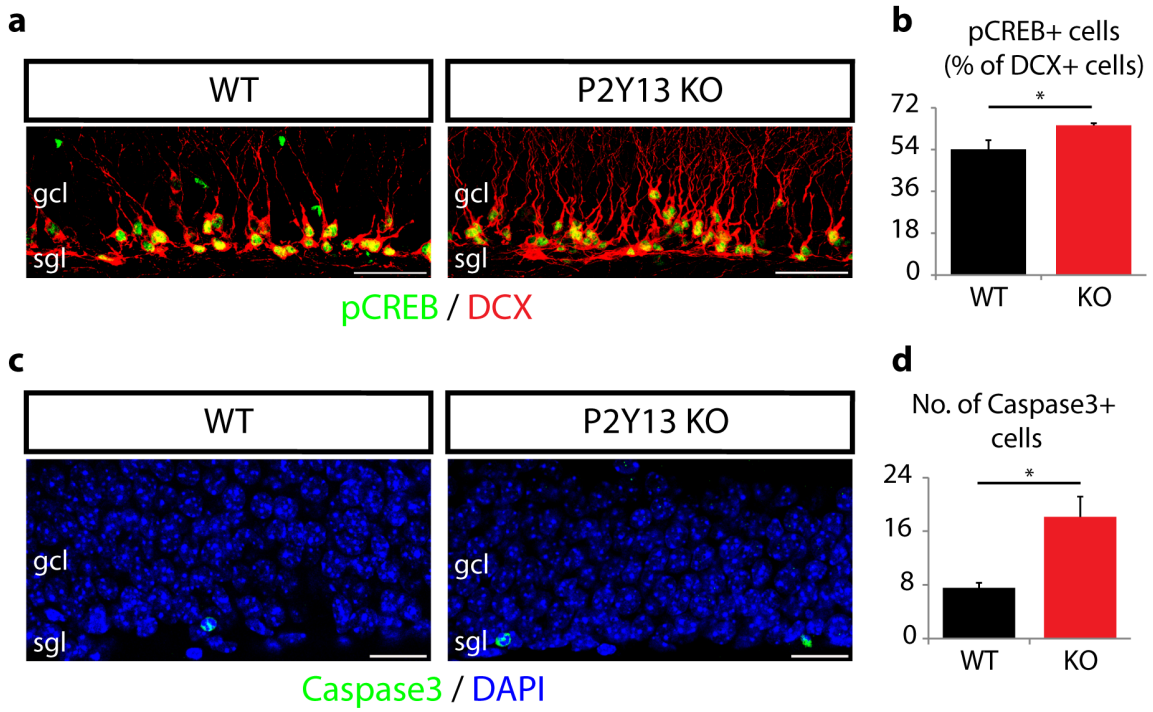

Figure 22: Increased CREB phosphorylation and apoptosis in the GCL upon *P2ry13* deletion. **a:** Immunofluorescence for pCREB (green) and DCX (red) in the SGL of adult WT and KO mice. **b:** Corresponding quantification pCREB-labeled DCX-positive cells (number of pCREB+/DCX+ cells presented as percentage of the total number of DCX+ cells, six sections per animal, n=11 for both genotypes). **c:** Immunolabeling for cleaved caspase-3 (green) in the SGL. DAPI shown in blue. Cleaved caspase-3+ cells were exclusively found in the SGL in relatively low numbers in both genotypes. **d:** Quantitative evaluation corresponding to **c** (total number of caspase-3-labeled cells, 14 sections per animal, n=7). Bar graphs represent means ± SEM. *$p<0.05$, significant relative to control. gcl, granule cell layer; sgl, subgranular layer. Confocal images were taken with a Leica TCS SP5 II microscope. (Scale bars, 50 µm, a; 20 µm, c)

2.1.2.5 The extent of neuron formation but not the neurogenic capacity is increased in $P2Y_{13}$ KO mice

A strong increase in apoptosis was detected in *P2ry13* KO mice (comp. Figure 22d). However, the number of surviving cells 4 weeks after BrdU labeling was strongly increased in the mutant mice (comp. Figure 20e). This indicates that increased apoptosis cannot compensate for the high number of surplus progenitor cells. To corroborate this hypothesis, the extent of neuron formation was determined (Figure 23). The contribution of NeuN-positive cells to the total of BrdU-positive cells, four weeks after BrdU-injection was analyzed (Figure 23a). The number of BrdU/NeuN double-positive cells was increased by 93% in the KO (Figure 23b), suggesting that more mature neurons integrate into the GCL of knockout animals. However, the neurogenic capacity, meaning the percentage of stem or progenitor cells that finally differentiate into neurons, was unchanged. In both genotypes around 70% of all initially labelled BrdU+ cells were found to be immunopositive for NeuN (Figure 23c), indicating that nearly three-quarters of all precursor cells differentiated into neurons.

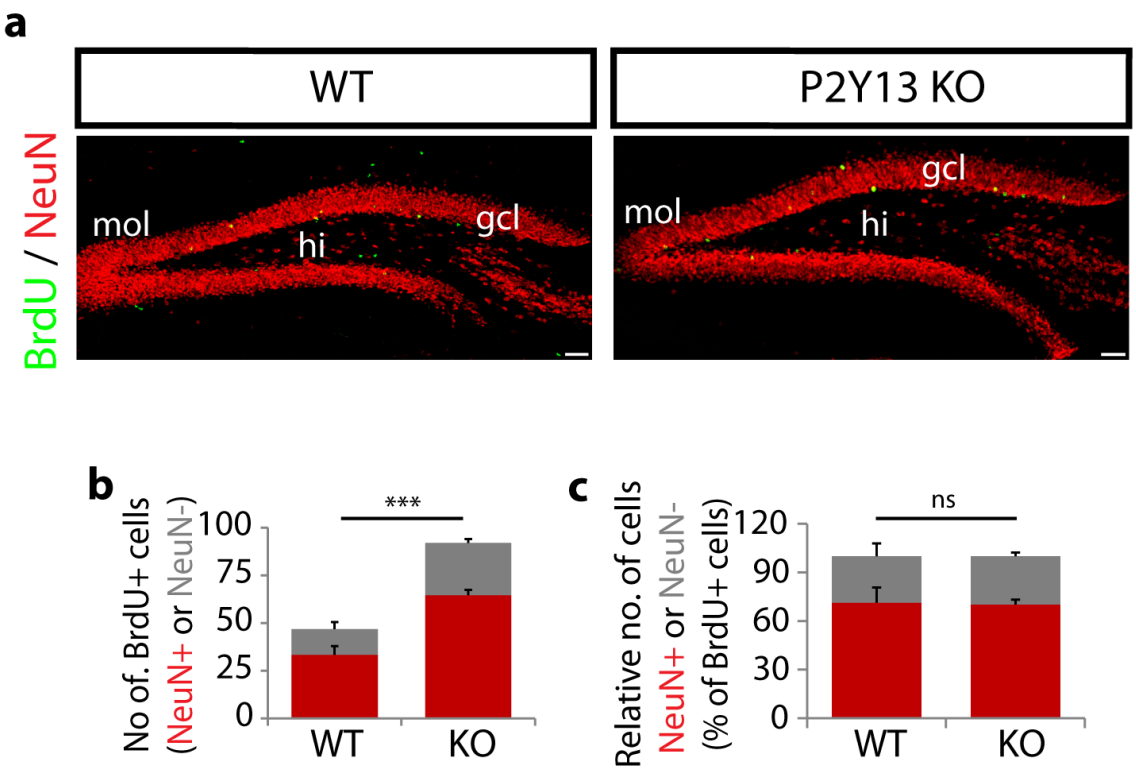

Figure 23: Increased number of neurons 28 d after BrdU injection in KO mice. a: Immunostaining for BrdU (green) and NeuN (red) in the GCL of WT and KO mice four weeks after BrdU labeling. **b:** Quantitative evaluation of BrdU/NeuN double-labeled cells corresponding to **a** (total number of cells,. six sections per animal, n=7) **c:** Corresponding quantification of NeuN+ or NeuN- cells represented as percentage of the number of BrdU+ cells (six sections per animal, n=7 for both

genotypes). 100% corresponds to the total number of BrdU-positive cells counted in the GCL (46.86 ± 4.43 cells in the WT and 92 ± 2.88 cells in the KO). Red graphs represent double-labeled cells; grey graphs correspond to cells labeled for BrdU only. Bar graphs represent means ± SEM. ***p<0.001, significant relative to control, ns, difference not significant. gcl, granule cell layer; hi, hilus; mol, molecular layer. Confocal images were taken with a Leica TCS SP5 II microscope. (Scale bars, 50 µm)

2.1.2.6 Neuronal activity is increased in the hippocampal dentate gyrus of *P2ry13* null mice

Neural network activity modulates the rate of adult neurogenesis matching it to the physiological needs of the synaptic network (Lledo et al., 2006; Piatti et al., 2011; Babu et al., 2009). Upon neuronal activity, expression of immediate early genes is rapidly induced (Smeyne et al., 1992; Barth, 2007; Inoue et al., 2010; Okuno, 2011). Among these immediate early genes,

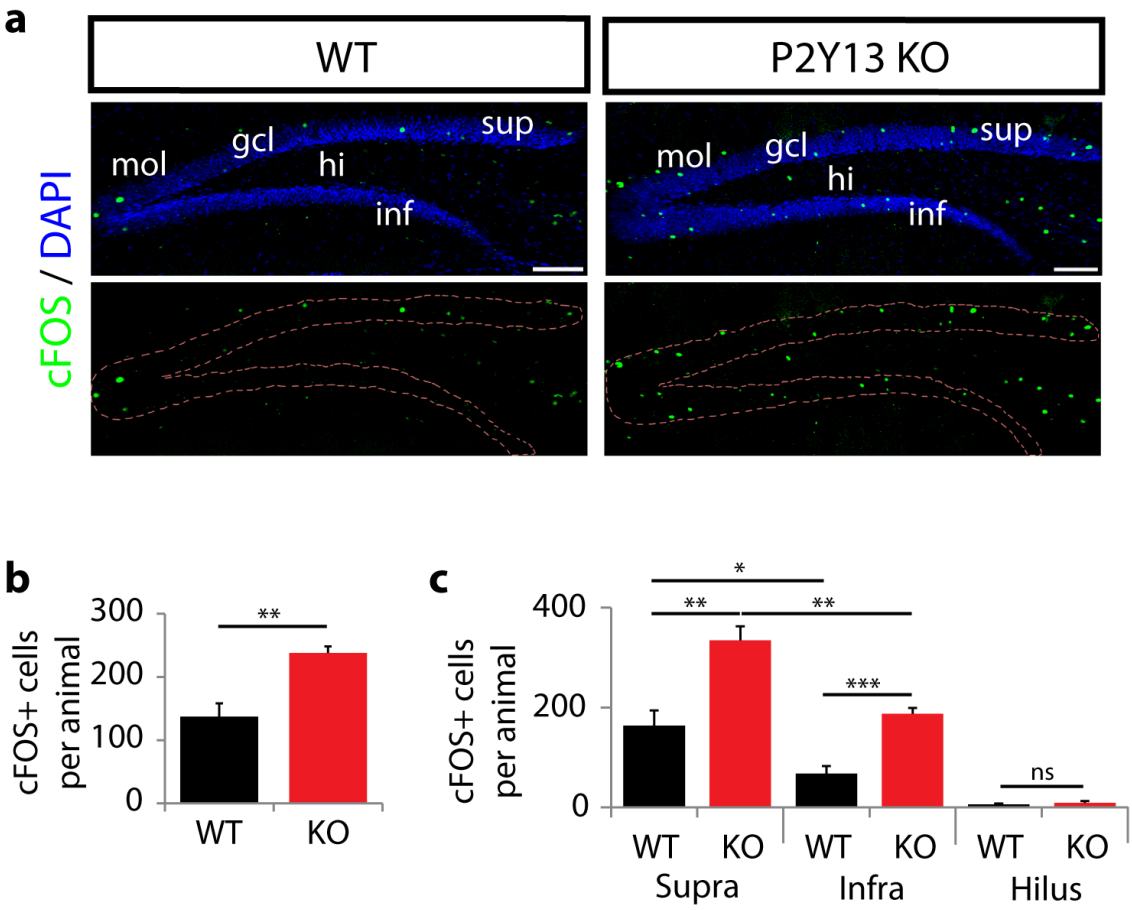

Figure 24: Analysis of neuronal activity in the hippocampal DG of wild type and mutant mice. **a:** Analysis of immunofluorescence for c-Fos (green) and DAPI (blue) in the GCL of adult WT and KO mice. **b:** Increased number of c-Fos+ cells in the GCL of KO mice as revealed by quantitative evaluation of immunofluorescence (total number of c-Fos+ cells, 7 sections per animal, n=6-7). **c:** Corresponding quantification in individual DG blades (total number of cells, 14 sections per animal, n=6-7). Bar graphs represent means ± SEM. *p<0.05, **p<0.01, ***p<0.001, significant relative to control, ns, difference not significant. gcl, granule cell layer; hi, hilus; inf, infrapyramidal blade; mol, molecular layer; sup, suprapyramidal blade. Confocal images were taken with a Leica TCS SP5 II microscope. (Scale bars, 100 µm)

c-Fos (Schilling et al., 1991) is used as a well characterized and frequently used tool to detect and map neuronal activity in situ (Kawashima et al., 2014). To scrutinize potential effects of *P2ry13* deletion on neuronal activity, the expression of c-Fos was analyzed. Immunolabeling was performed and c-Fos+ cells were quantified in the granule cell layer of WT and KO mice (Figure 24a). A strong increase of 74% in the number of c-Fos labeled cells was detected in KO animals (Figure 24b). In both genotypes higher numbers of c-Fos-positive cells were detected in the suprapyramidal blade than in the infrapyramidal blade (Figure 24c). Individual quantification of both blades revealed higher levels of c-Fos in KO animals with an increase of 104% in the suprapyramidal blade and an increase of 178% in the infrapyramidal blade, respectively (Figure 24c). Only few cells were found to be immunopositive for c-Fos in the hilus of WT and KO mice. Quantification of these cells did not reveal significant differences between WT and KO (Figure 24c). This suggests that neuronal activity is higher in the suprapyramidal blade of the DG in adult mice. Moreover, deletion of *P2ry13* leads to increased expression of immediate early genes like c-Fos, indicating higher levels of neuronal activity in the dentate granule cell layer of mutant mice.

2.1.2.7 Deletion of *P2ry13* does not alter levels of proliferation and long-term survival of precursor cells in the ventral dentate gyrus

Hippocampal function and properties vary along the dorsoventral axis (Bannerman et al., 2004; Fanselow and Dong, 2010), with the dorsal pole affecting spatial learning and memory (Moser et al., 1995) and the ventral pole playing a role in emotional and anxiolytic behavior (Kjelstrup et al., 2002). The dorsal dentate gyrus of mice exhibits higher levels of progenitor cell proliferation than the ventral dentate gyrus (Jinno, 2011; Snyder et al., 2012). But survival rates were reported not to differ along the dorsoventral axis (Snyder et al., 2012). In order to evaluate whether properties of the dorsal and ventral dentate gyrus differ in $P2Y_{13}$ receptor-deleted mice, levels of proliferation and long-term survival of precursor cells were analyzed in the ventral dentate gyrus of WT and KO mice (Figure 25a) in the same sections used for quantification of the dorsal DG (comp. Figure 20). In both genotypes the number of BrdU-labeled cells was apparently lower at all time points in the ventral DG as compared to cell numbers counted in the dorsal DG (comp. Figure 20). In contrast to the values obtained for the dorsal hippocampus (Figure 20) no significant differences between wild type and KO animals was found by BrdU labeling 2 h, 3 d, and 28 d after the final BrdU pulse and no

significant difference could be observed between upper and lower blades (Figure 25 b-d). This suggests that levels of progenitor cell proliferation and long-term survival in the ventral dentate gyrus are not affected by deletion of the $P2Y_{13}$ receptor.

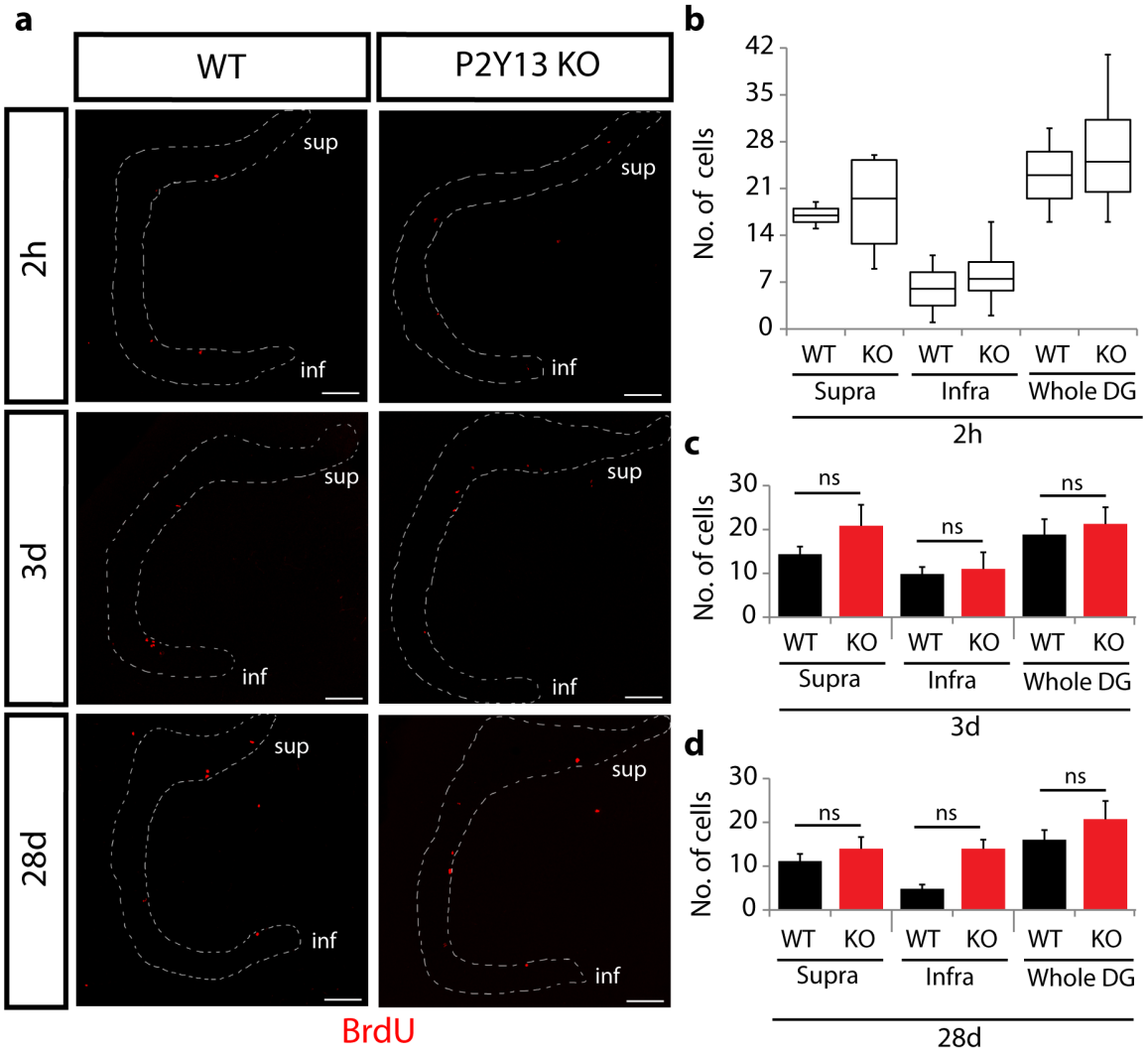

Figure 25: Analysis of progenitor proliferation and survival in the ventral dentate gyrus. a: Immunofluorescence for BrdU (red) in the ventral DG of adult WT and KO mice 2 h (upper panel), 3 d (middle panel) and 28 d (lower panel) after BrdU injection. **b:** Evaluation of BrdU+ cells 2 h after BrdU labeling. Boxplot diagram showing median, maximum and minimum levels in WT and KO animals in both blades and in the whole ventral DG corresponding to **a**, upper panel (six sections per animal, n=2-4). **c:** Quantification of BrdU-labeling 3 d after the final BrdU pulse corresponding to **a**, middle panel (five sections per animal, n=6-7). **d:** Quantification corresponding to **a** (lower panel) 28 d after BrdU-labeling (seven sections per animal, n=7 for both genotypes). Bar graphs in **c** and **d** represent means ± SEM. ns, difference not significant. inf, infrapyramidal blade; sup, suprapyramidal blade. Confocal images were taken with a Leica TCS SP5 II microscope. (Scale bars, 100 µm)

2.1.2.8 Also aged $P2Y_{13}$ receptor KO mice show increased levels of proliferation and long-term survival of precursor cells

Neurons are continuously generated in neurogenic niches throughout the life span of mammals, though the degree of neurogenesis strongly depends on animal age (Encinas and Sierra, 2012). In order to test whether increased progenitor cell proliferation and survival in *P2ry13*-depleted animals persists during aging, 6 month old WT and mutant mice were injected with BrdU three times a day at 2 hours interval for one day or three consecutive days and perfused 2 h or 28 d after the last BrdU pulse (Figure 26a, b). Coronal sections were used for immunostaining for BrdU and NeuN (Figure 26c). Quantitative evaluation of BrdU-positive cells 2 h after the final BrdU pulse (Figure 26c, upper panel) revealed an increase in the total

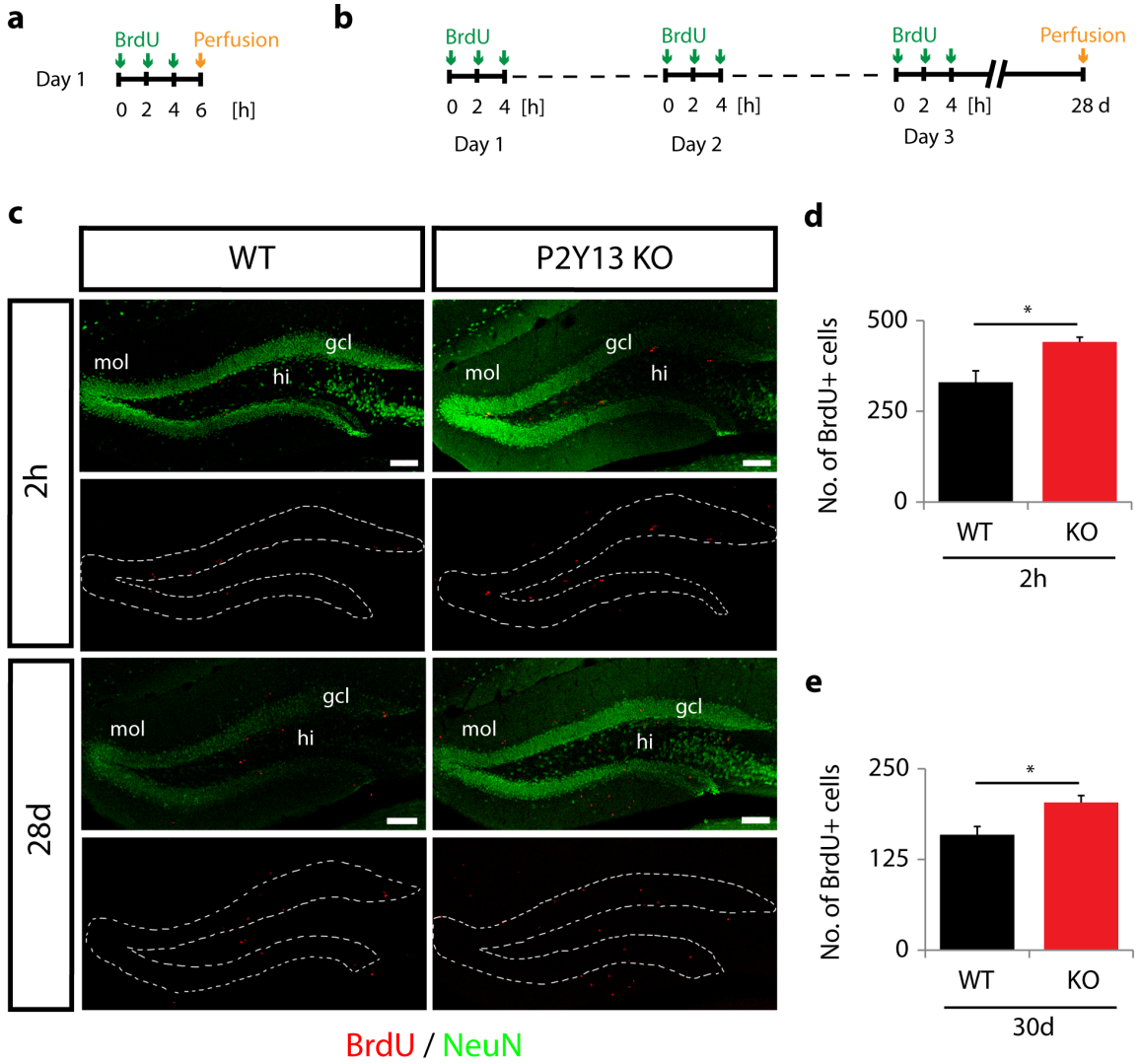

Figure 26: Sustained increase of progenitor cell proliferation and survival in the DG of aged KO mice. a: Schematic overview of BrdU injection protocol for analysis of progenitor cell proliferation. **b:** Schematic overview of BrdU injection protocol for analysis of long-term progenitor cell

survival. **c:** Immunofluorescence for BrdU (red) and NeuN (green) in the DG of aged WT and KO mice 2 h (upper panel) or 28 d (lower panel) after the final BrdU pulse following BrdU injection. **d:** Quantification of progenitor cell proliferation corresponding to **c**, upper panel (total number of cells, eight sections per animal, n=7). **e:** Quantitative evaluation corresponding to **c**, lower panel (total number of cells, eight sections per animal, n=7). Bar graphs represent means ± SEM. *p<0.05, significant relative to control. gcl, granule cell layer; hi, hilus; mol, molecular layer. Confocal images were taken with a Leica TCS SP5 II microscope. (Scale bars, 100 μm)

number of cells in aged KO mice of 34% (Figure 26d). Differences in the number of BrdU-labeled cells were further detected 28 d after BrdU injections (Figure 26c, lower panel). 28% more BrdU+ cells were found in the granule cell layer of mutant mice as compared to the wild type controls (Figure 26e). These results indicate that changes in the levels of progenitor cell proliferation and long-term survival in *P2ry13* null mice persist in older animals.

In summary, these data further support the notion that extracellular nucleotides significantly contribute to the control of neurogenesis in the dentate gyrus. Under basal conditions activation of the $P2Y_{13}$ receptor apparently attenuates progenitor cell proliferation, new neuron formation, and neuronal activity.

2.2 Analysis of purinergic signaling in adult hypothalamic neurogenesis

In mammals, energy balance is tightly regulated by the two actions of calorie intake and energy expenditure (Dietrich and Horvath, 2013). In this context the hypothalamus functions as central regulator of energy balance in the CNS (Morton et al., 2006). Increasing evidence suggests that, in addition to the classic neurogenic niches, active neurogenesis takes place in various additional regions of the adult rodent brain, including the hypothalamus (Migaud et al., 2010). Adult hypothalamic neurogenesis was reported to contribute to the regulation of food intake (Kokoeva et al., 2007; Pierce and Xu, 2010; Lee et al., 2012). Tanycytes, lining the lateral wall of the third ventricle in the hypothalamus, together with supependymal astrocytes are considered to represent adult hypothalamic neural stem and precursor cells (hNSPCs) (Lee et al., 2012; Robins et al., 2013; Haan et al., 2013). Adult born hypothalamic neurons originate from these proliferative cells and migrate to the hypothalamic parenchyma, finally integrating into appetite-regulating circuits (Xu et al., 2005; Werner et al., 2012; Haan et al., 2013). hNSPCs can sense and integrate nutritional signals from the periphery (Sousa-Ferreira et al.,

2014). Signaling actions in tanycytes depend on changes in intracellular Ca^{2+} (Bolborea and Dale, 2013). Noteworthy, sensing of altered blood glucose levels by tanycytes has been reported to involve $P2Y_1$ receptors and ATP release (Frayling et al., 2011; Orellana et al., 2012). Moreover, α-tanycytes express the ectoenzyme NTPDase2 and show high levels of ecto-ATPase activity (Firth and Bock, 1976; Braun et al., 2003). Together these findings implicate purinergic signaling mechanisms in the control of adult hypothalamic neurogenesis. A pilot study was therefore undertaken to investigate whether the $P2Y_{13}$ receptor could also be involved in the control of hypothalamic neurogenesis.

2.2.1 Functional characterization of adult hypothalamic neurogenesis in *P2ry13* knockout mice

Tanycytes express NTPDase2 and show high levels of ecto-ATPase activity (Firth and Bock, 1976; Braun et al., 2003). Furthermore, glucose sensing in tanycytes involves $P2Y_1$ receptors and ATP release (Frayling et al., 2011; Orellana et al., 2012). This suggests that ATP released upon a glucose stimulus is rapidly broken down to ADP by NTPDase2. ADP might induce intracellular signaling pathways by activating ADP-sensitive P2Y receptors. It has been shown in this thesis that ADP-sensitive $P2Y_{13}$ receptors play an essential role in the control of adult hippocampal neurogenesis (see previous chapter). To investigate the contribution of purinergic mechanisms in adult hypothalamic neurogenesis and to reveal the potential involvement of $P2Y_{13}$ receptors in this context, BrdU-proliferation and progenitor survival studies were performed. Moreover, neuron formation and neuronal activity in hypothalamic nuclei including the arcuate nucleus (ARC), ventromedial nucleus (VMN) and dorsomedial nucleus (DMN) was analyzed.

2.2.1.1 Deletion of *P2ry13* increases levels of progenitor cell proliferation at the third ventricle of the adult hypothalamus

In a first set of experiments progenitor cell proliferation at the third ventricle was analyzed. Mice received three daily injections of BrdU at 2 h interval for three consecutive days and were perfused 2 h after the final BrdU pulse (Figure 27a). To date, no consensus about the identity of adult hNSPCs exists. Two distinct proliferative zones harboring hNSPCs were identified at the third ventricle, the ventral part including β-tanycytes in the median eminence (Lee et al., 2012; Haan et al., 2013) and the medial part including tanycytes (α-tanycytes) and

proliferative subependymal astrocytes (Perez-Martin et al., 2010; Robins et al., 2013). Therefore the number of BrdU+ cells 2 h after BrdU labeling was analyzed around the entire third ventricle wall (Figure 27b, upper panel) and separately in the median eminence (Figure 27b, enlarged image in lower panel). Tanycytes at the third ventricle are depicted by immunostaining for GFAP (Figure 27b, upper panel). By eye, no gross alterations in the distribution or morphology of GFAP+ tanycytes were detected between WT and KO mice. Quantitative

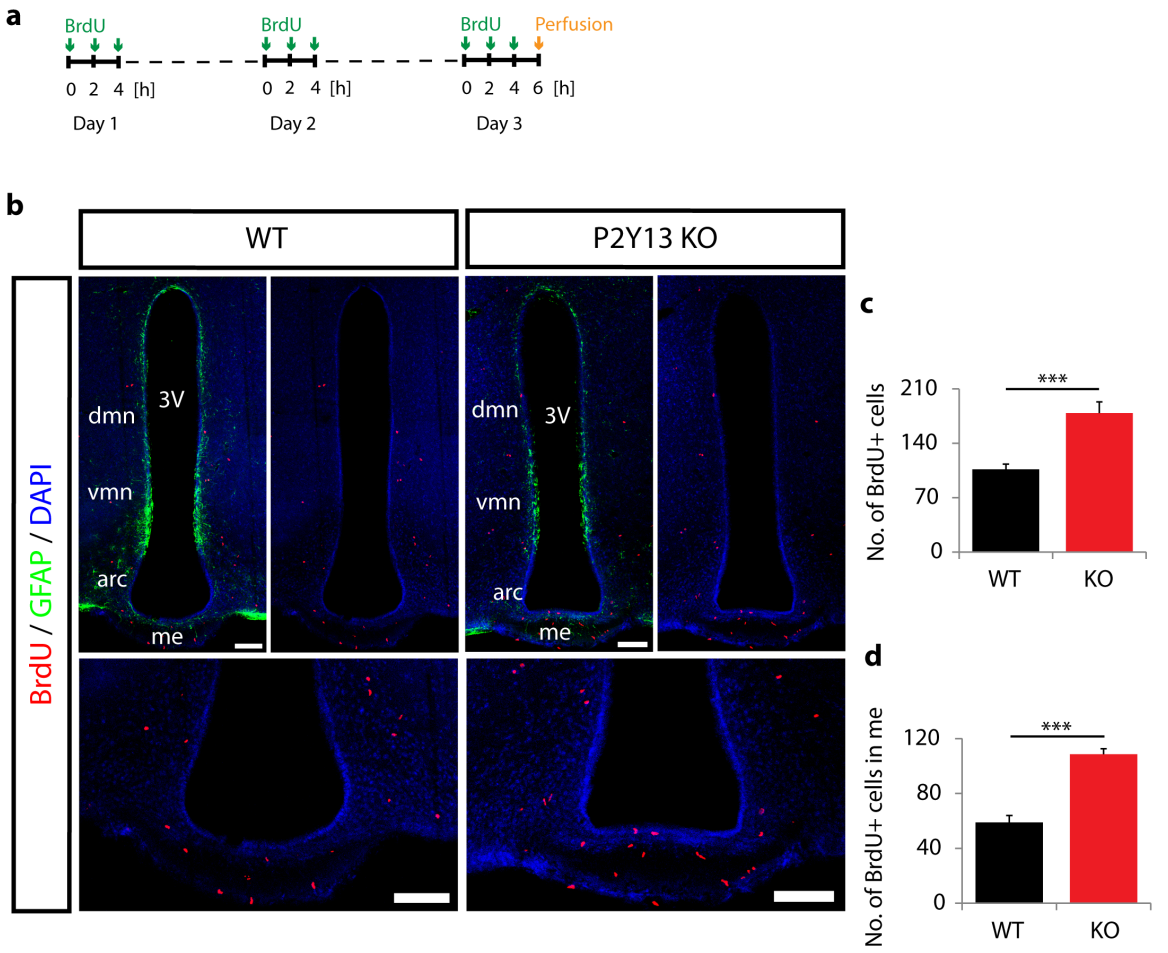

Figure 27: Increased progenitor cell proliferation at the 3rd ventricle in *P2ry13* KO mice. a: Schematic overview of BrdU injection protocol for analysis of progenitor cell proliferation 2 h after BrdU injection. **b:** Immunolabeling for BrdU (red), GFAP (green), and DAPI (blue) at the third ventricle in the adult hypothalamus of WT and KO mice 2 h after the final BrdU pulse. Enlarged images in the lower panel represent BrdU labeling in the median eminence. **c:** Quantitative evaluation of BrdU+ cells corresponding to **b**, upper panel (total number of cells, 4-5 sections per animal, n=5 for both genotypes). **d:** Quantification of progenitor cell proliferation in the median eminence only corresponding to **b**, lower panel, indicating an increase in the number of BrdU+ cells in KO animals (total number of cells, 4-5 sections per animal, n=5-6). Bar graphs represent means ± SEM. ***p<0.001, significant relative to control. 3V, third ventricle; arc, arcuate nucleus; dmn, dorsomedial nucleus; me, median eminence; vmn, ventromedial nucleus. Confocal images were taken with a Leica TCS SP5 II microscope. (Scale bars, 100 µm)

evaluation of BrdU-positive cells revealed an increase in cell number of 68% around the entire third ventricle wall in KO animals (Figure 27c). In addition the median eminence was separately evaluated. There 85% more BrdU-labeled cells were detected in *P2ry13* knockout mice (Figure 27d). This suggests that, in line with findings in the adult hippocampus, $P2Y_{13}$ receptors function as a brake on nucleotide-mediated progenitor cell proliferation in the neurogenic niche at the third ventricle in the adult mouse hypothalamus.

2.2.1.2 *P2ry13* KO mice exhibit increased long-term survival of precursor cells and neuron formation in hypothalamic nuclei

Upon activation, ventricular proliferative cells migrate to the hypothalamic parenchyma and incorporate into the appetite-controlling circuits composed of various hypothalamic nuclei (Sousa-Ferreira et al., 2014). To address the question of changes in long-term progenitor survival and neuron formation in hypothalamic nuclei of KO animals, mice received three daily injections of BrdU at 2 h interval for three consecutive days and were perfused 28 d after the final BrdU pulse. Immunolabeling for BrdU and the neuronal markers NeuN and HuC/D, allowed for solid discrimination of hypothalamic nuclei (Figure 28a). Four weeks after the initial BrdU-labeling, progenitor cells had migrated deeper into the parenchyma to their target regions including the dorsomedial nucleus (dmn), the ventromedial nucleus (vmn) and the arcuate nucleus (arc) (Figure 28a). The total number of BrdU-labeled cells in the hypothalamus of KO mice was nearly duplicated (increase of 95%) (Figure 28b, left bars). To further validate the extent of neuron formation, the contribution of HuC/D+ cells to the total of BrdU-labeled cells was analyzed. Indeed, doubling in the number of BrdU+ cells co-expressing HuC/D was identified in KO animals (Figure 28b, right bars), suggesting that more mature neurons integrate into appetite-regulating circuits in the adult hypothalamus in knockout animals. This was particularly obvious in the dorsomedial nucleus with an increase of 152% in the number of BrdU+/HuC/D+ cells (Figure 28c, left bars) and in the arcuate nucleus with increased cell numbers in KO animals of 100% (Figure 28d, left bars). However, no significant changes in neuron formation were detected in the ventromedial nucleus (Figure 28c, right bars). The increase in cell numbers in the KO mice was only identified by trend ($p=0.15$). In both genotypes only few BrdU+/HuC/D+ cells were detected in the median eminence four weeks after labeling (Figure 28d, right bars), indicating that most of the initially labeled cells had migrated to their upper target regions. No difference in the number of BrdU-

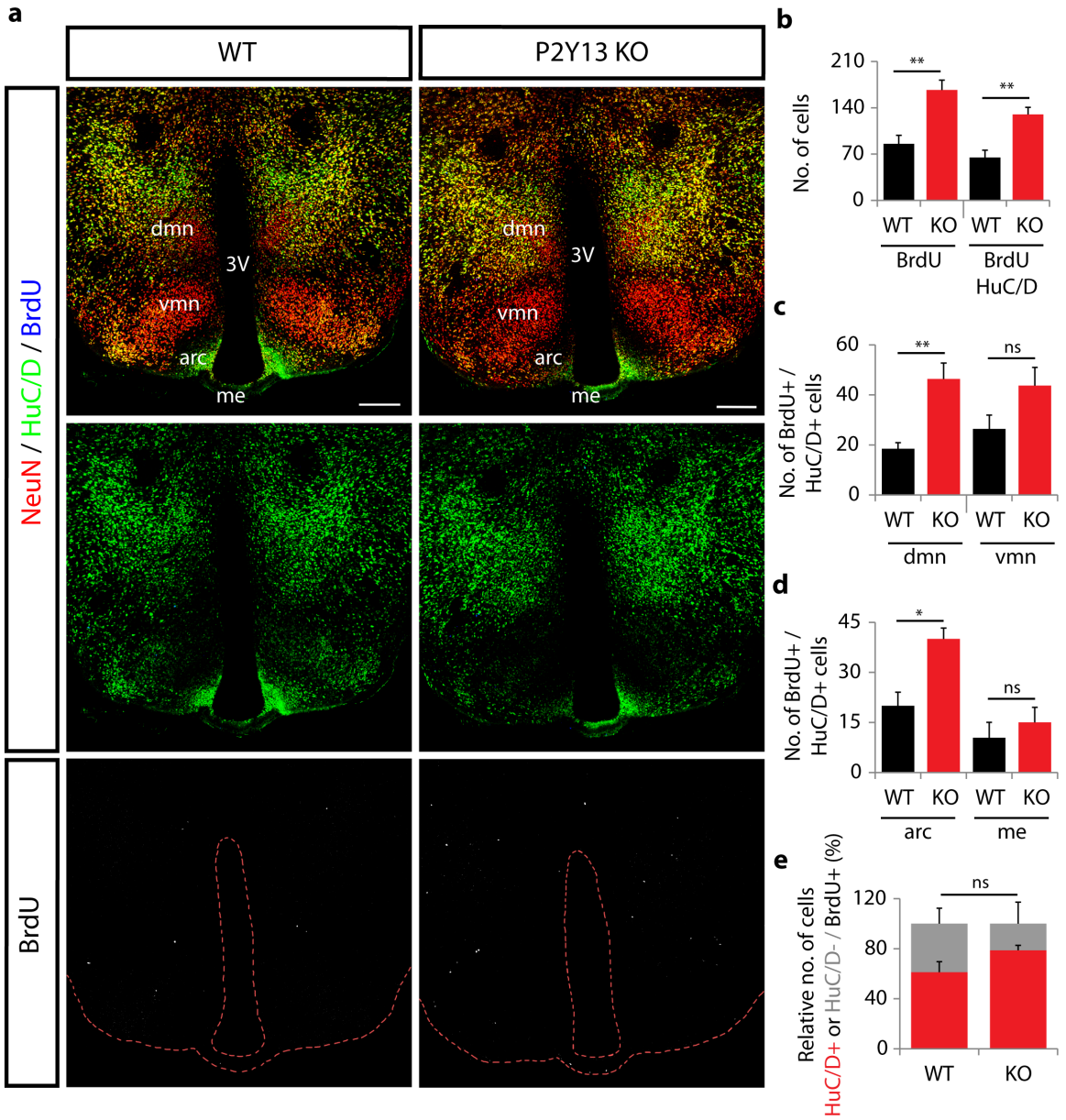

Figure 28: Increased progenitor survival and number of neurons 28 d after BrdU injections in KO mice. a: Immunostaining for BrdU (blue), NeuN (red) and HuC/D (green) in the adult hypothalamus of WT and KO mice four weeks after BrdU injections. The lower panel depicts BrdU+ cells in the parenchyma of the hypothalamus. **b:** Left bars represent quantification of BrdU-labeled cells corresponding to **a**. Right bars represent quantitative evaluation of BrdU/HuC/D double-labeled cells corresponding to **a**, middle panel (total number of cells, 4 sections per animal, n=6 for left and right bars). **c:** Quantification of BrdU+/HuC/D+ cells 28 d after BrdU injections in WT and KO mice in the dmn (left bars) and vmn (right bars) (total number of cells, 4 sections per animal, n=6). **d:** Quantification of BrdU+/HuC/D+ 28 d after BrdU injections in WT and KO mice in the arc (left bars) and me (right bars) (total number of cells, 4 sections per animal, n=6). **e:** Corresponding quantification of HuC/D+ or HuC/D- cells represented as percentage of the number of BrdU+ cells (four sections per animal, n=6). 100% corresponds to the total number of BrdU-positive cells counted (85.6 ± 12.82 in the WT and 167 ± 14.75 in the KO). Red bar sections correspond to double-labeled cells; grey bar sections correspond to cells labeled for BrdU only. Bar graphs represent means ± SEM. *p<0.05, **p<0.01, significant relative to control, ns, difference not significant. 3V, third ventricle; arc, arcuate nucleus; dmn, dorsomedial nucleus; me, median eminence; vmn, ventromedial nucleus. Confocal images were taken with a Leica TCS SP5 II microscope. (Scale bars, 250 µm)

positive cells expressing HuC/D between WT and KO was observed in the median eminence (Figure 28d, right bars). In line with previous findings in the adult hippocampus (comp. Figure 23) the neurogenic capacity - defined as the percentage of progenitor cells that differentiated into neurons rather than other cell types - was unchanged between WT and KO (Figure 28e). Around 74% of all initially labelled BrdU+ cells were found to be immunopositive for HuC/D in the WT, whereas in KO animals it was 79%, implicating a high neurogenic capacity of BrdU-labeled progenitors in both genotypes.

2.2.1.3 Neuronal activity is decreased in hypothalamic nuclei of *P2ry13* null mice

Neuronal surplus in the hippocampal neurogenic niche was associated with increased overall neuronal activity in the GCL of *P2ry13* KO mice (comp. Figure 24). To scrutinize potential effects of $P2Y_{13}$ receptor deletion on neuronal activity in hypothalamic nuclei, neuronal activity was monitored by the expression of the immediate early gene c-Fos (Figure 29a). Individual nuclei were easily identified via expression of the neuronal marker HuC/D (Figure 29a). In contrast to findings in the adult hippocampal GCL (Figure 24b), an overall decrease in neuronal activity in *P2ry13*-/- mice was observed in all nuclei examined (Figure 29a). In the dorsomedial nucleus (Figure 29a, enlarged images 1 in WT and a in KO) 60% less c-Fos+ cells were detected in KO animals compared to the WT controls (Figure 29b). The ventromedial nucleus (Figure 29a, enlarged images 2 in WT and b in KO) displayed 39% less c-Fos+ cells (Figure 29c) and 40% less c-Fos-labeled cells (Figure 29d) were counted in the arc (Figure 29a, enlarged images, lower right panels). Together these findings indicate that more inhibitory neurons incorporate into food-intake regulating circuits upon deletion of *P2ry13*, damping neuronal network activity.

In summary these data suggest a major contribution of purinergic mechanisms in adult hypothalamic neurogenesis and energy metabolism and a direct involvement of $P2Y_{13}$ receptors in this context. Under basal conditions $P2Y_{13}$ receptors diminish progenitor cell proliferation, survival and neuron formation and decrease inhibition of appetite-regulating circuits by newborn neurons in the hypothalamus of adult mice.

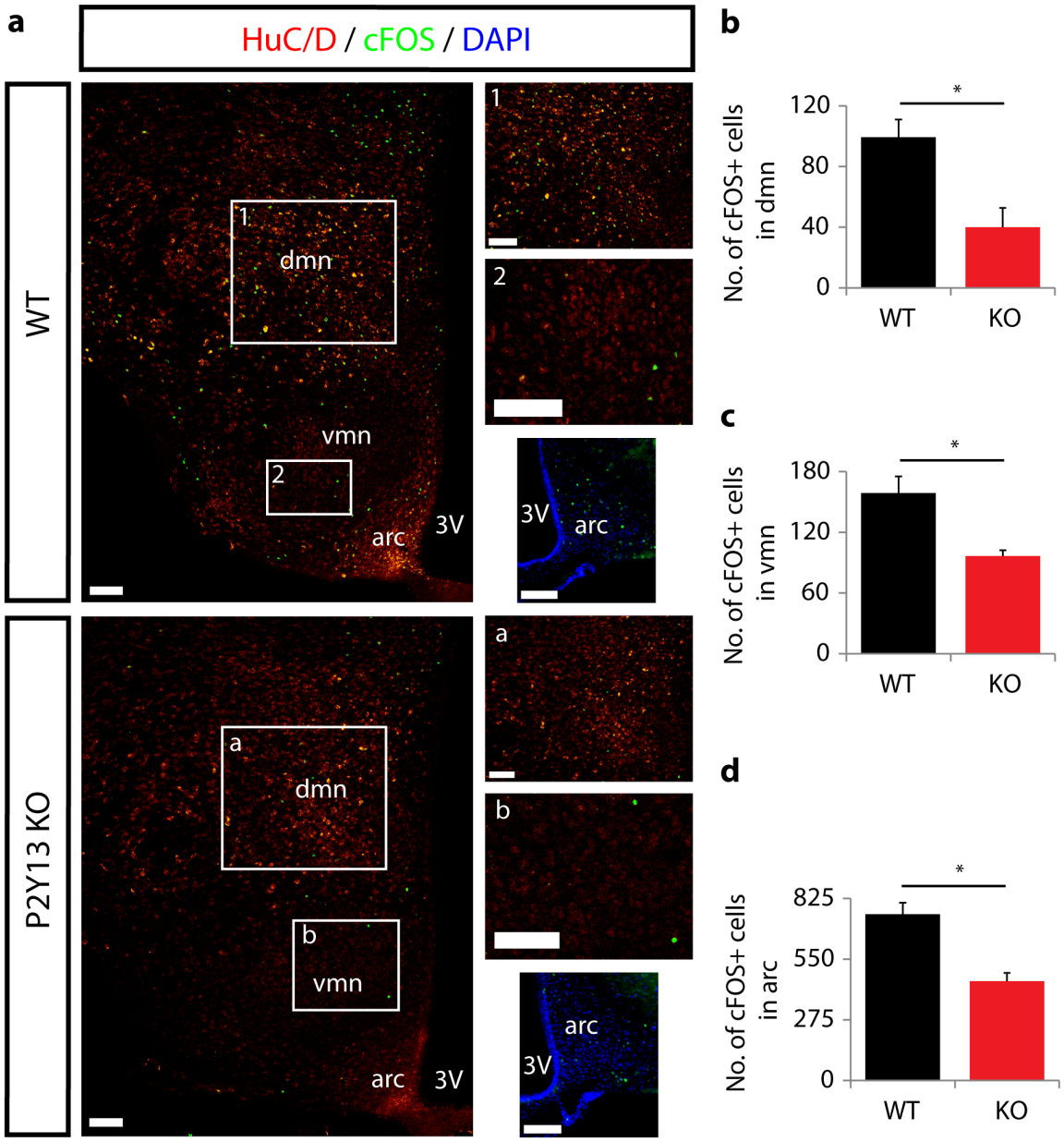

Figure 29: Decreased neuronal activity in hypothalamic nuclei of mutant mice. a: Analysis of immunofluorescence for c-Fos (green), HuC/D (red) and DAPI (blue) in the dmn, vmn and arc of adult WT and KO mice. In contrast to analysis of confocal images (Leica TCS SP5 II) in dmn and vmn, analysis of arc was performed in fluorescence images taken with the Keyence BZ-9000 II microscope. **b:** Quantitative evaluation of c-Fos+ cells in the dmn corresponding to **a** (close-up images labeled with 1 in the upper panel and a in the lower panel, total number of cells, 4 sections per animal, n=3-4). **c:** Quantification of c-Fos-labeled cells in the vmn corresponding to **a** (close-up images labeled with 2 in the upper panel and b in the lower panel, total number of cells, 3 sections per animal, n=3-4). **d:** Quantification of fluorescence images of arc corresponding to **a** (total number of cells, 4-5 sections per animal, n=3-4. Bar graphs represent means ± SEM. *p<0.05, significant relative to control. 3V, third ventricle; arc, arcuate nucleus; dmn, dorsomedial nucleus; me, median eminence; vmn, ventromedial nucleus. (Scale bars, 100 µm)

2.3 The $P2Y_1$ receptor and the $P2Y_{13}$ receptor – Co-Players in the control of adult neurogenesis?

This thesis provides strong evidence for direct involvement of the $P2Y_{13}$ receptor in the control of adult hippocampal and hypothalamic neurogenesis. Several lines of evidence indicate an antagonistic impact of the $P2Y_1$ receptor and the $P2Y_{13}$ receptor in controlling different cellular mechanisms, including axonal elongation in primary hippocampal neurons (del Puerto et al., 2012), insulin release in pancreatic beta cells (Amisten et al., 2010) and nociceptive signaling (Malin and Molliver, 2010). The $P2Y_1$ receptor has in addition been functionally implicated in the control of adult neurogenesis. The receptor is expressed on cultured neural stem cells derived from the mouse SVZ, mediates elevations in intracellular calcium, and controls cell proliferation in these cultured stem cells (Mishra et al., 2006). Moreover, in vivo studies showed that infusion of a selective $P2Y_1$ receptor antagonist reduced neurogenic proliferation in the SVZ (Suyama et al., 2012) whereas ventricular infusion of $P2Y_1$ receptor agonists slightly promoted the expansion of progenitor cells and neuroblasts in the SVZ (Boccazzi et al., 2014). In vitro hippocampal progenitor cell proliferation is enhanced by $P2Y_1$ receptor-mediated purinergic signaling (Cao et al., 2013). The $P2Y_1$ receptor is also expressed in hypothalamic nuclei (Bjelobaba et al., 2015). Glucose-sensing by tanycytes involves $P2Y_1$ receptor action (Frayling et al., 2011) and infusion of stable $P2Y_1$ receptor agonists or antagonists enhanced or decreased food intake in vivo, respectively (Kittner et al., 2006). Moreover, food restriction led to decreased expression levels of the $P2Y_1$ receptor in the hypothalamus of rats (Seidel et al., 2006). Together these findings are indicative of a potential antagonistic action of the nucleotide receptors $P2Y_1$ and $P2Y_{13}$ in the control of adult neurogenesis.

2.3.1 Analysis of *P2ry1* knockout mice

To address the imposing question on the role of the $P2Y_1$ receptor as a potential antagonist of the $P2Y_{13}$ receptor in adult hippocampal and hypothalamic neurogenesis, progenitor cell proliferation and neuronal activity was analyzed in *P2ry1*-depleted mice.

2.3.1.1 Deletion of *P2ry1* does not alter levels of progenitor cell proliferation but decreases neuronal activity in the adult dentate gyrus

Mice were injected with BrdU three times a day at 2 h interval for three consecutive days and progenitor cell proliferation was analyzed 2 h after the final BrdU pulse (Figure 30b, f). In the adult dentate gyrus quantification of BrdU-labeled cells did not reveal changes in progenitor

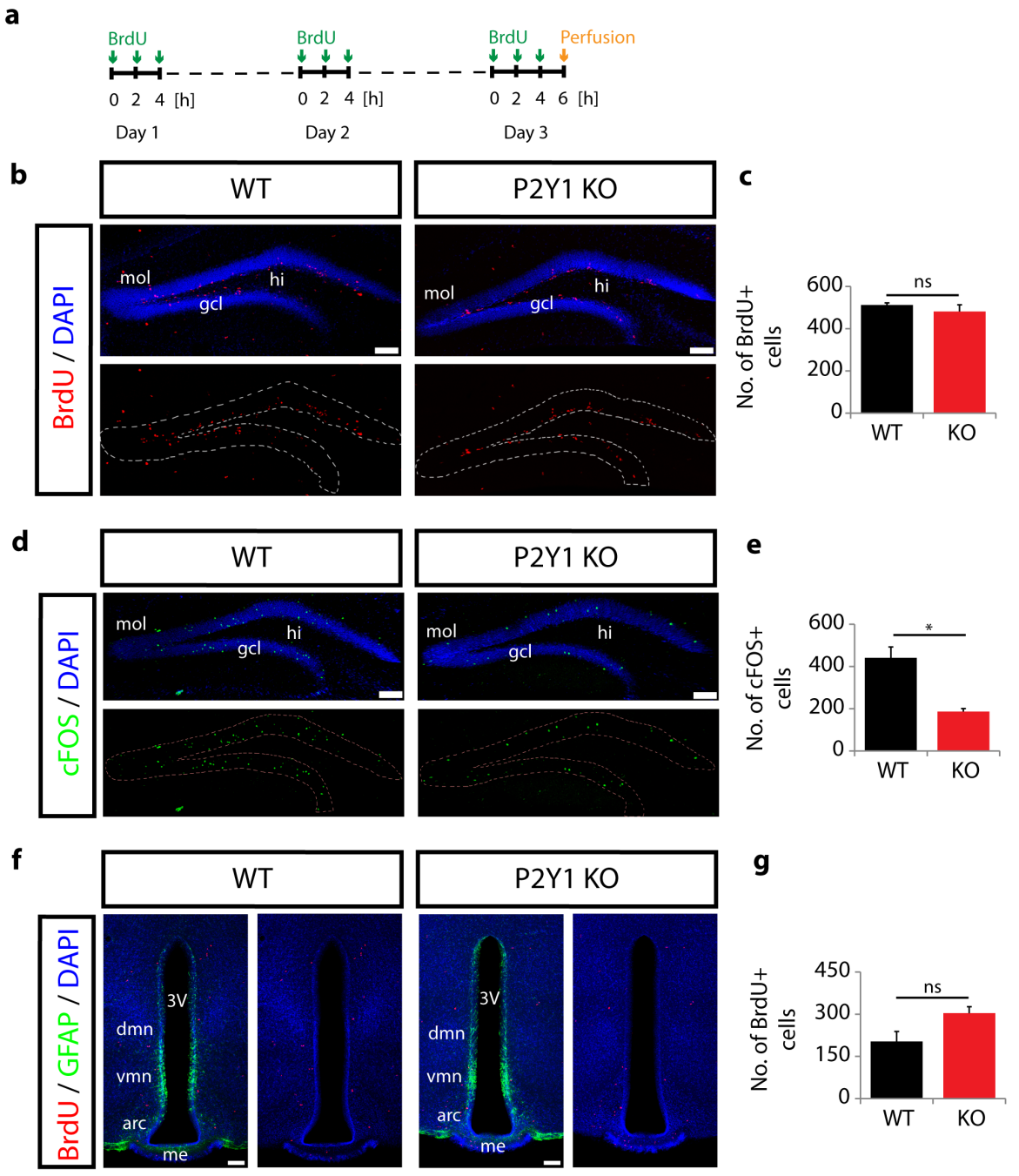

Figure 30: Analysis of progenitor cell proliferation and neuronal activity in *P2ry1* KO mice. a: Schematic overview depicting the BrdU injection protocol for analysis of progenitor cell proliferation

in the adult hippocampal and hypothalamic neurogenic niche. **b:** Analysis of fluorescence for BrdU (red) and DAPI (blue) in the DG of WT and KO mice **c:** Quantification of BrdU+ cells in the DG of WT and mutant mice corresponding to **b** (total number of cells, five sections per animal, n=5-6). **d:** Immunolabeling for c-Fos (green) and DAPI (blue) in the adult DG. **e:** Quantitative evaluation of c-Fos-labeled cells corresponding to **d** (total number of cells, five sections per animal, n=4). **f:** Immunostaining for BrdU (red), GFAP (green) and DAPI (blue) at the third ventricle in the adult hypothalamus of WT and KO mice. **g:** Quantification of BrdU+ cells corresponding to **f** (total number of cells, 5-6 sections per animal, n=4). 3V, third ventricle; arc, arcuate nucleus; dmn, dorsomedial nucleus; gcl, granule cell layer; hi, hilus; me, median eminence; mol, molecular layer; vmn, ventromedial nucleus. Bar graphs represent means ± SEM. *$p<0.05$, significant relative to control. Confocal images were taken with a Leica TCS SP5 II microscope. (Scale bars, 100 μm)

cell proliferation between WT and KO mice (Figure 30c). However, quantification of c-Fos+ cells (Figure 30d) as a marker for neuronal activity disclosed a decrease of 42% of the number of c-Fos-labeled cells in the adult DG of *P2ry1* mutant mice (Figure 30e). BrdU-labeling was also analyzed at the third ventricle (Figure 30f) but the quantitative evaluation of BrdU-labeled cells did not show significant differences between WT and mutant mice (Figure 30g).

Taken together these data, obtained with the respective knockout mice, provide no support for the direct involvement of the $P2Y_1$ receptor in the control of progenitor cell proliferation in the hippocampal and hypothalamic neurogenic niches. Moreover, no clear evidence for an antagonizing mechanism of the $P2Y_1$ receptor and the $P2Y_{13}$ receptor in the control of adult neurogenesis could be obtained. The analysis of c-Fos+ cells suggests, that at least neuronal activity in the hippocampal dentate gyrus might be controlled by antagonistic purinergic mechanisms, balancing the activation of ATP-sensitive, activity-increasing $P2Y_1$ receptors and ADP-sensitive, activity-decreasing $P2Y_{13}$ receptors. The nucleoside triphosphate diphosphohydrolase NTPDase2 could play a balancing role in this.

3 Discussion

3.1 The ectonucleotidase NTPDase2 and the purinergic receptor $P2Y_{13}$ are major regulators of adult hippocampal neurogenesis

In this thesis functional implications of purinergic signaling mechanisms in the control of adult hippocampal neurogenesis were investigated using knockout mouse models for the extracellular nucleotide-hydrolyzing enzyme NTPDase2 and the purinergic P2Y receptors $P2Y_{13}$ and $P2Y_1$. NTPDase2 was identified as the major ectonucleotidase within neurogenic niches of the adult mouse brain. Immunohistochemical analysis in NTPDase2 knockout mice revealed increased expansion of the hippocampal stem cell pool as well as of intermediate progenitor cell types in vivo. However, cell expansion is lost at the level of immature double-cortin-expressing young neurons, paralleled by decreases in the phosphorylation of the survival factor CREB and increases in apoptosis. Deletion of the ADP-sensitive $P2Y_{13}$ receptor increases progenitor cell proliferation, long-term progeny survival and new neuron formation in vivo. This is accompanied by thickening of the granule cell layer, increased CREB phosphorylation in maturing neurons, and elevated neuronal activity in the dentate gyrus. In contrast, a contribution of the $P2Y_1$ receptor in adult hippocampal neurogenesis could not be confirmed in this thesis.

Data presented in this work indicate that extracellular nucleotide signaling plays a pivotal role in the control of hippocampal neurogenesis in the adult rodent brain. My findings implicate that NTPDase2 is functional in balancing extracellular nucleotide concentrations in neurogenic niches thereby controlling purinergic receptor activation and nucleotide-mediated progenitor cell proliferation and expansion in the adult dentate gyrus. Activation of the $P2Y_{13}$ receptor reduces progenitor cell proliferation, new neuron formation, and neuronal activity in the hippocampal neurogenic niche.

3.1.1 NTPDase2 is the major nucleotide-hydrolyzing enzyme within the two major neurogenic niches

Various cell surface-located enzymes in the adult mouse brain are capable of hydrolyzing extracellular nucleotides, thereby controlling the availability of purinergic receptor ligands and

modulating or terminating purinergic signaling pathways (Abbracchio et al., 2009). Highest expression levels of the AMP-hydrolyzing ecto-5'-nucleotidase have been allocated to the caudoputamen and the adjacent olfactory tubercle (Langer et al., 2008). Ecto-nucleotide pyrophosphatase/phosphodiesterases (E-NPPs) are mainly associated with microglia and brain vessels, including microvessels and large brain vessels (Langer et al., 2008), neuronal cell bodies in the cortex, hypothalamus, thalamus and hippocampus, and cells of the choroid plexus (Bjelobaba et al., 2006). However, in neurogenic niches, catalytic activity for both subtypes was low or absent (Langer et al., 2008). Alkaline phosphatases show highest catalytic activity at an alkaline pH around 9 whereas their catalytic activity at near to neutral pH of 7 to 7.5 can almost be neglected (Langer et al., 2008). The tissue non-specific alkaline phosphatase (TNAP) is the only isoform expressed in the mammalian brain (Zimmermann and Langer, 2015). TNAP activity, as measured at alkaline pH, is widely distributed throughout the brain with strong activity reported in the caudoputamen, cerebral cortex, hypothalamus, medulla oblongata, within the subventricular neurogenic niche, along the rostral migratory stream and in the olfactory bulb, but not in the hippocampal dentate gyrus (Langer et al., 2007; Langer et al., 2008). Among all isoforms of E-NTPDases, only NTPDase1, NTPDase2, NTPDase3 and NTPDase8 are typically cell-surface located, and in the rodent brain only NTPDase1-3 were found to be expressed (Zimmermann et al., 2012). NTPDase1 expression is associated with microglia and blood vessel, particularly with endothelial cells, pericytes and smooth muscle cells, and the neuropil in defined brain regions (Braun et al., 2000; Langer et al., 2008). Expression levels are particularly high in the cortex and hypothalamus (Langer et al., 2008). Distinct subpopulations of neurons in the cortex, hippocampus and the hypothalamus express NTPDase3 (Belcher et al., 2006). NTPDase2 represents the only ectonucleotidase that is expressed by the neural stem and progenitor cell population in neurogenic niches (Braun et al., 2003; Shukla et al., 2005; Gampe et al., 2015).

We have previously reported that deletion of NTPDase2 does not alter stem cell morphology in the adult dentate gyrus (Gampe et al., 2015). In line with these findings, immunohistochemical analysis of nestin-EGFP+ NTPDase2-/- mice in the present study did not disclose gross morphological changes in brain morphology or the distribution of nestin-expressing progenitor cells in the hippocampal neurogenic niche between wild type and knockout mice. But how and to which extent does deletion of the ATP/ADP-hydrolyzing enzyme NTPDase2 affect ectonucleotidase activity in the adult brain, particularly in neurogenic niches?

In this thesis enzymehistochemical staining revealed, that ATPase catalytic activity is completely absent from the adult subventricular zone and the hippocampal neurogenic niche in NTPDase2-/- mice. Residual staining on blood vessels presumably results from NTPDase1 expression. This leads to the conclusion that NTPDase2 is the major nucleotide-hydrolyzing enzyme within neurogenic niches of the adult mouse brain. Under physiological conditions, extracellular ATP is present at nanomolar concentrations (Di Virgilio, 2000). Microdialysis in the rat dorsal hippocampus revealed basal ATP levels of around 60 nM (Dona et al., 2016). Inhibition of NTPDase catalytic activity with the specific inhibitor PV4 increased extracellular ATP levels in the rat striatum by 12-fold (Melani et al., 2012). Moreover, extracellular ATP concentrations were increased upon deletion or knockdown of the NTPDase2 (Vandenbeuch et al., 2013; Ho et al., 2013). In line with these studies, deletion of NTPDase2 strongly decreases extracellular ATP hydrolysis throughout the entire brain and abrogates ectonucleotidase activity in stem and progenitor cell rich regions at the lateral ventricles and in the hippocampal dentate gyrus. In turn deletion of NTPDase2 may possibly lead to the accumulation of extracellular ATP in neurogenic niches in situ. In vitro studies in rat cortical astrocytes demonstrate an upregulation of several ectonucleotidases in the presence of high concentrations of ATP (Brisevac et al., 2015). In contrast my data presented in this thesis indicate, that increased extracellular ATP concentrations upon knockdown of *Entpd2* do not lead to upregulation of other ectonucleotidases in situ. In the work of Brisevac et al. (2015) cortical astrocytes were challenged with the unphysiologically high concentration of 1 mM ATP which might have led to non-physiological results.

3.1.2 The hippocampal progenitor pool is expanded in NTPDase2 knockout mice in vivo

In this thesis I could show that depletion of *Entpd2* leads to expansion of the progenitor pool of type-1 and type-2 cells in the adult hippocampal niche, presumably due to increased proliferation. This is supported by the finding that incorporation of BrdU in type-1 cells is disproportionally increased in knockout animals. Self-renewal of stem cells via symmetric division has recently been reported (Bonaguidi et al., 2011). Remarkebly, I could observe horizontal cleavage planes, typical for symmetric cell division (Götz and Huttner, 2005), in NTPDase2 knockout animals. Therefore, symmetric division and self-renewal might reflect one potential explanation for expansion of the type-1 cell pool. However, extensive analysis of cleavage planes of dividing progenitor cells would be needed to further support this hypo-

thesis. Shortening in the length of the cell cycle increased BrdU incorporation in neural stem and progenitor cells (Farioli-Vecchioli et al., 2014) and might reflect another possible explanation for the observed increase in the level of BrdU incorporation in *Entpd2* knockout animals.

3.1.3 Increased apoptosis and microglial phagocytosis might prevent excessive progenitor survival in NTPDase2-/- mice

We have previously reported that the increased progenitor cell proliferation observed in the dentate gyrus of NTPDase2 knockout mice does not necessarily lead to increased survival and increased numbers of mature granule neurons (Gampe et al., 2015). In line with this observation, staging analysis of individual progenitor cell types in the present study suggests, that surplus progenitors are lost at around type-3 stage, reflecting DCX-expressing immature neurons that retain the capacity to proliferate, before they become postmitotic and mature into granule neurons (Kempermann et al., 2004). The majority of cells reaches this transition stage within 3 days and this is reportedly a critical time point for the maturation and survival of precursor cells (Sierra et al., 2010). Microglial phagocytosis contributes to the elimination of apoptotic precursor cells (Sierra et al., 2010). The analysis of caspase-3 positive cells in the dentate granule cell layer I performed in this thesis revealed increased apoptosis in *Entpd2* null mice, further supporting the notion that proliferating progenitors are lost at type-3 cell stage. Expression of functional P2 receptors, including the ADP-activated $P2Y_{12}$ receptor on resting microglia and the UDP-activated $P2Y_6$ receptor on activated microglia, controls activity and motility of microglia (Koizumi et al., 2007; Domercq et al., 2013). My analysis of cells expressing *P2ry12* mRNA suggests, that the number of resting microglial cells is increased in the inner part of the dentate granule cell layer that is orientated towards the hilus, where stem and progenitor cells reside. Microglial NTPDase1 hydrolyzes nucleoside triphosphates (NTPs) to NDPs (Braun et al., 2000) and loss of NTPDase1 was shown to attenuate microglial phagocytosis (Bulavina et al., 2013). Pharmacological blockage of P2 receptors in the work of Bulavina et al. (2013) copied that phenotype and suggests that decreased microglial phagocytosis presumably is the result of missing activation of $P2Y_6$ receptors by NDPs. This further supports the notion that surplus progenitor clearance in NTPDase2 knockout mice is mediated by microglial phagocytosis. Depletion of NTPDase2 would result in the accumulation of NTPs in neurogenic niches that is partially broken down by NTPDase1, expressed on microglia residing in the granule cell layer, and would subsequently act on neighboring $P2Y_6$ receptors, inducing phagocytosis.

Other P2 receptors can contribute to nucleotide-mediated progenitor cell death. Functional $P2X_7$ receptors were found to be located in the adult nestin-EGFP-expressing stem and progenitor cell population of the mouse SVZ and SGL (Messemer et al., 2013; Rozmer et al., 2016). Prolonged activation of $P2X_7$ induced apoptosis in progenitor cells in vitro (Delarasse et al., 2009) whereas deletion of $P2X_7$ resulted in a slight increase in BrdU incorporation in the hippocampal granule cell layer (Csölle et al., 2013). Under physiological conditions the $P2X_7$ receptor is only minimally activated as its activation requires ATP concentration in the higher micromolar range (Zimmermann, 2016). Epileptic seizures lead to the release of large amounts of nucleotides into the extracellular space (Dale and Frenguelli, 2009). After induction of status epilepticus (SE) expression of the $P2X_7$ receptor was highly increased in microglia and dentate granule neurons (Jimenez-Pacheco et al., 2016), and neural precursor cells in the juvenile mouse dentate gyrus (Rozmer et al., 2016). High levels of extracellular ATP induced $P2Y_1$-dependent increases in proliferation and ectopic migration of neural precursor cells that were counterbalanced by activation of $P2X_7$ receptors via induction of apoptosis/necrosis (Rozmer et al., 2016). As stated above, depletion of NTPDase2 would increase extracellular ATP levels. This in turn might induce apoptosis in progenitor cells and might mediate hippocampal microglia activation through activation of $P2X_7$ receptors.

Apart from its functional implication in mediating apoptosis activation of $P2X_7$ receptors can stimulate glutamate release in the CNS (Zimmermann, 2016). Glutamate-dependent neuronal hyperexcitation impaired hippocampal neurogenesis (Sierra et al., 2015). Sierra et al. injected low doses of kainic acid, a glutamate receptor agonist, in the dentate gyrus to model neuronal hyperactivity without hippocampal pathology. In this model, stem cell proliferation was strongly increased, however long term neurogenesis was impaired even in the absence of seizures (Sierra et al., 2015). ATP-induced activation of $P2X_7$ receptors might increase glutamate release in the hippocampal neurogenic niche in *Entpd2* null mice. This might boost progenitor cell proliferation, however at the same time impairing long-term progeny survival.

3.1.4 Neuroblasts in *Entpd2* null mice loose trophic support by survival factors

Stem and progenitor cell proliferation is strongly increased in NTPDase2 knockout animals. However, at the same time internal regulatory mechanisms might prevent surplus progenitor survival, presumably through induction of apoptosis and microglial phagocytosis. This raises the question which could be the potential mechanism underlying increased progenitor cell

death in *Entpd2* null mice? Phosphorylation of CREB is associated with structural maturation (Jungenitz et al., 2014), survival, and integration of DCX-positive neuroblasts (Jagasia et al., 2009). CREB phosphorylation in the dentate gyrus is transient and overlaps with DCX expression (Merz et al., 2011). The present study demonstrates that levels of phosphorylated CREB in DCX positive cells are reduced upon deletion of *Entpd2*. This further supports the notion that in NTPDase2 knockout mice type-3 cells loose trophic support by survival factors and therefore undergo increased apoptosis which presumably induces microglial phagocytosis. At present it is not clear which factors could in fact contribute to maintenance of the increased progenitor cell pool and might be missing in the NTPDase2 KO model. Different exogenous stimuli have been reported to positively affect progenitor cell proliferation and/or survival including running (Kobilo et al., 2011; Garrett et al., 2012) and physical exercise (Fabel et al., 2009), environmental enrichment (Kempermann et al., 1997), and social interaction (Lieberwirth and Wang, 2012). Also growth factor signaling of the neurotrophin family such as BDNF (brain-derived neurotrophic factor) was shown to promote adult neurogenesis (Pencea et al., 2001; Scharfman et al., 2005). It might be possible that these stimuli are missing in the underlying experiments and that they might have positive effects on neuroblast survival in *Entpd2* depleted mice.

In conclusion this work provides strong evidence that NTPDase2 is the major ectonucleotidase within the two major neurogenic niches of the adult mouse brain. Under basal conditions NTPDase2 is functional in balancing extracellular nucleotide concentrations and therefore acts as a homeostatic regulator of neural progenitor cell proliferation and expansion.

3.1.5 The ADP-sensitive $P2Y_{13}$ receptor functions as a negative regulator of adult hippocampal neurogenesis in vivo

This work provides strong evidence that NTPDase2 regulates neural progenitor cell proliferation and expansion presumably by balancing extracellular NTP and NDP concentrations and subsequent activation of either pro-mitotic acting receptors or anti-mitotic acting receptors. In turn both ATP and ADP receptors could contribute to the control of neurogenesis in the dentate gyrus. Increasing evidence suggests that ATP-induced activation of the $P2Y_1$ receptor promotes progenitor proliferation and expansion in neurogenic niches. Studies in acute brain slices revealed increased intracellular Ca^{2+} levels upon ATP-mediated $P2Y_1$ receptor activation in mouse SVZ B1 cells (Lacar et al., 2012). Ventricular infusion of ATP or ADPβS promoted

$P2Y_1$ receptor-dependent progenitor cell proliferation and expansion in the adult SVZ in situ (Suyama et al., 2012; Boccazzi et al., 2014). Moreover, hippocampal progenitor cell proliferation was enhanced by $P2Y_1$ receptor-mediated purinergic signaling in vitro (Cao et al., 2013). Little is known about neurogenic effects mediated by P1 adenosine receptor subtypes. Neurogenesis was shown to be increased in cultured mouse fetal midbrain-derived neural precursor cells upon adenosine stimulation (Delic and Zimmermann, 2010). In postnatal neurogenesis, A1 receptor activation attenuated neuronal differentiation but promoted astrogliogenesis of neurosphere cultures derived from the adult SVZ (Benito-Munoz et al., 2016).

How could ADP-induced purinergic signaling affect the neural progenitor cell pool in the dentate gyrus? ADP stimulation of cultured vascular endothelial cells induced cell cycle arrest in S-Phase, inhibited cell proliferation and induced apoptosis in these cells (Wang et al., 2014b). This suggests that ADP-receptor activation could mediate anti-mitotic effects in progenitor cells in the hippocampal neurogenic niche. Upon deletion of *Entpd2* extracellular ATP levels possibly increase at the expense of extracellular ADP levels. If ADP-receptor activation in the dentate gyrus exerts anti-mitotic effects this should be decreased in *Entpd2* null mice. Moreover, in ADP-receptor knockout mice anti-mitotic effects should be reverted.

Which ADP-sensitive receptor subtype could be involved in the control of hippocampal neurogenesis? The $P2Y_{13}$ receptor is expressed in SVZ-derived neural precursor cells (Grimm et al., 2010) and the Allen Brain Atlas allocates high levels of *P2ry13* mRNA to neurogenic regions, particularly the SGL of the dentate gyrus. Therefore the $P2Y_{13}$ receptor would be a candidate. In this study I could show for the first time that the $P2Y_{13}$ receptor is highly involved in the control of adult hippocampal neurogenesis. My results strongly suggest that the $P2Y_{13}$ receptor attenuates adult neurogenesis in the adult dentate gyrus of mice under basal conditions. I could demonstrate that upon deletion of the receptor, progenitor cell proliferation and survival, as well as neuron formation were highly increased. The constant increase of supply of newborn cells to the dentate granule cell layer results in thickening of granule cell layers in knockout animals. Quantification of BrdU positive cells in the hilus of wild type and knockout mice revealed no difference in total cell numbers at all time points analyzed. Therefore ectopic proliferation or migration of precursor cells can be excluded. This finding further suggests that deletion of *P2ry13* presumably does not affect proliferation rates of other proliferative cell types such as NG2 glia in the hilar region of the dentate gyrus. Together, these

findings are highly indicative for a negative regulatory role of the ADP-sensitive $P2Y_{13}$ receptor in adult hippocampal neurogenesis.

3.1.6 Potential mechanism underlying increased progenitor cell proliferation and survival in *P2ry13* knockout mice in vivo

How could this ADP receptor affect neural progenitor proliferation and survival and which could be the intracellular signaling cascade induced upon ADP-binding to the receptor? Purinergic signaling controls glycogen synthase kinase 3β (GSK3β) function (Neary and Kang, 2006) and studies in cerebellar granule neurons revealed that GSK3 signaling depends on $P2Y_{13}$ receptor activation (Perez-Sen et al., 2015). The regulation of skin pigmentation and melanogenesis by melanocortins was shown to involve the cAMP pathway and GSK3β-signaling (Khaled et al., 2002). In B16 melanoma cells cAMP decreased phosphorylation of GSK3β which in turn stimulated its activity (Khaled et al., 2002). The G_i-protein-coupled $P2Y_{13}$ receptor inhibits adenylate cyclase activity which leads to reduced formation of intracellular cyclic AMP (cAMP) (Abbracchio et al., 2006). Upon deletion of *P2ry13* levels of intracellular cAMP should accumulate which in turn might stimulate GSK3β intracellular signaling. Notably, GFAP promoter-driven overexpression of GSK3β in neural precursor cells during dentate gyrus development copies parts of the phenotype of *P2ry13* knockout mice, including increased number of precursor cells including DCX+ neuroblasts, higher numbers of mature granule neurons, and a higher dentate gyrus volume in transgenic mice (Jurado-Arjona et al., 2016). However, in contrast to my findings in *P2ry13* knockout mice, no changes in progenitor proliferation, differentiation and maturation were observed in GFAP/GSK3β-overexpressing mice. The authors attribute changes in neurogenesis to an expansion of the slow proliferating stem and progenitor cell pool in transgenic mice. I could not detect expansion of the type-1 cell pool in $P2Y_{13}$ receptor knockout mice in this thesis. My data suggest that the increased BrdU incorporation into the progenitor cell pool of *P2ry13* KO mice 2 h and 3 d after BrdU injection is mainly due to enhanced proliferation of amplifying progenitor type-2 cells and type-3 neuroblasts. Further studies on expression levels and phosphorylation states of second messenger molecules via Western blot analysis would be needed, to unravel the molecular mechanism underlying the purinergic control of adult hippocampal progenitor proliferation by $P2Y_{13}$ receptors and to confirm potential implications of GSK3β activity in this context.

As discussed earlier, maturation, survival and integration of DCX-positive neuroblasts highly depends on transient CREB expression and phosphorylation in this cell type (Jagasia et al., 2009). I could demonstrate that levels of phosphorylated CREB in the DCX-expressing cell population are increased in *P2ry13* null mice. The notion that under physiological conditions, $P2Y_{13}$ receptor activation reduces cell survival is further supported by this finding. Surplus generation and later selection for long-term survival is a general principle of hippocampal neurogenesis (Kempermann et al., 2003). Two critical periods of survival have been reported: one main period in the first four days at the transition to the neuroblast state (Sierra et al., 2010) and a second, 1-3 weeks after birth of a young immature neuron, dependent upon synaptic integration (Tashiro et al., 2006). A slight drop in the net increase in progenitor cell proliferation was observed in my experiments 3 d after BrdU injection (40% increase in BrdU in knockout animals 2 h after injection versus 30% increase in BrdU in knockout animals 3 d after injection). This is overlapping with the first critical wave of apoptosis. However, the duplication of BrdU levels in knockout animals by four weeks suggests that surplus progenitor cells pass the second selection process and survive and integrate into local neuronal circuits.

Apoptosis-induced microglial phagocytosis is one potent regulator of adult neurogenesis in the hippocampal dentate gyrus (Sierra et al., 2010). One might assume that increased cell survival in *P2ry13* depleted mice correlates to reduced levels of apoptosis. Increased levels of apoptosis, as revealed by analysis of caspase-3 positive cells, were detected in *P2ry13* knockout mice. However, this could obviously not compensate for the net surplus of progenitor cell proliferation and survival. Of note, Abiega et al. (2016) recently reported that microglial phagocytic efficiency strongly depends on apoptosis/microglial phagocytosis coupling that is mediated by ATP microgradients released by apoptotic cells. Massive ATP release under pathological conditions such as mesial temporal lobe epilepsy (MTLE) led to uncoupling of apoptosis and microglial phagocytosis and to an accumulation of apoptotic newborn cells in the hippocampal neurogenic niche that was not associated with decreased survival of progenitor cells but due to delayed cell clearance by microglia (Abiega et al., 2016). Expression of the $P2Y_{13}$ receptor in the brain was also allocated to microglia (von Kügelgen, 2006). Moreover, in cultured dorsal spinal cord microglia, the $P2Y_{13}$ receptor was shown to mediate intracellular Ca^{2+} increases (Zeng et al., 2014). Further studies would need to be performed to examine whether deletion of *P2ry13* alters microglial morphology, distribution and/or behavior of microglia and whether this might in turn affect microglial phagocytic efficiency and/or hippocampal neurogenesis.

3.1.7 Progenitor cell proliferation and survival is still increased in aged *P2ry13* knockout animals, however, to a lower extent

It is known that the amount of neurogenesis strongly depends on the age of the animal (Encinas and Sierra, 2012). Lineage tracing experiments suggested that activated radial-glia-like stem cells loose their stem cell capabilities and differentiate into astrocytes after a few rounds of asymmetric cell division, resulting in a decline of the hippocampal stem cell pool (Encinas et al., 2011). In this model increased activation of neural stem cells would lead to an initial boost of neurogenesis, however on the long run, neurogenesis would be attenuated, which could explain age-related decreases in neurogenesis (Encinas et al., 2011). To address the question whether increased neurogenesis in *P2ry13* knockout animals might alter progenitor cell proliferation and survival in aged animals, 6 month old wild type and knockout mice were analyzed. My data suggest that increased progenitor cell proliferation and survival in *P2ry13* null mice persists during aging. 2 h and 28 d after injections more BrdU-labeled cells were found in 6 month old knockout animals compared to age-matched wild type controls. However, whereas in young knockout mice the number of BrdU-labeled cells almost doubled by four weeks, only 28% more cells were observed in old knockout animals. Increased activation of the neural stem cell population in young knockout animals might lead to a faster exhaustion of the progenitor cell pool which could explain this observation in old mice. However, this was not examined in the present study and further experiments would be needed to prove this hypothesis. Another possible explanation could relate to the survival rate of amplifying progenitor cells in young and old knockout animals. Increased levels of apoptosis in older animals would also result in reduced levels of mature neurons. Immunolabeling of cells with BrdU, cleaved caspase-3 and cell type-specific markers and/or lineage tracing experiments would be needed to elaborate on this observation.

3.1.8 Heterogeneity between dentate gyrus blades differently affects neurogenesis in suprapyramidel blades and infraprymidal baldes

Differences between dentate gyrus blades concerning dendritic length and spine density, abundance and ratio of cell types and cell density, and also connectivity were described (Schmidt et al., 2012). However, extensive studies addressing the functional differences of dentate gyrus blades are still missing. My finding that neurogenesis was differentially affected in the suprapyramidal and infrapyramidal blade of the dentate gyrus is in line with data

describing strong differences in neurogenesis along the transverse axis (Snyder et al., 2012). Cell proliferation was found to be initially higher in the infrapyramidal blade than in the suprapyramidal blade, however decreased survival in the infrapyramidal blade compensated for that and resulted in similar numbers of neurons in both blades (Snyder et al., 2012). In this thesis I showed that the number of BrdU-labeled cells was higher in knockout animals as compared to the wild type in both dentate gyrus blades at all time points analyzed. However, in contrast to the findings of Snyder et al. (2012), proliferation rates 2 h after BrdU injection were higher in the suprapyramidal blade than in the infrapyramidal blade. Additionally, more BrdU-labeled and thus surviving cells were found in the suprapyramidal blade in wild type and knockout animals by four weeks. In contrast to my work performed in mice, Snyder et al. used adult Sprague Dawley rats for their experiments. It is possible that differences in neurogenesis across the transverse axis reflect species-dependent differences in blade heterogeneity. Other evidence for blade heterogeneity comes from experiments with enriched environment and chronic stress. Enriched environment increased neurogenesis within the dorsal dentate gyrus whereas chronic stress decreased neurogenesis primarily within the ventral dentate gyrus (Tanti et al., 2012). Even though subregion-specific studies of neurogenesis along the transverse axis are missing in this context, it might also be possible that differences in external factors such as housing or animal handling could explain the discordance between studies.

3.1.9 Increased neuronal activity in *P2ry13* knockout mice might be indicative for improved pattern separation

I could not only show that proliferation and long-term progeny survival are significantly increased in *P2ry13* null mice. Also analysis of neuronal activity revealed a strong increase in c-Fos expression in the dentate gyrus of knockout mice. A recent publication identified the $P2Y_{13}$ receptor as key regulator of presynaptic inhibition of acetylcholine release at the mouse neuromuscular junction (Guarracino et al., 2016). This study supports the notion, that deletion of *P2ry13* might alter neurotransmitter release also in the dentate gyrus. Further experimentation could clarify whether increased neuronal activity in the dentate gyrus of $P2Y_{13}$ receptor knockout mice is neurogenesis-related, resulting from increased neuron formation or whether changes in neurotransmitter release upon deletion of *P2ry13* affect neuronal activity.

Several studies suggest that dentate granule cells in the suprapyramidal blade are more active than in the infrapyramidal blade (Schmidt et al., 2012). In line with these studies, I observed

that c-Fos expression was in general higher in the suprapyramidal blade. In the infrapyramidal blade the expression pattern of immediate early genes did not change upon spatial exploration of a novel environment or solving a maze task (Schmidt et al., 2012). These findings strongly suggest that pattern separation involves activity of granule cells in the suprapyramidal blade, rather than of granule cells in the infrapyramidal blade. Pattern separation is one key function of the dentate gyrus and various studies demonstrated functional implications of adult neurogenesis in pattern discrimination tasks (Leutgeb et al., 2007; Aimone et al., 2014). Higher levels of neurogenesis and neuronal activity in the knockout mice, particularly in the suprapyramidal blade of the dentate gyrus, suggest that *P2ry13* null mice probably show higher rating in hippocampus-dependent and neurogenesis-related learning and memory tasks involving pattern separation such as the radial arm maze, fear contextual discrimination or two-choice discrimination. Additional behavioral experiments using wild type and *P2ry13* knockout littermates could verify this hypothesis.

3.1.10 The expression pattern of *P2ry13* might differ along the dorsoventral axis of the hippocampus

Heterogenity is not only observed along the transverse axis of the dentate gyrus. Increasing evidence suggests that gene expression, connectivity pattern and hippocampal function vary also along the dorsoventral axis (Bannerman et al., 2004; Fanselow and Dong, 2010; Kheirbek et al., 2013). Changes in neurogenesis upon deletion of *P2ry13* seem to be restricted to the dorsal dentate gyrus. In the ventral dentate gyrus progenitor cell proliferation or long-term progeny survival were unaffected in knockout animals. Interestingly, recent work by Jhaveri et al. (2015) identified two distinct heterogeneous subpopulations of stem cells within the hippocampus that were specifically activated by different stimuli. Of note, the distribution, reactivity to neurogenic modulators such as GABA and stress and the gene expression pattern, including those of several neurotransmitter receptors and ion channels, of these subpopulations varied along the dorsoventral axis. Taking into account that deletion of *P2ry13* differentially affects neurogenesis in the dorsal and ventral pole of the hippocampus, one can assume that the expression pattern of purinergic receptors might similarly differ along the dorsoventral axis, and that the $P2Y_{13}$ receptor shows higher expression levels in the dorsal pole. In turn, this would suggest an involvement of the $P2Y_{13}$ receptor in dorsal pole-related spatial learning and memory (Moser et al., 1995), rather than anxiolytic behavior, to which the ventral pole has been related to (Kjelstrup et al., 2002).

In summary, I could substantiate that purinergic signaling mechanisms contribute to the regulation of adult neurogenesis in the rodent hippocampal neurogenic niche in vivo. For the first time, the $P2Y_{13}$ receptor was identified as a key mediator of adult hippocampal neurogenesis. While most signaling cues identified to date result in stimulation of neurogenesis, ADP acting at the $P2Y_{13}$ receptor is an example of a neurogenesis-attenuating cue, thus contributing to the homeostasis in the adult hippocampal neurogenic niche. The results obtained in *P2ry13* null mice are also highly indicative of a functional involvement of the receptor in hippocampus-dependent learning and memory such as pattern separation. But this would require further experimentation.

3.1.11 Deletion of the $P2Y_1$ receptor does not alter progenitor cell proliferation in the hippocampus in vivo

In this work I provide strong evidence that NTPDase2 regulates neural progenitor cell proliferation and expansion presumably by balancing extracellular nucleotide concentrations. Upon release, ATP is rapidly broken down by the NTPDase2. In turn, activation of either pro-mitotic acting ATP-sensitive receptors or anti-mitotic acting ADP-sensitive receptors would control levels of adult neurogenesis in situ. I could identify the ADP-sensitive $P2Y_{13}$ receptor as key mediator of adult hippocampal neurogenesis, attenuating progenitor cell proliferation and survival under basal conditions. The $P2Y_1$ receptor is activated by ADP but also by ATP in rodents (Zimmermann, 2016). Previous studies demonstrated that $P2Y_1$ receptor activation, presumably mediated by ATP, enhanced progenitor cell proliferation and expansion in the SVZ and DG in vitro (Mishra et al., 2006; Grimm et al., 2009; Cao et al., 2013) and in the SVZ in vivo (Suyama et al., 2012; Boccazzi et al., 2014). These studies suggest that the $P2Y_1$ receptor might boost progenitor cell proliferation in the dentate gyrus in situ. However, up to date in vivo studies on the functional role of $P2Y_1$ in the control of adult hippocampal neurogenesis are missing. Further evidence for an antagonistic involvement of $P2Y_1$ and $P2Y_{13}$ receptors in the control adult hippocampal neurogenesis comes from experiments in various other cellular mechanisms such as axonal elongation (del Puerto et al., 2012), insulin release in pancreatic beta cells (Amisten et al., 2010) and nociceptive signaling (Malin and Molliver, 2010), all suggesting an antagonistic action of $P2Y_1$ and $P2Y_{13}$ receptors.

BrdU-labeling experiments in the present in vivo study did not reveal changes in progenitor cell proliferation in the hippocampal neurogenic niche following deletion of the $P2Y_1$ recep-

tor. Although in vitro systems resemble to some extent in situ conditions, limitations of the neurosphere culture system, particularly concerning changes in gene expression profile of progenitor cells and sensitivity to methodological variations have been reviewed in detail (Reynolds and Rietze, 2005; Jensen and Parmar, 2006; Pastrana et al., 2011). Therefore the comparability of in vitro model systems to the situation in situ is questionable. The adult neurogenic niche provides a highly complex microenvironment composed of diverse cell-to-cell contacts and interactions of stem and progenitor cells with extracellular matrix proteins or secreted molecules to regulate quiescence or activation of stem cells (Urban and Guillemot, 2014). Moreover, each neurogenic niche displays unique features including niche architecture or contact of stem and progenitor cells to blood vessels and the cerebrospinal fluid in periventricular niches (Urban and Guillemot, 2014). Hence, purinergic signaling may underlie different regulatory mechanisms in different neurogenic niches in vivo and this could account for divergent results of progenitor cell proliferation in the subventricular zone and the dentate gyrus.

3.1.12 Compensatory mechanisms might prevent phenotypic changes in neurogenesis in *P2ry1* depleted mice

Deletion of genes does not necessarily result in phenotypic changes, presumably due to compensatory changes in gene expression of functionally related proteins or regulatory network changes (Kim et al., 2015). Deletion of *P2ry1* may lead to upregulation of closely related purinergic receptors such as the ATP/UTP-sensitive $P2Y_2$ receptor, the UTP-sensitive $P2Y_4$ receptor (Zimmermann, 2016) or ATP-sensitive P2X receptors that might compensate phenoytic effects of *P2ry1* deletion. Activation of the $P2Y_2$ receptor increases in vitro progenitor cell proliferation in the presence of growth factors (Mishra et al., 2006). Semi-quantitative Western blot analysis or real-time PCR experiments would be needed to prove this hypothesis. Compensatory mechanisms resulting from global knockout could be limited by cell-specific deletion of the receptor. Using newly generated floxed $P2Y_1$ mice crossed to astrocyte-specific, tamoxifen-inducible Cre DNA recombinase (GLAST-$CreER^{T2}$) mice (Bohn et al., 2015) would allow to selectively knockdown *P2ry1* in the glial-like stem cell population and to limit compensatory mechanisms.

3.1.13 $P2Y_1$ and $P2Y_{13}$ receptors antagonistically affect neuronal activity in the dentate gyrus

Previous studies reported that $P2Y_1$ receptor activation mediated glutamate exocytosis in cultured astrocytes (Domercq et al., 2006; Zeng et al., 2008). Thus, deletion of the $P2Y_1$ receptor might alter neurotransmitter release that might in turn impact neuronal activity. Indeed, neuronal activity in the adult dentate gyrus, as assayed via expression of the immediate early gene c-Fos, was significantly decreased in $P2Y_1$ knockout mice. Progenitor cell proliferation was unchanged between wild type and $P2Y_1$ knockout mice. However, whether deletion of $P2Y_1$ affected long-term progeny survival and/or neuron formation was not examined in the present work. Decreased levels of surviving progenitor cells and mature neurons in knockout animals could also account for decreased neuronal activity. Additional BrdU-labeling experiments would be needed to further support this hypothesis.

Recent work by Lopatar et al. (2015) suggested an involvement of ATP-induced $P2Y_1$ receptor action on metabotropic glutamate receptor-mediated oscillations in neuronal activity in rat CA3 regions. The authors used dihydroxyphenylglycol (DHPG) as a potent agonist of group I metabotropic glutamate receptors, including mGlu5 that induced adenosine release in CA1 and CA3 regions and ATP release in CA3 regions of the rat hippocampus, respectively. Adenosine binding to A1 receptors decreased DHPG-induced bursting activity whereas oscillations were induced by activation of mGlu5 and $P2Y_1$ receptors (Lopatar et al., 2015). Of note, mGlu5 is also expressed in postnatal neural stem cells in both neurogenic niches (Romano et al., 1995; Shigemoto et al., 1997; Manahan-Vaughan et al., 2003; Di Giorgi Gerevini et al., 2004) where it is involved in the control of progenitor cell proliferation and survival (Di Giorgi-Gerevini et al., 2005). Taking into account that neuronal activity in the dentate gyrus of $P2Y_1$ and $P2Y_{13}$ receptor knockout mice was decreased and increased, respectively, these data might indicate a regulatory function of the antagonistically acting purinergic receptors $P2Y_1$ and $P2Y_{13}$ in the control of neuronal activity in the hippocampus that might in turn control adult neurogenesis.

3.2 The purinergic receptor $P2Y_{13}$ is involved in the control of adult hypothalamic neurogenesis

The second part of this thesis aimed at providing insight into the potential implication of purinergic signaling in the control of adult neurogenesis in the newly discovered neurogenic niche at the third ventricle in the rodent hypothalamus. Using knockout mouse models for the purinergic P2Y receptors $P2Y_{13}$ and $P2Y_1$, functional implications of purinergic receptor signaling were investigated. The nucleotide receptor $P2Y_{13}$ was identified as major contributor to the control of neurogenesis within the hypothalamic neurogenic niche. BrdU-labeling experiments and immunohistochemical analysis in mice lacking *P2ry13* revealed that deletion of the receptor increases progenitor cell proliferation, long-term progeny survival and new neuron formation but decreases neuronal activity in vivo. In contrast, changes in progenitor cell proliferation upon deletion of $P2Y_1$ at the third ventricle could not be confirmed in this thesis.

My data suggest that purinergic signaling, particularly via the ADP-sensitive $P2Y_{13}$ receptor, plays an essential role in controlling adult hypothalamic progenitor cell proliferation and expansion as well as new neuron formation. Findings in this thesis implicate that ADP-mediated activation of $P2Y_{13}$ reduces progenitor cell proliferation at the third ventricle wall and new neuron formation in the murine hypothalamus. Moreover, $P2Y_{13}$ receptor action controls levels of neuronal activity in hypothalamic appetite-regulating circuits.

3.2.1 Purinergic signaling is involved in regions associated with the regulation of food intake and adult hypothalamic neurogenesis

Several studies have demonstrated active neurogenesis in the adult hypothalamus (Kokoeva et al., 2005; Xu et al., 2005; Kokoeva et al., 2007; Perez-Martin et al., 2010; Robins et al., 2013; Batailler et al., 2014; Chaker et al., 2016) and neurogenesis in this region is proposed to be predominantly associated with feeding control (Kokoeva et al., 2005; Li et al., 2012; Lee et al., 2012; McNay et al., 2012; Haan et al., 2013).

Ectonucleotidase expression is widely distributed in hypothalamic regions including expression of ecto-nucleotide pyrophosphatase/phosphodiesterase 1 (NPP1) (Bjelobaba et al., 2006),

as well as expression of NTPDase2 and 3 (Braun et al., 2003; Stojilkovic et al., 2010; Homola et al., 2015). These studies provided the first line of evidence for a direct involvement of purinergic signaling mechanisms in regions associated with adult hypothalamic neurogenesis and feeding control. This is further supported by the notion that a variety of purinergic receptors are present in this regions (Bjelobaba et al., 2015). Cells in the mediobasal hypothalamus, including the ventromedial nucleus, lateral hypothalamic area and the arcuate nucleus express functional $P2X_2$ and $P2X_4$ receptors, P1 receptor subtypes including A_1 and $A_{2,}$ and $P2Y_1$ receptors (Stojilkovic, 2009). In the rat arcuate nucleus $P2X_2$ colocalizes with the orexigenic peptides neuropeptide Y (NPY) and agouti-related protein (AgRP) (Collden et al., 2010). Orexin-expressing neurons that are involved in the control of appetite, express $P2X_2$ (Florenzano et al., 2006) and A_1 receptors (Thakkar et al., 2002).

Two studies in rats demonstrated a contribution of purinergic mechanisms in the regulation of food intake. Intraventricular infusion of specific $P2Y_1$ receptor agonists or antagonists enhanced or decreased food intake, respectively (Kittner et al., 2006). In the arcuate nucleus, food restriction led to decreased expression of the $P2Y_1$ receptor (Seidel et al., 2006). Lateral hypothalamic neurons co-release ATP and GABA in vitro (Jo and Role, 2002). Moreover, upon glucose stimulation, tanycytes release ATP via connexin43 hemichannels and activate $P2Y_1$ receptors, resulting in increases in intracellular Ca^{2+} (Frayling et al., 2011; Orellana et al., 2012). These studies suggest functional implications of purinergic signaling mechanisms in the regulation of food intake and raised the question whether purinergic signaling might be involved in adult hypothalamic neurogenesis.

3.2.2 The $P2Y_{13}$ receptor functions as a negative regulator of hypothalamic progenitor cell proliferation

In the present study, the $P2Y_{13}$ receptor was identified as a central regulator of adult hypothalamic neurogenesis. BrdU labeling experiments demonstrate that upon deletion of *P2ry13*, progenitor cell proliferation is highly increased in periventricular areas, particularly in the median eminence. Moreover, more newborn neurons integrate into hypothalamic nuclei, including the arcuate nucleus and the dorsomedial nucleus. There was a tendency for an increase in the number of newborn neurons also in the ventromedial nucleus of $P2Y_{13}$ receptor knockout mice. But this result was not significant ($p=0.15$). Around 74% of all initially labelled BrdU+ cells were found to be immunopositive for the neuron marker HuC/D in

the wild type, whereas in *P2ry13* knockout animals it was 79%, implicating a high neurogenic capacity of BrdU-labeled progenitors in both genotypes This data fits very well with findings of McNay et al. (2012) that attribute the neurogenic capacity of hypothalamic progenitor cells to 70-80%. Taken together findings in this thesis strongly indicate that the $P2Y_{13}$ receptor functions as an in situ negative regulator also of adult hypothalamic neurogenesis.

Although functional $P2Y_1$ receptors were shown to be expressed in hypothalamic regions involved in neurogenesis (Bjelobaba et al., 2015), no changes in progenitor cell proliferation in the hypothalamic neurogenic niche were observed in the present thesis upon deletion of the $P2Y_1$ receptor. As discussed earlier for the hippocampal dentate gyrus, compensatory mechanisms might prevent phenotypic changes in hypothalamic neurogenesis following deletion of *P2ry1*. However, additional experiments would be needed to verify this hypothesis.

3.2.3 Potential mechanisms underlying purinergic control of adult hypothalamic neurogenesis

Which could be the mechanism underlying increased progenitor cell proliferation and neuron formation in $P2Y_{13}$ receptor knockout mice? The microarchitecture of the hypothalamic neurogenic niche is rather special. Hypothalamic stem and progenitor cells line the third ventricle wall and receive signaling cues either through the cerebrospinal fluid or through the bloodstream. Endothelial cells of the blood-brain-barrier in the median eminence are fenestrated and allow the passive extravasation of blood-derived hormones and nutrients (Yu and Kim, 2012). Therefore one could assume either a direct, central control of hypothalamic neurogenesis or an indirect, peripheral control that could both be mediated by $P2Y_{13}$ receptor action.

Could $P2Y_{13}$ receptor-mediated microglial phagocytosis control hypothalamic neurogenesis? High fat diet induced microglia-mediated inflammation in hypothalamic regions which reduced adult hypothalamic neurogenesis (Li et al., 2012). Microglial-mediated phagocytosis is also one key regulator in the control of adult hippocampal neurogenesis (Sierra et al., 2010) and activity of cultured dorsal spinal cord microglia is tightly controlled by $P2Y_{13}$ receptor activation (Zeng et al., 2014). This indicates a potential role of $P2Y_{13}$ receptor-mediated microglial control of adult hypothalamic neurogenesis. However, it is still to be demonstrated if

the $P2Y_{13}$ receptor is indeed expressed on hypothalamic microglia and how microglial activation in turn controls progenitor cell proliferation and expansion.

As stated above the impact on adult hypothalamic neurogenesis mediated by $P2Y_{13}$ receptor action may also be indirect. Peripheral purinergic receptor activation and subsequent release of circulating blood-derived factors such as nutrients or hormones or release of factors into the cerebrospinal fluid may indirectly influence neurogenesis at the third ventricle. This hypothesis is supported by a study of Pencea et al. (2001), demonstrating that infusion of growth factors into the lateral ventricle increased neurogenesis not only in the subventricular zone lining the lateral ventricle but also in other periventricular areas such as the hypothalamus. Extracellular nucleotides are involved in the regulation of insulin secretion from pancreatic β-cells (Petit et al., 2009) and insulin release was reported to be regulated by antagonistic action of $P2Y_1$ and $P2Y_{13}$ receptors (Amisten et al., 2010). Global knockout of *P2ry13* might alter peripheral glucose metabolism therefore affecting blood-glucose levels and glucose-sensing, mediated by tanycytes (Bolborea and Dale, 2013), which in turn could impact on progenitor cell proliferation and neuron formation. Comparing the impact of central versus peripheral inhibition of the $P2Y_{13}$ receptor via intraventricular or intraperitoneal injection of the specific antagonist MRS2211 could clarify if and to which extent peripheral inhibition of purinergic signaling influences adult hypothalamic neurogenesis.

Induction of changes in the barrier properties at the third ventricle upon deletion of *P2ry13* could also explain changes in progenitor cell proliferation. Tight junctions of β-tanycytes form a barrier between the median eminence and the ventricular cerebrospinal fluid (Peruzzo et al., 2000; Mullier et al., 2010) and between the median eminence and the arcuate nucleus (Rodriguez et al., 2005). However, barrier properties are not static but adapt in response to diet changes such as altered blood-glucose levels to allow a wider distribution of blood-derived factors in periventricular areas (Langlet, 2014). As discussed earlier, glucose-sensing in tanycytes is mediated by ATP release and activation of $P2Y_1$ receptors (Frayling et al., 2011). Experiments analyzing the distribution of a blood-derived dye such as cadaverine-Alexa-Fluor555 that cannot cross the blood-brain-barrier but leaks out of fenestrated vessels in the median eminence and diffuses into the hypothalamic parenchyma, and analysis of the tight junction protein Zo-1 could reveal whether deletion of the $P2Y_{13}$ receptor alters barrier properties at the third ventricle.

3.2.4 $P2Y_{13}$ receptor action might control inhibition of appetite-regulating circuits in the adult murine hypothalamus

Deletion of *P2ry13* decreased neuronal activity as measured by c-Fos expression in the dorsomedial nucleus, the ventromedial nucleus and the arcuate nucleus. This suggests that either more inhibitory new-born neurons are incorporated into hypothalamic nuclei or more inhibitory neurons in appetite-regulating circuits are activated upon deletion of *P2ry13* which in turn leads to overall decreased neuronal activity in hypothalamic neural circuits. These findings suggest that under wild type conditions $P2Y_{13}$ diminishes progenitor cell proliferation, survival and neuron formation and decreases the inhibition of appetite-regulating circuits by new-born inhibitory neurons in the hypothalamus of adult mice. Crossing of $P2Y_{13}$ knockout mice to (*Nestin*)CreER^{T2}_*Rosa26*(EYFP) mice would allow to induce EYFP expression in tanycytes and all their progeny. Taking advantage of this tool, lineage-tracing experiments could unravel where exactly newborn neurons integrate into hypothalamic nuclei, which neurotransmitters they express and whether they differentiate to anorexigenic POMC-expressing neurons, or orexigenic NPY/AgRP-expressing neurons.

3.3 Therapeutic implications of purinergic control of adult neurogenesis

In summary, the data provided in this thesis substantiate the notion that purinergic signaling plays a pivotal role in the control of adult neurogenesis in vivo. I could show that NTPDase2 is the major ectonucleotidase within the two major neurogenic niches of the adult mouse brain. Deletion of this enzyme increases progenitor cell proliferation of type-1 and type-2 cells that is abrogated at the type-3 cell stage, presumably due to lack of support by survival factors and increased apoptosis. Under basal conditions NTPDase2 clears mitogenic extracellular nucleoside triphosphate concentrations and contributes to progenitor cell homeostasis by limiting nucleotide-mediated cell proliferation and expansion. Extracellular ATP might be elevated at the expense of ADP in neurogenic niches of *Entpd2* null mice. This might indicate that purinergic control of adult neurogenesis could implicate both, ATP-sensitive and ADP-sensitive purinergic receptors, acting antagonistically and promoting or blocking neurogenesis, respectively. Based on the analysis of $P2Y_{13}$ knockout mice I could provide strong evidence, for the first time, that activation of the ADP-sensitive $P2Y_{13}$ receptor attenuates progenitor cell proliferation, new neuron formation, and neuronal activity in the hippocampal neurogenic

niche. The $P2Y_{13}$ receptor therefore would function as negative regulator of adult hippocampal neurogenesis in vivo. Moreover, a functional involvement of the $P2Y_{13}$ receptor in the control of neurogenesis in the newly identified hypothalamic neurogenic niche was demonstrated. Activation of the $P2Y_{13}$ receptor dampens progenitor cell proliferation at the third ventricle and survival, maturation and integration of inhibitory neurons into food intake-regulating circuits in hypothalamic nuclei. This suggests a regulatory function of purinergic signaling mechanisms in adult hypothalamic neurogenesis and energy homeostasis.

How could findings on the regulatory function of purinergic signaling mechanisms in the control of adult hippocampal and hypothalamic neurogenesis help to identify or improve therapeutic applications to treat neurological or metabolic disorders or diseases?

The role of adult neurogenesis in neurological disorders and diseases is still poorly characterized and studies are often contradictory (van Doze and Perez, 2012). After traumatic brain injury increased neurogenesis has been reported (Yu et al., 2008; Zheng et al., 2013). Moreover, replacement of dying neurons after ischemic stroke was demonstrated (Arvidsson et al., 2002; Nakatomi et al., 2002). Whereas neurogenesis initially increases at sites of epileptic seizures (Ferland et al., 2002; Jessberger et al., 2005), chronic temporal lobe epilepsy is associated with declined dentate neurogenesis, decreased cognitive function (Hattiangady et al., 2004; Hattiangady et al., 2011) and ectopic neuron formation (Thom et al., 2002). In many neurodegenerative diseases such as Alzheimer's disease, Huntigton's disease or Parkinson's disease alterations in neurogenesis have been implicated. Of note, key components in the progression of these diseases such as α-synuclein, tau and presenilin-1, or huntingtin are involved in the physiological modulation of neurogenesis and brain plasticity (Winner et al., 2011). Alterations in neurogenesis might also contribute to neuropsychiatric disorders such as schizophrenia (Kempermann et al., 2008). Understanding the cellular and molecular mechanisms that guide the progression from a progenitor cell to a functional neuron or glial cell is essential to target neurological disorders with neural stem cell-based therapies via either transplantation of exogenous neural stem and progenitor cells, endogenous stimulation, or reprogramming of these cells. Remarkable success has been achieved on this field (van Doze and Perez, 2012; Braun and Jessberger, 2014). Therapeutic strategies could also involve purinergic signaling mechanisms resulting in either direct stimulation of adult neural stem and progenitor cells or indirect stimulation via the modulation of purine-induced neurotransmitter release. Specific modulation of ectonucleotidase activity and of agonizing or antagonizing

purinergic receptors could represent a promising strategy to promote self-repair or regeneration of the damaged or diseased mammalian brain (Burnstock, 2013).

Emerging evidence suggests that tanycytes at the third ventricle act as chemo-sensory gatekeepers, sensing and implementing signaling cues from the periphery, controlling neuroendocrine output at the median eminence and regulating hypothalamic neurogenesis, which is clearly associated with feeding control and energy metabolism (Bolborea and Dale, 2013; Rizzoti and Lovell-Badge, 2016). Significant postnatal turn-over of appetite-regulating neurons in the arcuate nucleus indicates high plasticity in this region that allows continuous adaptation to changes in diet or energy consumption (McNay et al., 2012). Diet-induced modulation of hypothalamic neurogenesis was reported. Particularly high fat diet induced inflammation that increased progenitor apoptosis, inhibited hypothalamic neurogenesis and was clearly associated with subsequent obesity and chronic metabolic diseases (Li et al., 2012; Lee et al., 2014; Lee et al., 2012; McNay et al., 2012; Valdearcos et al., 2015). Of note, activation of the purinergic receptor $P2Y_1$ in vivo increased food intake in rats (Kittner et al., 2006) and food restriction led to downregulation of the receptor in the rat hypothalamus (Seidel et al., 2006). Pharmacological manipulation of hypothalamic neurogenesis that might also target purinergic signaling, may have therapeutic benefits particularly in the context of metabolic syndrome. Unraveling the cellular and molecular mechanisms of hypothalamic neurogenesis that control peripheral glucose, fat and energy metabolism and to understand how in turn peripheral signaling cues are sensed and integrated by hypothalamic neural stem and progenitor cells, is crucial to therapeutically target hypothalamic neurogenesis and to improve regenerative applications for hypothalamus-relevant metabolic pathologies. The fact that the hypothalamus functions as a central regulator not only in feeding behavior and energy expenditure but also in vital functions such as growth, reproduction, circadian rhythms, blood pressure, mood and stress (Morton et al., 2006; Rizzoti and Lovell-Badge, 2016; Kriegsfeld and Silver, 2006) is pointing at the importance of additional studies that could rule out potential implications of adult hypothalamic neurogenesis in other physiological processes and related pathologies. Purinergic signaling mechanisms in the endocrine system have been widely studied (Burnstock, 2014; Bjelobaba et al., 2015), however, it appears essential to further validate functional implications of purinergic signaling in hypothalamic neurogenesis, controlling neuroendocrine functions.

4 Material and Methods

4.1 Material

4.1.1 Animals

The mouse lines used in this work are listed in Table 1 with original reference.

Table 1: List of mouse lines

Mouse line	Symbol	MGI ID	Original Reference
Wild type	C57BL/6		
Entpd2-/-	Entpd2^{tm1Srob}	MGI:5545886	Vandenbeuch et al., 2013
P2ry1-/-	P2ry1^{tm1Gac}	MGI:2181709	Léon et al., 1999
P2ry13-/-	P2ry13^{tm1Loma}	MGI:4839758	Fabre et al., 2010
Nestin-EGFP	Tg(Nes-EGFP)33Enik	MGI:5523870	Mignone et al., 2004

4.1.1.1 Knockout mouse lines

***Entpd2-/-* mice**

Entpd2 constructs to generate null mice were designed at BIDMC, Harvard University, Boston, USA by Simon C. Robson and Keiichi Enjyoji by deleting the exons I and II, including the entire promoter region. Knockout animals, where the mutant allele is carried on a genetic background mixture of the strains Sv129 and C57BL/6, were then generated by homologous recombination in murine embryonic stem cells at GenOway, Lyon, France.

***P2ry1-/-* mice**

In this mouse line (genetic background C57BL/6) the expression of the functional $P2Y_1$ receptor was blocked by the insertion of a PGK-neo-PolyA-cassette into the cDNA sequence of the *P2ry1* wild type gene at position 3208 bp.

P2ry13-/- mice

In *P2ry13*-deficient mice a neomycin resistance cassette replaced a 1.2-kb fragment containing the first non-coding exon, the only intron and the first 182 bp of the second exon. The $P2Y_{13}$ receptor mutation was crossed into the C57BL/6 genetic background for 10 generations.

4.1.1.2 Reporter mouse lines

Nestin-EGFP mice

This reporter mouse line eases the study of neural stem and progenitor cells. In this mouse line neural stem cells are marked by the expression of the enhanced green fluorescent protein (EGFP). Nestin is an intermediate filament protein that is characteristically expressed by neural stem and progenitor cells in the developing and adult mouse brain. Enhancer elements located in the intronic regions of the nestin gene regulate its expression. EGFP was placed under control of the 5.8-kb promoter and the 1.8-kb second intron, thus matching the arrangement of the regulatory sequences in the nestin gene (Mignone et al., 2004).

4.1.2 Chemicals and reagents

Table 2: List of chemicals, reagents and commercial solutions

Chemical, reagent, solution	Manufacturer
0.9% Sodium chloride	B. Braun, Melsungen, Germany
4' ,6-Diamidin-2'-phenylindoldihydrochlorid (DAPI)	Sigma-Aldrich, Taufkirchen, Germany
β-mercapto ethanol	Promega, Mannheim, Germany
Acetic acid (CH_3COOH)	J.T. Baker, Griesheim, Germany
Acetone	Carl Roth, Karlsruhe, Germany
Acrylamide	Carl Roth, Karlsruhe, Germany
Agarose	Bio & Sell, Feucht, Germany
Albumin Fraktion V (BSA)	AppliChem, Darmstadt, Germany
Ammonium sulfate $(NH_4)_2SO_4$	Sigma-Aldrich, Taufkirchen, Germany

Ammonium sulfide $(NH_4)_2S$	Sigma-Aldrich, Taufkirchen, Germany
Ammonium peroxodisulfate (APS)	Carl Roth, Karlsruhe, Germany
Aqua-Poly/Mount	Polysciences Europe, Eppelheim, Germany
Amersham ECL reagent	GE Lifesciences, Frankfurt am Main, Germany
Adenosine 5'-diphosphate (ADP)	Sigma-Aldrich, Taufkirchen, Germany
Adenosine 5'-monosphate (AMP)	Roche Diagnostics, Mannheim, Germany
Adenosine 5'-triphosphate (ATP)	Sigma-Aldrich, Taufkirchen, Germany
Bis-acrylamide	Carl Roth, Karlsruhe, Germany
Bromodeoxyuridine (BrdU)	Sigma-Aldrich, Taufkirchen, Germany
Bromophenol blue	Sigma-Aldrich, Taufkirchen, Germany
Calcium chloride ($CaCl_2$)	AppliChem, Darmstadt, Germany
Dextran T250	Carl Roth, Karlsruhe, Germany
Donkey serum	Sigma-Aldrich, Taufkirchen, Germany
dNTP mix	Fermentas, St. Leon-Rot, Germany
Ethylenediaminetetraacetic acid (EDTA)	AppliChem, Darmstadt, Germany
Ethylene glycol tetraacetic acid (EGTA)	Sigma-Aldrich, Taufkirchen, Germany
Ethanol	Merck, Darmstadt, Germany
Ethylene glycol	Sigma-Aldrich, Taufkirchen, Germany
Ethidium bromide (EtBr)	AppliChem, Darmstadt, Germany
Formaldehyde 10%, methanol free, Ultra Pure	Polysciences Europe, Eppelheim, Germany
Gene ruler DNA ladder mix	Fermentas, St. Leon-Rot, Germany
Glucose	Sigma-Aldrich, Taufkirchen, Germany
Glycerol	Merck, Darmstadt, Germany
Glycine	AppliChem, Darmstadt, Germany

HEPES	AppliChem, Darmstadt, Germany
Hydrochloric acid (HCl)	Merck, Darmstadt, Germany
Isoflurane (Forene)	Abbott, Wiesbaden, Germany
Ketamine (Ketavet, 100 mg/ml)	Pfizer Pharma, Berlin, Germany
Lead(II) nitrate ($Pb(NO_3)_2$)	Merck, Darmstadt, Germany
Levamisole-hydrochloride	AppliChem, Darmstadt, Germany
Magnesium chloride ($MgCl_2$)	AppliChem, Darmstadt, Germany
Magnesium sulfate ($MgSO_4$)	Merck, Darmstadt, Germany
Maleic acid	AppliChem, Darmstadt, Germany
Manganese(II) chloride ($MnCl_2$)	Merck, Darmstadt, Germany
Methanol	Merck, Darmstadt, Germany
Non-fat dry milk powder	AppliChem, Darmstadt, Germany
Pentobarbital sodium (Narcoren, 16 g/100 ml)	Merial, Hallbergmoos; Germany
Potassium chloride (KCl)	AppliChem, Darmstadt, Germany
Potassium dihydrogen phosphate (KH_2PO_4)	AppliChem, Darmstadt, Germany
Proteinase K	Sigma-Aldrich, Taufkirchen, Germany
Roti Histokitt II	Carl Roth, Karlsruhe, Germany
Sigma Fast BCIP/NBT-buffered substrate	Sigma-Aldrich, Taufkirchen, Germany
Sodium azide (NaN_3)	Merck, Darmstadt, Germany
Sodium bicarbonate ($NaHCO_3$)	Sigma-Aldrich, Taufkirchen, Germany
Sodium citrate	Sigma-Aldrich, Taufkirchen, Germany
Sodium chloride (NaCl)	AppliChem, Darmstadt, Germany
Sodium dodecyl sulfate (SDS)	AppliChem, Darmstadt, Germany
Sodium hydroxide (NaOH)	AppliChem, Darmstadt, Germany

Sodium phosphate dibasic (Na_2HPO_4)	Sigma-Aldrich, Taufkirchen, Germany
Sodium phosphate monobasic (NaH_2PO_4)	Sigma-Aldrich, Taufkirchen, Germany
Sucrose	AppliChem, Darmstadt, Germany
***Taq* DNA Polymerase**	New England Biolabs, Frankfurt am Main, Germany
Tetramethylethylenediamine (TEMED)	Carl Roth, Karlsruhe, Germany
Tissue-tek compound	Sakura Finetek, Staufen, Germany
Trizma base (Tris)	Sigma-Aldrich, Taufkirchen, Germany
Tween20	AppliChem, Darmstadt, Germany
Triton X-100	AppliChem, Darmstadt, Germany
Xylazine (Rompun 2%)	Bayer Vital, Leverkusen, Germany
Xylene cyanol FF	Sigma-Aldrich, Taufkirchen, Germany

4.1.3 Consumables

Table 3: List of consumable materials

Consumable	Manufacturer
Cell culture plates (6 well, 24 well)	BD Falcon, Heidelberg, Germany
Cell culture plates (96 well, flat bottom)	Greiner Bio-One, Frickenhausen, Germany
Cell Strainer (100 µm),	BD Falcon, Heidelberg, Germany
Cover slips (24 x 60 mm)	Diagonal, Münster, Germany
Embedding molds Peel-A-Way®	Polysciences Europe, Eppelheim, Germany
Falcon tubes (15 ml, 50 ml)	Sarstedt; Nümbrecht, Germany
Fine pen needles Omnican F® (1 ml)	B. Braun, Melsungen, Germany
Hydrophobic pen	Dako, Hamburg, Germany
Nitrocellulose	GE, Frankfurt am Main, Germany

Parafilm	Bemis Packaging, Meckenheim, Germany
Pasteur pipettes	Brand, Wertheim, Germany
Perfusion needle Vasufluo®	Dispomed Witt, Gelnhausen, Germany
PCR tubes (0.2 ml, domed cap)	Biozym, Hessisch Oldendorf, Germany
Reaction tubes (1.5 ml, 2 ml)	Sarsted, Nümbrecht, Germany
SafeSeal-Tips (10 µl, 20 µl, 100 µl, 200 µl, 1000 µl)	Biozym, Hessisch Oldendorf, Germany
Serological pipettes CELLSTAR® (1 ml, 5 ml, 10 ml, 25 ml, 50 ml)	Greiner Bio-One, Frickenhausen, Germany
Superfrost plus slides (Menzel Glas)	Thermo Fisher Scientific, Braunschweig, Germany
Syringes (5 ml, 30 ml, 50 ml)	Henry Schein, Berlin, Germany
Tips (2.5 µl, 10 µl, 20 µl, 200 µl, 1000 µl, 5000 µl)	Sarstedt, Nümbrecht, Germany
Whatmann paper	GE Holding, Frankfurt am Main, Germany

4.1.4 Kits

Table 4: List of kits

Kit	Manufacturer
Pierce BCA Protein Assay	ThermoFischer, Darmstadt, Germany

4.1.5 Media and solutions

4.1.5.1 Standard solutions

Phosphate-buffered saline (PBS)	**Tris-buffered saline (TBS)**
137 mM NaCl	0.15 M NaCl
2.7 mM KCl	0.1 M Tris-HCl
8 mM Na_2HPO_4	pH 7.5
2 mM KH_2PO_4	
pH 7.4	

4.1.5.2 Solutions for molecular biology

Lysis buffer	**10x Gitschier buffer**
1.7 µm SDS (sodium dodecyl sulfate)	166 mM ammonium sulfate
100 µg/ml proteinase K	670 mM Tris-HCl, pH 8.8
1x Gitschier buffer	67 mM $MgCl_2$
	50 mM β-mercapto ethanol
	67 µM EDTA
50x Tris-acetate-EDTA (TAE) buffer	**10x DNA-loading dye**
2 M Tris	0.42% (w/v) Bromophenol blue
2 M Acetic acid	0.42% (w/v) Xylene cyanol FF
50 mM EDTA	50% (w/v) Glycerol
pH 8.3	

4.1.5.3 Solutions for histology

Tris-maleate buffer (TM) 50 mM Tris 50 mM Maleic acid	**Tris-maleate-sucrose-buffer (TMS)** 0.25 M Sucrose 50 mM TM 2 mM $MgCl_2$ pH 7.4
TMS-buffered substrate solution 2 mM $Pb(NO_3)_2$ 5 mM $MnCl_2$ 2 mM $MgCl_2$ 50 mM TM 0.25 M Sucrose 3% Dextran T 250 pH 7.4	**Saline-sodium citrate buffer (SSC)** 0.3 M NaCl 0.03 M Sodium citrate pH 7.0
0.2 M Sodium phosphate buffer 154 mM Na_2HPO_4 46 mM NaH_2PO_4	**Tissue cryoprotectant solution (TCS)** 250 ml Glycerol 300 ml Ethylene glycol 450 ml 0.1 M Sodium phosphate buffer pH 6.7

4.1.5.4 Solutions for biochemistry

Homogenization buffer	**4x Sample buffer**
10 mM HEPES	250 mM Tris/HCl
150 mM NaCl	40% Glycerol
1 mM EGTA	8% SDS
0.1 mM $MgCl_2$	0.04% Bromophenol Blue
pH 7.4	pH 6.8
Electrophoresis buffer	**Transfer buffer**
100 mM Tris Base	25 mM Tris
100 mM Glycine	192 mM Glycine
3.5 mM SDS	1 mM EDTA
0.04% Bromophenol Blue	20% Methanol
pH 8.35	0.05% SDS
	pH 8.35

4.1.6 Antibodies

Table 5: List of primary antibodies

Antibody	Host	Order number	Manufacturer	Application and dilution
anti-Actin	rabbit	A2066	Sigma-Aldrich, Taufkirchen, Germany	WB 1:1000
anti-BrdU	rat	OBT0030	AbD Serotec, Düsseldorf, Germany	IHC 1:500
anti-c-Fos	rabbit	sc-52	Santa Cruz, Heidelberg, Germany	IHC 1:500
anti-Cleaved Caspase3 (Asp175)	rabbit	9661	Cell Signaling, Leiden, Netherlands	IHC 1:500
anti-DCX	goat	sc-8066	Santa Cruz, Heidelberg, Germany	IHC 1:200
anti-GFAP	mouse	G-3893	Sigma-Aldrich, Taufkirchen, Germany	IHC 1:500
anti-GFAP	rabbit	G-9269	Sigma-Aldrich, Taufkirchen, Germany	IHC 1:500
anti-GFP	chicken	ab13970	Abcam, Cambridge, United Kingdom	IHC 1:500
anti-HuC/D	mouse	A-21271	Molecular probes (Thermo Fisher Scientific), Dreieich, Germany	IHC 1:500
anti-NeuN	mouse	MAB377	Merck Millipore, Darmstadt, Germany	IHC 1:500
anti-NTPDase1	rabbit	C10F	Jean Sévigny, Quebec, Canada	WB 1:1000
anti-NTPDase2	rabbit	BZ3-B4F	Jean Sévigny, Quebec, Canada	IHC 1:1000 WB 1:1000
anti-NTPDase3	guinea pig	mN3-3I4	Jean Sévigny, Quebec, Canada	WB 1:1000
anti-pCREB (Ser133)	rabbit	9198	Cell Signaling, Leiden, Netherlands	IHC 1:100
anti-Sox2	goat	sc-17320	Santa Cruz, Heidelberg, Germany	IHC 1:50
anti-TNAP	rabbit		gift from Yukio Ikehara, Fukuoka, Japan	WB 1:1000

Table 6: List of secondary antibodies

Antibody	Order number	Manufacturer (Distributor)	Application and dilution	Type
Donkey anti-chicken Alexa Fluor 488	703-546-155	Dianova, Hamburg, Germany	IHC 1:200	IgY (H+L)
Donkey anti-goat Alexa Fluor 488	A-11055	Molecular probes (Thermo Fisher Scientific), Dreieich, Germany	IHC 1:200	IgG (H+L)
Donkey anti-mouse Alexa Fluor 488	A-21202	Molecular probes (Thermo Fisher Scientific), Dreieich, Germany	IHC 1:200	IgG (H+L)
Donkey anti-rabbit Alexa Fluor 488	A-21206	Molecular probes (Thermo Fisher Scientific), Dreieich, Germany	IHC 1:200	IgG (H+L)
Donkey anti-goat Alexa Fluor 647	A-21447	Molecular probes (Thermo Fisher Scientific), Dreieich, Germany	IHC 1:200	IgG (H+L)
Donkey anti-mouse AMCA	715-155-150	Dianova, Hamburg, Germany	IHC 1:200	IgG (H+L)
Donkey anti-goat Cy3	705-165-147	Jackson Immuno Research (Dianova), Hamburg, Germany	IHC 1:200	IgG (H+L)
Donkey anti-mouse Cy3	715-165-151	Jackson Immuno Research (Dianova), Hamburg, Germany	IHC 1:200	IgG (H+L)
Donkey anti-rabbit Cy3	711-165-152	Jackson Immuno Research (Dianova), Hamburg, Germany	IHC 1:200	IgG (H+L)
Donkey anti-rat Cy3	711-165-153	Jackson Immuno Research (Dianova), Hamburg, Germany	IHC 1:200	IgG (H+L)
Donkey anti-mouse Cy5	715-175-151	Dianova, Hamburg, Germany	IHC 1:200	IgG (H+L)
Donkey anti-rabbit Cy5	711-175-152	Jackson Immuno Research (Dianova), Hamburg, Germany	IHC 1:200	IgG (H+L)
Donkey anti-rabbit HRP	NA934	GE Lifesciences, Frankfurt am Main, Germany	WB 1:2000	IgG (H+L)
Goat anti-guinea pig HRP	A7289	Sigma-Aldrich, Taufkirchen, Germany	WB 1:2000	IgG (H+L)
Sheep anti-mouse HRP	NA931	GE Lifesciences, Frankfurt am Main, Germany	WB 1:2000	IgG (H+L)

4.1.7 Oligonucleotides

All oligonucleotides used for genotyping of transgenic mice are listed in Table 7. In general, oligonucelotides were ordered at BioSpring (Frankfurt, Germany).

Table 7: Oligonucleotides used for genotyping PCR reactions

Amplified sequence	Forward /Reverse primer (5'-3')	Product size (bp)
Entpd2	GTTAGGGGGTGTCTGTCTGG AAATGCTGCCTGGAAATGG	309
Entpd2/neo-cassette	CCGTAAAGCACGAGGAAG CTGGACGAAGAGCATCAGG	263
P2ry1	ACAGTACTGTCGCCTCAACTGCAGCAGTTT CCGAAGATCCAGTCAGTCTTGTTGAAGTAG	290
P2ry1/neo-cassette	GCCTTCTATCGCCTTCTTGACGAGTTCTTC CCGAAGATCCAGTCAGTCTTGTTGAAGTAG	660
P2ry13	ATCCCCAGCAATTCCACCT CCTGCTGTCCTTACTCCTAAACTTC	500
P2ry13/neo-cassette	GGCTCGACTAGAGGATCAGCTTG CCTGCTGTCCTTACTCCTAAACTTC	700
Nestin-EGFP	GGAGCTGCAGAGAAGGGATTGCC GATCACTCTCGGCATGGACGAGC	510

4.1.8 Equipment

4.1.8.1 General laboratory equipment

Table 8: List of laboratory equipment

Device	Type	Manufacturer
Balance (Fine balance)	Explorer pro	Ohaus, Nänikon, Switzerland
Balance (Universal balance)	Entris	Sartorius, Göttingen, Germany
Centrifuge (Benchtop centrifuge)	5415 C	Eppendorf, Hamburg, Germany
Centrifuge (Cooling centrifuge)	2K 15	Sigma, Osterode, Germany

Centrifuge (Mini centrifuge)	Mini Star silverline	VWR, Darmstadt, Germany
Centrifuge (Universal centrifuge)	Z 360 K	Hermle, Hamburg, Germany
Centrifuge (Ultracentrifuge)	TLX Optima	Beckmann Coulter, Krefeld, Germany
Cryostat	CM 3050 S	Leica Biosystems, Wetzlar, Germany
Digital black/white camera	AxioCAM MRm	Carl Zeiss, Oberkochen, Germany
Digital camera colored	AxioCAM HR	Carl Zeiss, Oberkochen, Germany
Electrophoresis chamber (SDS-Page)		custom-made
Electrophoresis chamber (Agarose gel electrophoresis)	Compact XS/S and M	Biometra, Göttingen, Germany
Electrophoresis power supply	Power Pack P25	Biometra, Göttingen, Germany
Freezer -20 °C	Premium	Liebherr, Biberach an der Riß, Germany
Freezer -80 °C	Herafreezer	Thermo Scientific, Darmstadt, Germany
Fridge +4 °C	CUP 3503, 960154	Liebherr, Biberach an der Riß, Germany
Heating block	Thermomixer R	Eppendorf, Hamburg, Germany
Gel documentation system	ImageQuant LAS 4000	GE Healthcare, Frankfurt am Main, Germany
Glas homogenizer/ Teflon pistil	Elvehjem Tissue grinder	Gerresheimer, Düsseldorf, Germany
Glas pipettes	5 mL, 10 mL, 20 mL	Brand, Wertheim, Germany
Glas plates	010-003	BioRad, München, Germany
Magnetic stirrer (heatable)	RET basic + IKATRON ETS D3	IKA-Werke, Staufen, Germany
Magnetic stirrer (heatable)	IKA C-MAG HS7	IKA-Werke, Staufen, Germany
Microwave	Alaska M900G	Bauknecht, Stuttgart, Germany
PCR cycler	T-gradient	Biometra, Göttingen, Germany

Perfusion pump	Minipuls	Gilson, Limburg-Offheim, Germany
Perfusion pump	Pumpdrive 5001	Heidolph, Kelheim, Germany
pH meter	Seven easy	Mettler Toledo, Gießen, Germany
Pipettes	0.1 µl – 1000 µl	Eppendorf, Hamburg, Germany
Pipette boy	Pipetus	Hirschmann Laborgeräte, Eberstadt, Germany
Plate reader	Infinite M200 pro	Tecan, Crailsheim, Germany
Rocker	Rocker 25	Labnet, Edison, USA
Safety bench	Herasafe	Heraeus, Hanau, Germany
Semidry blotting apparatus	Trans-Blot SD Semi-Dry Transfercell	BioRad, München, Germany
Shaker	WT12	Biometra, Göttingen, Germany
Ultrasonic Device	Sonifier 250	Branson Ultrasonics, Danbury, USA
UV transilluminator	FLX-20M	Biometra, Göttingen, Germany
Vibratome	7000smz	Campden Instruments, Loughborough, United Kingdom
Vortex	Genie 2 G-560 E	Fisher Scientific, Schwerte, Germany
Water bath	MB-5A	JULABO Labortechnik, Seelbach, Germany
Water bath (shakeable)	Thermolab 1083	GFL, Burgwedel, Germany
Water purification system	Milli-Q Biocel A10	Merck Millipore, Darmstadt, Germany

4.1.8.2 Microscopes

Table 9: List of microscopes

Microscope	Type	Manufacturer
Binocular	Stemi SV 6	Carl Zeiss, Oberkochen, Germany
Confocal laser scan microscope	TCS SP5 II	Leica Microsystems, Wetzlar, Germany
Fluorescence microscope	Axiovert 200	Carl Zeiss, Oberkochen, Germany
Fluorescence microscope	BZ-9000 II	Keyence, Neu-Isenburg, Germany

4.1.9 Software and online data bases

Table 10: List of software and online data bases

Software, data base	Supplier
Adobe Acrobat X Pro	Adobe Systems Incorporated, San Jose, USA
Adobe Design Standard CS5.5	Adobe Systems Incorporated, San Jose, USA
AxioVision LE Rel 4.1	Carl Zeiss, Oberkochen, Germany
Citavi 5	Swiss Academic Software, Wädenswil, Switzerland
GraphPad Prism 7	GraphPad Software Inc., San Diego, USA
ImageJ	National Institute of Mental Health, Bethesda, USA
Image Quant LAS 4000	GE Healthcare, Frankfurt am Main, Germany
Image Quant TL	GE Healthcare, Frankfurt am Main, Germany
Imaris 4.1.0	Bitplane, Zürich, Switzerland
Microsoft Office 2010	Microsoft Corporation, Redmond, USA
NCBI Genome (Nucleotide BLAST Tool)	National Institute of Mental Health, Bethesda, USA
NCBI PubMed	National Institute of Mental Health, Bethesda, USA
NCBI Gene	National Institute of Mental Health, Bethesda, USA
Windows 7	Microsoft Corporation, Redmond, USA

4.2 Methods

4.2.1 Animal breeding

All animal experiments were approved by the local government and performed under veterinary supervision in accordance with European regulations. If not stated otherwise animals were kept under 12 h light and dark cycle with food and water *ad libitum*. Experiments were generally performed using mice aged 8–12 weeks. Only analysis of neurogenesis in old animals was carried out using mice aged 20-24 weeks. Mutant and wild type mice were bred in house. *Entpd2* heterozygous mice were inbred to obtain wild type and homozygous animals in a litter. For *P2ry1* and *P2ry13* knockout lines, homozygous animals were bred and wild type mice were obtained from C57BL6/J breedings. The mouse lines used for this work are all listed in Table 1 with references.

Generation of a *Entpd2*-deficient, nestin-EGFP-expressing mouse line

Entpd2-/- mice were bred to mice homozygously carrying the nestin-EGFP transgene. Mice heterozygous for *Entpd2* and expressing nestin-EGFP were further inbred and litters were genotyped. EGFP-positive wild type and knockout animals were further processed.

Generation of a *P2ry13*-deficient, nestin-EGFP-expressing mouse line

P2ry13 knockout mice were crossed to *Entpd*2 wild type mice expressing nestin-EGFP. Litters were genotyped. *P2ry13*+/- mice expressing nestin-EGFP were inbred. Nestin-EGFP positive wild type and knockout mice were further processed.

4.2.2 Molecular Biology

4.2.2.1 Genotyping transgenic mice

Discrimination between wild type, heterozygous and homozygous animals of either mouse line based on genotyping via polymerase chain reaction (PCR) and subsequent agarose gel electrophoresis.

Genomic DNA extraction

Mouse tail biopsies were used to extract genomic DNA. After biopsy each animal was assigned to a specific earmark code consisting of bars and holes for later recognition. Tissue digestion was performed by either boiling tail tips in 100 µl 50 mM NaOH for 2 h at 95 °C or incubating them over night at 55 °C in 100 µl lysis buffer. After digestion in NaOH the lysates were neutralized by adding 10 µl 1.5 M Tris-HCl, pH 8.8. In case of tissue digestion in lysis buffer the lysates were heated to 95 °C for 30 min to inactivate residual proteinase K. In either case the lysates were then centrifuged at 21.460 g for 1 min to remove hair and tissue debris and directly used for PCR.

Genotyping PCR

The PCR master mix was prepared as indicated in Table 11. Taq DNA polymerase was added just before use. 2 µl lysate (10-50 ng DNA) was used for PCR reactions of 25 µl in total.

Table 11: PCR master mix

Component	End concentration	*Entpd2*	*P2ry1*	*P2ry13*	Nestin-EGFP
10x ThermoPol reaction buffer (NEB)	1x				
dNTPs (10 mM each)	200 µm each				
Primer 1 (10 µM)		1 µM	0.5 µM	0.5 µM	0.5 µM
Primer 2 (10 µM)		1 µM	1 µM	1 µM	0.5 µM
Primer 3 (10 µM)		0.5 µM	0.5 µM	0.5 µM	-
Primer 4 (10 µM)		0.5 µM	-	-	-
***Taq* polymerase (250 U/µl)**	2,5 U/µl				
Sterile dH_2O					
Genomic DNA	10-50 ng				

Primers used for the different PCR reactions are listed in Table 7. PCR reaction conditions for either allele are indicated in Table 12.

Table 12: PCR reaction conditions

Reaction program for *Entpd2* & Nestin-EGFP			**Reaction program for *P2ry1***			**Reaction program for *P2ry13***		
temp. (°C)	**time (sec)**	**cycles**	**temp. (°C)**	**time (sec)**	**cycles**	**temp. (°C)**	**time (sec)**	**cycles**
95	30	1	94	120	1	94	240	1
95	30	35	94	30	35	94	30	35
60	30	35	60	30	35	60	30	35
72	90	35	72	90	35	72	50	35
72	420	1	72	480	1	72	600	1
4	∞	1	4	∞	1	4	∞	1

Agarose gel electrophoresis

2% agarose gels were prepared to run PCR products to separate DNA fragments. The corresponding amount of agarose was dissolved in 50-100 ml 1x TAE (for small or large gels) by heating in the microwave. The agarose solution was allowed to cool down to approximately 60 °C before 0.2 µg/ml ethidium bromide was added. To solidify, the solution was poured into a gel tank and a comb was inserted. DNA ladder mix was loaded as a standard to clearly identify DNA fragment sizes. 15 µl PCR reaction mix (including approximately 1µl of 10x DNA loading dye) was loaded per lane. Constant voltage of 100 V and current intensity of 250 mA were applied for 45 min. Individual bands were visualized using a UV-Transilluminator at a wavelength of 302 nm. Gel documentation was performed using a gel documentation system that was connected to a digital camera.

4.2.3 Animal experiments

4.2.3.1 BrdU injection

Analysis of neural stem and progenitor cell proliferation in the dentate gyrus

8-12 week old wild type and knockout mice received daily intraperitoneal injections of the thymidine analog 5-bromo-2‘-deoxyuridine (BrdU). As a thymidine analog, BrdU incorporates into the DNA during S-phase of the cell cycle. Therefore it is an ideal marker for mitotic cells that can easily be detected via subsequent antibody-staining. BrdU concentrations of 50 mg/kg of bodyweight were used for analysis of progenitor cell proliferation in *P2ry13* animals

(one BrdU pulse) as well as in *Entpd2*, nestin-EGFP expressing mice (three pulses at 2 h interval). BrdU was dissolved in 0.9% NaCl for at least 2 h at room temperature, filtered and mice were injected and perfused with 4% paraformaldehyde (PFA) in PBS 2 h after the final BrdU pulse. Analysis of progenitor cell proliferation in old *P2ry13* animals was performed in mice aged 20-24 weeks. Again a BrdU concentration of 50 mg/kg of bodyweight was chosen. However, due to the fact that hippocampal neurogenesis declines in aged animals (Kuhn et al., 1996; Heine et al., 2004), mice received three daily injections at 2 h interval and were perfused 2 h after the final pulse. Proliferation analysis in *P2ry1* animals was carried out using a BrdU concentration of 150 mg/kg of bodyweight. Mice were injected for three consecutive days, three times a day at 2 h interval and were again perfused with 4% paraformaldehyde (PFA) in PBS 2 h after the final BrdU pulse. Brains were further processed for BrdU detection and immunolabeling.

Analysis of progenitor cell proliferation at the third ventricle of the hypothalamus

P2ry1 and *P2ry13* wild type and knockout mice were treated with BrdU (150 mg/kg of body-weight) as described above for proliferation analysis in *P2ry1* animals in the dentate gyrus. 2 h after the final BrdU pulse animals were perfused with 4% PFA in PBS and brains were further processed for BrdU detection and immunolabeling.

Analysis of differentiation and survival of neural stem cells in the dentate gyrus

P2ry13 wild type and knockout animals aged 8-12 weeks were injected with BrdU intra-peritoneally (50 mg/kg of body weight) three times a day at 2 h interval. The animals were perfused with 4% PFA in PBS either 3 d or 28 d after the last BrdU pulse leaving enough time for migration of progenitor cells to the target region, namely the granule cell layer of the hippocampal dentate gyrus, and differentiation of the initially BrdU-labelled stem cells. *P2ry13* animals aged 20-24 weeks were injected with BrdU concentrations of 150 mg/kg of body-weight three times a day at 2 h intervals on three consecutive days and perfused 28 d after the final BrdU pulse. Perfused brains were further processed for detection and analysis of BrdU and immunohistochemistry.

Analysis of differentiation and survival of neural stem cells in the olfactory bulb

P2ry13 wild type and knockout animals aged 8-12 weeks were injected with BrdU intraperitoneally (50 mg/kg of body weight) as described earlier for the hippocampal dentate gyrus. To ensure that initially labeled cells in the subventricular zone at the lateral ventricle have migrated to their target region, namely the olfactory bulb, perfusion of the animals was performed 28 d after the final BrdU pulse. BrdU detection and immunohistochemistry were subsequently performed.

Analysis of differentiation and survival of neural stem cells in hypothalamic nuclei

At the age of 8-12 weeks *P2ry1* and *P2ry13* wild type and knockout animals were injected intraperitoneally with BrdU at a concentration of 150 mg/kg of body weight. Mice received 3 injections per day for 3 consecutive days as described earlier. The animals were perfused on day 30 before immunohistochemistry and BrdU detection were carried out.

4.2.4 Histology

4.2.4.1 Intracardial perfusion and tissue processing

Animals received an anesthetic overdose by intraperitoneal injection of ketamine (180 mg/kg of body weight; Ketavet) and xylazine (10 mg/kg of body weight; Rompun). Depth of anesthesia was tested via a pinch method. When the animals showed no more reflexes their extremities were fixed on a preparation plate. When the animals were finally reaching the state of asphyxia, thorax and abdominal cavity were opened and the perfusion cannula was inserted into the right heart chamber. Immediately after positioning the perfusion cannula, an incision was made at the left atrium. Animals were perfused for 1-2 min with ice-cold 0.9% NaCl at a constant flow rate of 6-7 ml/min to rinse all blood from the cardiovascular system. Perfusion with ice-cold 4% PFA in PBS followed for 17-20 min (flow rate 6-7 ml/min). Brains were isolated and postfixed over night at 4 °C in the same fixative. For cryosections brains were subsequently cryoprotected with 30% sucrose/PBS for 24-48 h at 4 °C. Hemispheres were divided, embedded in TissueTek and frozen in isopentane pre-cooled to -80 °C. Using a cryotome, brains were serially cut into 40 µm thick sagittal free floating sections. Sections were collected in 12 well chambers of a 24 well plate filled with Tissue Cryoprotectant Solution (TCS) (as a 1 in 12 series). For analysis in the hippocampal dentate gyrus, sections were

collected from medial to lateral 2.725mm to 0.225mm according to Allen Brain Reference Atlas. Cryosections were stored at -20 °C until further processing.

For vibratome sections brains were directly embedded in 4% agarose in PBS after post-fixation. After polymerization of agarose, the agarose block was glued on the metal block of the vibratome and cut into 50 µm thick coronal sections. Sections were collected in 12 well chambers filled with PBS (as a 1 in 12 series). For analysis in the hippocampal dentate gyrus, sections were collected from bregma -1.355mm to -2.555mm according to Allen Brain Reference Atlas. Sections from bregma -1.155mm to -2.155mm were collected for analysis in the third ventricle. For long-term storage, sections were transferred to TCS and kept at -20 °C until further processing.

4.2.4.2 Immunohistochemical staining

For standard immunohistochemical procedures cryosections or vibratome sections were washed in PBS several times and permeabilized with 0.1% Triton-X 100 for 30 min at room temperature. Non-specific binding of antibodies was blocked with 5% BSA (bovine serum albumin) in PBS for 30 min at room temperature following incubation with primary antibodies in 1% BSA in PBS over night or over two nights at 4 °C. Sections were then rinsed in PBS and subsequently incubated with secondary antibodies in 1% BSA in PBS containing 1 µg/ml DAPI (4', 6-Diamidino-2-phenylindole) as a nuclear counterstain, for 2 h at room temperature. Sections were washed in PBS, transferred onto glass slides and mounted with Aqua-Poly/Mount for subsequent analysis.

For detection of BrdU labeling in either region of interest, floating sections (cryosections or vibratome sections) were incubated in 50% formamide in 2x saline-sodium citrate buffer (SSC) at 65 °C for 2 h in order to destabilize the hydrogen bonds of the DNA double helix. Sections were rinsed in 2x SSC followed by 30 min incubation in 2 M HCl at 37 °C to remove chromatin proteins and to further open the helical structure of the genomic DNA. Sections were neutralized in 0.1 M boric acid (pH 8.5) for 10 min, washed in Tris-buffered saline (TBS) and blocked with 3% normal donkey serum in TBS containing 0.1 % Triton-X-100 for 30 min at room temperature. The sections were incubated with an anti-BrdU antibody in the same blocking solution overnight at 4°C. For double or even triple fluorescent immunostaining (BrdU and additional antigens) additional primary antibodies were added to the primary anti-

body solution. The next day the sections were rinsed in TBS several times, before incubation with secondary antibodies was performed for 2 h at room temperature. Sections were washed in TBS, transferred onto glass slides and mounted with Aqua-Poly/Mount.

4.2.4.3 Enzymehistochemical staining

ATPase, ADPase, and AMPase activity were visualized applying a method modified from Wachstein and Meisel, 1957) as previously described by Langer et al. (2008). In brief, cryo-sections were preincubated for 30 min at room temperature with Tris-maleate sucrose buffer. The enzyme reaction was performed at 37 °C in TMS-buffered substrate solution for 30 min, containing either 1 mM ATP, ADP or AMP as a substrate. During the enzyme reaction substrates were stabilized by addition of 3% dextran. After rinsing with dH_2O, lead ortho-phosphate, precipitated as a result of nucleotidase activity, was visualized as a brown deposit by incubating sections in an aqueous solution of 1% (vol/vol) $(NH_4)_2S$. Detection of alkaline phosphatase activity was carried out by applying the nitro-blue tetrazolium chloride (NBT)/ 5-bromo-4-chloro-30-indolyl phosphate p-toluidine salt (BCIP) system (Sigma-Aldrich) according to the manufacturer's protocol. Sections were dehydrated in graded ethanol (70% EtOH, 80% EtOH, 100% EtOH, 100% isopropanol, 100% xylol) and mounted with Roti-Histokit II.

4.2.5 Biochemical methods

4.2.5.1 Tissue preparation and membrane fractionation

Total mouse brains from *Entpd2* wild type and knockout animals were dissected, washed in ice cold PBS and homogenized in homogenization buffer (containing protease inhibitor) using a potter homogenizer following a treatment with 10-15 ultrasonic pulses. Insoluble material was removed by centrifugation for 10 min at 300 g at 4° C. To isolate membrane fractions, super-natants were collected and centrifuged at 100.000 g for 45 min at 4 °C. The precipitate was resuspended in homogenization buffer and directly used to measure the protein concentration.

4.2.5.2 Determination of protein concentration

Sample protein concentration was determined using the Pierce BCA assay kit. The BCA assay was performed in 96-well plates using a microplate absorbance reader at 562 nm according to the manufacturer's instruction. The standard curve was created in duplicates by a serial dilution of BSA in homogenization buffer (0-10 µg/µl) and was assayed together with the samples (in triplicate). Based on the standard curve, protein concentrations per sample were determined and samples were diluted in concentrated sample buffer in the absence of reducing agent to reach a final concentration of 3 µg/µl. Samples were boiled at 95 ºC for 5 min and either processed directly or snap frozen in liquid nitrogen and stored at -80 °C.

4.2.5.3 SDS Polyacrylamide gel electrophoresis and immunoblotting

Equal volumes of prepared protein samples were loaded and run on a 10% Tris-glycine sodium dodecyl sulfate polyacrylamide gel (Laemmli, 1970) at 25 mA for 60 min in electrophoresis buffer. Separated proteins were transferred in transfer buffer onto a nitrocellulose membrane at 90 mA for 1 h using semi-dry blotting techniques. Membranes were blocked with 5% skimmed milk powder in PBS containing 0.1% Tween20 (PBS/T) over night at 4 °C. Incubation with the primary antibodies was performed overnight at 4 °C in PBS/T containing 0.02% NaN_3 and 5% bovine serum albumin (BSA). Following several washing steps in 5% skimmed milk powder in PBS/T, incubation with an anti-actin antibody was performed for 1 h at room temperature. Membranes were again blocked for 5x10 min with 5% skimmed milk powder in PBS/T and incubated with the respective horseradish peroxidase (HRP)-conjugated secondary antibodies (in 5% skimmed milk powder in PBS/T) for 1 h at room temperature. A final washing step in PBS/T (5x10 min) was performed. Immunoblots were then incubated with Amersham ECL Western Blotting Detection Reagents and bands were visualized using ImageQuant LAS 4000.

Table 13: Composition of stacking gel and running gel

Chemical	Stacking gel 5%	Running gel 10%
30% Acrylamide	1.67 ml	10 ml
1% Bisacrylamide	1.3 ml	3.9 ml
1 M Tris/HCl pH 8.7	11.2 ml	-
0.25 M Tris/HCl pH 6.8	-	5 ml
dH_2O	4.3 ml	1.95 ml
20% SDS	0.15 ml	0.05 ml
TEMED	0.03 ml	0.01 ml
10% APS	0.15 ml	0.05 ml

4.2.6 Quantification and data analysis

4.2.6.1 Semi-quantitative Western blot analysis

Individual levels of ectoenzyme immunostaining (anti-TNAP or anti-NTPDase1–3, see Table 5) were standardized to the according levels of actin immunostaining using ImageQuant TL software. Data were presented as percentage of protein expression (wild type control defined as 100%).

4.2.6.2 Quantification of fluorescent-labeled cells

To avoid multiple counts of identical cells and for quantification of double or triple immuno-staining, z-stacks (1 ± 0.05 µm for analysis of the dentate gyrus, 2 ± 0.05 µm for analysis of the olfactory bulb and the third ventricle) were recorded with a Leica TCS SP5 II confocal laser scanning microscope and analyzed using Imaris (x64 7.6.1). Identical exposure times and parameters were chosen between wild type and knockout. All quantification procedures were performed in a double-blinded manner.

Cleaved caspase-3 was analyzed in serial coronal cryosections with an interspace of 160 µm from wild type and *Entpd2* knockout mice as well as *P2ry13*+/+ and *P2ry13*-/- mice in the granule cell layer of the hippocampal dentate gyrus. 6 (*Entpd2)* or 14 sections (*P2ry13)* per animal were counted.

Expression of the transcription factor c-Fos in the hippocampal dentate gyrus was analyzed in serial sagittal cryosections from wild type and *P2ry13* knockout mice spaced 160 µm apart (7 sections per animal) as a readout for neuronal activity. Furthermore serial coronal vibratome sections from *P2ry1* wild type and knockout mice were analyzed. c-Fos positive cells were counted in 5 sections per animal with an interspace of 200 µm.

Serial coronal vibratome sections from wild type, *P2ry13*-/- and *P2ry1*-/- mice (section intervals of 200 µm) were labeled with anti-c-Fos and additional markers as described before. High resolution images were obtained with a Leica TCS SP5 II confocal laser scanning microscope or a fluorescence microscope (Keyence) and regions of interest (ROI) were semi-automatically drawn in ImageJ. DAPI staining and/or labeling with the neuronal marker anti-Human Neuronal Protein HuC/HuD (anti-HuC/D) were used for discrimination of hypothalamic areas. The MaximumFinder plugin-filter was used to automatically count the total number of c-Fos-positive cells (defined as pixels with a level above the lower threshold) per ROI. All hypothalamic nuclei were analyzed bilaterally and mean values were calculated. 4-5 sections per animal were analyzed (Bregma -1.155 mm to -2.155 mm). The same parameters were chosen for quantification of wild type and knockout images.

4.2.6.3 Quantification of chromogenic-labeled cells

In situ hybridization data for *P2ry12* was obtained from Allen Brain Atlas (http://mouse.brain-map.org/gene/show/46680). 6 sections per animal were analyzed. In each section the hippocampal dentate gyri were analyzed bilaterally and mean values were calculated. The granule cell layer of the dentate gyrus was manually divided into two identical halves, an inner part, orientated towards the hilus, and an outer part, orientated towards the molecular layer of the dentate gyrus, and chromogenic labeled cells were counted for each part.

4.2.6.4 Cell type-specific quantification

Subtypes of hippocampal progenitor cells (type-1 to type-3) were quantified in sagittal cryosections from EGFP-expressing *Entpd2* wild type or knockout mice that were immunostained for GFAP, Sox2 and DCX. Individual sagittal cryosections were assigned to specific brain

levels. Four sections with an interspace of 240 µm were analyzed and cells located within the SGL and up to 10 µm deep into the granule cell layer were included.

Subtypes of hippocampal progenitor cells were further quantified in sagittal cryosections from EGFP-expressing *P2ry13* wild type or knockout mice that were immunostained for GFAP and DCX. Processes positive for nestin-EGFP, nestin-EGFP and GFAP, or DCX were counted in 4-6 sections per animal.

Similarly, pCREB immunostaining in DCX-immunopositive cells was quantified in 4 sagittal cryosections from *Entpd2* wild type and knockout mice as well as in 6 sagittal cryosections from *P2ry13* wild type or knockout mice.

4.2.6.5 Quantification of BrdU-labeled cells in neurogenic niches

Quantification of BrdU-labeled cells in the hippocampal dentate gyrus

Serial sagittal cryosections (160 µm section intervals) from *P2ry13* wild type and knockout mice or serial coronal vibratome sections from *P2ry1* wild type and knockout mice were analyzed. The total number of BrdU-positive cells in the hippocampal granule cell layer was counted. In *P2ry13*+/+ and *P2ry13*-/- animals the number of BrdU-positive cells in the supra- and infrapyramidal blade of the dorsal dentate gyrus and the hilus were also counted separately. Furthermore the ventral dentate gyrus was analyzed in these animals.

In order to determine the frequency of newly formed neurons, serial sagittal sections from *P2ry13* wild type and knockout mice spaced 160 µm apart were stained for double immuno-fluorescence using antibodies against BrdU and NeuN. 6 sections per animal were analyzed for marker colocalization, yielding the percentage of the NeuN-expressing BrdU-positive cell population.

For quantification of cells positive for EGFP/GFAP/BrdU (type-1 cells positive for BrdU) serial sagittal sections from *Entpd2*+/+ and *Entpd2*-/- mice spaced 160 µm apart (10 sections per animal) were analyzed.

Quantification of BrdU-labeled cells at the third ventricle and in hypothalamic nuclei

Serial coronal vibratome sections (Bregma -1.155 mm to -2.155 mm) from wild type, *P2ry13* knockout, and *P2ry1* knockout mice (section intervals of 200 µm) were labeled with an anti-BrdU antibody and additional markers as described before. High resolution imaging was performed and regions of interest (ROI) were semi-automatically defined in ImageJ. Hypothalamic areas were discriminated by DAPI staining and/or labeling with the neuronal marker anti-Human Neuronal Protein HuC/HuD (anti-HuC/D). The total number of BrdU-positive cells per ROI was calculated using the MaximumFinder plugin-filter as described before for quantification of c-Fos. Quantification of images from wild type and knockout animals was performed using the same parameters.

Quantification of BrdU-labeled cells in the olfactory bulb

BrdU-positive cells were analyzed in the olfactory bulb in 4 defined serial sagittal cryosections from *P2ry13* wild type and knockout mice with section intervals of 160 µm. Z-stacks of the olfactory bulb were recorded. Focal planes were combined to one single image. Color images were inverted and converted to grayscale (8 bit). The ITCN (Image-based Tool for Counting Nuclei) plugin in ImageJ was used to automatically count the total number of BrdU-positive cells per olfactory bulb. The same parameters were chosen for all images.

4.2.6.6 Determination of the area of the hippocampal granule cell layer

Serial sagittal cryosections from *P2ry13* wild type and knockout mice spaced 160 µm apart were stained using an antibody against NeuN. Individual sagittal cryosections were assigned to specific brain levels. Based on NeuN immunofluorescence, the area of the whole granule cell layer was calculated in six defined sections per animal using the semi-automatic Contour Surface Tool in Imaris, which allows to extract a 3D object by manually drawing the object contours on 2D slices.

4.2.7 Statistics

Unless stated otherwise, MS Excel was used for statistical calculations. Analysis of one mouse per genotype represents one independent experiment (abbreviated as n). For all data sets the arithmetic average (mean) was determined and the standard deviation and the standard error

of the mean (SEM) were calculated. Mean values of independent experimental groups were compared and data are presented as mean values ± SEM. Differences between independent experimental groups were evaluated by the unpaired, two-sided Student's t-test and were considered significant at the 5% level distinguishing significance levels of: * $p < 0.05$; ** $p < 0.01$;*** and $p < 0.001$.

5 References

Abbracchio MP, Burnstock G, Boeynaems JM, Barnard EA, Boyer JL, Kennedy C, Knight GE, Fumagalli M, Gachet C, Jacobson KA, Weisman GA (2006) International Union of Pharmacology LVIII: update on the P2Y G protein-coupled nucleotide receptors: from molecular mechanisms and pathophysiology to therapy. Pharmacol Rev. 58:281–341.

Abbracchio MP, Burnstock G, Verkhratsky A, Zimmermann H (2009) Purinergic signalling in the nervous system: an overview. Trends Neurosci. 32:19–29.

Abiega O et al. (2016) Neuronal Hyperactivity Disturbs ATP Microgradients, Impairs Microglial Motility, and Reduces Phagocytic Receptor Expression Triggering Apoptosis/Microglial Phagocytosis Uncoupling. PLoS biology 14:e1002466.

Ables JL, Decarolis NA, Johnson MA, Rivera PD, Gao Z, Cooper DC, Radtke F, Hsieh J, Eisch AJ (2010) Notch1 is required for maintenance of the reservoir of adult hippocampal stem cells. J Neurosci. 30:10484–10492.

Abraham WC, Robins A (2005) Memory retention-the synaptic stability versus plasticity dilemma. Trends Neurosci. 28:73–78.

Ahn S, Joyner AL (2005) In vivo analysis of quiescent adult neural stem cells responding to Sonic hedgehog. Nature. 437:894–897.

Aimone JB, Li Y, Lee SW, Clemenson GD, Deng W, Gage FH (2014) Regulation and function of adult neurogenesis: from genes to cognition. Physiol Rev. 94:991–1026.

Akers KG, Martinez-Canabal A, Restivo L, Yiu AP, Cristofaro A de, Hsiang HLL, Wheeler AL, Guskjolen A, Niibori Y, Shoji H, Ohira K, Richards BA, Miyakawa T, Josselyn SA, Frankland PW (2014) Hippocampal neurogenesis regulates forgetting during adulthood and infancy. Science. 344:598–602.

Akmayev IG, Popov AP (1977) Morphological aspects of the hypothalamic-hypophyseal system. VII. The tanycytes: Their relation to the hypophyseal adrenocorticotrophic function. An ultrastructural study. Cell Tissue Res. 180:263–282.

Altman J, Bayer SA (1978) Development of the diencephalon in the rat. II. Correlation of the embryonic development of the hypothalamus with the time of origin of its neurons. J Comp Neurol. 182:973–993.

Altman J, Das GD (1965) Autoradiographic and histological evidence of postnatal hippocampal neurogenesis in rats. J Comp Neurol. 124:319–335.

Alvarez-Bolado G, Paul FA, Blaess S (2012) Sonic hedgehog lineage in the mouse hypothalamus: from progenitor domains to hypothalamic regions. Neural Dev. 7:4.

Amisten S, Meidute-Abaraviciene S, Tan C, Olde B, Lundquist I, Salehi A, Erlinge D (2010) ADP mediates inhibition of insulin secretion by activation of P2Y13 receptors in mice. Diabetologia. 53:1927–1934.

Anand BK, Brobeck JR (1951) Localization of a "Feeding Center" in the Hypothalamus of the Rat. Exp Biol Med. (Maywood) 77:323–325.

Arvidsson A, Collin T, Kirik D, Kokaia Z, Lindvall O (2002) Neuronal replacement from endogenous precursors in the adult brain after stroke. Nat Med. 8:963–970.

Ashton RS, Conway A, Pangarkar C, Bergen J, Lim KI, Shah P, Bissell M, Schaffer DV (2012) Astrocytes regulate adult hippocampal neurogenesis through ephrin-B signaling. Nat Neurosci. 15:1399–1406.

Babu H, Ramirez-Rodriguez G, Fabel K, Bischofberger J, Kempermann G (2009) Synaptic Network Activity Induces Neuronal Differentiation of Adult Hippocampal Precursor Cells through BDNF Signaling. Front Neurosci. 3:49.

Balland E, Dam J, Langlet F, Caron E, Steculorum S, Messina A, Rasika S, Falluel-Morel A, Anouar Y, Dehouck B, Trinquet E, Jockers R, Bouret SG, Prevot V (2014) Hypothalamic tanycytes are an ERK-gated conduit for leptin into the brain. Cell Metab. 19:293–301.

Bannerman DM, Rawlins JNP, McHugh SB, Deacon RMJ, Yee BK, Bast T, Zhang WN, Pothuizen HHJ, Feldon J (2004) Regional dissociations within the hippocampus-memory and anxiety. Neurosci Biobehav Rev. 28:273–283.

Barth AL (2007) Visualizing circuits and systems using transgenic reporters of neural activity. Curr Opin Neurobiol. 17:567–571.

Batailler M, Droguerre M, Baroncini M, Fontaine C, Prevot V, Migaud M (2014) DCX-expressing cells in the vicinity of the hypothalamic neurogenic niche: a comparative study between mouse, sheep, and human tissues. J Comp Neurol. 522:1966–1985.

Bath KG, Mandairon N, Jing D, Rajagopal R, Kapoor R, Chen ZY, Khan T, Proenca CC, Kraemer R, Cleland TA, Hempstead BL, Chao MV, Lee FS (2008) Variant Brain-Derived Neurotrophic Factor (Val66Met) Alters Adult Olfactory Bulb Neurogenesis and Spontaneous Olfactory Discrimination. J Neurosci. 28:2383–2393.

Belcher SM, Zsarnovszky A, Crawford PA, Hemani H, Spurling L, Kirley TL (2006) Immunolocalization of ecto-nucleoside triphosphate diphosphohydrolase 3 in rat brain: implications for modulation of multiple homeostatic systems including feeding and sleep-wake behaviors. Neuroscience. 137:1331–1346.

Benito-Munoz M, Matute C, Cavaliere F (2016) Adenosine A1 receptor inhibits postnatal neurogenesis and sustains astrogliogenesis from the subventricular zone. Glia. 64:1465–1478.

Berg DA, Yoon KJ, Will B, Xiao AY, Kim NS, Christian KM, Song HJ, Ming GL (2015) Tbr2-expressing intermediate progenitor cells in the adult mouse hippocampus are unipotent neuronal precursors with limited amplification capacity under homeostasis. Front Biol. 10:262–271.

Biver G, Wang N, Gartland A, Orriss I, Arnett TR, Boeynaems JM, Robaye B (2013) Role of the P2Y13 receptor in the differentiation of bone marrow stromal cells into osteoblasts and adipocytes. Stem Cells. 31:2747–2758.

Bjelobaba I, Janjic MM, Stojilkovic SS (2015) Purinergic signaling pathways in endocrine system. Auton Neurosci. 191:102–116.

Bjelobaba I, Nedeljkovic N, Subasic S, Lavrnja I, Pekovic S, Stojkov D, Rakic L, Stojiljkovic M (2006) Immunolocalization of ecto-nucleotide pyrophosphatase/phosphodiesterase 1 (NPP1) in the rat forebrain. Brain Res. 1120:54–63.

Blom D, Yamin TT, Champy MF, Selloum M, Bedu E, Carballo-Jane E, Gerckens L, Luell S, Meurer R, Chin J, Mudgett J, Puig O (2010) Altered lipoprotein metabolism in P2Y(13) knockout mice. Biochim Biophys Acta. 1801:1349–1360.

Blouet C, Schwartz GJ (2010) Hypothalamic nutrient sensing in the control of energy homeostasis. Behav Brain Res. 209:1–12.

Boccazzi M, Rolando C, Abbracchio MP, Buffo A, Ceruti S (2014) Purines regulate adult brain subventricular zone cell functions: contribution of reactive astrocytes. Glia. 62:428–439.

Bohn C, Jahn H, Bai X, Scheller A, Kirchhoff F (2015) Analysis of purinergic P2Y1 receptors in cortical astrocytes and cerebellar bergmann glia.

Bolborea M, Dale N (2013) Hypothalamic tanycytes: potential roles in the control of feeding and energy balance. Trends Neurosci. 36:91–100.

Bonaguidi MA, Song J, Ming GL, Song HJ (2012) A unifying hypothesis on mammalian neural stem cell properties in the adult hippocampus. Curr Opin Neurobiol. 22:754–761.

Bonaguidi MA, Wheeler MA, Shapiro JS, Stadel RP, Sun GJ, Ming GL, Song HJ (2011) In vivo clonal analysis reveals self-renewing and multipotent adult neural stem cell characteristics. Cell. 145:1142–1155.

Bonfanti L, Peretto P (2011) Adult neurogenesis in mammals-a theme with many variations. Eur J Neurosci. 34:930–950.

Bracko O, Singer T, Aigner S, Knobloch M, Winner B, Ray J, Clemenson GD, Suh H, Couillard-Despres S, Aigner L, Gage FH, Jessberger S (2012) Gene expression profiling of neu-

ral stem cells and their neuronal progeny reveals IGF2 as a regulator of adult hippocampal neurogenesis. J Neurosci. 32:3376–3387.
Braun N, Sevigny J, Mishra SK, Robson SC, Barth SW, Gerstberger R, Hammer K, Zimmermann H (2003) Expression of the ecto-ATPase NTPDase2 in the germinal zones of the developing and adult rat brain. Eur J Neurosci. 17:1355–1364.
Braun N, Sevigny J, Robson SC, Enjyoji K, Guckelberger O, Hammer K, Di Virgilio F, Zimmermann H (2000) Assignment of ecto-nucleoside triphosphate diphosphohydrolase-1/cd39 expression to microglia and vasculature of the brain. Eur J Neurosci. 12:4357–4366.
Braun SMG, Jessberger S (2014) Adult neurogenesis: mechanisms and functional significance. Development. 141:1983–1986.
Breunig JJ, Silbereis J, Vaccarino FM, Sestan N, Rakic P (2007) Notch regulates cell fate and dendrite morphology of newborn neurons in the postnatal dentate gyrus. Proc Natl Acad Sci USA. 104:20558–20563.
Brisevac D, Adzic M, Laketa D, Parabucki A, Milosevic M, Lavrnja I, Bjelobaba I, Sevigny J, Kipp M, Nedeljkovic N (2015) Extracellular ATP Selectively Upregulates Ecto-Nucleoside Triphosphate Diphosphohydrolase 2 and Ecto-5'-Nucleotidase by Rat Cortical Astrocytes In Vitro. J Mol Neurosci. 57:452–462.
Brobeck JR, Tepperman J, Long CN (1943) Experimental Hypothalamic Hyperphagia in the Albino Rat. Yale J Biol Med. 15:831–853.
Brun-Heath I, Ermonval M, Chabrol E, Xiao J, Palkovits M, Lyck R, Miller F, Couraud PO, Mornet E, Fonta C (2011) Differential expression of the bone and the liver tissue non-specific alkaline phosphatase isoforms in brain tissues. Cell Tissue Res. 343:521–536.
Bulavina L, Szulzewsky F, Rocha A, Krabbe G, Robson SC, Matyash V, Kettenmann H (2013) NTPDase1 activity attenuates microglial phagocytosis. Purinergic Signal. 9:199–205.
Burnstock G (2007) Purine and pyrimidine receptors. Cell Mol Life Sci. 64:1471–1483.
Burnstock G (2008) Purinergic signalling and disorders of the central nervous system. Nat Rev Drug Discov. 7:575–590.
Burnstock G (2013) Purinergic signalling: pathophysiology and therapeutic potential. Keio J Med. 62:63–73.
Burnstock G (2014) Purinergic signalling in endocrine organs. Purinergic Signal. 10:189–231.
Burnstock G, Knight GE (2004) Cellular distribution and functions of P2 receptor subtypes in different systems. Int Rev Cytol. 240:31–304.
Burnstock G, Verkhratsky A (2009) Evolutionary origins of the purinergic signalling system. Acta Physiol (Oxf). 195:415–447.
Cao L, Jiao X, Zuzga DS, Liu Y, Fong DM, Young D, During MJ (2004) VEGF links hippocampal activity with neurogenesis, learning and memory. Nat Genet. 36:827–835.
Cao X, Li LP, Qin XH, Li SJ, Zhang M, Wang Q, Hu HH, Fang YY, Gao YB, Li XW, Sun LR, Xiong WC, Gao TM, Zhu XH (2013) Astrocytic adenosine 5'-triphosphate release regulates the proliferation of neural stem cells in the adult hippocampus. Stem Cells. 31:1633–1643.
Carlson AJ (1919) The control of hunger in health and disease. University of Chicago Press.
Carro E, Nunez A, Busiguina S, Torres-Aleman I (2000) Circulating insulin-like growth factor I mediates effects of exercise on the brain. J Neurosci. 20:2926–2933.
Cavaliere F, Donno C, D'Ambrosi N (2015) Purinergic signaling: a common pathway for neural and mesenchymal stem cell maintenance and differentiation. Front Cell Neurosci. 9:211.
Chaker Z, George C, Petrovska M, Caron J-B, Lacube P, Caillé I, Holzenberger M (2016) Hypothalamic neurogenesis persists in the aging brain and is controlled by energy-sensing IGF-I pathway. Neurobiol Aging. 41:64–72.

Cheng M-F (2013) Hypothalamic neurogenesis in the adult brain. Front Neuroendocrinol. 34:167–178.

Christian KM, Song HJ, Ming GL (2014) Functions and dysfunctions of adult hippocampal neurogenesis. Annu Rev Neurosci. 37:243–262.

Ciofi P, Garret M, Lapirot O, Lafon P, Loyens A, Prevot V, Levine JE (2009) Brain-endocrine interactions: a microvascular route in the mediobasal hypothalamus. Endocrinology. 150:5509–5519.

Clelland CD, Choi M, Romberg C, Clemenson GD, Fragniere A, Tyers P, Jessberger S, Saksida LM, Barker RA, Gage FH, Bussey TJ (2009) A functional role for adult hippocampal neurogenesis in spatial pattern separation. Science. 325:210–213.

Collden G, Mangano C, Meister B (2010) P2X2 purinoreceptor protein in hypothalamic neurons associated with the regulation of food intake. Neuroscience. 171:62–78.

Communi D, Gonzalez NS, Detheux M, Brezillon S, Lannoy V, Parmentier M, Boeynaems JM (2001) Identification of a novel human ADP receptor coupled to G(i). J Biol Chem. 276:41479–41485.

Cortes-Campos C, Elizondo R, Llanos P, Uranga RM, Nualart F, Garcia MA (2011) MCT expression and lactate influx/efflux in tanycytes involved in glia-neuron metabolic interaction. PLoS ONE. 6:e16411.

Craig CG, Tropepe V, Morshead CM, Reynolds BA, Weiss S, van der Kooy D (1996) In vivo growth factor expansion of endogenous subependymal neural precursor cell populations in the adult mouse brain. J Neurosci. 16:2649–2658.

Creer DJ, Romberg C, Saksida LM, van Praag H, Bussey TJ (2010) Running enhances spatial pattern separation in mice. Proc Natl Acad Sci USA. 107:2367–2372.

Csölle C, Baranyi M, Zsilla G, Kittel A, Goloncser F, Illes P, Papp E, Vizi ES, Sperlagh B (2013) Neurochemical Changes in the Mouse Hippocampus Underlying the Antidepressant Effect of Genetic Deletion of P2X7 Receptors. PLoS ONE. 8:e66547.

Dale N (2008) Dynamic ATP signalling and neural development. J Physiol. 586:2429–2436.

Dale N, Frenguelli BG (2009) Release of adenosine and ATP during ischemia and epilepsy. Curr Neuropharmacol. 7:160–179.

Dayer AG, Cleaver KM, Abouantoun T, Cameron HA (2005) New GABAergic interneurons in the adult neocortex and striatum are generated from different precursors. J Cell Biol. 168:415–427.

Decarolis NA, Mechanic M, Petrik D, Carlton A, Ables JL, Malhotra S, Bachoo R, Götz M, Lagace DC, Eisch AJ (2013) In vivo contribution of nestin- and GLAST-lineage cells to adult hippocampal neurogenesis. Hippocampus. 23:708–719.

Deisseroth K, Singla S, Toda H, Monje M, Palmer TD, Malenka RC (2004) Excitation-neurogenesis coupling in adult neural stem/progenitor cells. Neuron. 42:535–552.

del Puerto A, Diaz-Hernandez JI, Tapia M, Gomez-Villafuertes R, Benitez MJ, Zhang J, Miras-Portugal MT, Wandosell F, Diaz-Hernandez M, Garrido JJ (2012) Adenylate cyclase 5 coordinates the action of ADP, P2Y1, P2Y13 and ATP-gated P2X7 receptors on axonal elongation. J Cell Sci. 125:176–188.

del Puerto A, Wandosell F, Garrido JJ (2013) Neuronal and glial purinergic receptors functions in neuron development and brain disease. Front Cell Neurosci. 7:197.

Delarasse C, Gonnord P, Galante M, Auger R, Daniel H, Motta I, Kanellopoulos JM (2009) Neural progenitor cell death is induced by extracellular ATP via ligation of P2X7 receptor. J Neurochem. 109:846–857.

Delic J, Zimmermann H (2010) Nucleotides affect neurogenesis and dopaminergic differentiation of mouse fetal midbrain-derived neural precursor cells. Purinergic Signal. 6:417–428.

Deng W, Aimone JB, Gage FH (2010) New neurons and new memories: how does adult hippocampal neurogenesis affect learning and memory? Nat Rev Neurosci. 11:339–350.

Deng W, Saxe MD, Gallina IS, Gage FH (2009) Adult-born hippocampal dentate granule cells undergoing maturation modulate learning and memory in the brain. J Neurosci. 29:13532–13542.

Dhaliwal J, Lagace DC (2011) Visualization and genetic manipulation of adult neurogenesis using transgenic mice. Eur J Neurosci. 33:1025–1036.

Di Giorgi Gerevini VD, Caruso A, Cappuccio I, Ricci Vitiani L, Romeo S, Della Rocca C, Gradini R, Melchiorri D, Nicoletti F (2004) The mGlu5 metabotropic glutamate receptor is expressed in zones of active neurogenesis of the embryonic and postnatal brain. Brain Res Dev Brain Res. 150:17–22.

Di Giorgi-Gerevini V, Melchiorri D, Battaglia G, Ricci-Vitiani L, Ciceroni C, Busceti CL, Biagioni F, Iacovelli L, Canudas AM, Parati E, Maria R de, Nicoletti F (2005) Endogenous activation of metabotropic glutamate receptors supports the proliferation and survival of neural progenitor cells. Cell Death Differ. 12:1124–1133.

Di Virgilio F (2000) Dr. Jekyll/Mr. Hyde: the dual role of extracellular ATP. J Auton Nerv Syst. 81:59–63.

Dietrich MO, Horvath TL (2013) Hypothalamic control of energy balance: insights into the role of synaptic plasticity. Trends Neurosci. 36:65–73.

Doetsch F, Caillé I, Lim DA, García-Verdugo JM, Alvarez-Buylla A (1999) Subventricular Zone Astrocytes Are Neural Stem Cells in the Adult Mammalian Brain. Cell. 97:703–716.

Domercq M, Brambilla L, Pilati E, Marchaland J, Volterra A, Bezzi P (2006) P2Y1 receptor-evoked glutamate exocytosis from astrocytes: control by tumor necrosis factor-alpha and prostaglandins. J Biol Chem. 281:30684–30696.

Domercq M, Vazquez-Villoldo N, Matute C (2013) Neurotransmitter signaling in the pathophysiology of microglia. Front Cell Neurosci. 7:49.

Dona F, Conceicao IM, Ulrich H, Ribeiro EB, Freitas TA, Nencioni ALA, da Silva Fernandes, Maria Jose (2016) Variations of ATP and its metabolites in the hippocampus of rats subjected to pilocarpine-induced temporal lobe epilepsy. Purinergic Signal. 12:295–302.

Ebling FJP (2015) Hypothalamic control of seasonal changes in food intake and body weight. Front Neuroendocrinol. 37:97–107.

Ekdahl CT, Claasen JH, Bonde S, Kokaia Z, Lindvall O (2003) Inflammation is detrimental for neurogenesis in adult brain. Proc Natl Acad Sci USA. 100:13632–13637.

Elizondo-Vega R, Cortes-Campos C, Barahona MJ, Oyarce KA, Carril CA, Garcia-Robles MA (2015) The role of tanycytes in hypothalamic glucosensing. J Cell Mol Med. 19:1471–1482.

Encinas JM, Michurina TV, Peunova N, Park JH, Tordo J, Peterson DA, Fishell G, Koulakov A, Enikolopov G (2011) Division-coupled astrocytic differentiation and age-related depletion of neural stem cells in the adult hippocampus. Cell Stem Cell. 8:566–579.

Encinas JM, Sierra A (2012) Neural stem cell deforestation as the main force driving the age-related decline in adult hippocampal neurogenesis. Behav Brain Res. 227:433–439.

Eriksson PS, Perfilieva E, Björk-Eriksson T, Alborn AM, Nordborg C, Peterson DA, Gage FH (1998) Neurogenesis in the adult human hippocampus. Nat Med. 4:1313–1317.

Espada S, Ortega F, Molina-Jijon E, Rojo AI, Perez-Sen R, Pedraza-Chaverri J, Miras-Portugal MT, Cuadrado A (2010) The purinergic P2Y(13) receptor activates the Nrf2/HO-1 axis and protects against oxidative stress-induced neuronal death. Free Radic Biol Med. 49:416–426.

Esposito MS, Piatti VC, Laplagne DA, Morgenstern NA, Ferrari CC, Pitossi FJ, Schinder AF (2005) Neuronal differentiation in the adult hippocampus recapitulates embryonic development. J Neurosci. 25:10074–10086.

Evans J, Sumners C, Moore J, Huentelman MJ, Deng J, Gelband CH, Shaw G (2002) Characterization of mitotic neurons derived from adult rat hypothalamus and brain stem. J Neurophysiol. 87:1076–1085.

Fabel K, Fabel K, Tam B, Kaufer D, Baiker A, Simmons N, Kuo CJ, Palmer TD (2003) VEGF is necessary for exercise-induced adult hippocampal neurogenesis. Eur J Neurosci. 18:2803–2812.

Fabel K, Wolf SA, Ehninger D, Babu H, Leal-Galicia P, Kempermann G (2009) Additive effects of physical exercise and environmental enrichment on adult hippocampal neurogenesis in mice. Front Neurosci. 3:50.

Fabre AC, Malaval C, Ben Addi A, Verdier C, Pons V, Serhan N, Lichtenstein L, Combes G, Huby T, Briand F, Collet X, Nijstad N, Tietge UJF, Robaye B, Perret B, Boeynaems JM, Martinez LO (2010) P2Y13 receptor is critical for reverse cholesterol transport. Hepatology. 52:1477–1483.

Fanselow MS, Dong HW (2010) Are the dorsal and ventral hippocampus functionally distinct structures? Neuron. 65:7–19.

Farioli-Vecchioli S, Mattera A, Micheli L, Ceccarelli M, Leonardi L, Saraulli D, Costanzi M, Cestari V, Rouault JP, Tirone F (2014) Running rescues defective adult neurogenesis by shortening the length of the cell cycle of neural stem and progenitor cells. Stem Cells. 32:1968–1982.

Ferland RJ, Gross RA, Applegate CD (2002) Increased mitotic activity in the dentate gyrus of the hippocampus of adult C57BL/6J mice exposed to the flurothyl kindling model of epileptogenesis. Neuroscience. 115:669–683.

Ferri ALM, Cavallaro M, Braida D, Di Cristofano A, Canta A, Vezzani A, Ottolenghi S, Pandolfi PP, Sala M, DeBiasi S, Nicolis SK (2004) Sox2 deficiency causes neurodegeneration and impaired neurogenesis in the adult mouse brain. Development. 131:3805–3819.

Firth JA, Bock R (1976) Distribution and properties of an adenosine triphosphatase in the tanycyte ependyma of the IIIrd ventricle of the rat. Histochemistry. 47:145–157.

Florenzano F, Viscomi MT, Mercaldo V, Longone P, Bernardi G, Bagni C, Molinari M, Carrive P (2006) P2X2R purinergic receptor subunit mRNA and protein are expressed by all hypothalamic hypocretin/orexin neurons. J Comp Neurol. 498:58–67.

Frankland PW, Kohler S, Josselyn SA (2013) Hippocampal neurogenesis and forgetting. Trends Neurosci. 36:497–503.

Frayling C, Britton R, Dale N (2011) ATP-mediated glucosensing by hypothalamic tanycytes. J Physiol. 589:2275–2286.

Fumagalli M, Trincavelli L, Lecca D, Martini C, Ciana P, Abbracchio MP (2004) Cloning, pharmacological characterisation and distribution of the rat G-protein-coupled P2Y(13) receptor. Biochem Pharmacol. 68:113–124.

Gage FH (2000) Mammalian Neural Stem Cells. Science. 287:1433–1438.

Gampe K, Stefani J, Hammer K, Brendel P, Pötzsch A, Enikolopov G, Enjyoji K, Acker-Palmer A, Robson SC, Zimmermann H (2015) NTPDase2 and purinergic signaling control progenitor cell proliferation in neurogenic niches of the adult mouse brain. Stem Cells. 33:253–264.

Gao Z, Ure K, Ables JL, Lagace DC, Nave KA, Goebbels S, Eisch AJ, Hsieh J (2009) Neurod1 is essential for the survival and maturation of adult-born neurons. Nat Neurosci. 12:1090–1092.

Gao ZG, Ding Y, Jacobson KA (2010) P2Y(13) receptor is responsible for ADP-mediated degranulation in RBL-2H3 rat mast cells. Pharmacol Res. 62:500–505.

Garrett L, Lie DC, Hrabe de Angelis M, Wurst W, Holter SM (2012) Voluntary wheel running in mice increases the rate of neurogenesis without affecting anxiety-related behaviour in single tests. BMC Neurosci. 13:61.

Ge S, Sailor KA, Ming GL, Song HJ (2008) Synaptic integration and plasticity of new neurons in the adult hippocampus. J Physiol. 586:3759–3765.

Ge S, Yang CH, Hsu KS, Ming GL, Song HJ (2007) A critical period for enhanced synaptic plasticity in newly generated neurons of the adult brain. Neuron. 54:559–566.

Gebara E, Bonaguidi MA, Beckervordersandforth R, Sultan S, Udry F, Gijs P-J, Lie DC, Ming GL, Song HJ, Toni N (2016) Heterogeneity of Radial Glia-Like Cells in the Adult Hippocampus. Stem Cells. 34:997–1010.

Glaser T, Cappellari AR, Pillat MM, Iser IC, Wink MR, Battastini AMO, Ulrich H (2012) Perspectives of purinergic signaling in stem cell differentiation and tissue regeneration. Purinergic Signal. 8:523–537.

Gonzalez JA, Reimann F, Burdakov D (2009) Dissociation between sensing and metabolism of glucose in sugar sensing neurones. J Physiol. 587:41–48.

Götz M, Huttner WB (2005) The cell biology of neurogenesis. Nat Rev Mol Cell Biol. 6:777–788.

Gould E (2007) How widespread is adult neurogenesis in mammals? Nat Rev Neurosci. 8:481–488.

Gould E, Cameron HA, Daniels DC, Woolley CS, McEwen BS (1992) Adrenal hormones suppress cell division in the adult rat dentate gyrus. J Neurosci. 12:3642–3650.

Gould E, Reeves AJ, Graziano MS, Gross CG (1999) Neurogenesis in the neocortex of adult primates. Science. 286:548–552.

Grimm I, Messemer N, Stanke M, Gachet C, Zimmermann H (2009) Coordinate pathways for nucleotide and EGF signaling in cultured adult neural progenitor cells. J Cell Sci. 122:2524–2533.

Grimm I, Ullsperger SN, Zimmermann H (2010) Nucleotides and epidermal growth factor induce parallel cytoskeletal rearrangements and migration in cultured adult murine neural stem cells. Acta Physiol (Oxf). 199:181–189.

Guarracino JF, Cinalli AR, Fernandez V, Roquel LI, Losavio AS (2016) P2Y13 receptors mediate presynaptic inhibition of acetylcholine release induced by adenine nucleotides at the mouse neuromuscular junction. Neuroscience. 326:31–44.

Haan N, Goodman T, Najdi-Samiei A, Stratford CM, Rice R, El Agha E, Bellusci S, Hajihosseini MK (2013) Fgf10-expressing tanycytes add new neurons to the appetite/energy-balance regulating centers of the postnatal and adult hypothalamus. J Neurosci. 33:6170–6180.

Han J, Calvo CF, Kang TH, Baker KL, Park JH, Parras C, Levittas M, Birba U, Pibouin-Fragner L, Fragner P, Bilguvar K, Duman RS, Nurmi H, Alitalo K, Eichmann AC, Thomas JL (2015) Vascular endothelial growth factor receptor 3 controls neural stem cell activation in mice and humans. Cell Rep. 10:1158–1172.

Hattiangady B, Kuruba R, Shetty AK (2011) Acute Seizures in Old Age Leads to a Greater Loss of CA1 Pyramidal Neurons, an Increased Propensity for Developing Chronic TLE and a Severe Cognitive Dysfunction. Aging Dis. 2:1–17.

Hattiangady B, Rao MS, Shetty AK (2004) Chronic temporal lobe epilepsy is associated with severely declined dentate neurogenesis in the adult hippocampus. Neurobiol Dis. 17:473–490.

Heine P, Braun N, Heilbronn A, Zimmermann H (1999) Functional characterization of rat ecto-ATPase and ecto-ATP diphosphohydrolase after heterologous expression in CHO cells. Eur J Biochem. 262:102–107.

Heine VM, Maslam S, Joëls M, Lucassen PJ (2004) Prominent decline of newborn cell proliferation, differentiation, and apoptosis in the aging dentate gyrus, in absence of an age-related hypothalamus–pituitary–adrenal axis activation. Neurobiol Aging. 25:361–375.

Ho CL, Yang CY, Lin WJ, Lin CH (2013) Ecto-nucleoside triphosphate diphosphohydrolase 2 modulates local ATP-induced calcium signaling in human HaCaT keratinocytes. PLoS ONE. 8:e57666.

Hodge RD, Kowalczyk TD, Wolf SA, Encinas JM, Rippey C, Enikolopov G, Kempermann G, Hevner RF (2008) Intermediate progenitors in adult hippocampal neurogenesis: Tbr2 expression and coordinate regulation of neuronal output. J Neurosci. 28:3707–3717.

Holmes AP, Wong SQ, Pulix M, Johnson K, Horton NS, Thomas P, Magalhaes JP de, Plagge A (2016) Reductions in hypothalamic Gfap expression, glial cells and alpha-tanycytes in lean and hypermetabolic Gnasxl-deficient mice. Mol Brain. 9:39.

Homola M, Pfeffer M, Fischer C, Zimmermann H, Robson SC, Korf HW (2015) Expression of ectonucleotidases in the prosencephalon of melatonin-proficient C3H and melatonin-deficient C57Bl mice: spatial distribution and time-dependent changes. Cell Tissue Res. 362:163–176.

Hsieh J (2012) Orchestrating transcriptional control of adult neurogenesis. Genes Dev. 26:1010–1021.

Huszar D, Lynch CA, Fairchild-Huntress V, Dunmore JH, Fang Q, Berkemeier LR, Gu W, Kesterson RA, Boston BA, Cone RD, Smith FJ, Campfield LA, Burn P, Lee F (1997) Targeted disruption of the melanocortin-4 receptor results in obesity in mice. Cell. 88:131–141.

Inoue M, Yagishita-Kyo N, Nonaka M, Kawashima T, Okuno H, Bito H (2010) Synaptic activity-responsive element (SARE): A unique genomic structure with an unusual sensitivity to neuronal activity. Commun Integr Biol. 3:443–446.

Jagasia R, Steib K, Englberger E, Herold S, Faus-Kessler T, Saxe M, Gage FH, Song HJ, Lie DC (2009) GABA-cAMP response element-binding protein signaling regulates maturation and survival of newly generated neurons in the adult hippocampus. J Neurosci. 29:7966–7977.

Jang MH, Bonaguidi MA, Kitabatake Y, Sun J, Song J, Kang E, Jun H, Zhong C, Su Y, Guo JU, Wang MX, Sailor KA, Kim JY, Gao Y, Christian KM, Ming GL, Song HJ (2013) Secreted frizzled-related protein 3 regulates activity-dependent adult hippocampal neurogenesis. Cell Stem Cell. 12:215–223.

Jensen JB, Parmar M (2006) Strengths and Limitations of the Neurosphere Culture System. Mol Neurobiol. 34:153–162.

Jessberger S, Romer B, Babu H, Kempermann G (2005) Seizures induce proliferation and dispersion of doublecortin-positive hippocampal progenitor cells. Exp Neurol. 196:342–351.

Jhaveri DJ, O'Keeffe I, Robinson GJ, Zhao QY, Zhang ZH, Nink V, Narayanan RK, Osborne GW, Wray NR, Bartlett PF (2015) Purification of neural precursor cells reveals the presence of distinct, stimulus-specific subpopulations of quiescent precursors in the adult mouse hippocampus. J Neurosci. 35:8132–8144.

Jimenez-Pacheco A, Diaz-Hernandez M, Arribas-Blazquez M, Sanz-Rodriguez A, Olivos-Ore LA, Artalejo AR, Alves M, Letavic M, Miras-Portugal MT, Conroy RM, Delanty N, Farrell MA, O'Brien DF, Bhattacharya A, Engel T, Henshall DC (2016) Transient P2X7 Receptor Antagonism Produces Lasting Reductions in Spontaneous Seizures and Gliosis in Experimental Temporal Lobe Epilepsy. J Neurosci. 36:5920–5932.

Jin K, Zhu Y, Sun Y, Mao XO, Xie L, Greenberg DA (2002) Vascular endothelial growth factor (VEGF) stimulates neurogenesis in vitro and in vivo. Proc Natl Acad Sci USA. 99:11946–11950.

Jinno S (2011) Topographic differences in adult neurogenesis in the mouse hippocampus: a stereology-based study using endogenous markers. Hippocampus. 21:467–480.

Jo YH, Role LW (2002) Coordinate release of ATP and GABA at in vitro synapses of lateral hypothalamic neurons. J Neurosci. 22:4794–4804.

Jungenitz T, Radic T, Jedlicka P, Schwarzacher SW (2014) High-Frequency Stimulation Induces Gradual Immediate Early Gene Expression in Maturing Adult-Generated Hippocampal Granule Cells. Cereb Cortex. 24:1845–1857.

Jurado-Arjona J, Llorens-Martin M, Avila J, Hernandez F (2016) GSK3beta Overexpression in Dentate Gyrus Neural Precursor Cells Expands the Progenitor Pool and Enhances Memory Skills. J Biol Chem. 291:8199–8213.

Kaebisch C, Schipper D, Babczyk P, Tobiasch E (2015) The role of purinergic receptors in stem cell differentiation. Comput Struct Biotechnol J. 13:75–84.

Karalay O, Doberauer K, Vadodaria KC, Knobloch M, Berti L, Miquelajauregui A, Schwark M, Jagasia R, Taketo MM, Tarabykin V, Lie DC, Jessberger S (2011) Prospero-related homeobox 1 gene (Prox1) is regulated by canonical Wnt signaling and has a stage-specific role in adult hippocampal neurogenesis. Proc Natl Acad Sci USA. 108:5807–5812.

Kawaguchi D, Furutachi S, Kawai H, Hozumi K, Gotoh Y (2013) Dll1 maintains quiescence of adult neural stem cells and segregates asymmetrically during mitosis. Nat Comms. 4:1880.

Kawashima T, Okuno H, Bito H (2014) A new era for functional labeling of neurons: activity-dependent promoters have come of age. Front Neural Circuits. 8:37.

Kee N, Teixeira CM, Wang AH, Frankland PW (2007) Preferential incorporation of adult-generated granule cells into spatial memory networks in the dentate gyrus. Nat Neurosci. 10:355–362.

Kempermann G, Gast D, Kronenberg G, Yamaguchi M, Gage FH (2003) Early determination and long-term persistence of adult-generated new neurons in the hippocampus of mice. Development. 130:391–399.

Kempermann G, Jessberger S, Steiner B, Kronenberg G (2004) Milestones of neuronal development in the adult hippocampus. Trends Neurosci. 27:447–452.

Kempermann G, Krebs J, Fabel K (2008) The contribution of failing adult hippocampal neurogenesis to psychiatric disorders. Curr Opin Psychiatry. 21:290–295.

Kempermann G, Kuhn HG, Gage FH (1997) More hippocampal neurons in adult mice living in an enriched environment. Nature. 386:493–495.

Khaled M, Larribere L, Bille K, Aberdam E, Ortonne JP, Ballotti R, Bertolotto C (2002) Glycogen synthase kinase 3beta is activated by cAMP and plays an active role in the regulation of melanogenesis. J Biol Chem. 277:33690–33697.

Kheirbek MA, Drew LJ, Burghardt NS, Costantini DO, Tannenholz L, Ahmari SE, Zeng H, Fenton AA, Hen R (2013) Differential control of learning and anxiety along the dorsoventral axis of the dentate gyrus. Neuron. 77:955–968.

Khodosevich K, Zuccotti A, Kreuzberg MM, Le Magueresse C, Frank M, Willecke K, Monyer H (2012) Connexin45 modulates the proliferation of transit-amplifying precursor cells in the mouse subventricular zone. Proc Natl Acad Sci USA. 109:20107–20112.

Kim S, Titcombe RF, Zhang H, Khatri L, Girma HK, Hofmann F, Arancio O, Ziff EB (2015) Network compensation of cyclic GMP-dependent protein kinase II knockout in the hippocampus by Ca2+-permeable AMPA receptors. Proc Natl Acad Sci USA. 112:3122–3127.

Kitamura T, Saitoh Y, Takashima N, Murayama A, Niibori Y, Ageta H, Sekiguchi M, Sugiyama H, Inokuchi K (2009) Adult neurogenesis modulates the hippocampus-dependent period of associative fear memory. Cell. 139:814–827.

Kittner H, Franke H, Harsch JI, El-Ashmawy IM, Seidel B, Krugel U, Illes P (2006) Enhanced food intake after stimulation of hypothalamic P2Y1 receptors in rats: modulation of feeding behaviour by extracellular nucleotides. Eur J Neurosci. 24:2049–2056.

Kjelstrup KG, Tuvnes FA, Steffenach HA, Murison R, Moser EI, Moser MB (2002) Reduced fear expression after lesions of the ventral hippocampus. Proc Natl Acad Sci USA. 99:10825–10830.

Kobilo T, Liu QR, Gandhi K, Mughal M, Shaham Y, van Praag H (2011) Running is the neurogenic and neurotrophic stimulus in environmental enrichment. Learn Mem. 18:605–609.

Koizumi S, Shigemoto-Mogami Y, Nasu-Tada K, Shinozaki Y, Ohsawa K, Tsuda M, Joshi BV, Jacobson KA, Kohsaka S, Inoue K (2007) UDP acting at P2Y6 receptors is a mediator of microglial phagocytosis. Nature. 446:1091–1095.

Kokoeva MV, Yin H, Flier JS (2005) Neurogenesis in the hypothalamus of adult mice: potential role in energy balance. Science. 310:679–683.

Kokoeva MV, Yin H, Flier JS (2007) Evidence for constitutive neural cell proliferation in the adult murine hypothalamus. J Comp Neurol. 505:209–220.

Kriegsfeld LJ, Silver R (2006) The regulation of neuroendocrine function: Timing is everything. Horm Behav. 49:557–574.

Kronenberg G, Reuter K, Steiner B, Brandt MD, Jessberger S, Yamaguchi M, Kempermann G (2003) Subpopulations of proliferating cells of the adult hippocampus respond differently to physiologic neurogenic stimuli. J Comp Neurol. 467:455–463.

Kuhn HG, Dickinson-Anson H, Gage FH (1996) Neurogenesis in the dentate gyrus of the adult rat: age-related decrease of neuronal progenitor proliferation. J Neurosci. 16:2027–2033.

Kuipers SD, Schroeder JE, Trentani A (2015) Changes in hippocampal neurogenesis throughout early development. Neurobiol Aging. 36:365–379.

Kukekov VG, Laywell ED, Suslov O, Davies K, Scheffler B, Thomas LB, O'Brien TF, Kusakabe M, Steindler DA (1999) Multipotent stem/progenitor cells with similar properties arise from two neurogenic regions of adult human brain. Exp Neurol. 156:333–344.

Kukulski F, Levesque SA, Lavoie EG, Lecka J, Bigonnesse F, Knowles AF, Robson SC, Kirley TL, Sevigny J (2005) Comparative hydrolysis of P2 receptor agonists by NTPDases 1, 2, 3 and 8. Purinergic Signal. 1:193–204.

Kukulski F, Levesque SA, Sevigny J (2011) Impact of ectoenzymes on p2 and p1 receptor signaling. Adv Pharmacol. 61:263–299.

Kunze A, Congreso MR, Hartmann C, Wallraff-Beck A, Huttmann K, Bedner P, Requardt R, Seifert G, Redecker C, Willecke K, Hofmann A, Pfeifer A, Theis M, Steinhauser C (2009) Connexin expression by radial glia-like cells is required for neurogenesis in the adult dentate gyrus. Proc Natl Acad Sci USA. 106:11336–11341.

Lacar B, Herman P, Hartman NW, Hyder F, Bordey A (2012) S phase entry of neural progenitor cells correlates with increased blood flow in the young subventricular zone. PLoS ONE. 7:e31960.

Laemmli UK (1970) Cleavage of Structural Proteins during the Assembly of the Head of Bacteriophage T4. Nature. 227:680–685.

Langer D, Hammer K, Koszalka P, Schrader J, Robson SC, Zimmermann H (2008) Distribution of ectonucleotidases in the rodent brain revisited. Cell Tissue Res. 334:199–217.

Langer D, Ikehara Y, Takebayashi H, Hawkes R, Zimmermann H (2007) The ectonucleotidases alkaline phosphatase and nucleoside triphosphate diphosphohydrolase 2 are associated with subsets of progenitor cell populations in the mouse embryonic, postnatal and adult neurogenic zones. Neuroscience. 150:863–879.

Langlet F (2014) Tanycytes: a gateway to the metabolic hypothalamus. J Neuroendocrinol. 26:753–760.

Langlet F, Levin BE, Luquet S, Mazzone M, Messina A, Dunn-Meynell AA, Balland E, Lacombe A, Mazur D, Carmeliet P, Bouret SG, Prevot V, Dehouck B (2013) Tanycytic VEGF-A boosts blood-hypothalamus barrier plasticity and access of metabolic signals to the arcuate nucleus in response to fasting. Cell Metab. 17:607–617.

Lavado A, Lagutin OV, Chow LML, Baker SJ, Oliver G (2010) Prox1 is required for granule cell maturation and intermediate progenitor maintenance during brain neurogenesis. PLoS Biol. 8.

Lee DA, Bedont JL, Pak T, Wang H, Song J, Miranda-Angulo A, Takiar V, Charubhumi V, Balordi F, Takebayashi H, Aja S, Ford E, Fishell G, Blackshaw S (2012) Tanycytes of the hypothalamic median eminence form a diet-responsive neurogenic niche. Nat Neurosci. 15:700–702.

Lee DA, Yoo S, Pak T, Salvatierra J, Velarde E, Aja S, Blackshaw S (2014) Dietary and sex-specific factors regulate hypothalamic neurogenesis in young adult mice. Front Neurosci. 8:157.

Léon C, Hechler B, Freund M, Eckly A, Vial C, Ohlmann P, Dierich A, Lemeur M, Cazenave JP, Gachet C (1999) Defective platelet aggregation and increased resistance to thrombosis in purinergic P2Y(1) receptor-null mice. J Clin Invest. 104:1731–1737.

Leutgeb JK, Leutgeb S, Moser MB, Moser EI (2007) Pattern separation in the dentate gyrus and CA3 of the hippocampus. Science. 315:961–966.

Li J, Tang Y, Cai D (2012) IKKbeta/NF-kappaB disrupts adult hypothalamic neural stem cells to mediate a neurodegenerative mechanism of dietary obesity and pre-diabetes. Nat Cell Biol. 14:999–1012.

Lichtenstein L, Serhan N, Espinosa-Delgado S, Fabre A, Annema W, Tietge UJF, Robaye B, Boeynaems JM, Laffargue M, Perret B, Martinez LO (2015) Increased atherosclerosis in P2Y13/apolipoprotein E double-knockout mice: contribution of P2Y13 to reverse cholesterol transport. Cardiovasc Res. 106:314–323.

Lie DC, Colamarino SA, Song HJ, Desire L, Mira H, Consiglio A, Lein ES, Jessberger S, Lansford H, Dearie AR, Gage FH (2005) Wnt signalling regulates adult hippocampal neurogenesis. Nature. 437:1370–1375.

Lieberwirth C, Wang Z (2012) The social environment and neurogenesis in the adult Mammalian brain. Front Hum Neurosci. 6:118.

Lin JHC, Takano T, Arcuino G, Wang X, Hu F, Darzynkiewicz Z, Nunes M, Goldman SA, Nedergaard M (2007) Purinergic signaling regulates neural progenitor cell expansion and neurogenesis. Dev Biol. 302:356–366.

Liu X, Hashimoto-Torii K, Torii M, Ding C, Rakic P (2010) Gap junctions/hemichannels modulate interkinetic nuclear migration in the forebrain precursors. J Neurosci. 30:4197–4209.

Lledo PM, Alonso M, Grubb MS (2006) Adult neurogenesis and functional plasticity in neuronal circuits. Nat Rev Neurosci. 7:179–193.

Lohman AW, Billaud M, Isakson BE (2012) Mechanisms of ATP release and signalling in the blood vessel wall. Cardiovasc Res. 95:269–280.

Lopatar J, Dale N, Frenguelli BG (2015) Pannexin-1-mediated ATP release from area CA3 drives mGlu5-dependent neuronal oscillations. Neuropharmacology. 93:219–228.

Lugert S, Basak O, Knuckles P, Haussler U, Fabel K, Götz M, Haas CA, Kempermann G, Taylor V, Giachino C (2010) Quiescent and active hippocampal neural stem cells with distinct morphologies respond selectively to physiological and pathological stimuli and aging. Cell Stem Cell. 6:445–456.

Maggi R, Zasso J, Conti L (2014) Neurodevelopmental origin and adult neurogenesis of the neuroendocrine hypothalamus. Front Cell Neurosci. 8:440.

Malin SA, Molliver DC (2010) Gi- and Gq-coupled ADP (P2Y) receptors act in opposition to modulate nociceptive signaling and inflammatory pain behavior. Mol Pain. 6:21.

Manahan-Vaughan D, Ngomba RT, Storto M, Kulla A, Catania MV, Chiechio S, Rampello L, Passarelli F, Capece A, Reymann KG, Nicoletti F (2003) An increased expression of the mGlu5 receptor protein following LTP induction at the perforant path-dentate gyrus synapse in freely moving rats. Neuropharmacology. 44:17–25.

Marin-Burgin A, Mongiat LA, Pardi MB, Schinder AF (2012) Unique processing during a period of high excitation/inhibition balance in adult-born neurons. Science. 335:1238–1242.

Markakis EA, Palmer TD, Randolph-Moore L, Rakic P, Gage FH (2004) Novel neuronal phenotypes from neural progenitor cells. J Neurosci. 24:2886–2897.

Marteau F, Le Poul E, Communi D, Communi D, Labouret C, Savi P, Boeynaems JM, Gonzalez NS (2003) Pharmacological characterization of the human P2Y13 receptor. Mol Pharmacol. 64:104–112.

Mayer J (1953) Glucostatic mechanism of regulation of food intake. N Engl J Med. 249:13–16.
McNay DEG, Briancon N, Kokoeva MV, Maratos-Flier E, Flier JS (2012) Remodeling of the arcuate nucleus energy-balance circuit is inhibited in obese mice. J Clin Invest. 122:142–152.
McTighe SM, Mar AC, Romberg C, Bussey TJ, Saksida LM (2009) A new touchscreen test of pattern separation: effect of hippocampal lesions. Neuroreport. 20:881–885.
Melani A, Corti F, Stephan H, Muller CE, Donati C, Bruni P, Vannucchi MG, Pedata F (2012) Ecto-ATPase inhibition: ATP and adenosine release under physiological and ischemic in vivo conditions in the rat striatum. Exp Neurol. 233:193–204.
Merz K, Herold S, Lie DC (2011) CREB in adult neurogenesis--master and partner in the development of adult-born neurons? Eur J Neurosci. 33:1078–1086.
Messemer N, Kunert C, Grohmann M, Sobottka H, Nieber K, Zimmermann H, Franke H, Norenberg W, Straub I, Schaefer M, Riedel T, Illes P, Rubini P (2013) P2X7 receptors at adult neural progenitor cells of the mouse subventricular zone. Neuropharmacology. 73:122–137.
Migaud M, Batailler M, Segura S, Duittoz A, Franceschini I, Pillon D (2010) Emerging new sites for adult neurogenesis in the mammalian brain: a comparative study between the hypothalamus and the classical neurogenic zones. Eur J Neurosci. 32:2042–2052.
Migita H, Kominami K, Higashida M, Maruyama R, Tuchida N, McDonald F, Shimada F, Sakurada K (2008) Activation of adenosine A1 receptor-induced neural stem cell proliferation via MEK/ERK and Akt signaling pathways. J Neurosci Res. 86:2820–2828.
Mignone JL, Kukekov V, Chiang AS, Steindler D, Enikolopov G (2004) Neural stem and progenitor cells in nestin-GFP transgenic mice. J Comp Neurol. 469:311–324.
Ming GL, Song HJ (2011) Adult neurogenesis in the mammalian brain: significant answers and significant questions. Neuron. 70:687–702.
Mira H, Andreu Z, Suh H, Lie DC, Jessberger S, Consiglio A, San Emeterio J, Hortiguela R, Marques-Torrejon MA, Nakashima K, Colak D, Götz M, Farinas I, Gage FH (2010) Signaling through BMPR-IA regulates quiescence and long-term activity of neural stem cells in the adult hippocampus. Cell Stem Cell. 7:78–89.
Mishra SK, Braun N, Shukla V, Fullgrabe M, Schomerus C, Korf HW, Gachet C, Ikehara Y, Sevigny J, Robson SC, Zimmermann H (2006) Extracellular nucleotide signaling in adult neural stem cells: synergism with growth factor-mediated cellular proliferation. Development. 133:675–684.
Miyata S (2015) New aspects in fenestrated capillary and tissue dynamics in the sensory circumventricular organs of adult brains. Front Neurosci. 9:390.
Moraes JC, Coope A, Morari J, Cintra DE, Roman EA, Pauli JR, Romanatto T, Carvalheira JB, Oliveira ALR, Saad MJ, Velloso LA (2009) High-fat diet induces apoptosis of hypothalamic neurons. PLoS ONE. 4:e5045.
Morente V, Perez-Sen R, Ortega F, Huerta-Cepas J, Delicado EG, Miras-Portugal MT (2014) Neuroprotection elicited by P2Y13 receptors against genotoxic stress by inducing DUSP2 expression and MAPK signaling recovery. Biochim Biophys Acta. 1843:1886–1898.
Morrison SJ, Spradling AC (2008) Stem cells and niches: mechanisms that promote stem cell maintenance throughout life. Cell. 132:598–611.
Morton GJ, Cummings DE, Baskin DG, Barsh GS, Schwartz MW (2006) Central nervous system control of food intake and body weight. Nature. 443:289–295.
Moser MB, Moser EI, Forrest E, Andersen P, Morris RG (1995) Spatial learning with a minislab in the dorsal hippocampus. Proc Natl Acad Sci USA. 92:9697–9701.
Mu L, Berti L, Masserdotti G, Covic M, Michaelidis TM, Doberauer K, Merz K, Rehfeld F, Haslinger A, Wegner M, Sock E, Lefebvre V, Couillard-Despres S, Aigner L, Berninger B, Lie DC (2012) SoxC transcription factors are required for neuronal differentiation in adult hippocampal neurogenesis. J Neurosci. 32:3067–3080.

Mullier A, Bouret SG, Prevot V, Dehouck B (2010) Differential distribution of tight junction proteins suggests a role for tanycytes in blood-hypothalamus barrier regulation in the adult mouse brain. J Comp Neurol. 518:943–962.

Nakashiba T, Cushman JD, Pelkey KA, Renaudineau S, Buhl DL, McHugh TJ, Rodriguez Barrera V, Chittajallu R, Iwamoto KS, McBain CJ, Fanselow MS, Tonegawa S (2012) Young dentate granule cells mediate pattern separation, whereas old granule cells facilitate pattern completion. Cell. 149:188–201.

Nakatomi H, Kuriu T, Okabe S, Yamamoto SI, Hatano O, Kawahara N, Tamura A, Kirino T, Nakafuku M (2002) Regeneration of hippocampal pyramidal neurons after ischemic brain injury by recruitment of endogenous neural progenitors. Cell. 110:429–441.

Neary JT, Kang Y (2006) P2 purinergic receptors signal to glycogen synthase kinase-3beta in astrocytes. J Neurosci Res. 84:515–524.

Neary JT, Zimmermann H (2009) Trophic functions of nucleotides in the central nervous system. Trends Neurosci. 32:189–198.

Oh J, McCloskey MA, Blong CC, Bendickson L, Nilsen-Hamilton M, Sakaguchi DS (2010) Astrocyte-derived interleukin-6 promotes specific neuronal differentiation of neural progenitor cells from adult hippocampus. J Neurosci Res. 88:2798–2809.

Okuno H (2011) Regulation and function of immediate-early genes in the brain: beyond neuronal activity markers. Neurosci Res. 69:175–186.

Ollmann MM, Wilson BD, Yang YK, Kerns JA, Chen Y, Gantz I, Barsh GS (1997) Antagonism of central melanocortin receptors in vitro and in vivo by agouti-related protein. Science. 278:135–138.

Olney JW (1969) Brain lesions, obesity, and other disturbances in mice treated with monosodium glutamate. Science. 164:719–721.

Ono N, Ono W, Nagasawa T, Kronenberg HM (2014) A subset of chondrogenic cells provides early mesenchymal progenitors in growing bones. Nat Cell Biol. 16:1157–1167.

Orellana JA, Saez PJ, Cortes-Campos C, Elizondo RJ, Shoji KF, Contreras-Duarte S, Figueroa V, Velarde V, Jiang JX, Nualart F, Saez JC, Garcia MA (2012) Glucose increases intracellular free Ca(2+) in tanycytes via ATP released through connexin 43 hemichannels. Glia. 60:53–68.

Orriss I, Syberg S, Wang N, Robaye B, Gartland A, Jorgensen N, Arnett T, Boeynaems JM (2011) Bone phenotypes of P2 receptor knockout mice. Front Biosci. (Schol Ed) 3:1038–1046.

Ortega F, Perez-Sen R, Delicado EG, Miras-Portugal MT (2011) ERK1/2 activation is involved in the neuroprotective action of P2Y13 and P2X7 receptors against glutamate excitotoxicity in cerebellar granule neurons. Neuropharmacology. 61:1210–1221.

Palmer TD, Markakis EA, Willhoite AR, Safar F, Gage FH (1999) Fibroblast growth factor-2 activates a latent neurogenic program in neural stem cells from diverse regions of the adult CNS. J Neurosci. 19:8487–8497.

Palmer TD, Takahashi J, Gage FH (1997) The adult rat hippocampus contains primordial neural stem cells. Mol Cell Neurosci. 8:389–404.

Palmer TD, Willhoite AR, Gage FH (2000) Vascular niche for adult hippocampal neurogenesis. J Comp Neurol. 425:479–494.

Parent JM, Murphy GG (2008) Mechanisms and functional significance of aberrant seizure-induced hippocampal neurogenesis. Epilepsia. 49 Suppl 5:19–25.

Pastrana E, Silva-Vargas V, Doetsch F (2011) Eyes wide open: a critical review of sphere-formation as an assay for stem cells. Cell Stem Cell. 8:486–498.

Paton JA, Nottebohm FN (1984) Neurons generated in the adult brain are recruited into functional circuits. Science. 225:1046–1048.

Pearson RA, Dale N, Llaudet E, Mobbs P (2005) ATP released via gap junction hemichannels from the pigment epithelium regulates neural retinal progenitor proliferation. Neuron. 46:731–744.

Pencea V, Bingaman KD, Wiegand SJ, Luskin MB (2001) Infusion of brain-derived neurotrophic factor into the lateral ventricle of the adult rat leads to new neurons in the parenchyma of the striatum, septum, thalamus, and hypothalamus. J Neurosci. 21:6706–6717.

Perez-Martin M, Cifuentes M, Grondona JM, Lopez-Avalos MD, Gomez-Pinedo U, García-Verdugo JM, Fernandez-Llebrez P (2010) IGF-I stimulates neurogenesis in the hypothalamus of adult rats. Eur J Neurosci. 31:1533–1548.

Perez-Sen R, Queipo MJ, Morente V, Ortega F, Delicado EG, Miras-Portugal MT (2015) Neuroprotection Mediated by P2Y13 Nucleotide Receptors in Neurons. Comput Struct Biotechnol J. 13:160–168.

Peruzzo B, Pastor FE, Blazquez JL, Schobitz K, Pelaez B, Amat P, Rodriguez EM (2000) A second look at the barriers of the medial basal hypothalamus. Exp Brain Res. 132:10–26.

Petit P, Lajoix AD, Gross R (2009) P2 purinergic signalling in the pancreatic beta-cell: control of insulin secretion and pharmacology. Eur J Pharm Sci. 37:67–75.

Piatti VC, Davies-Sala MG, Esposito MS, Mongiat LA, Trinchero MF, Schinder AF (2011) The timing for neuronal maturation in the adult hippocampus is modulated by local network activity. J Neurosci. 31:7715–7728.

Pierce AA, Xu AW (2010) De novo neurogenesis in adult hypothalamus as a compensatory mechanism to regulate energy balance. J Neurosci. 30:723–730.

Porcheri C, Suter U, Jessberger S (2014) Dissecting integrin-dependent regulation of neural stem cell proliferation in the adult brain. J Neurosci. 34:5222–5232.

Ralevic V, Burnstock G (1998) Receptors for purines and pyrimidines. Pharmacol Rev. 50:413–492.

Reynolds BA, Rietze RL (2005) Neural stem cells and neurospheres--re-evaluating the relationship. Nat Methods. 2:333–336.

Reynolds BA, Weiss S (1992) Generation of neurons and astrocytes from isolated cells of the adult mammalian central nervous system. Science. 255:1707–1710.

Richards LJ, Kilpatrick TJ, Bartlett PF (1992) De novo generation of neuronal cells from the adult mouse brain. Proc Natl Acad Sci USA. 89:8591–8595.

Rizzoti K, Lovell-Badge R (2016) Pivotal role of median eminence tanycytes for hypothalamic function and neurogenesis. Mol Cell Endocrinol. doi: 10.1016/j.mce.2016.08.020:[Epub ahead of print].

Robins SC, Stewart I, McNay DE, Taylor V, Giachino C, Goetz M, Ninkovic J, Briancon N, Maratos-Flier E, Flier JS, Kokoeva MV, Placzek M (2013) alpha-Tanycytes of the adult hypothalamic third ventricle include distinct populations of FGF-responsive neural progenitors. Nat Comms. 4:2049.

Robson SC, Sevigny J, Zimmermann H (2006) The E-NTPDase family of ectonucleotidases: Structure function relationships and pathophysiological significance. Purinergic Signal. 2:409–430.

Rodriguez E, Blazquez J, Pastor F, Pelaez B, Pena P, Peruzzo B, Amat P (2005) Hypothalamic Tanycytes. A Key Component of Brain–Endocrine Interaction. Int Rev Cytol. 247:89–164.

Romano C, Sesma MA, McDonald CT, O'Malley K, van den Pol AN, Olney JW (1995) Distribution of metabotropic glutamate receptor mGluR5 immunoreactivity in rat brain. J Comp Neurol. 355:455–469.

Roy NS, Wang S, Jiang L, Kang J, Benraiss A, Harrison-Restelli C, Fraser RA, Couldwell WT, Kawaguchi A, Okano H, Nedergaard M, Goldman SA (2000) In vitro neurogenesis by progenitor cells isolated from the adult human hippocampus. Nat Med. 6:271–277.

Rozmer K, Gao P, Araujo MGL, Khan MT, Liu J, Rong W, Tang Y, Franke H, Krugel U, Fernandes MJS, Illes P (2016) Pilocarpine-Induced Status Epilepticus Increases the Sensitivity of P2X7 and P2Y1 Receptors to Nucleotides at Neural Progenitor Cells of the Juvenile Rodent Hippocampus. Cereb Cortex. doi: 10.1093/cercor/bhw178:[Epub ahead of print].

Sahay A, Hen R (2007) Adult hippocampal neurogenesis in depression. Nat Neurosci. 10:1110–1115.

Sahay A, Scobie KN, Hill AS, O'Carroll CM, Kheirbek MA, Burghardt NS, Fenton AA, Dranovsky A, Hen R (2011) Increasing adult hippocampal neurogenesis is sufficient to improve pattern separation. Nature. 472:466–470.

Samms RJ, Lewis JE, Lory A, Fowler MJ, Cooper S, Warner A, Emmerson P, Adams AC, Luckett JC, Perkins AC, Wilson D, Barrett P, Tsintzas K, Ebling FJP (2015) Antibody-Mediated Inhibition of the FGFR1c Isoform Induces a Catabolic Lean State in Siberian Hamsters. Curr Biol. 25:2997–3003.

Saxe MD, Malleret G, Vronskaya S, Mendez I, Garcia AD, Sofroniew MV, Kandel ER, Hen R (2007) Paradoxical influence of hippocampal neurogenesis on working memory. Proc Natl Acad Sci USA. 104:4642–4646.

Scemes E, Duval N, Meda P (2003) Reduced expression of P2Y1 receptors in connexin43-null mice alters calcium signaling and migration of neural progenitor cells. J Neurosci. 23:11444–11452.

Schanzer A, Wachs FP, Wilhelm D, Acker T, Cooper-Kuhn C, Beck H, Winkler J, Aigner L, Plate KH, Kuhn HG (2004) Direct stimulation of adult neural stem cells in vitro and neurogenesis in vivo by vascular endothelial growth factor. Brain Pathol. 14:237–248.

Scharfman H, Goodman J, Macleod A, Phani S, Antonelli C, Croll S (2005) Increased neurogenesis and the ectopic granule cells after intrahippocampal BDNF infusion in adult rats. Experimental neurology 192:348–356.

Schilling K, Luk D, Morgan JI, Curran T (1991) Regulation of a fos-lacZ fusion gene. A paradigm for quantitative analysis of stimulus-transcription coupling. Proc Natl Acad Sci USA. 88:5665–5669.

Schmidt B, Marrone DF, Markus EJ (2012) Disambiguating the similar: the dentate gyrus and pattern separation. Behav Brain Res. 226:56–65.

Schmidt-Hieber C, Jonas P, Bischofberger J (2004) Enhanced synaptic plasticity in newly generated granule cells of the adult hippocampus. Nature. 429:184–187.

Schwartz MW, Woods SC, Porte D, JR, Seeley RJ, Baskin DG (2000) Central nervous system control of food intake. Nature. 404:661–671.

Seib DRM, Corsini NS, Ellwanger K, Plaas C, Mateos A, Pitzer C, Niehrs C, Celikel T, Martin-Villalba A (2013) Loss of Dickkopf-1 restores neurogenesis in old age and counteracts cognitive decline. Cell Stem Cell. 12:204–214.

Seidel B, Bigl M, Franke H, Kittner H, Kiess W, Illes P, Krugel U (2006) Expression of purinergic receptors in the hypothalamus of the rat is modified by reduced food availability. Brain Res. 1089:143–152.

Seri B, García-Verdugo JM, McEwen BS, Alvarez-Buylla A (2001) Astrocytes give rise to new neurons in the adult mammalian hippocampus. J Neurosci. 21:7153–7160.

Shapiro LA, Ng KL, Kinyamu R, Whitaker-Azmitia P, Geisert EE, Blurton-Jones M, Zhou QY, Ribak CE (2007) Origin, migration and fate of newly generated neurons in the adult rodent piriform cortex. Brain Struct Funct. 212:133–148.

Shigemoto R, Kinoshita A, Wada E, Nomura S, Ohishi H, Takada M, Flor PJ, Neki A, Abe T, Nakanishi S, Mizuno N (1997) Differential presynaptic localization of metabotropic glutamate receptor subtypes in the rat hippocampus. J Neurosci. 17:7503–7522.

Shimazu K, Zhao M, Sakata K, Akbarian S, Bates B, Jaenisch R, Lu B (2006) NT-3 facilitates hippocampal plasticity and learning and memory by regulating neurogenesis. Learn Mem. 13:307–315.

Shors TJ, Miesegaes G, Beylin A, Zhao M, Rydel T, Gould E (2001) Neurogenesis in the adult is involved in the formation of trace memories. Nature. 410:372–376.

Shukla V, Zimmermann H, Wang L, Kettenmann H, Raab S, Hammer K, Sevigny J, Robson SC, Braun N (2005) Functional expression of the ecto-ATPase NTPDase2 and of nucleotide receptors by neuronal progenitor cells in the adult murine hippocampus. J Neurosci Res. 80:600–610.

Sierra A, Encinas JM, Deudero JJP, Chancey JH, Enikolopov G, Overstreet-Wadiche LS, Tsirka SE, Maletić-Savatić M (2010) Microglia shape adult hippocampal neurogenesis through apoptosis-coupled phagocytosis. Cell Stem Cell. 7:483–495.

Sierra A, Martín-Suárez S, Valcárcel-Martín R, Pascual-Brazo J, Aelvoet SA, Abiega O, Deudero JJ, Brewster AL, Bernales I, Anderson AE, Baekelandt V, Maletić-Savatić M, Encinas JM (2015) Neuronal hyperactivity accelerates depletion of neural stem cells and impairs hippocampal neurogenesis. Cell Stem Cell. 16:488–503.

Sierra A, Tremblay ME, Wake H (2014) Never-resting microglia: physiological roles in the healthy brain and pathological implications. Front Cell Neurosci. 8:240.

Smeyne RJ, Schilling K, Robertson L, Luk D, Oberdick J, Curran T, Morgan JI (1992) Fos-lacZ transgenic mice. Mapping sites of gene induction in the central nervous system. Neuron. 8:13–23.

Smith LK, He Y, Park JS, Bieri G, Snethlage CE, Lin K, Gontier G, Wabl R, Plambeck KE, Udeochu J, Wheatley EG, Bouchard J, Eggel A, Narasimha R, Grant JL, Luo J, Wyss-Coray T, Villeda SA (2015) beta2-microglobulin is a systemic pro-aging factor that impairs cognitive function and neurogenesis. Nat Med. 21:932–937.

Snyder JS, Ferrante SC, Cameron HA (2012) Late maturation of adult-born neurons in the temporal dentate gyrus. PLoS ONE. 7:e48757.

Snyder JS, Soumier A, Brewer M, Pickel J, Cameron HA (2011) Adult hippocampal neurogenesis buffers stress responses and depressive behaviour. Nature. 476:458–461.

Song HJ, Stevens CF, Gage FH (2002) Astroglia induce neurogenesis from adult neural stem cells. Nature. 417:39–44.

Song J, Zhong C, Bonaguidi MA, Sun GJ, Hsu D, Gu Y, Meletis K, Huang ZJ, Ge S, Enikolopov G, Deisseroth K, Luscher B, Christian KM, Ming GL, Song HJ (2012) Neuronal circuitry mechanism regulating adult quiescent neural stem-cell fate decision. Nature. 489:150–154.

Sousa-Ferreira L, Almeida LP de, Cavadas C (2014) Role of hypothalamic neurogenesis in feeding regulation. Trends Endocrinol Metab. 25:80–88.

Stafford MR, Bartlett PF, Adams DJ (2007) Purinergic receptor activation inhibits mitogen-stimulated proliferation in primary neurospheres from the adult mouse subventricular zone. Mol Cell Neurosci. 35:535–548.

Steiner B, Klempin F, Wang L, Kott M, Kettenmann H, Kempermann G (2006) Type-2 cells as link between glial and neuronal lineage in adult hippocampal neurogenesis. Glia. 54:805–814.

Stojilkovic SS (2009) Purinergic regulation of hypothalamopituitary functions. Trends Endocrinol Metab. 20:460–468.

Stojilkovic SS, He ML, Koshimizu TA, Balik A, Zemkova H (2010) Signaling by purinergic receptors and channels in the pituitary gland. Mol Cell Endocrinol. 314:184–191.

Striedinger K, Meda P, Scemes E (2007) Exocytosis of ATP from astrocyte progenitors modulates spontaneous Ca2+ oscillations and cell migration. Glia. 55:652–662.

Suh H, Consiglio A, Ray J, Sawai T, D'Amour KA, Gage FH (2007) In vivo fate analysis reveals the multipotent and self-renewal capacities of Sox2+ neural stem cells in the adult hippocampus. Cell Stem Cell. 1:515–528.

Sun GJ, Zhou Y, Stadel RP, Moss J, Yong JHA, Ito S, Kawasaki NK, Phan AT, Oh JH, Modak N, Reed RR, Toni N, Song HJ, Ming GL (2015) Tangential migration of neuronal precursors of glutamatergic neurons in the adult mammalian brain. Proc Natl Acad Sci USA. 112:9484–9489.

Suyama S, Sunabori T, Kanki H, Sawamoto K, Gachet C, Koizumi S, Okano H (2012) Purinergic signaling promotes proliferation of adult mouse subventricular zone cells. J Neurosci. 32:9238–9247.

Tan C, Voss U, Svensson S, Erlinge D, Olde B (2013) High glucose and free fatty acids induce beta cell apoptosis via autocrine effects of ADP acting on the P2Y(13) receptor. Purinergic Signal. 9:67–79.

Tanti A, Rainer Q, Minier F, Surget A, Belzung C (2012) Differential environmental regulation of neurogenesis along the septo-temporal axis of the hippocampus. Neuropharmacology. 63:374–384.

Tashiro A, Sandler VM, Toni N, Zhao C, Gage FH (2006) NMDA-receptor-mediated, cell-specific integration of new neurons in adult dentate gyrus. Nature. 442:929–933.

Tatsumi E, Yamanaka H, Kobayashi K, Yagi H, Sakagami M, Noguchi K (2015) RhoA/ROCK pathway mediates p38 MAPK activation and morphological changes downstream of P2Y12/13 receptors in spinal microglia in neuropathic pain. Glia. 63:216–228.

Teixeira CM, Kron MM, Masachs N, Zhang H, Lagace DC, Martinez A, Reillo I, Duan X, Bosch C, Pujadas L, Brunso L, Song HJ, Eisch AJ, Borrell V, Howell BW, Parent JM, Soriano E (2012) Cell-autonomous inactivation of the reelin pathway impairs adult neurogenesis in the hippocampus. J Neurosci. 32:12051–12065.

Thakkar MM, Winston S, McCarley RW (2002) Orexin neurons of the hypothalamus express adenosine A1 receptors. Brain Res. 944:190–194.

Thimm D, Knospe M, Abdelrahman A, Moutinho M, Alsdorf BBA, von Kügelgen I, Schiedel AC, Muller CE (2013) Characterization of new G protein-coupled adenine receptors in mouse and hamster. Purinergic Signal. 9:415–426.

Thom M, Sisodiya SM, Beckett A, Martinian L, Lin WR, Harkness W, Mitchell TN, Craig J, Duncan J, Scaravilli F (2002) Cytoarchitectural abnormalities in hippocampal sclerosis. J Neuropathol Exp Neurol. 61:510–519.

Thompson BAN, Storm MP, Hewinson J, Hogg S, Welham MJ, MacKenzie AB (2012) A novel role for P2X7 receptor signalling in the survival of mouse embryonic stem cells. Cell Signal. 24:770–778.

Toni N, Laplagne DA, Zhao C, Lombardi G, Ribak CE, Gage FH, Schinder AF (2008) Neurons born in the adult dentate gyrus form functional synapses with target cells. Nat Neurosci. 11:901–907.

Tozuka Y, Fukuda S, Namba T, Seki T, Hisatsune T (2005) GABAergic excitation promotes neuronal differentiation in adult hippocampal progenitor cells. Neuron. 47:803–815.

Trejo JL, Carro E, Torres-Aleman I (2001) Circulating insulin-like growth factor I mediates exercise-induced increases in the number of new neurons in the adult hippocampus. J Neurosci. 21:1628–1634.

Tsao HK, Chiu PH, Sun SH (2013) PKC-dependent ERK phosphorylation is essential for P2X7 receptor-mediated neuronal differentiation of neural progenitor cells. Cell Death Dis. 4:e751.

Urban N, Guillemot F (2014) Neurogenesis in the embryonic and adult brain: same regulators, different roles. Front Cell Neurosci. 8:396.

Valdearcos M, Xu AW, Koliwad SK (2015) Hypothalamic inflammation in the control of metabolic function. Annu Rev Physiol. 77:131–160.

van Doze A, Perez DM (2012) G-protein-coupled receptors in adult neurogenesis. Pharmacol Rev. 64:645–675.
van Praag H, Christie BR, Sejnowski TJ, Gage FH (1999) Running enhances neurogenesis, learning, and long-term potentiation in mice. Proc Natl Acad Sci USA. 96:13427–13431.
van Praag H, Schinder AF, Christie BR, Toni N, Palmer TD, Gage FH (2002) Functional neurogenesis in the adult hippocampus. Nature. 415:1030–1034.
Vandenbeuch A, Anderson CB, Parnes J, Enjyoji K, Robson SC, Finger TE, Kinnamon SC (2013) Role of the ectonucleotidase NTPDase2 in taste bud function. Proc Natl Acad Sci USA. 110:14789–14794.
Verkhratsky A, Burnstock G (2014) Biology of purinergic signalling: its ancient evolutionary roots, its omnipresence and its multiple functional significance. Bioessays. 36:697–705.
Villeda SA et al. (2011) The ageing systemic milieu negatively regulates neurogenesis and cognitive function. Nature. 477:90–94.
von Kügelgen I (2006) Pharmacological profiles of cloned mammalian P2Y-receptor subtypes. Pharmacol Ther. 110:415–432.
von Kügelgen I, Harden TK (2011) Molecular pharmacology, physiology, and structure of the P2Y receptors. Adv Pharmacol. 61:373–415.
von Kügelgen I, Hoffmann K (2016) Pharmacology and structure of P2Y receptors. Neuropharmacology. 104:50–61.
Voss U, Turesson MF, Robaye B, Boeynaems JM, Olde B, Erlinge D, Ekblad E (2014) The enteric nervous system of P2Y13 receptor null mice is resistant against high-fat-diet- and palmitic-acid-induced neuronal loss. Purinergic Signal. 10:455–464.
Wachstein M, Meisel E (1957) Histochemistry of hepatic phosphatases of a physiologic pH; with special reference to the demonstration of bile canaliculi. Am J Clin Pathol. 27:13–23.
Wang N, Robaye B, Gossiel F, Boeynaems JM, Gartland A (2014a) The P2Y13 receptor regulates phosphate metabolism and FGF-23 secretion with effects on skeletal development. FASEB J. 28:2249–2259.
Wang W, Luo J, Xiang F, Liu X, Jiang M, Liao L, Hu J (2014b) Nucleolin down-regulation is involved in ADP-induced cell cycle arrest in S phase and cell apoptosis in vascular endothelial cells. PLoS ONE. 9:e110101.
Weissman TA, Riquelme PA, Ivic L, Flint AC, Kriegstein AR (2004) Calcium waves propagate through radial glial cells and modulate proliferation in the developing neocortex. Neuron. 43:647–661.
Werner L, Muller-Fielitz H, Ritzal M, Werner T, Rossner M, Schwaninger M (2012) Involvement of doublecortin-expressing cells in the arcuate nucleus in body weight regulation. Endocrinology. 153:2655–2664.
Winner B, Kohl Z, Gage FH (2011) Neurodegenerative disease and adult neurogenesis. Eur J Neurosci. 33:1139–1151.
Wirenfeldt M, Dalmau I, Finsen B (2003) Estimation of absolute microglial cell numbers in mouse fascia dentata using unbiased and efficient stereological cell counting principles. Glia. 44:129–139.
Xu Y, Tamamaki N, Noda T, Kimura K, Itokazu Y, Matsumoto N, Dezawa M, Ide C (2005) Neurogenesis in the ependymal layer of the adult rat 3rd ventricle. Exp Neurol. 192:251–264.
Yano S, Tsukimoto M, Harada H, Kojima S (2012) Involvement of P2Y13 receptor in suppression of neuronal differentiation. Neurosci Lett. 518:5–9.
Yu JH, Kim MS (2012) Molecular mechanisms of appetite regulation. Diabetes Metab J. 36:391–398.
Yu TS, Zhang G, Liebl DJ, Kernie SG (2008) Traumatic brain injury-induced hippocampal neurogenesis requires activation of early nestin-expressing progenitors. J Neurosci. 28:12901–12912.

Zeng JW, Liu X, He WJ, Du L, Zhang JH, Wu XG, Ruan HZ (2008) Inhibition of ATP-induced glutamate release by MRS2179 in cultured dorsal spinal cord astrocytes. Pharmacology. 82:257–263.

Zeng JW, Wang G, Liu X, Wang C, Tian H, Liu A, Jin H, Luo X, Chen Y (2014) P2Y13 receptor-mediated rapid increase in intracellular calcium induced by ADP in cultured dorsal spinal cord microglia. Neurochem Res. 39:2240–2250.

Zhang FL, Luo L, Gustafson E, Palmer K, Qiao X, Fan X, Yang S, Laz TM, Bayne M, Monsma F (2002) P2Y(13): identification and characterization of a novel Galphai-coupled ADP receptor from human and mouse. J Pharmacol Exp Ther. 301:705–713.

Zhao C, Deng W, Gage FH (2008) Mechanisms and functional implications of adult neurogenesis. Cell. 132:645–660.

Zhao C, Teng EM, Summers RG, JR, Ming GL, Gage FH (2006) Distinct morphological stages of dentate granule neuron maturation in the adult mouse hippocampus. J Neurosci. 26:3–11.

Zhao M, Li D, Shimazu K, Zhou YX, Lu B, Deng CX (2007) Fibroblast growth factor receptor-1 is required for long-term potentiation, memory consolidation, and neurogenesis. Biol Psychiatry. 62:381–390.

Zhao M, Momma S, Delfani K, Carlen M, Cassidy RM, Johansson CB, Brismar H, Shupliakov O, Frisen J, Janson AM (2003) Evidence for neurogenesis in the adult mammalian substantia nigra. Proc Natl Acad Sci USA. 100:7925–7930.

Zheng WM, ZhuGe Q, Zhong M, Chen G, Shao B, Wang H, Mao XO, Xie L, Jin K (2013) Neurogenesis in adult human brain after traumatic brain injury. J Neurotrauma. 30:1872–1880.

Zimmermann H (2006) Nucleotide signaling in nervous system development. Pflugers Arch. 452:573–588.

Zimmermann H (2016) Extracellular ATP and other nucleotides-ubiquitous triggers of intercellular messenger release. Purinergic Signal. 12:25–57.

Zimmermann H, Langer D (2015) Tissue-Nonspecific Alkaline Phosphatase in the Developing Brain and in Adult Neurogenesis. Sub-cellular biochemistry 76:61–84.

Zimmermann H, Zebisch M, Strater N (2012) Cellular function and molecular structure of ecto-nucleotidases. Purinergic Signal. 8:437–502.

Appendix

A List of figures

B List of tables

C Abbreviations

-	Negative
%	Percentage
+	Positive
°C	Degree Celsius
α	Alpha
β	Beta
µg	Microgram
µl	Microliter
µm	Micrometer
µM	Micromolar
3V	Third ventricle
AdeR	Adenine receptor
ADO	Adenosine
ADP	Adenosine 5'-diphosphate
ADPβS	Adenosine 5'-O-(2-thiodiphosphate)
AgRP	Agouti-related protein
AMCA	Aminomethylcoumarin
AMP	Adenosine 5'-monophosphate
AMPA	α-amino-3-hydroxy-5-methyl-4-isoxazolepropionic acid
AP	Alkaline phosphatase
APS	Ammonium peroxodisulfate
ARC/arc	Arcuate nucleus
Asp	Aspartate
ATP	adenosine 5'-triphosphate
BCA	Bicinchoninic acid
BCIP	5-bromo-4-chloro-3-indolyl phosphate
BDNF	Bone derived neurotrophic factor
BMP	Bone morphogneic protein
bp	Base pair
BrdU	Bromodeoxyuridine
BSA	Bovine serum albumin
CA	Cornu ammonis

Ca^{2+}	Calcium
CB/cb	Cerebellum
CC/cc	Corpus callosum
cDNA	Copy DNA
cm	centimeter
CNS	Central nervous system
CNTF	Ciliary neurotrophic factor
CP/cp	Caudoputamen
CREB	cAMP response element binding protein
CRH	Corticotropin-releasing hormone
CSF	Cerebrospinal fluid
C-Terminus	Carboxy-Terminus
CTX/ctx	Cerebral cortex
d	Day
DAG	Diacylglycerol
DAPI	4' ,6-Diamidin-2'-phenylindoldihydrochlorid
DCX	Doublecortin
DEPC	Diethyl pyrocarbonate
DG	Dentate gyrus
dH_2O	Demineralized water
DMN/dmn	Dorsomedial nucleus
DNA	Deoxyribonucleic acid
dNTP	Deoxynucleoside triphosphate
EC	Entorhinal cortex
ECL	Enhanced chemiluminescence
EDTA	Ethylenediaminetetraacetic acid
EGF	Epidermal growth factor
EGFP	Enhanced green fluorescent protein
EGTA	Ethylene glycol tetraacetic acid
eN	Ecto-5'-nucleotidase
ELAV	Embryonic lethal abnormal vision
ERK	Extracellular signal–regulated kinase
EtBr	Ethidium bromide
EtOH	Ethanol

FGF	Fibroblast growth factor
g	Gram
GABA	Gamma-aminobutyric acid
GCL/gcl	Granule cell layer
GFAP	Glial fibrillary acidic protein
GFP	Green fluorescent protein
G_i / G_q / G_s	Types of G proteins
GLAST	L-Glutamate/L-Aspartate Transporter
GPCR	G protein coupled receptor
h	Hour
H_2O	Water
HCl	Hydrochloric acid
HEPES	4-(2-Hydroxyethyl)-1-piperazineethanesulfonic acid
Hi/hi	Hilus
hNSPC	Hypothalamic neural stem and progenitor cell
HP/hpf	Hippocampal formation
HuC/D	Neuronal ELAV-like (Hu) protein C/D
IGF	Insulin-like Growth Factor
IgG	Immunoglobulin G
IgY	Immunoglobulin Y
IHC	Immunohistochemistry
IL	Interleukin
INF/inf	Infrapyramidal
IP3	Inositol 1,4,5-trisphosphate
ISH	In situ hybridization
kb	kilobase
KCl	Potassium chloride
kg	kilogram
KO	knockout
l	Liter
LHA	Lateral hypothalamic area
LHX2	LIM/homeobox protein
LiCl	Lithium chloride

LIF	Leukemia inhibiting factor
LTP	Long-term potentiation
LV	Lateral ventricle
M	Molar
mA	Milliampere
MBH	Medio-basal hypothalamus
MC	Melanocortin
MCH	Melanin concentrating hormone
ME / me	Median eminence
mg	Milligram
Mg	Magnesium
mGlu	Glutamate metabotropic receptor
min	Minute
ml	Milliliter
mm	Millimeter
mM	Millimolar
Mol / mol	Molecular layer
mRNA	Messenger RNA
MSH	Melanocyte-stimulating hormone
NaCl	Sodium chloride
NaOH	Sodium hydroxide
NBT	Nitro blue tetrazolium
neo	Neomycin
Nes	Nestin
NeuN	Neuronal Nuclei
NeuroD1	Neurogenic differentiation 1
Neurog2	Neurogenin 2
ng	Nanogram
nm	Nanometer
NMDA	N-Methyl-D-aspartate
No.	Number
NPP	Nucleotide pyrophoshatase phosphodiester-ase
NPY	Neuropeptide Y

ns	Not significant
NSC	Neural stem cell
N-Terminus	Amino-Terminus
NTPDase	Nucleoside triphosphate diphosphohydrolase
OB	Olfactory bulb
ORX	Orexin
Pax6	Paired box 6
PBS	Phosphate-buffered saline
PCR	Polymerase chain reaction
pCREB	Phosphorylated cAMP response element binding protein
PFA	Paraformaldehyde
PLC	Phospholipase C
POMC	Proopiomelanocortin
Prox1	Prospero homeobox 1
PVN	Paraventricular nucleus
RAX	Retinal homeobox protein
RMS	Rostral migratory stream
RNA	Ribonucleic acid
ROI	Region of interest
rpm	Rotations per minute
RT	Room temperature
SDS	Sodium dodecyl sulfate
se	Septum
sec	Second
SEM	Standard error of the mean
Ser	Serine
Sfrp3	Secreted frizzled-related protein 3
SGL / sgl	Subgranular layer
Shh	Sonic hedge hog
sl	Stratum lacunosum
sn	Substantia nigra
Sox2	Sex determining region Y-box 2
SSC	Saline Sodium citrate

st	Striatum
SUB	Subiculum
SUP/ sup	Suprapyramidal
SVZ	Subventricular zone
TAP	transit-amplifying progenitor
Tbr2	T-box brain protein 2
TBS	Tris-buffered saline
TCS	Tissue cryoprotectant solution
Tg	Transgene
th	Thalamus
TM	Tris-maleate
TMS	Tris-maleate sucrose
TNAP	Tissue nonspecific alkaline phosphatase
TRH	Thyrotropin-releasing hormone
U	Unit
UDP	Uridine 5'-diphosphate
UTP	Uridine 5'-triphosphate
UV	Ultraviolet
V	Volts
VEGF	Vascular endothelial growth factor
VMN	Ventromedial nucleus
vol	Volume
w	Weight
WB	Western blot
WT	Wild type